

MASARYKOVA UNIVERZITA

Lékařská fakulta

Propojení preklinického a klinického výzkumu v orofaciální oblasti

Habilitační práce

MUDr., MUDr. Jan Štembírek, Ph.D.

Obor: Stomatologie

Ostrava 2023



Ústav živočišné fyziologie
a genetiky AV ČR, v. v. i.

Bibliografický záznam

Autor:	MUDr., MUDr. Jan Štembírek, Ph.D.
Pracoviště:	Klinika ústní, čelistní a obličejové chirurgie Fakultní nemocnice Ostrava
Laboratoř:	Laboratoř molekulární morfogeneze Ústav živočišné fyziologie a genetiky Akademie věd Brno, v.v.i
Obor:	Stomatologie
Název práce česky:	Propojení preklinického a klinického výzkumu v orofaciální oblasti
Rok:	2023
Počet stran:	157
Klíčová slova:	Orofaciální region, odontogeneze, odontogenní tumor, temporomandibulární kloub, biomodel, retromarginální zlomeniny očnice

Bibliographic record

Author: MUDr., MUDr. Jan Štembírek, Ph.D.

Department: Department of Maxillofacial Surgery
University Hospital Ostrava

Laboratory: Laboratory of Molecular Morphogenesis
Institute of Animal Physiology and Genetics
Academy of Science, Brno

Field: Stomatology

Title of Thesis: Connecting preclinical and clinical research of orofacial area

Year: 2023

Number of Pages: 157

Keywords: Orofacial region, odontogenesis, odontogenic tumor,
temporomandibular joint, biomodel, blowout orbital fractures

Anotace

Orofaciální oblast patří mezi složité regiony vzhledem k embryonálnímu vývoji, ale později i díky relativně velkému počtu anatomických struktur. Samotný základní výzkum, ale ani samotný klinický výzkum, mohou v takto komplikované oblasti samy o sobě přinést jen dílčí úspěchy, a pro dosažení komplexního pokroku v této oblasti je nezbytně nutné jejich propojení. Význam tohoto propojení je ilustrován na třech příkladech výzkumných projektů, které se uskutečnily v rámci spolupráce Akademie věd jako výzkumné instituce a Fakultní nemocnice Ostrava jako klinického pracoviště. První část se věnuje odontogenezi a jejímu možnému vlivu na vznik odontogenních tumorů, druhá ukazuje možné využití zvířecího biomodelu pro výzkum čelistního kloubu, poslední se pak zaměřuje na problematiku retromarginální zlomeniny očnice.

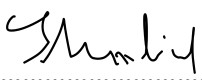
Abstract

The orofacial region is complicated not only from the perspective of embryonal development, but also later throughout the individual's life due to a large number of anatomical structures. Isolated primary or isolated clinical research can, in such a complicated region, bring only partial success and for complex progress in the field, joining forces of these two branches of research is of utmost importance. Here, we illustrate the significance of such linkage on three examples of research projects performed in cooperation of the Czech Academy of Sciences as an institution of primary research and the University Hospital Ostrava as a clinical department. The first part is devoted to odontogenesis and its possible influence on the formation of odontogenic tumors. The second one exhibits the possible usage of an animal biomodel for jaw joint research, and the last part focuses on retromarginal orbital fractures.

Prohlášení

Prohlašuji, že jsem tuto práci vypracoval samostatně s použitím uvedených literárních pramenů.

V Ostravě, dne 26.2.2023


.....

Poděkování

Můj největší dík patří především doc. RNDr. Marcele Buchtové, Ph.D., která mi ochotně a trpělivě pomáhala designovat experimenty, zpracovávat a publikovat výsledky. Bez ní bych těžko procházel úskalími vědecké činnosti a tato práce by zřejmě nikdy nevznikla.

Velkým přínosem pro mě byly připomínky RNDr. Jaroslava Janoška, Ph.D. a MVDr. Ivety Putnové, Ph.D., kterým děkuji za věcné připomínky a jazykovou korekci.

Kromě Laboratoře molekulární morfogeneze Ústavu živočišné fyziologie a genetiky Akademie věd ČR, v.v.i., bych za poskytnuté zázemí pro klinický ale i vědecký rozvoj rád poděkoval také Klinice ústní, čelistní a obličejové chirurgie Fakultní nemocnice v Ostravě, hlavně jejímu přednostovi MUDr. Jiřímu Stránskému, Ph.D. a primáři MUDr. Oldřichovi Resovi, Ph.D., za podporu, trpělivost a předávání klinických zkušeností, které jsem se snažil promítnout i do vědeckých experimentů.

Poděkování patří samozřejmě i mým kolegům a kolegyním za jejich podporu a přátelský přístup. Dále bych chtěl poděkovat všem spoluautorům, se kterými jsem měl možnost spolupracovat a řešit grantové projekty.

V neposlední řadě bych chtěl poděkovat své rodině, že mě trpělivě podporovala ve vědecké práci.

Obsah

Seznam obrázků	10
Seznam zkratk.....	11
1. Úvod.....	12
2. Odontogeneze a její možný vliv na vznik odontogenních tumorů.....	13
3. Experimentální chirurgie v oblasti temporomandibulárního kloubu.....	63
4. Retromarginální zlomeniny očnice.....	113
4. Závěr.....	152
5. Literatura.....	153

Seznam obrázků

Obr. 1: Ortopantomogram pacienta s ameloblastomem

Obr. 2: Aplikace autologní krve u pacienta s hypermobilitou temporomandibulárního kloubu

Obr. 3: Retromarginální zlomenina levé očnice

Seznam zkratek

ASC - adipose stem cell
BRAF - B-Raf proto-oncogene
CCND1- Cell Cycle Regulators Cyclin 1
CT - Počítačová tomografie
DNA – Deoxyribonukleová kyselina
ED - Embryonální den
FANCA - Fanconiho anemia completion group A
FZD - Frizzled
FZD1- Frizzled 1
FZD4- Frizzled 4
FZD7 - Frizzled 7
FZD8 - Frizzled 8
GLI1 - Glioma - associated oncogene family zinc finger 1
IFT20 - Interflagellar transport 20
IFT80 - Interflagellar transport 80
IFT88 - Interflagellar transport 88
LRP5 - Low- density lipoprotein receptor-related protein 5
MMP2 - Metaloproteináza 2
MRi - Magnetická rezonance
OPG - Ortopantomogram
PTCH1- Protein patched homolog 1
SHH - Sonic Hedgehog
SNAI2 - Snail Family Transcriptional Repressor 2
PITX2 - Paired like homeodomain 2
RNA – Ribonukleová kyselina
SFRP1 - Secreted frizzled related protein 1
scRNA-seq - single-cell RNA sequencing
TMK - Temporomandibulární kloub
Wnt - Wingless/Int - 1
Wnt3a - Wingless 3a

1. Úvod

Cílem této práce je zdůraznit důležitost propojení preklinického výzkumu orofaciální oblasti s klinickou praxí. Význam tohoto propojení bude ilustrován na třech příkladech výzkumných projektů. Právě vznik vědeckovýzkumných týmů zahrnujících jak vědce, tak i klinické pracovníky schopné a ochotné přistupovat k dané problematice ne pouze na základě svých individuálních úhlů pohledu, ale skutečně multidisciplinárně, může být cestou k zefektivnění (nejen) medicínského výzkumu (Beger a Schwarz, 1998, Campanelli, 2020).

Prvním příkladem, který bude v této práci uveden, je výzkum vývoje zubu, kde modelový organismus (prase) pomáhá pochopit jednotlivé fáze vývoje zubu a patologických jevů s tímto vývojem spojených, jako je např. vznik epiteliálních perel při degradaci zubní lišty. Tyto epiteliální perly pak mohou tvořit potenciální základ pro vznik odontogenních tumorů, jako je ameloblastom.

Dalším tématem, kterému se práce věnuje, je využití prasečího a králičího modelu pro výzkum čelistního kloubu. V první části tohoto výzkumu jsme využili čelistní kloub prasete k experimentu spočívajícímu v aplikaci autologní krve do tohoto kloubu a k následnému sledování účinku. Tato metoda se v klinické praxi sice rutinně využívá, ale princip není jednoznačně znám. V druhé části výzkumu jsme využili králíka, jehož čelistní kloub je ve srovnání s prasetem lépe dostupný a chov méně nákladný. Na tomto modelu jsme se zabývali reparačním účinkem kmenových buněk na defekt v oblasti čelistního kloubu.

Poslední část je věnována retromarginálním zlomeninám očnice. V tomto případě jsme ve spolupráci s oftalmologem využili naše zkušenosti získané při vývoji skórovacího systému, který by měl usnadnit rozhodování o způsobu terapie takto postiženého pacienta (chirurgická vs konzervativní terapie). Samotné chirurgické řešení takovéto fraktury je další výzvou, protože vyžaduje co nej přesnější rekonstrukci defektu na spodině očnice. Cílem našeho současného výzkumu je vyvinout vstřebatelné rekonstrukční lastury vymodelované pomocí softwarové aplikace na základě CT snímků. Pro takovýto výzkum je použití vhodného biomodelu v preklinické fázi nezbytné a právě prasečí model by mohl být ideálním kandidátem.

Odontogeneze a její možný vliv na vznik odontogenních tumorů

Do vývoje zubu se zapojuje jak ektodermální, tak i ektomezenchymová tkáň. Z ektodermální tkáně vzniká sklovinný orgán a následně sklovina, naopak ektomezenchymová tkáň představuje základ pro dentinovou složku, cement pokrývající zubní kořen, zubní dřeň se strukturami zajišťujícími inervaci, cévní zásobení, imunitní systém (buňky prostupují přes cévy a natrvalo osídlují pulpu zubu) a periodont nutný k uchycení zubu v alveolu (Krivánek et al., 2020).

U difyodontních druhů se vyvíjí nejprve primární zubní lišta, která dává základ primární dentici. Poté, v průběhu dalšího embryonálního vývoje, kdy dochází k vývoji samotných zubů, primární zubní lišta degraduje, ale současně se začíná vyvíjet i sekundární zubní lišta jako základ pro trvalou dentici. Po dokončení vývoje zubů degraduje i tato sekundární dentální lišta. Právě proces degradace zubní lišty, při které vznikají shluky buněk v podobě epiteliálních perel, pak může být jedním z buněčných zdrojů pro vznik odontogenních tumorů, jako je ameloblastom (Stock et al., 1997, Fraser et Smith, 2011, Liu et al., 2021).

Celý proces začíná po vytvoření neurální trubice, která vzniká invaginací ektodermu z dorzálního středového regionu do vyvíjejících se faryngových oblouků (Bronner-Fraser, 1995, Morikawa et al., 2016). Tyto buňky jsou schopny prodělat fenotypovou změnu z ektodermového základu na mezenchymový, a vytvořit tak základy zubního ektomezenchymu (Imai et al., 1996, Krivánek et al., 2017). Nejprve dojde ke ztenčení epitelové tkáně, poté pak v oblasti budoucích zubních zárodků ke kondenzaci mezenchymové tkáně, kde naopak epitelová tkáň ztlušťuje a dochází k tvorbě zubního *pupene* (Thesleff et al., 1995, Krivánek et al., 2017). Poté epitelové buňky prolifерují a postupně se vnořují do okolního mezenchymu, až vytvoří stadium zubního *pohárku*, ve kterém se v oblasti korunky začne tvořit sklovinný orgán a v oblasti budoucí zubní dřeně díky kondenzaci ektomezenchymu vzniká zubní papila a následně odontoblasty produkující dentin. Spojením vnějšího a vnitřního sklovinného epitelu vzniká Hertwigova epiteliální pochva (HERS), která apikálně prorůstá do mezenchymu a enkapsuluje zubní papilu, což nazýváme stadiem zubního *zvonku* (Thesleff et al., 1995). Poté se mezenchymální buňky přiléhající k vnitřnímu sklovinnému epitelu diferencují

v odontoblasty a začnou produkovat organickou matrix. Po počáteční mineralizaci pre-dentinu se přilehlé epitelální buňky mění v ameloblasty produkující organickou matrix skloviny.

Po skončení ukládání sklovinné hmoty část ameloblastů apoptoticky zaniká a zbylé buňky regulují maturaci skloviny ve vysoce mineralizovanou tkáň s minimální přítomností organických složek. Ameloblasty a ostatní epitelální buňky jsou na povrchu skloviny až do okamžiku erupce (Fleischmanová et al., 2007). S pokračující odontogenezí vznikají epitelové zbytky z vnějšího sklovinného epitelu, které nazýváme Serresovy buňky. Právě tyto buněčné shluky mohou být potenciálním zdrojem pro vznik odontogenního tumoru v čelisti (Eversole, 1999, Buchtova et al. 2012).

Během vývoje zubů dochází nejprve k vytvoření korunkové části zubu, poté následuje vytváření zubního kořene. Apikální část HERS hraje důležitou roli v prodlužování zubního kořene, což má vliv na jeho výsledný tvar a na počet kořenů (Ten Cate, 1996). Následně Hertwigova epitelální pochva fenestruje, což umožňuje buňkám mezenchymového zubního vaku kontakt s formujícím se povrchem zubního kořene. Mezenchymové buňky vnitřní vrstvy dentálního vaku se dostávají do kontaktu s kořenovým dentinem a diferencují v cementoblasty. Folikulární buňky hraničící s HERS (mezenchymové buňky vnější vrstvy zubního vaku) obsahují populaci buněk schopných diferencovat v periodontální buňky, včetně cementoblastů, fibroblastů a osteoblastů. Společně se podílejí na vytvoření periodontálního aparátu (Zeichner-David et al., 2003). Některé buňky z HERS migrují od zubního kořene do prostoru budoucích periodontálních vláken, kde se shlukují do Malassezových ostrůvků. Ty mohou následně ovlivňovat reparaci cementu, ale mohou být také zodpovědné za tvorbu odontogenních tumorů (Kaneko et al., 1999, Zeichner-David et al., 2003, Xiong et al., 2013).

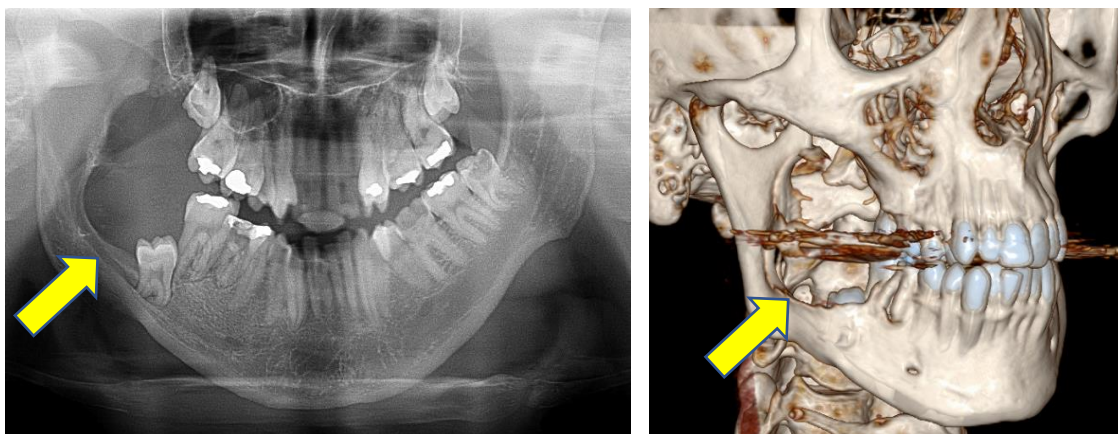
Interdentální i dentální oblasti zubní lišty během dalšího vývoje zubů degradují, i když přesný mechanismus zatím přesně neznáme. Podle různých teorií jde o programovanou buněčnou smrt (apoptózu), jejíž zapojení již bylo do vývoje zubu prokázáno (Matalova et al., 2004). Rovněž byly zaznamenány projevy epitelální-mezenchymální transformace neboli přeměna fenotypu buněk z epitelového na mezenchymový (Kang and Svoboda, 2005), či migrace buněk (Lee et al., 2004). I tyto zbytky buněk ze zubní lišty (epitelální perly) pak mohou teoreticky být základem pro vznik odontogenního tumoru.

V klinické praxi se mezi nejčastější odontogenní tumory řadí zmiňovaný ameloblastom. Jedná se o epitelový odontogenní nádor původem z ameloblastů, který je dominantně benigní s lokálně destrukčním potenciálem, ale v klinické praxi můžeme vzácně nalézt i maligní formy. Nádor se vyskytuje především v dolní čelisti (nejčastěji je lokalizován v úhlu nebo v těle dolní čelisti, vzácně v čelisti horní) a diagnostikován bývá obvykle mezi 20. a 40. rokem života (Kreppel a Zoller, 2018).

Nádor roste pomalu a vede ke zvětšení objemu kosti, přičemž zduřelá kost je palpačně nebolestivá, většinou bez otoku, kryta zdravou sliznicí. Zajímavostí je, že v klinické praxi se s poruchou citlivosti v oblasti mandibulárního nervu setkáváme pouze minimálně. Tento klinicky bezpříznakový růst bývá hlavním důvodem pozdních záchytů ameloblastomu u pacientů s tímto onemocněním (Singh et al., 2021).

V pokročilých případech už ale nacházíme resorpci kořenů způsobujících nestabilitu zubů nebo parestézii či hypestézií. Klinicky se rozeznává forma solidní a cystická. Solidní forma je vzácnější, makroskopicky se skládá z bělavě žlutých granulovaných mas, které jsou zevně dobře opouzdřené nebo alespoň ohraničené. Cystická forma je buď monocystická, nebo polycystická, a obsahem dutin je nažloutlá cystická tekutina (Mendenhall et al., 2007).

Standardním RTG vyšetřením je OPG (**Obr. 1**), kde se nádor prokáže buď jako jedna dobře ohraničená dutina připomínající cystu, nebo jako skupina různě velkých dutin oddělených od sebe kostními přepážkami (to směřuje diagnostiku k ameloblastomu). Tyto přepážky mohou někdy dokonce i zcela chybět a pak jsou na snímku patrné polokruhovitě výřezy v kosti, oddělené od sebe nízkými zbytky kostních sept. V pokročilejším stadiu jsou patrné resorpce kořenů zubů. Při podezření na ameloblastom je vhodné doplnit diagnostiku i CT vyšetřením (Kitisubkanchana et al., 2021).



Obr. 1: Vlevo: Zobrazení ameloblastomu na OPG. Vpravo: 3D rekonstrukce z CT vyšetření stejného pacienta. Zajímavostí je přítomnost neprořezaného zubu 47 a ageneze zubu 48 v místě vzniku ameloblastomu.

Histologicky se rozlišuje šest typů ameloblastomů: folikulární, plexiformní, akantozomatozní, z granulárních buněk, desmoplastický a bazaloidní. Z klinického hlediska je ovšem terapie pro všechny stejná, tzn. chirurgická léčba v podobě extirpace nebo dokonce resekce čelisti (Shi et al., 2021).

Přesné mechanismy kontrolující iniciaci odontogenních nádorů stále nejsou detailně známy. Proto je vhodné využívat tkáňové kultury, ale i zvířecí biomodely, které nám mohou pomoci při odhalování patologických procesů v rámci signalizace a buněčné komunikace mezi epitelovými a mezenchymovými složkami v průběhu vývojových procesů. V našem výzkumu se v této souvislosti ukazuje být jedním z nejvhodnějších kandidátů prasečí model (*Sus scrofa f. domestica*), neboť jsme u tohoto modelu při vývoji primární dentice zachytili rozpad dentální lišty s tvorbou epiteliálních perel, které se formují do shluků buněk, obdobně jako je tomu u člověka. Právě tyto buňky mohou být v budoucnu zdrojem možných patologií. Vzhledem k tomu, že problematika vývoje ameloblastomů je z velké části neprozkoumaná, spojení klinických nálezů s molekulárními analýzami u jednotlivých pacientů a dále využití vhodného zvířecího biomodelu by nám mohlo pomoci lépe pochopit etiologii vzniku těchto patologií a umožnit rozšíření možného terapeutického spektra v podobě biologické léčby.

Komentář k přiložené publikaci č. 1

STEMBIREK, Jan, Marcela BUCHTOVA, Tomas KRAL, Eva MATALOVA, Scott LOZANOFF a Ivan MISEK. Early morphogenesis of heterodont dentition in minipigs. *European Journal of Oral Sciences* [online]. 2010, 118(6), 547–558. ISSN 0909-8836. Dostupné z: doi:[10.1111/j.1600-0722.2010.00772.x](https://doi.org/10.1111/j.1600-0722.2010.00772.x)

IF = 1,890; Kvartil Q2

V literatuře se prase domácí uvádí jako vhodný biomodel pro výzkum embryonálního vývoje zubů, protože stejně jako člověk má dvě série zubů (tzn. difyodontní dentici) s více typy zubů (heterodontní dentice; Liu et al., 2021). Detailní informace o jednotlivých stádiích vývoje dentice u tohoto biomodelu v literatuře přesto chyběly. Cílem naší studie proto bylo u prasete identifikovat a charakterizovat raná vývojová stadia odontogeneze, konkrétně období od iniciace primární dentice až po pozdní fázi zvonku, kdy se začíná vyvíjet i sekundární dentice. V nejranějších stádiích byla zubní lišta podél celé délky čelisti kontinuální. Následně se začaly objevovat dentální a interdentalní oblasti, které byly charakteristické nejen založením zubních zárodků a vrůstáním zubní lišty v lingválním směru, ale také zmenšováním zubní lišty v interdentalní oblasti. Stran dalšího výzkumu v souvislosti se vznikem možných patologií považujeme za nejdůležitější stádium zvonku primárních zubů (ED50), kdy zubní lišta začíná degradovat a oddělovat se od orálního epitelu. Většina buněk dentální lišty během tohoto procesu postupně zmizela, některé však perzistovaly v podobě epitelových perel. Právě vznik těchto perel při degradaci zubní lišty a jejich perzistence může představovat v dalším vývoji riziko vzniku patologických struktur, jako je odontogenní tumor.

Early morphogenesis of heterodont dentition in minipigs

Jan Štebáček^{1,2,3*}, Marcela Buchtová^{1,4*}, Tomáš Král^{1,2}, Eva Matalová^{1,5}, Scott Lozanoff⁶, Ivan Míšek^{1,4}

Štebáček J, Buchtová M, Král T, Matalová E, Lozanoff S, Míšek I. Early morphogenesis of heterodont dentition in minipigs.

Eur J Oral Sci 2010; 118: 547–558. © 2010 Eur J Oral Sci

The minipig provides an excellent experimental model for tooth morphogenesis because its diphyodont and heterodont dentition resemble that of humans. However, little information is available on the processes of tooth development in the pig. The purpose of this study was to classify the early stages of odontogenesis in minipigs from the initiation of deciduous dentition to the late bell stage when the successional dental lamina begins to develop. To analyze the initiation of teeth anlagen and the structural changes of dental lamina, a three-dimensional (3D) analysis was performed. At the earliest stage, 3D reconstruction revealed a continuous dental lamina along the length of the jaw. Later, the dental lamina exhibited remarkable differences in depth, and the interdental lamina was shorter. The dental lamina grew into the mesenchyme in the lingual direction, and its inclined growth was underlined by asymmetrical cell proliferation. After the primary tooth germ reached the late bell stage, the dental lamina began to disintegrate and fragmentize. Some cells disappeared during the process of lamina degradation, while others remained in small islands known as epithelial pearls. The minipig can therefore, *inter alia*, be used as a model organism to study the fate of epithelial pearls from their initiation to their contribution to pathological structures, primarily because of the clinical significance of these epithelial rests.

¹Institute of Animal Physiology and Genetics, v.v.i., Academy of Sciences of the Czech Republic, Brno, Czech Republic; ²Faculty of Medicine, Masaryk University, Brno, Czech Republic; ³Department of Oral and Maxillofacial Surgery, University Hospital Ostrava, Czech Republic; ⁴Department of Anatomy, Histology and Embryology, University of Veterinary and Pharmaceutical Sciences, Brno, Czech Republic; ⁵Department of Physiology, University of Veterinary and Pharmaceutical Sciences, Brno, Czech Republic; ⁶Department of Anatomy, Biochemistry & Physiology, University of Hawaii School of Medicine, Honolulu, HI, USA

*Authors who contributed equally to the work presented in this article.

Dr Marcela Buchtová, Institute of Animal Physiology and Genetics, v.v.i., Academy of Sciences of the Czech Republic, Veverí 97, 602 00 Brno, Czech Republic

Telefax: +420–5–41212988
E-mail: buchtova@iach.cz

Key words: dental lamina; epithelial pearls; odontogenesis; three-dimensional reconstruction

Accepted for publication August 2010

The minipig is currently used as an experimental model for human systems in many biomedical fields because of its apparent similarities in anatomy and physiology, as well as for economic advantages. Many different porcine strains have been utilized to investigate numerous diseases, such as diabetes mellitus or melanomas, which affect humans (1–3). Pigs are widely used for salivary gland research because they have a salivary flow rate that corresponds closely to that of humans (4, 5). The pig is also similar to the human with respect to the meniscotemporal and condylomeniscal joint, making it suitable for experiments on abnormal or harmful function of the temporomandibular joint (6). Furthermore, pig jaws are used for testing implant materials as well as for investigating the introduction of new techniques in implantology (7, 8). The porcine model facilitates testing of stem cells/scaffold constructs in the restoration of orofacial skeletal defects and provides a rapid translation of the stem-cell-based therapeutics in orofacial reconstructions (9). The pig is also suitable for periodontal disease research as inflammation of the gingiva can be present after 6 months of age, characterized by swelling, accumulated plaque, and calculus, consistent with the common features seen in human gingivitis. Even though the mouse is the most common laboratory animal used for dental research, it displays a heterodont

and monofyodont dentition. However, pigs have normodont diphyodont dentition without diastema, so they have the potential to become an excellent model organism for studying the mechanisms of replacement and patterning of heterodont teeth.

Pig deciduous teeth exhibit numerous morphological similarities compared with the human dental pattern. The dental formula of the deciduous dentition for the miniature pig is $i3/3$, $c1/1$, and $p3/3 = 28$, and for the permanent dentition is $I3/3$, $C1/1$, $P4/4$, and $M3/3 = 44$. The pig adult dentition with three incisors, one canine, four premolars, and three molars represents the general eutherian dental formula. The number of premolars varies among animals because the first premolar may be absent (10, 11). Incisors and canines have a simple conical shape with one tooth cusp and one root, while premolars are multicuspid and possess multiple roots (Fig. S1). The curved canine teeth (tusks) of boars possess an open root canal and continue growing throughout life. Piglets are born with the third incisor and canine already erupted, and a detailed analysis of eruption has been published recently (12). In contrast, humans are born toothless, and the first primary teeth usually erupt between 6 and 8 months postnatally. As a general rule, the mandibular teeth erupt before the maxillary teeth, and teeth appear earlier in females than in males.

Tooth development is characterized by a complex series of reciprocal interactions that occur between the epithelium (stomodeal ectoderm) and the underlying cranial neural crest-derived mesenchyme (ectomesenchyme) that regulates tooth morphogenesis and differentiation at the molecular level (13–16). Despite the differences in final shape, teeth undergo successive developmental stages common to all mammals, including epithelial thickening, and bud, cap, and bell stages (17). Epithelial thickening is the first morphological feature of tooth development and is characterized by cell proliferation and invagination of the dental placode into the surrounding ectomesenchyme.

The monophodont mouse is the most common model used for experimental investigations of tooth development and offers many advantages (18). However, certain limitations exist. In the mouse, the epithelium forms a tooth bud in close proximity to the oral epithelium without any significant invagination into the mesenchyme. The mouse also lacks the full spectrum of teeth. There is an incisor that grows permanently and three molars in each jaw quadrant separated by a large, toothless gap (19). Diphyodont species (including humans) display epithelial growth that invaginates into the underlying mesenchyme to form a distinct dental lamina that is necessary for the development of both primary and secondary generations of teeth (20, 21). The pig has a normodont and heterodont dentition, with all tooth families being present and without an obvious diastema (22). These morphological features facilitate analysis of pattern formation in the heterodont dentition with the potential to address hypotheses concerning the morphogenetic specificity of incisor–canine–premolar–molar areas. The pig develops two generations of teeth, similarly to humans, and thus has the potential to serve as a suitable model for the analysis of successional tooth development. Furthermore, cloning of the porcine genome is well underway, providing increased opportunities to use molecular methods to address the underlying mechanisms of pattern formation of specific tooth types.

Despite all the advantages of the pig model in odontology, detailed descriptive information concerning tooth development in the pig is lacking. The purpose of this study was to identify and classify early stages of odontogenesis in minipigs, focusing on morphogenesis of the dental lamina utilizing computerized three-dimensional (3D) analyses. This study also compared the development of individual teeth in different positions along the jaw and aimed to obtain basic information about their development for further molecular studies. Finally, we addressed whether or not temporal and positional overlap occurs between the initiation of dental lamina regression and the beginning of replacement tooth formation.

Material and methods

Embryonic material

All procedures were conducted following a protocol approved by the Institutional Ethics Committee. Minipig

embryos and fetuses were obtained from Liběchov animal facility (strain LiM; Liběchov, Czech Republic). The day after insemination was established as day 1 of gestation. Staged embryos and fetuses were obtained by hysterectomy and collected between embryonic days (E)20 and 67. Specimens were fixed in 4% neutral formaldehyde (E20, E25, E30, E35, E41, E45, E50, E56, and E67) and processed for routine paraffin embedding. Five-micrometer serial tissue sections were prepared and stained with hematoxylin and eosin for 3D reconstruction analysis. Tissues were observed and photographed using a Leica microscope (DMLB2) with a Leica camera (DFC480) attached (Leica Microsystems, Wetzlar, Germany). In addition, tissues were collected for immunohistochemical staining and analysis.

3D reconstruction

Gestation in the minipig takes 115 d, which is similar to that of the common domestic pig. Serial histological sections were used to analyze the initiation of teeth anlagen and dental lamina morphology. To evaluate continuity of the dental lamina and the corresponding arrangement of tooth anlagen within the jaw during development, 3D analysis at four developmental stages (E25, E30, E35, and E45) was performed. Computerized 3D reconstructions were matched with transverse histological sections through the dental lamina along the lower right mandibular corpus, and the pictures of individual teeth anlagen were arranged in the rostrocaudal direction to elucidate details of heterodont dentition development. Three-dimensional reconstruction of the right mandibular corpus from representative specimens was performed using SURFdriver software (WINSURF, v. 3.6; SURFdriver Software, Kailua, HI, USA) and subsequently viewed with SURFviewer (1.1). Sequential transverse serial sections were photographed (magnification 200 × or 100 ×) and opened in WINSURF. Relevant tissue boundaries were identified and manually segmented.

Immunohistochemical staining

The location of proliferating (positive) cell populations was detected by immunohistochemical detection of the proliferation marker, proliferating cell nuclear antigen (PCNA). After deparaffinization and rehydration, the sections were incubated for 1 h at room temperature with primary mouse anti-PCNA IgG (clone PC10, 1:100 dilution; Dako, Copenhagen, Denmark). The secondary biotinylated anti-mouse IgG (1:500 dilution, ABC kit; Vectastain, Vector Laboratories, Burlingame, CA, USA) and the avidin–biotin complex (ABC kit; Vectastain) were applied for 30 min each. Visualization was performed by diaminobenzidine (DAB). Slides were counterstained with hematoxylin and the non-proliferating (negative) cells were stained blue.

Proliferation index

To quantify temporo-spatial differences in proliferation, the proliferation index [i.e. the ratio of positive cells out of the total number of cells (approximately 100)] was determined. Deeper vs. superficial parts of the dental lamina (E36), the interdental vs. the dental areas of lamina, and the labial vs. the lingual areas of the lamina at E36, E56, and E67 were evaluated.

Proliferating and non-proliferating cells were counted using the IMAGE J plugin Cell counter (Wayne Rasband, Research Services Branch, Bethesda, Maryland, USA)

allowing individual cell tagging in different colors. The results were evaluated using the Student's *t*-test and multi-factorial ANOVA (MANOVA) with Tukey's *post-hoc* testing ($P < 0.05$; STATISTICA; StatSoft, Tulsa, OK, USA).

Results

Definition of individual tooth stages

All pig teeth, regardless of shape or identity, displayed developmental stages (Fig. 1) equivalent to those of other mammalian species where epithelial thickening was the first morphological indication of tooth development (Fig. 1A). In contrast to the mouse, we defined the dental lamina stage in minipig embryos (Fig. 1B) as the epithelium that proliferates into the mesenchyme without any obvious bud formation. We distinguished the early cap stage, where the central area of the primordium is formed by the enamel knot (Fig. 1D), and the late cap stage, where the enamel organ cells are loosened (Fig. 1E). Diphyodont species exhibit a distinct asymmetry with the dental lamina located on the lingual side of the tooth anlagen (Fig. 1G). The histodifferentiation and morpho-differentiation of epithelial cells occurred in conjunction with the dental papilla deeply protruding into anlagen, forming an acute-angled apex. The dental lamina became reduced, which disrupted its connection to the oral epithelium (Fig. 1G). Differentiation of odontoblasts at

the bell stage was followed by the production of predentin and dentin, which are typical for the secretory stage (Fig. 1H). Epithelial pearls appeared in the dental lamina at this stage of odontogenesis (Fig. 1H).

Odontogenesis at early prenatal stages

The first signs of invagination of the oral epithelium into the underlying mesenchyme occurred at E20 (Fig. S2). The epithelial thickening was continuous along one quadrant of the mandibular corpus. Right and left dental thickenings were not connected in the midline and tooth anlagen had not yet been initiated. The dental epithelium became thinner and straightened close to the caudal end of the epithelial thickening. At this developmental stage, the primary and secondary palates were still open.

At E25, the epithelial thickening had grown more deeply into the mesenchyme to reach the dental lamina stage (Fig. 2). The right and left laminae were in close proximity in the midline area. Computerized 3D reconstruction revealed a continuous dental lamina along the jaw (Fig. 2A,A''). There was no interruption of the dental lamina in the region of the presumptive canine. There were differences in the depth of the invagination of the dental lamina into the mesenchyme, with the deepest projections occurring in the area of the future canine and the first incisor in the

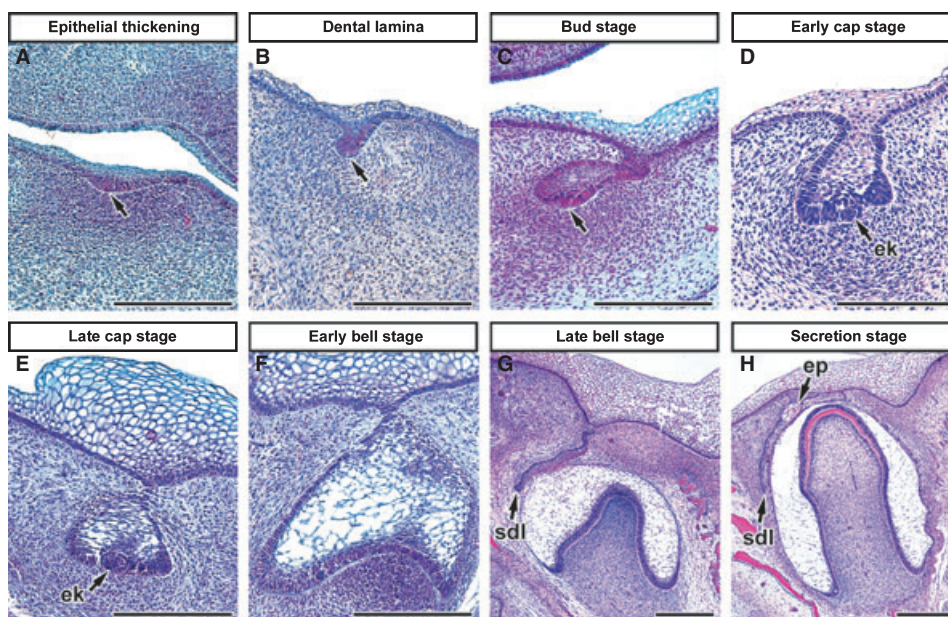


Fig. 1. Staging of tooth development in the minipig. (A) Epithelial thickening was the first morphological sign of odontogenesis. (B) The epithelium grew into the mesenchyme to form the dental lamina. (C) Localized thickening of epithelium (arrow) appeared along the dental lamina, which was characteristic for the bud stage of tooth anlagen with condensations of the surrounding mesenchymal cells (D) The enamel organ differentiated into the early cap stage with the enamel knot (37). (E) Loosening of enamel organ cells was evident at the late cap stage. The outer and the inner enamel epithelium and formation of dental papilla were distinguishable. (F) Stellate reticulum cells differentiated and the dental papilla increased in size at the early bell stage. (G) Tooth anlage showed a distinct asymmetry with the dental lamina located on the lingual surface at the late bell stage. The dental lamina was disrupted and detached from the oral epithelium (arrow). Successional dental lamina (sdl) was observed as projecting into the mesenchyme. (H) Differentiation of odontoblasts and their production of dentin (d) characterized the secretion stage. Epithelial pearls became visible in the superficial part of the lamina (ep). Scale bars = 200 μ m.

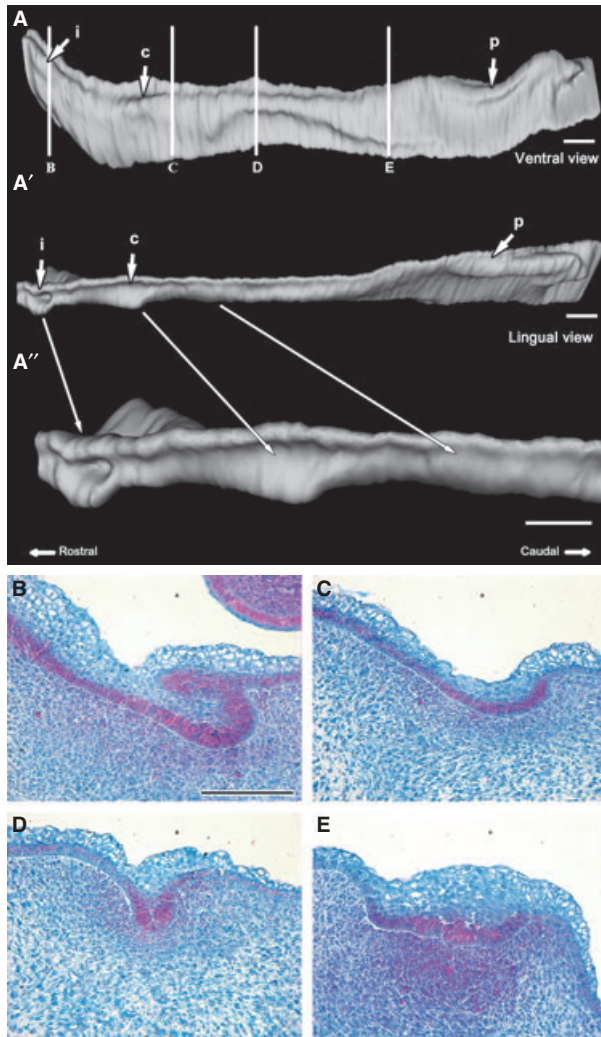


Fig. 2. Odontogenesis in a minipig embryo at embryonic day 25 (E25). Computerized three-dimensional (3D) reconstruction of the right mandibular dental lamina viewed from ventral (A) and lateral (A') perspectives. (A'') A detail of the rostral area showing the continuity of the dental lamina between the rostral and caudal areas. The labeled lines in (A) correspond to the histological section below. (B) Section of the incisiform rostral area. (C) The interdental area between canine and premolar areas. Note the small epithelial thickening and differential staining of basal layers (red) of the dental epithelium in comparison to the oral surface. (D) More caudally, the epithelium of the interdental area protruded into the underlying mesenchyme. (E) Epithelial thickening in the future premolar formation zone exhibiting a diffuse growth pattern contrasted against localized formation of the lamina rostrally. Scale bar = 100 μ m.

rostral mandibular corpus (Fig. 2A'A''). The epithelial anlagen of the future fourth premolar also protruded deeply. Lamina between anlagen showed small ingrowths into the mesenchyme and proliferative regions were easily distinguishable by the presence of epithelial cell condensations (Fig. 2C). The primary palate and lips were fused at this stage, but the secondary palate remained open.

At E30 (Fig. 3), the oral epithelium was thicker and superficial cells became cornified. Right and left dental

laminae were connected in the midline. The dental lamina projected deeply into the mesenchyme (Fig. 3C,E). In the rostral area, bud stages of the deciduous first, second, and third incisors as well as the canines were evident (Fig. 3B,D,G, Table S1). In the caudal region, the fourth premolar progressed into the cap stage (Fig. 3J). The third premolar was at the bud stage with the enamel knot protruding into the mesenchyme (Fig. 3I) and the second premolar had not yet been initiated (Fig. 3A,H). Interdental lamina was morphologically obvious at this stage and had expanded into the mesenchyme; however, it was shorter and lagged behind the tooth-forming regions (Fig. 3A'). The dental lamina projected into the mesenchyme with a curved trajectory and in a lingual direction rather than as a simple straight protrusion and perpendicular (Fig. 3E). An epithelial ingrowth forming the vestibular lamina began to protrude in the lateral direction from tooth anlagen (Fig. 3B,C). These epithelial ingrowths were most prominent in the rostral area in a close relationship to the incisor anlagen (Fig. 3A').

The dental lamina was still connected to the oral epithelium along the length of the mandibular corpus at E35 (Fig. 4), except in the most caudal area where this connection was lost. Teeth anlagen were initiated superficially close to the oral epithelium and the dental lamina did not overgrow the tooth anlagen (Fig. 4B,C,I,J). Further growth of the dental lamina continued asymmetrically into the mesenchyme with a tendency to turn lingually (Fig. 4D,H). The dental lamina was connected to all deciduous teeth anlagen (Fig. 4A). The early cap stages of the deciduous first, second, and third incisors were present at E35 (Fig. 4B,C,E, Table S1) whereas the late cap stages were observed in the deciduous canine and the third premolar (Fig. 4G,I, Table S1). The most developed tooth anlagen were the deciduous fourth premolars that had reached the early bell stage, as indicated by the stellate reticulum (Fig. 4J). Vestibular lamina appeared in the frontal area of the dental lamina (Fig. 4B,D in contrast to J) and was associated with incisor and canine teeth. The vestibular lamina became shorter in the caudal direction and was well developed in the interdental areas just anterior to the teeth anlagen (Fig. 4A,A').

At E41 of fetal development, the dental lamina was still connected to the oral epithelium. The depression of epithelium appeared at the junction of the dental lamina and the oral epithelium. The deciduous incisors were at the late cap stage, whereas the canine was at the early bell stage (Table S1). The fourth premolar progressed to the late bell stage; however, the third premolar was still at the late cap stage (Table S1). The second premolar appeared for the first time at this developmental stage. Growth of the interdental lamina lagged behind growth of the dental lamina in the anlagen areas.

The dental lamina remained connected to the oral epithelium at E45 (Fig. 5C,F). The depression of epithelium appeared at the junction of the dental lamina and the oral epithelium. The vestibular lamina

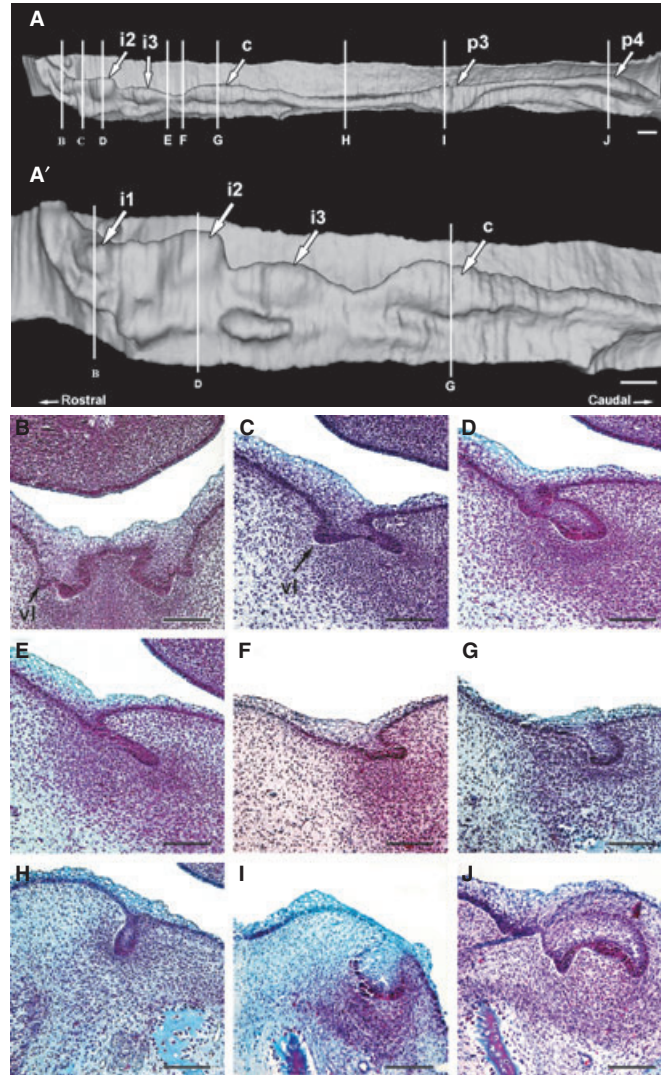


Fig. 3. Odontogenesis in a minipig embryo at embryonic day 30 (E30). (A) Computerized three-dimensional (3D) reconstruction of the right mandibular dental lamina viewed from a ventral (A') perspective with the rostral area showing initiation of individual anlagen along the mandibular lamina. The labeled lines in (A) correspond to the histological sections shown below. (B) Transverse section of the first incisors. (C) Interdental area between the first and second incisors with invaginating vestibular lamina (vl). (D) The second incisor reached the bud stage while the vestibular lamina decreased in height. (E,F) Interdental lamina between the third incisor and canine showed continuity of lamina along the mandibular corpus. The growth of interdental lamina was slower during this early developmental stage. (G) Cross-section of the bud stage of canine anlagen. (H) Interdental lamina between canine and premolars. (I) The third premolar proceeded into the early cap stage. (J) The fourth premolar reached the late cap stage, at which time it was fully developed. Scale bars = 100 μ m.

protruded into the mesenchyme of the first incisor region (Fig. 5A,B) but became reduced in size caudally (Fig. 5B–I). The first, second, and third incisors had progressed to the early bell stage, whereas the fourth premolar was still at the late bell stage and the third premolar at the late cap stage (Fig. 5J,I). The second premolar had reached the early cap stage. The dental lamina became reduced in size and thickness in the interdental region (Fig. 5C,F), particularly in the area connecting to the oral epithelium.

At E50, the dental lamina and the oral epithelium were disconnected (Fig. S3A,B). The dental lamina projected deeply into the mesenchyme in the lingual direction, and had overgrown the deciduous tooth

anlagen forming the second generation at its tip (Fig. S3C,F,H). The first occurrence of odontoblast differentiation occurred in the presumptive canine as it entered the secretory stage, which was characterized by predentin production (Fig. S3F). The second premolars were at the late cap stage (Fig. S3G), while all incisors were at the bell stage (Fig. S3A–D). The dental lamina of the interdental region was interrupted and reduced in size (Fig. S3E).

At E56, the dental lamina was disconnected from the oral epithelium (Fig. S4A,C). In the caudal area of the jaw where the lamina was retained, superficial portions of the lamina were composed of flat cells forming a thin layer (Fig. S4F). Deeper portions of the lamina were

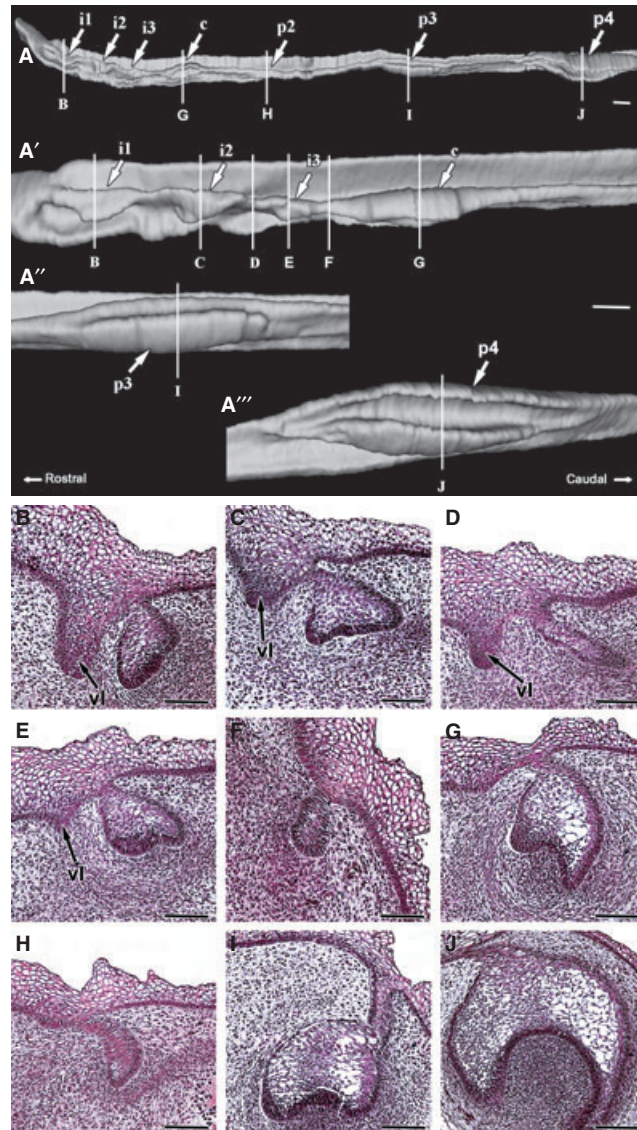


Fig. 4. Odontogenesis in a minipig embryo at embryonic day 35 (E35). (A) Computerized three-dimensional (3D) reconstruction of the right mandibular dental lamina viewed from the ventral perspective. (A') The rostral area shows the progress of individual tooth anlage development along the mandibular corpus. Detailed view of the third (A'') and the fourth (A''') premolars; the labeled lines in (A) correspond to the histological sections shown below. (B) Transverse section of the first incisor. (C) Transverse section of the second incisor. (D) Interdental area between the second and third incisors with well-developed vestibular lamina (vl). (E) The third incisor reached the bud stage with the vestibular lamina displaying a decreased height (vl). (F) Dental lamina between the third incisor and the canine anlagen. (G) The deciduous canine reached the late cup stage. Note that the vestibular lamina was not present at this stage. (H) Interdental lamina between rostral and caudal dentigenous areas retained continuity at this stage. (I) The third premolar progressed into the late cap stage. (J) The fourth premolar reached the early bell stage. Scale bars = 100 μm .

characterized by three layers of cells, including superficial cylindrical cells underlying the basal membrane and dispersed central polygonal cells. The cell layer facing the tooth anlagen was covered with large acidophilic cells. The dental lamina was rudimental in the region between the canine and the premolar (Fig. S4E). The fourth premolar reached the secretion stage, as indicated by dentin production (Fig. S4I). The second premolar progressed into the early bell stage (Fig. S4G) and the third premolar into the late bell stage (Fig. S4H, Table S1). Incisors persisted at the late bell stage (Fig. S4A–C).

Complete detachment of the dental lamina from the oral epithelium occurred at E67. The superficial portion had fragmented into numerous independent tissue islands (Fig. S5A,B). The number of cells with acidophilic cytoplasm appeared to increase while the total mass of the dental lamina decreased (Fig. S5G). Alveolar bone was observed to surround the base of teeth and formed an alveolar pocket (Fig. S5D,F). Numerous osteoclasts were located on the superficial bone lamellae adjacent to the corresponding tooth. All teeth, except for the second premolar, had reached the secretory stage. Enamel production was obvious in

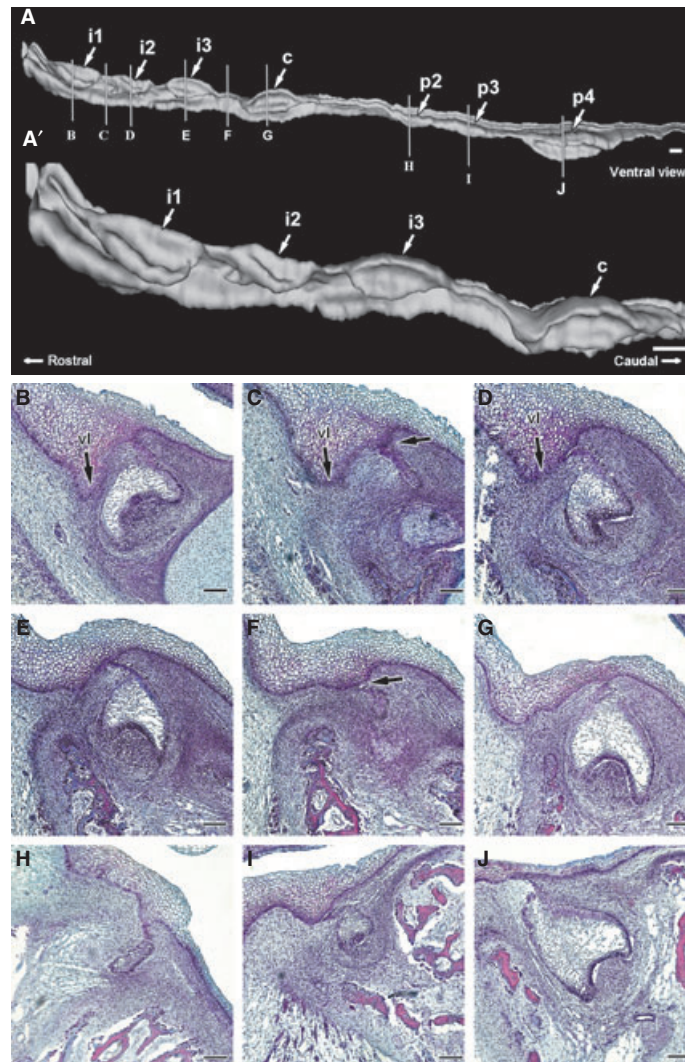


Fig. 5. Odontogenesis in a minipig embryo at embryonic day 45 (E45). (A) Computerized three-dimensional (3D) reconstruction of the right mandibular dental lamina viewed from the lateral perspective. (A') The rostral area shows continued progress of individual anlagen development along the mandibular corpus. The labelled lines in (A) correspond to the histological sections shown below. (B) Transverse section of the first incisor at the early bell stage and related vestibular lamina (vl). (C) Interdental lamina between the first and second incisors. (D) The early bell stage of the second incisor and the third incisor. (E) The vestibular lamina decreased in size in the caudal direction. (F) The interdental lamina between the third incisor and the canine was small and narrow. (G) The canine was more developed than the incisor and reached the late bell stage. (H) Transverse section of the interdental region, where the dental lamina was still continuous. (I, J) No obvious progress in development of the third and fourth premolars was seen in comparison to the previous stage. Scale bars = 100 μm .

the third incisor, canine, and the fourth premolar (Fig. S5A,C,D).

Inclined growth of the dental lamina is underlined by asymmetrical cell proliferation

Immunohistochemical detection of PCNA was used to determine the proliferation rate during development of the dentition, and differences in the growth capacity of the dental lamina were noted.

At E20, PCNA-positive cells were dispersed in the mesenchyme around the dental thickening and in the epithelial portion of the tooth germ (Fig. 6A). Later in development (E25 and E36), proliferating cells were located primarily at the tip of the growing dental

lamina, with a significantly higher number of positive cells positioned labially (Fig. 6C, S6B, S7). The distribution of PCNA-positive cells in the mesenchyme was irregular, with condensations of these cells around the lingual tip of the lamina (Fig. 6C). The interdental region was characterized by a slightly decreased number of proliferating cells compared with the dental region. However, this difference was only marginally significant for the superficial part of the lamina (Fig. 6B,C, S7). A significantly lower number of proliferating cells were located in the dental stalk of both regions (Fig. 6B,C, S7). Condensation of positively stained cells preceded morphological signs of bud formation at the distal tip of the lamina (Fig. S6B) and appeared to persist to the late bud stage (Fig. 6C).

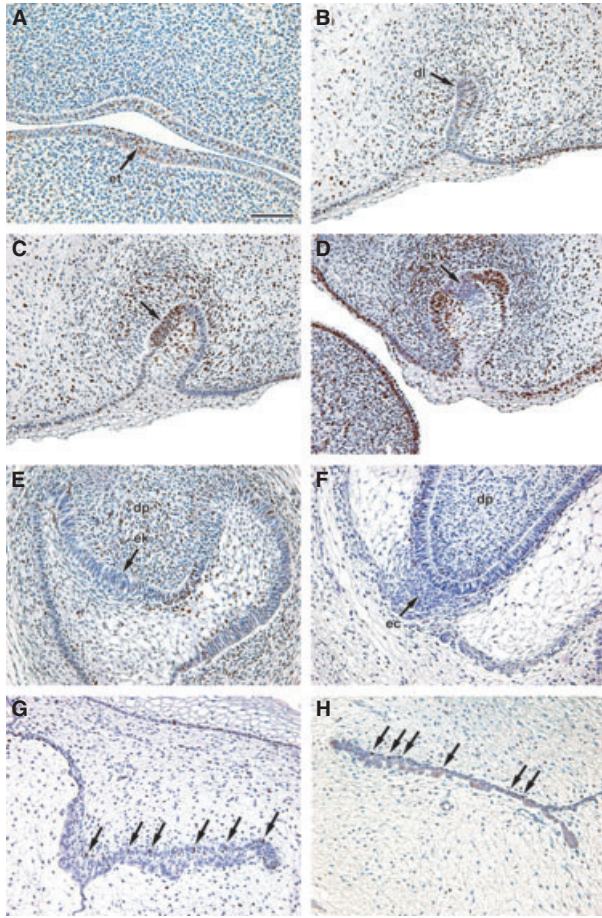


Fig. 6. Proliferation in teeth anlagen and dental lamina at early stages of odontogenesis. Positive cells were visualized by diaminobenzidine (DAB) (brown) and counterstained by hematoxylin (blue). (A) Proliferating cell nuclear antigen (PCNA)-positive cells were dispersed in the epithelium and the adjacent mesenchyme at the early stages of odontogenesis E20. (B) The tip of the growing dental lamina contained more proliferating cells than superficial lamina (E36). (C) Tooth anlagen at the bud stage with positive cells concentrated in the forming inner enamel epithelium (E36). (D) At the cup stage, positive cells were concentrated in the cervical loop, whereas the enamel knot area was PCNA-negative (E36). (E) At the early bell stage, there appeared to be a decrease in the number of positive cells. The enamel knot was PCNA-negative through the early (E) and late (F) bell stages (E56). (G) There was an asymmetrical distribution of proliferating cells in the dental lamina at E56. PCNA-positive cells were located on the side adjacent to the oral epithelium. (H) The dental lamina became thinner at E67 and only a few PCNA-positive cells were located on the side adjacent to the oral epithelium. Scale bars = 100 μ m.

Cells of the lateral epithelial ingrowth in the interdental area were PCNA-negative (Fig. S6A), while a cluster of positive cells appeared in the dental region (Fig. S6B). There were no proliferating cells in the enamel knot area (Fig. 6D). At the later stages (E56 and E67), the number of proliferating cells significantly decreased in the dental lamina (Fig. 6G,H, S7) and they were situated in the region adjacent to the oral epithelium (lingual side). Furthermore, positively stained cells were located in the cervical loop area of the early bell

(Fig. 6E) and also of the late bell (Fig. 6F) stages. An apparent increase in the number of positive cells in the inner enamel epithelium of the late bell stage was evident just before enamel and dentin production (Fig. S6 – compare E and F). In contrast, the enamel cord cells were PCNA-negative (Fig. S6F).

Successional dental lamina follows the bell stage deciduous dentition

The deciduous dentition was initiated superficially close to the oral epithelium. The penetration of the successional dental lamina into the mesenchyme was apparent at the late bell stage, when the tooth anlage had moved away from the oral epithelium. The successional lamina had overgrown the primary tooth anlage and elongated into the mesenchyme to initiate the secondary dentition. Budding of the successional lamina initiated from the lingual aspect of the primary teeth.

Initiation of replacement lamina was not apparent until E41 when the fourth premolar reached the late bell stage and the lamina started to elongate. By E56, all deciduous teeth had progressed into the late bell stage with a well-developed successional lamina (Fig. S4). Any permanent tooth anlagen were not observed during the time period under investigation. Disconnection of the tooth anlage from the adjacent dental lamina occurred by E67, particularly of the most developed teeth (c, p4) that also displayed enamel production (Fig. S5). The teeth with reduced enamel production, including the incisors and premolars (p2, p3), were still connected to the dental lamina by a thin dental stalk (Fig. S5).

Epithelial pearls

After the primary tooth germ had reached the late bell stage, the dental lamina began to fragment and disintegrate (Fig. S4A). During the process of lamina degradation, selected cells remained as epithelial pearls (Fig. S4F). The epithelial pearls were localized to the superficial region of the dental lamina between the tooth anlage and the oral epithelium. The first observation of these structures occurred at E56 (Fig. S4F). The epithelial pearls appeared as groups of circumferentially positioned cells situated separately or as components of the dental lamina. In the course of further development, they lost their reticular structure and became more compact (compare Fig. S4F and S5B,I). The epithelial cells assumed a flattened appearance as they became arranged into several concentric layers.

Discussion

The minipig provides a good model for dental research, in particular because of its normodont dentition with all four types of teeth. The current study was initiated to provide a detailed analysis of individual tooth development in the minipig using a comprehensive documentation approach. Data from this study should facilitate

further dental experiments in the pig model, particularly selection of appropriate developmental stages for experiments.

Heterodont dentition development

The shapes of all minipig tooth anlagen showed a similar appearance at early stages of development. Differences became obvious at the beginning of the late bell stage when characteristic shaping of the inner enamel epithelium occurred. The premolar (a multicuspid tooth type) displayed a complex inner enamel epithelium shape compared with the incisor and canine that had a simple conical shape. The canine reached the early bell stage at E41 and dentin production was visible at E50, whereas the fourth premolar reached the early bell stage at E35, but dentin production was not first visible until E56. Similar observations were reported for the albino ferret (*Mustela putorius*) where the enamel organ was observed in the canine and the fourth premolar at E30, and dentin production was first seen in the canine at E35 and in the fourth premolar at E40 (23). This result suggests that a complex tooth needs longer to achieve its final shape before dentin production commences. Even in the mouse, where the gestational period for tooth development is very brief, individual tooth types maintain different temporal trajectories. For example, incisors reach the bell stage by E17 and the predentine production is obvious at E18, while the first molar achieves the bell stage at E17.5 and predentine secretion is apparent at E19 (24). This temporal difference in tooth-type morphogenesis is consistent among mouse, ferret, and pig when compared with the length of the entire gestational period. One possible explanation is that the longer developmental period is necessary in the multicuspid teeth to increase the number of inner enamel cells and re-organize cells sufficiently to form folds on epithelial–mesenchymal junctions. This formation is followed by cusp morphogenesis accompanied by odontoblast differentiation in specific temporal and special patterns (25). Because the simple conical shape of incisors and canine teeth corresponds to the embryonic shape of the tooth anlage, the re-arrangement of inner enamel cells is not necessary and histodifferentiation of odontoblasts can occur in a shorter period of time.

There is a wide distance separating the earliest initiated teeth in heterodont dentition (Fig. 7). This may reflect an independent morphogenetic potential of the specific tooth types in normodont dentition, similar to the mouse. In the minipig, deciduous incisors and canines (rostral field) differentiate anteriorly in the mandibular corpus to the caudally positioned presumptive fourth deciduous premolar (caudal field), which differentiates at the same time. While incisors trigger in the caudal direction, premolars are initiated in the rostral direction (Fig. 7). The space between both fields is formed by the dental lamina. Similar observations of premolar rostral initiation, with p1 developing last, were observed also in other Eutherians (17). This direction of prenatal development underlying subsequent initiation of more rostral premo-

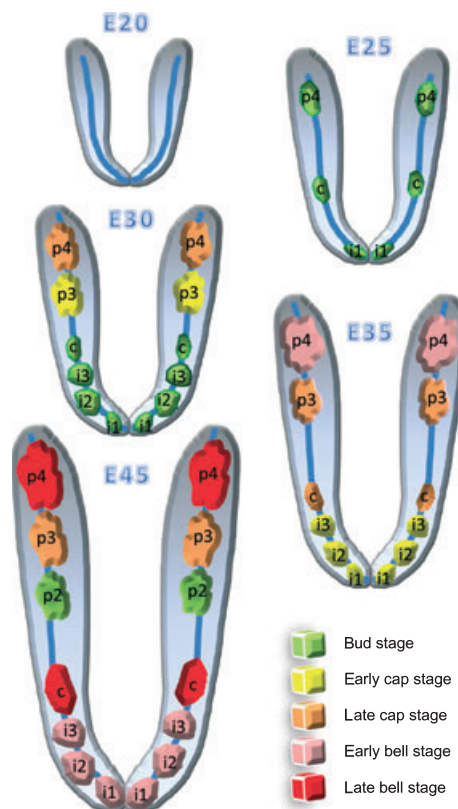


Fig. 7. Schematic drawing of initiation and early development of the individual teeth anlagen in minipig embryos. E, embryonic day.

lars probably played a major role in the reduction and loss of rostral premolars during therian phylogeny (17).

Dental lamina is continuous along the jaw in normodont dentition

In the mouse, the oral epithelium thickens in the anterior and posterior areas of the jaw to form incisiform and molariform dental laminae separated by a diastema (26). The computerized 3D reconstruction revealed additional small thickenings in the diastema area that may represent remnants of additional canines and premolars lost during evolution (27, 28). Discontinuity of the dental lamina in the diphyodont dentition was previously described also in human embryos (29) where the presence of two thickenings of dental epithelia, based on 3D reconstructions, was reported. These investigators observed a gap between both laminae that probably arose as a secondary effect reflecting the dual origin of the upper jaw derived from the frontonasal mass and maxillary prominence. To avoid the effect of fusion from two different prominences, we prepared 3D reconstructions of the mandible that arises uniformly from the first pharyngeal arch. We focused on answering the question of whether the incisor and molar placodes arise separately as in the mouse, or from a continuous epithelial lamina. Computerized 3D reconstruction of normodont dentition in the minipig revealed a continuous dental lamina along the jaw at

the early stage of tooth development (E25). There was no interruption of the lamina in the rostral half of the mandible in the area of the presumptive canine similar to the human condition.

Initiation of replacement lamina

Primary teeth are initiated at the tip of the dental lamina, and the second generation grows from the successional lamina. Successional teeth form at the lingual aspect of the primary teeth budding from the dental lamina. However, the mechanism of tooth replacement related to re-organization of the outer epithelium of the primary tooth germ to form a cervical extension of dental lamina remains unclear (30). The minipig model may contribute to understanding these developmental processes. The lamina of the diphyodont dentition initially invades into the mesenchyme before successional dentition morphogenesis commences, in contrast to the monophyodont mouse where teeth develop in close proximity to the oral epithelium (31). However, the minipig deciduous teeth are also positioned close to the surface during early development (up to E45) subsequently becoming embedded more deeply into the mesenchyme as teeth anlagen enter the late bell stage (E50). This observation was unexpected because it occurred simultaneously with the initiation of dental lamina disruption and, moreover, detachment from the oral epithelium is distinguishable. The tip of successional dental lamina elongates at this late bell stage as the deciduous dentition emerges.

The timing of initiation differs in premolar and canine successional teeth. The dental lamina of the ferret is disconnected from the deciduous premolar anlagen before the permanent teeth begin to develop (20), while the deciduous canine anlagen is still attached to the lamina. We observed the disconnection of dental lamina from tooth anlagen before the replacement dentition was initiated in canine, as well as in premolar, areas. For the ferret, it was suggested that temporal differences in the initiation of successional teeth can result in differences in the progression of replacement (20) based on shrew data, where early development of the permanent dentition leads to the inhibition of deciduous tooth development (32). Previously published observations are consistent with the fact that in the pig, a very early, even prenatal, eruption of canines occurs. Therefore, impeding the development of canine permanent teeth is required to ensure rapid replacement of the deciduous tooth germ. In contrast to pig, the ferret canine erupts 2 wk after birth.

Proliferation during diphyodont dentition development

In the mouse (33, 34) as well as in the pig, proliferating cells are dispersed diffusely throughout the dental epithelium and dental mesenchyme at the initiation stage of tooth development. The tip of the dental epithelium adjacent to the mesenchyme contains proliferating cells at E13.5 in the mouse similar to the early developmental

stage of the minipig dentition. The enamel knot encloses PCNA-negative cells from the cup through the bell stages corresponding to the situation in the mouse and vole (33, 35).

While the early development and morphogenesis are remarkably similar in the mouse and pig, the later phases of odontogenesis undertake divergent developmental pathways. Whereas the mouse has a short dental stalk where apoptosis is present from early stages (E15) (35), there are numerous proliferating cells present in the minipig throughout all developmental periods, as determined in this study. This finding is in agreement with morphological differences and timing, where the pig dental lamina requires a prolonged growing capacity, ensuring penetration into the mesenchyme at a proper depth.

At E30, differences in the dental lamina depth became apparent in minipig. The interdental lamina was shorter in length and lagged in development. Analysis of PCNA staining demonstrated that cellular proliferation starts to decrease in the interdental area, in contrast to the pattern in python embryos, where proliferation remains consistent throughout the length of the mandible (36). This observation suggests that differentiation of the dentition is associated with regional variation of cellular proliferation in the dental lamina. This idea is further supported by the observation that tooth anlagen project unequally into the dental lamina and achieve different depths in minipigs, in contrast to the python where the dental lamina invaginates consistently into the mesenchyme as a sheet (37). Similarly to the snake, there was an asymmetrical growth of the dental lamina into the mesenchyme, the mandibular lamina was growing in the lingual direction, and the distribution of proliferating cells in the epithelium was asymmetrical, supporting the inclined lamina growth.

Appearance of epithelial rests and their function during odontogenesis

The dental lamina begins to disintegrate when the primary tooth germ achieves the late bell stage. During the process of lamina degradation, some of its cells disappear, while others remain in small islands known as the rests of Serres or epithelial pearls. As odontogenesis continues, the epithelial cell remnants arise from two different sources, including the dental lamina and the outer enamel epithelium. Epithelial rests are of clinical interest in humans because these cellular masses can give rise to cysts or ameloblastomas (38–40).

In the minipig embryos, the presence of the epithelial pearls occurred in the deeper portions of the lamina in the area between tooth anlagen and oral epithelium. This finding contrasts with that of rat where the pearls are situated in the central area of the short dental stalk connecting the tooth anlagen to the oral epithelium. They form in close proximity or within the oral epithelium of the rat (41). We suggest that this difference may relate to the length of the lamina in the rat, which is shorter than that of the diphyodont pig. How pearls development is initiated and why they arise remains

unknown. Owing to the clinical significance of epithelial rests, it will be necessary to provide a detailed analysis of their fate from the initial development up to their contribution to pathological structure formation. The minipig may provide an important experimental model for answering these questions.

Acknowledgements – We would like to thank to Dušan Usvald for help with the collection of pig embryos and Katarina Marečková and Zdenka Matoušová for their valuable technical assistance. This research was supported by GACR (grant 304/08/P289). The laboratory is funded by IRP IPAG No. AVOZ 5045015.

References

- MILLIKAN LE, BOYLON JL, HOOK RR, MANNING PJ. Melanoma in Sinclair swine: a new animal model. *J Invest Dermatol* 1974; **62**: 20–30.
- LARSEN MO, ROLIN B. Use of the Gottingen minipig as a model of diabetes, with special focus on type 1 diabetes research. *ILAR J* 2004; **45**: 303–313.
- HORAK V, FORTYN K, HRUBAN V, KLAUDY J. Hereditary melanoblastoma in miniature pigs and its successful therapy by devitalization technique. *Cell Mol Biol (Noisy-le-grand)* 1999; **45**: 1119–1129.
- SHAN Z, LI J, ZHENG C, LIU X, FAN Z, ZHANG C, GOLDSMITH CM, WELLNER RB, BAUM BJ, WANG S. Increased fluid secretion after adenoviral-mediated transfer of the human aquaporin-1 cDNA to irradiated miniature pig parotid glands. *Mol Ther* 2005; **11**: 444–451.
- WANG S, LIU Y, FANG D, SHI S. The miniature pig: a useful large animal model for dental and orofacial research. *Oral Dis* 2007; **13**: 530–537.
- BERMEJO A, GONZALEZ O, GONZALEZ JM. The pig as an animal model for experimentation on the temporomandibular articular complex. *Oral Surg Oral Med Oral Pathol* 1993; **75**: 18–23.
- SCHULTZE-MOSGAU S, SCHLIEPHAKE H, RADESPIEL-TROGER M, NEUKAM FW. Osseointegration of endodontic endosseous cones: zirconium oxide vs. titanium. *Oral Surg Oral Med Oral Pathol Radiol Endod* 2000; **89**: 91–98.
- BUCHTER A, WIECHMANN D, KOERDT S, WIESMANN HP, PIFFKO J, MEYER U. Load-related implant reaction of mini-implants used for orthodontic anchorage. *Clin Oral Implants Res* 2005; **16**: 473–479.
- ZHENG Y, LIU Y, ZHANG CM, ZHANG HY, LI WH, SHI S, LE AD, WANG SL. Stem cells from deciduous tooth repair mandibular defect in swine. *J Dent Res* 2009; **88**: 249–254.
- BIVIN WS, MCCLURE RC. Deciduous tooth chronology in the mandible of the domestic pig. *J Dent Res* 1976; **55**: 591–597.
- WEAVER ME, JUMP EB, MCKEAN CF. The eruption pattern of permanent teeth in miniature swine. *Arch Oral Biol* 1969; **14**: 323–331.
- TUCKER AL, WIDOWSKI TM. Normal profiles for deciduous dental eruption in domestic piglets: effect of sow, litter, and piglet characteristics. *J Anim Sci* 2009; **87**: 2274–2281.
- THESLEFF I, VAAHTOKARI A, KETTUNEN P, ABERG T. Epithelial-mesenchymal signaling during tooth development. *Connect Tissue Res* 1995; **32**: 9–15.
- THESLEFF I, VAAHTOKARI A, VAINIO S, JOWETT A. Molecular mechanisms of cell and tissue interactions during early tooth development. *Anat Rec* 1996; **245**: 151–161.
- THESLEFF I. The genetic basis of tooth development and dental defects. *Am J Med Genet* 2006; **140**: 2530–2535.
- TUCKER A, SHARPE P. The cutting-edge of mammalian development; how the embryo makes teeth. *Nat Rev Genet* 2004; **5**: 499–508.
- LUCKETT WP. Ontogenetic staging of the mammalian dentition, and its value for assessment of homology and heterochrony. *J Mamm Evol* 1993; **1**: 269–282.
- FLEISCHMANNOVA J, MATALOVA E, TUCKER AS, SHARPE PT. Mouse models of tooth abnormalities. *Eur J Oral Sci* 2008; **116**: 1–10.
- VIRIOT L, PETERKOVA R, VONESCH JL, PETERKA M, RUCH JV, LESOT H. Mouse molar morphogenesis revisited by three-dimensional reconstruction. III. Spatial distribution of mitoses and apoptoses up to bell-staged first lower molar teeth. *Int J Dev Biol* 1997; **41**: 679–690.
- JARVINEN E, TUMMERS M, THESLEFF I. The role of the dental lamina in mammalian tooth replacement. *J Exp Zool B Mol Dev Evol* 2009; **312B**: 281–291.
- LUCKETT WP, MAIER W. Development of deciduous and permanent dentition in Tarsius and its phylogenetic significance. *Folia Primatol (Basel)* 1982; **37**: 1–36.
- SACK WO. *Pig anatomy and atlas*. New York: Veterinary textbooks Ithaca, 1982.
- BERKOVITZ BK. Tooth development in the albino ferret (*Mustela putorius*) with special reference to the permanent carnassial. *Arch Oral Biol* 1973; **18**: 465–471.
- DEPEW M, TUCKER A, SHARPE PT. Craniofacial development. In: ROSSANT J, TAM PPL, ed. *Mouse development*. London: Academic Press, 2002; 421–499.
- LISI S, PETERKOVA R, PETERKA M, VONESCH J, RUCH JV, LESOT H. Tooth morphogenesis and pattern of odontoblast differentiation. *Connect Tissue Res* 2003; **44**(Suppl 1): 167–170.
- HAY MF. The development *in vivo* and *in vitro* of the lower incisor and molars of the mouse. *Arch Oral Biol* 1961; **3**: 86–109.
- LESOT H, PETERKOVA R, VIRIOT L, VONESCH JL, TURECKOVA J, PETERKA M, RUCH JV. Early stages of tooth morphogenesis in mouse analyzed by 3D reconstructions. *Eur J Oral Sci* 1998; **106**(Suppl 1): 64–70.
- PETERKOVA R, PETERKA M, VONESCH JL, RUCH JV. Contribution of 3-D computer-assisted reconstructions to the study of the initial steps of mouse odontogenesis. *Int J Dev Biol* 1995; **39**: 239–247.
- HOVORAKOVA M, LESOT H, PETERKOVA R, PETERKA M. Origin of the deciduous upper lateral incisor and its clinical aspects. *J Dent Res* 2006; **85**: 167–171.
- COBOURNE MT, SHARPE PT. Making up the numbers: the molecular control of mammalian dental formula. *Semin Cell Dev Biol* 2010; **21**: 314–324.
- PETERKOVA R, LESOT H, VONESCH JL, PETERKA M, RUCH JV. Mouse molar morphogenesis revisited by three dimensional reconstruction. I. Analysis of initial stages of the first upper molar development revealed two transient buds. *Int J Dev Biol* 1996; **40**: 1009–1016.
- JARVINEN E, VALIMAKI K, PUMMILA M, THESLEFF I, JERNVALL J. The taming of the shrew milk teeth. *Evol Dev* 2008; **10**: 477–486.
- SHIGEMURA N, KIYOSHIMA T, KOBAYASHI I, MATSUO K, YAMAZA H, AKAMINE A, SAKAI H. The distribution of BrdU- and TUNEL-positive cells during odontogenesis in mouse lower first molars. *Histochem J* 1999; **31**: 367–377.
- LESOT H, VONESCH JL, PETERKA M, TURECKOVA J, PETERKOVA R, RUCH JV. Mouse molar morphogenesis revisited by three-dimensional reconstruction. II. Spatial distribution of mitoses and apoptosis in cap to bell staged first and second upper molar teeth. *Int J Dev Biol* 1996; **40**: 1017–1031.
- SETKOVA J, LESOT H, MATALOVA E, WITTER K, MATULOVA P, MISEK I. Proliferation and apoptosis in early molar morphogenesis – voles as models in odontogenesis. *Int J Dev Biol* 2006; **50**: 481–489.
- BUCHTOVA M, BOUGHNER JC, FU K, DIEWERT VM, RICHMAN JM. Embryonic development of Python sebae – II: Craniofacial microscopic anatomy, cell proliferation and apoptosis. *Zoology (Jena)* 2007; **110**: 231–251.
- BUCHTOVA M, HANDRIGAN GR, TUCKER AS, LOZANOFF S, TOWN L, FU K, DIEWERT VM, WICKING C, RICHMAN JM. Initiation and patterning of the snake dentition are dependent on Sonic hedgehog signaling. *Dev Biol* 2008; **319**: 132–145.
- BUCHNER A, SCIUBBA JJ. Peripheral epithelial odontogenic tumors: a review. *Oral Surg Oral Med Oral Pathol* 1987; **63**: 688–697.

39. HAMAMOTO Y, HAMAMOTO N, NAKAJIMA T, OZAWA H. Morphological changes of epithelial rests of Malassez in rat molars induced by local administration of N-methylnitrosourea. *Arch Oral Biol* 1998; **43**: 899–906.
40. EVERSOLE LR. Malignant epithelial odontogenic tumors. *Semin Diagn Pathol* 1999; **16**: 317–324.
41. KHAEJORN BUT J, WILSON DJ, OWENS PD. The development and fate of the dental lamina of the mandibular first molar tooth in the rat. *J Anat* 1991; **179**: 85–96.

Supporting Information

Additional Supporting Information may be found in the online version of this article:

Table S1. The initiation of deciduous tooth anlagen in early prenatal period.

Fig. S1. Deciduous dentition of the pig in the lower jaw.

Fig. S2. Odontogenesis in a minipig embryo at E20.

Fig. S3. Odontogenesis in a minipig embryo at E50.

Fig. S4. Odontogenesis in a minipig embryo at E56.

Fig. S5. Odontogenesis in a minipig embryo at E67.

Fig. S6. Distribution of proliferating cells during odontogenesis.

Fig. S7. Temporo-spatial analysis of cell proliferation during odontogenesis.

Please note: Wiley-Blackwell is not responsible for the content or functionality of any supporting materials supplied by the authors. Any queries (other than missing material) should be directed to the corresponding author for the article.

Komentář k přiložené publikaci č. 2

BUCHTOVA, M., J. STEMIREK, K. GLOCOVA, E. MATALOVA a A. S. TUCKER. Early Regression of the Dental Lamina Underlies the Development of Diphyodont Dentitions. *Journal of Dental Research* [online]. 2012, 91(5), 491–498. ISSN 0022-0345. Dostupné z: doi:[10.1177/0022034512442896](https://doi.org/10.1177/0022034512442896)

IF = 3,826; kvartil Q1

Vzhledem k tomu, že rozpad dentální lišty může být v průběhu vývoje zubů jedním z klíčových mechanismů, které brání ve vývoji další generace zubů, zaměřili jsme se v této studii provedené na prasečím modelu na mechanismy zodpovědné za rozpad zubní lišty. Mezi tyto mechanismy, které se mohou vzájemně kombinovat, může patřit i migrace buněk, přeměna jedné zárodečné tkáně na jinou (tzv. epiteliálně-mezenchymální transformace) a/nebo apoptóza. Pro rozpad zubní lišty je charakteristická ztráta bazální membrány, která epitelové buňky „drží“ pohromadě. Dochází k tomu právě díky procesu epiteliálně-mezenchymální transformace, kdy dojde k oddělení buněk od ostatních a k jejich následné migraci. Pro tyto buňky je typická ztráta epitelových markerů, jako jsou E-cadherin zodpovědný za buněčné spoje nebo cytokeratin, tvořící cytoskelet epitelových buněk. Naopak, detekovat lze zvýšení exprese mezenchymových markerů, jako jsou transkripční faktor Slug typický pro mezenchymové buňky, matrix metaloproteináza 2 (MMP2), což je enzym degradující extracelulární matrix a umožňující buňce migraci, nebo vimentin, který tvoří cytoskeletální vlákna (Kang a Svoboda, 2005, Bazina et al., 2022).

V našem experimentu jsme pozorovali v oblasti dentální lišty na začátku odontogeneze relativně výraznou expresi E-cadherinu, která se v pozdějších stádiích, na rozdíl od zbytku ústního epitelu, snižovala. Zároveň docházelo v období degradace zubní lišty ke zvýšení hladiny MMP2, a to hlavně v ostrůvcích lokalizovaných v oblasti rozpadající se zubní lišty. Podobné změny jsme zachytili i u dalšího mezenchymálního faktoru SNAI2. Zajímavostí je, že zánik pomocí apoptózy jsme prokázali pouze u části buněk zubní lišty; část (být menší) se pak seskupovala do malých shluků označovaných jako epiteliální perly, které se zdají být klinicky významné i pro humánní medicínu, protože mohou představovat základ pro vznik patologií v čelistech (Palanisamy et al., 2022).

RESEARCH REPORTS

Biological

M. Buchtová^{1,3*}, J. Štembírek²,
K. Glocová³, E. Matalová^{1,4},
and A.S. Tucker⁵

¹Institute of Animal Physiology and Genetics, v.v.i., Academy of Sciences of the Czech Republic, Veveří 97, 602 00 Brno, Czech Republic; ²Department of Oral and Maxillofacial Surgery, University Hospital Ostrava, Ostrava, Czech Republic; ³Department of Anatomy, Histology and Embryology, Faculty of Veterinary Medicine, University of Veterinary and Pharmaceutical Sciences, Brno, Czech Republic; ⁴Department of Physiology, Faculty of Veterinary Medicine, University of Veterinary and Pharmaceutical Sciences, Brno, Czech Republic; and ⁵Department of Craniofacial Development and Stem Cell Biology and Department of Orthodontics, King's College London, Dental Institute, London, SE1 9RT, UK; *corresponding author, buchtova@iach.cz

J Dent Res 91(5):491-498, 2012

ABSTRACT

Functional tooth germs in mammals, reptiles, and chondrichthyans are initiated from a dental lamina. The longevity of the lamina plays a role in governing the number of tooth generations. Monophyodont species have no replacement dental lamina, while polyphyodont species have a permanent continuous lamina. In diphyodont species, the dental lamina fragments and regresses after initiation of the second tooth generation. Regression of the lamina seems to be an important mechanism in preventing the further development of replacement teeth. Defects in the complete removal of the lamina lead to cyst formation and has been linked to ameloblastomas. Here, we show the previously unknown mechanisms behind the disappearance of the dental lamina, involving a combination of cell migration, cell-fate transformation, and apoptosis. Lamina regression starts with the loss of the basement membrane, allowing the epithelial cells to break away from the lamina and migrate into the surrounding mesenchyme. Cells deactivate epithelial markers (E-cadherin, cytokeratin), up-regulate Slug and MMP2, and activate mesenchymal markers (vimentin), while residual lamina cells are removed by apoptosis. The uncovering of the processes behind lamina degradation allows us to clarify the evolution of diphyodonty, and provides a mechanism for future manipulation of the number of tooth generations.

KEY WORDS: developmental biology, dental morphology, tooth development, odontogenesis, apoptosis, epithelial-mesenchymal interactions.

DOI: 10.1177/0022034512442896

Received November 25, 2011; Last revision February 2, 2012; Accepted February 27, 2012

A supplemental appendix to this article is published electronically only at <http://jdr.sagepub.com/supplemental>.

© International & American Associations for Dental Research

Early Regression of the Dental Lamina Underlies the Development of Diphyodont Dentitions

INTRODUCTION

The dental lamina (DL) has been described in many different species of vertebrates and starts as an invagination of the epithelium growing deeply into the mesenchyme (Buchtová *et al.*, 2008; Jarvinen *et al.*, 2009; Fraser and Smith, 2011). Teeth bud off from the DL, with replacement teeth originating from the free end of the lamina. There are significant variations in the morphology of the DL during development in monophyodont, diphyodont, and polyphyodont species that relate to their ability to form replacement teeth. However, detailed accounts of the processes are unknown.

The mouse is the main model for the study of odontogenesis, but it forms only one tooth generation. Our knowledge of the processes involved in replacement tooth development is therefore limited. The mouse DL is very short; therefore, the teeth develop at the oral surface, and there is no evidence of a replacement lamina (Fig. 1A). In diphyodont species, such as the pig and ferret, the replacement lamina is evident as the primary dentition reaches the late bell stage, lying lingual to the deciduous tooth (Jarvinen *et al.*, 2009; Stembirek *et al.*, 2010). A second generation of teeth then buds off from this replacement lamina (Fig. 1B). After initiation of this second generation during mid-gestation, the pig lamina, like that of humans, undergoes degradation, preventing the initiation of further tooth generations (Moskow and Bloom, 1983; Stembirek *et al.*, 2010). In humans, incomplete lamina degradation has been linked to the formation of epithelial pearls, which can lead to the development of oral cysts or tumors (Moskow and Bloom, 1983; Eversole, 1999). In contrast to the pig and human, in species with multiple generations of teeth, such as snakes, the lamina persists, linking the developing teeth in a chain, and providing further generations from its leading edge (Fig. 1C) (Buchtová *et al.*, 2008).

Here, we have investigated the mechanisms behind the regression of the lamina in a diphyodont species, the pig. The pig has a dentition very similar to that of humans and therefore represents an excellent model.

There are three possible processes that have been proposed to play a role in loss of epithelial cells during development: apoptosis, migration, and epithelial-mesenchymal transformation (Prindull and Zipori, 2004; Ahlstrom and Erickson, 2009). We therefore proposed that a combination of these processes might be involved in loss of the replacement dental lamina in the pig.

MATERIALS & METHODS

Embryonic Material

Minipig embryos and fetuses (E56 and E67) were obtained from the Liběchov animal facility (Czech Republic, strain LiM). All procedures were conducted following the Guide for the Care and Use of Laboratory Animals and a protocol approved by the Animal Science Committee of the Institute of Animal Physiology and Genetics (Czech Republic).

In situ Staining

Standard protocol was used for immunohistochemical analysis as described previously (Stembirek *et al.*, 2010). Detailed lists of antibodies and protocols are summarized in Appendix Table 1 and Appendix Methods. The apoptotic DNA fragmentation was evaluated by the TUNEL method (ApopTag Peroxidase *In Situ* Apoptosis Detection Kit – S7101, Chemicon, Temecula, CA, USA).

Slice Cultures

Minipig mandibles were removed from 2 different developmental stages – E55 (2 embryos, 7 slices), and E60 (2 embryos, 6 slices) – and bone was dissected from the tissue for easier cutting. Slice cultures were prepared as described for mouse mandibles (Matalova *et al.*, 2005).

Cell Migration

We used a DiI labeling method to track groups of migrating epithelial cells. Using a FemtoJet microinjection system (Eppendorf, Hamburg, Germany), we injected CellTracker™ CM-DiI (Molecular Probes Inc., Eugene, OR, USA) dissolved in dimethyl sulfoxide (DMSO) and diluted in 0.3 M sucrose to a working concentration (0.5 mg/mL) into the dental lamina of the mandible slices.

RESULTS

Breakdown of the Lamina Starts with Disruption of the Basement Membrane

The first morphological sign of regression was visible at E50 (Stembirek *et al.*, 2010). At E56, the regression was obvious in: (a) the superficial part of the DL connecting the lamina to the oral epithelium, and (b) the dental stalk attaching the DL to the deciduous tooth anlagen (Figs. 1D–1F). The timing of regression corresponded with the initiation of the second generation of teeth from the replacement lamina. Later on, morphological changes became apparent in the deeper parts of the DL. The aboral part of the DL contained cells with acidophilic cytoplasm forming circular structures disconnected from the DL at E67 (Figs. 1G–1I), while, on the other side, the cells remained narrow and columnar (Figs. 1E, 1H). During these later stages, clusters of epithelial cells (pearls) were evident close to the oral epithelium (Figs. 1J, 1K) (Stembirek *et al.*, 2010). To follow these initial stages of degeneration, we dissected out the DL before overt signs of disintegration (E55) and used a slice

culture method to take a live frontal section (Fig. 2J). Over just a few days, the DL was seen to thicken, and the initially straight walls of the DL started to undulate and became rough on the aboral side nearest the tooth, mimicking the process shown by histology (Fig. 2M).

To determine the integrity of the basement membrane during lamina fragmentation, we detected the presence of laminin (Figs. 1L, 1M). Epithelial cells facing the oral side of the DL were tightly packed and surrounded by a continuous laminin-positive basement membrane (Fig. 1M). The aboral side of the DL showed no laminin expression. Notably, high levels of laminin expression were associated with the appearance of numerous laminin-positive vessels close to the DL (Fig. 1M), and the size and number of which increased along with lamina fragmentation (Appendix Fig. 1).

Cell Death Is Associated with Loss of Some Cells in the Fragmenting Lamina

Cell death by apoptosis during odontogenesis has been previously described (Kindaichi, 1980; Vaahtokari *et al.*, 1996; Sasaki *et al.*, 2001). Since the number of cells that make up the lamina appeared to reduce between E56 and E67, we analyzed apoptosis during minipig DL regression. TUNEL-positive cells were rarely located in the DL at early stages (Fig. 2A), but were concentrated in the enamel knot (Figs. 2D, 2E, 2G), as in the mouse. Only a few dispersed positive cells were in the dental papilla and surrounding mesenchyme (Fig. 2G). As the DL started to disintegrate, TUNEL-positive cells and apoptotic bodies were observed at the edges of the lamina, where the most fragmentation was visible (Figs. 2B, 2C, 2H, 2I), and in the dental stalk of the first tooth (Figs. 2D, 2F). The main body of the lamina, however, remained largely TUNEL-negative, with no evident increase in apoptosis on the aboral vs. the oral side (Figs. 2B, 2H).

Epithelial Cells Move Out of the Lamina

To test the possibility that the epithelial cells were moving out of the lamina, we labeled the epithelial cells by injection of DiI in the cultured slices of DL at E55 (before overt DL fragmentation) (Figs. 2J–2R). At this stage, DL cells appeared to have high migratory potential. After 2 days of incubation, the shape of the DL was modified, and protrusion of cell clusters was apparent (Figs. 2J, 2M). Some cells appeared to spread into the adjacent mesenchyme (Figs. 2N, 2O), this movement being more pronounced after 4 days (Figs. 2Q, 2R), when the DL was still evident but much reduced in size (Fig. 2P). Simultaneously, the lamina was also labeled at E60 (once degradation had started), but at this stage less movement from the site of injection was observed (Appendix Fig. 2), and the DL was no longer evident after 4 days in culture (Appendix Fig. 2G).

Epithelial Cells Transform to Mesenchymal during Lamina Regression

Epithelial-mesenchymal transformation (EMT) occurs during normal prenatal development as well as in tumor metastasis and wound healing (Jin and Ding, 2006; Baum *et al.*, 2008). Having

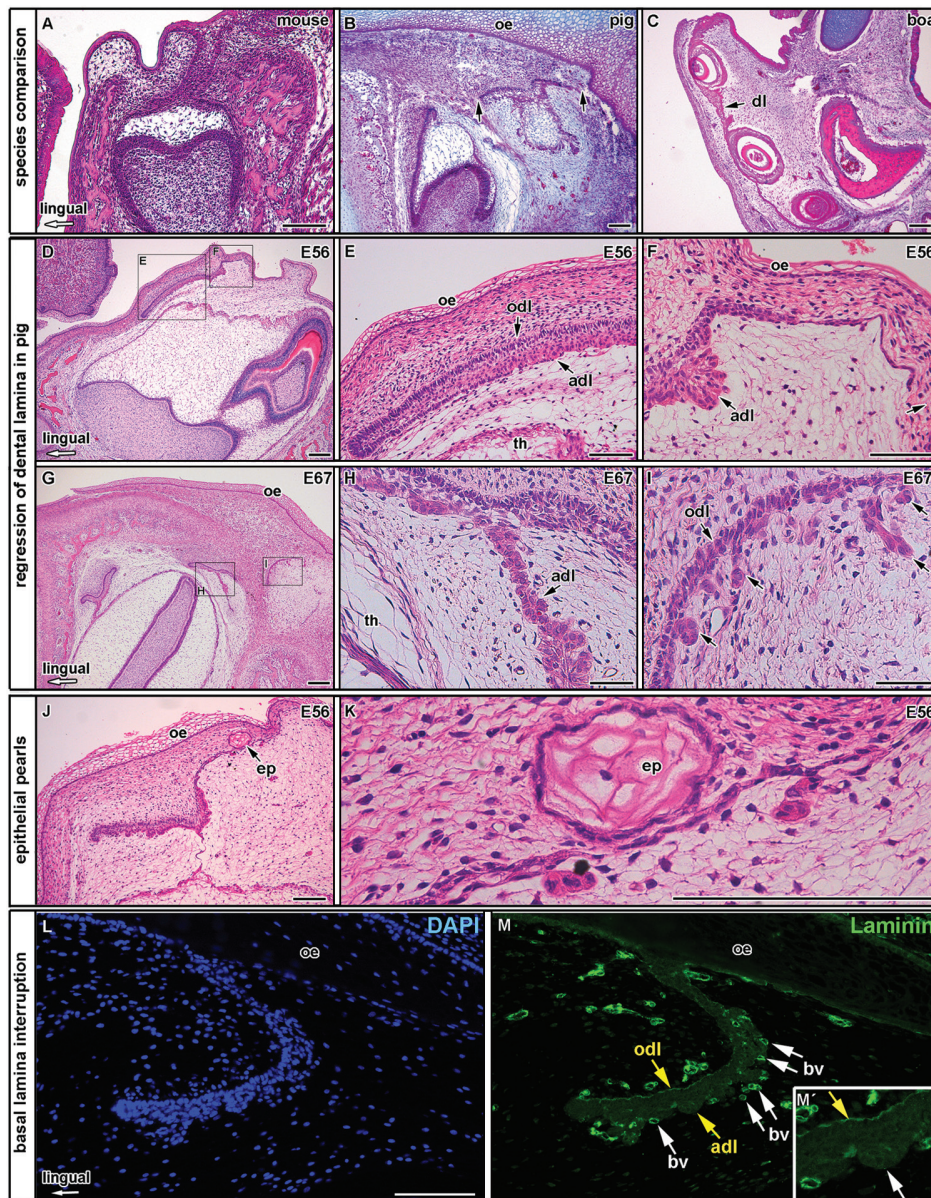


Figure 1. Dental lamina morphology and regression are connected with the disruption of the basement membrane. (A-C) Species comparison of dental lamina morphology. (A-K) Hematoxylin-eosin staining. (A) Monophyodont mouse with a stalk-like lamina connecting the tooth germ to the oral epithelium. (B) Disruption of the dental lamina (arrows) during mid-gestation in the diphyodont pig. (C) Long lamina (arrow) connecting 4 generations of tooth germs in the polyphyodont boa. (D-K) Degradation of the pig dental lamina. (D-F, J, K) The dental lamina at E56. (E, F) High-power views of boxed areas in (D). (E) In the deeper part of the lamina, on the side facing the tooth anlagen, the cells were rounded, while on the other side the cells were narrow and columnar and the tip of the lamina was uniformly columnar. (F) Close to the oral surface, the dental lamina showed signs of regression and was disconnected from the oral epithelium. Cells facing the tooth contained acidophilic cytoplasm and protruded from the lamina (arrow). (G-I) The dental lamina at E67 was fragmented into several pieces. (H, I) High-power views of boxed areas in (G). (H) Clear differences were observed in cell morphology between the oral and aboral sides of the lamina. The mesenchyme on either side of the lamina showed similar differences in morphology, being more closely packed on the oral side. (I) Close to the oral surface, the lamina was thinner, with cell cluster formation on the tooth side. Some acidophilic cells were localized out of the lamina (arrow). (J) Epithelial pearls are situated next to the lamina, close to the oral epithelium, by E56. (K) High-power view of pearl shown in (J), showing similarities to palatal epithelial pearls formed during loss of the midline seam. (L-M) Basement membrane confluence was analyzed in the minipig dentition using lamina at E67. (L) Background stained by DAPI (blue nuclei). (M, M', detail) Laminin was labeled by FITC (in green). Oral side of the dental lamina displayed a continuous basement membrane, while the aboral side was disrupted. Small blood vessels (bv) (white arrows) were attached to the aboral side of the dental lamina. dl – dental lamina, ep – epithelial pearls, oe – oral epithelium, th – tooth, odl – oral side of dental epithelium, adl – aboral side of dental lamina. Scale bar = 100 μ m.

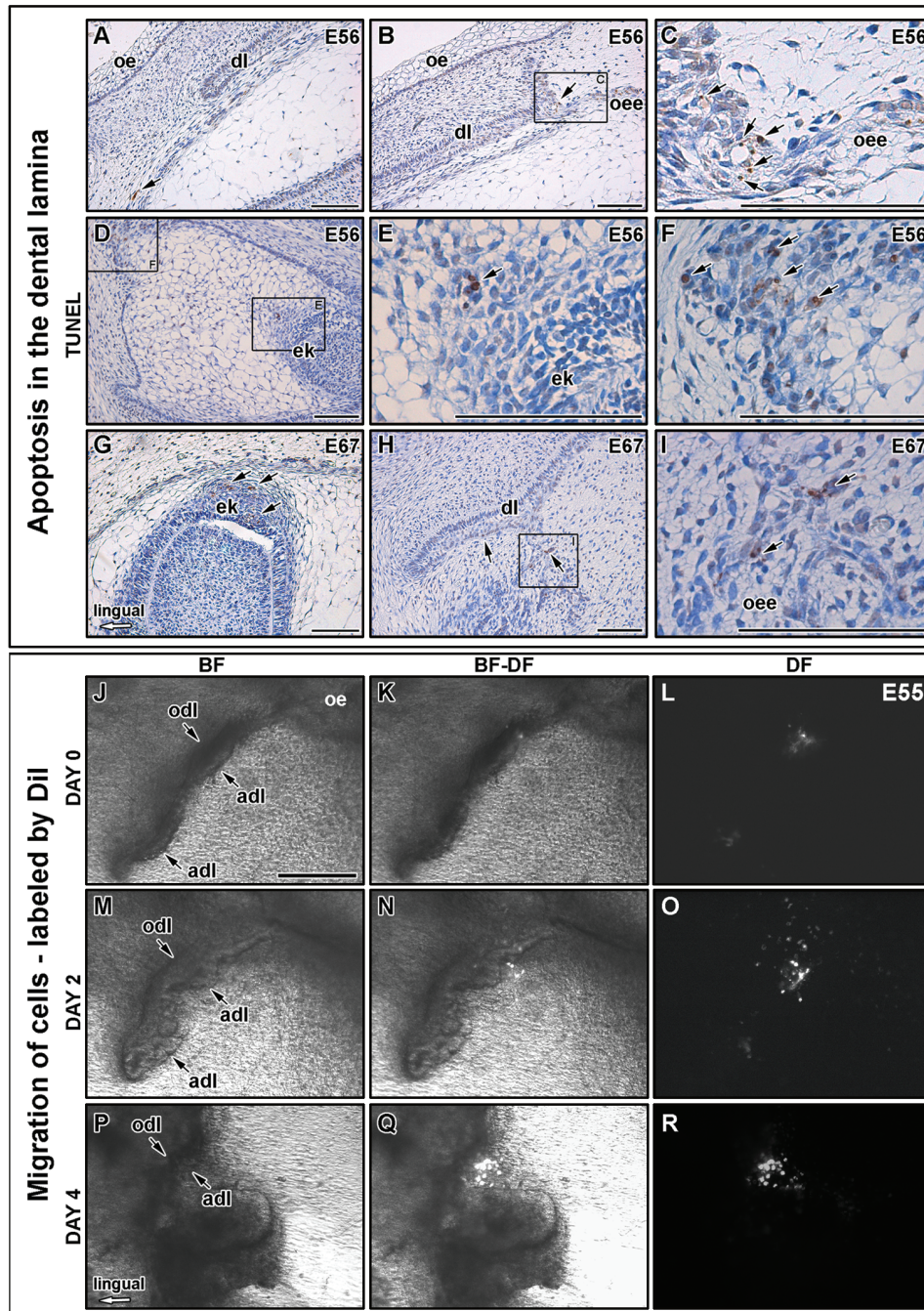


Figure 2. Apoptosis and cell migration of epithelial cells during dental lamina regression. (A-I) Apoptotic cells (dark brown) were labeled by TUNEL assay. Slides were counterstained with hematoxylin to contrast negative cells in blue. (A-F) E56. (G-I) E67. (A,B) Very few dispersed TUNEL-positive cells were associated with the main body of the dental lamina at E56. (C) High-power view of boxed area in (B). Positive cells were located in areas of lamina fragmentation near and in the outer enamel epithelium (oee). (D) Positive cells were associated with the enamel knot, highlighted in (E), and dental stalk, highlighted in (F). (G) Apoptosis was still evident in the enamel knot at E67 (positive cells arrowed). (H) A few positive cells were observed in the main body of the lamina (arrow), but the majority were found in the thin dental stalk close to the outer enamel epithelium, where the lamina had already degraded. (I) Boxed area in (H) highlighting positive cells (arrow). (J-R) Dil labeling of dental lamina cells at stage E55. (J,M,P) Slice cultures of minipig embryos in bright field (BF), (L,O,R) dark field (DF), and (K,N,Q) both fields merged. (J,K,L) Label just after injection (day 0) showed a small fluorescent spot in the dental lamina at E55. (M,N,O) Label after 2 days of incubation. (M) The initially straight outline of the lamina started to undulate and protruded into mesenchyme on the side facing the tooth germ. (N,O) Dil shows cells spread out of the lamina. (P,Q,R) Label after 4 days of incubation. (P) The outline of the lamina is less defined. (Q,R) Dil shows cells spread out at a distance from the lamina. adl – aboral side of dental lamina, dl – dental lamina, ek – enamel knot, odl – oral side of dental lamina, oe – oral epithelium, oee – outer enamel epithelium. Arrows show positive cells. Scale bar = 100 µm.

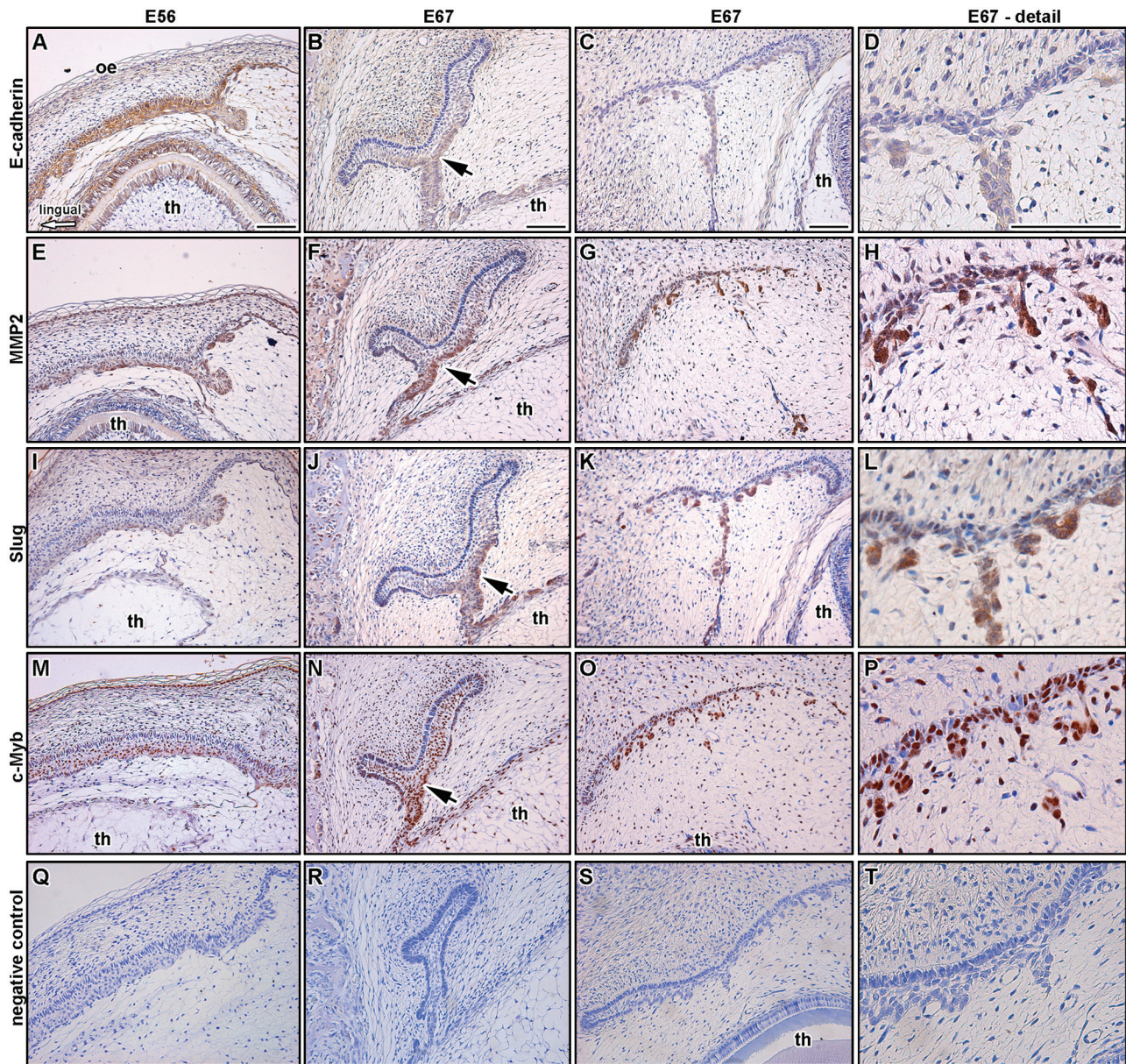


Figure 3. Detection of markers of an epithelial-mesenchymal transformation (EMT). (A-D) Expression of E-cadherin. (A) E-cadherin showed strong expression at the early stage of dental lamina degradation (E56). (B,C,D) As the lamina regressed, expression of E-cadherin was reduced (arrow) (E67). (E-H) Expression of matrix metalloproteinase 2 (MMP2). (E) MMP2 expression was detected at high levels on the side of the lamina facing the tooth germ at E56. (F,G,H) As the lamina regressed, expression increased (E67) (arrow). (H) Clusters of cells disconnected from the lamina appeared strongly positive for MMP2. (I-L) Expression of Slug. (I) Only a few Slug-positive cells were found at E56. (J,K,L) At E67, elevated Slug expression was visible on the oral side of the lamina (arrow). (M-P) Expression of c-Myb. Asymmetrical c-Myb expression overlapped with Slug-positive cells at E56 (M) and E67 (N,O,P) (arrow). (Q-T) Alternative sections were used as a negative control by omission of the primary antibody. Immunohistochemical reactions were visualized with diaminobenzidine (brown cells). Slides were counterstained with hematoxylin to contrast negative cells in blue. th – tooth, oe – oral epithelium. Scale bar = 100 μ m.

shown that DL cells appeared to move out, we looked for signs of EMT. The key EMT proteins reported in the palate and neural crest were analyzed: (1) loss of cell-cell attachment (E-cadherin), (2) degradation of the extracellular matrix (MMP2), (3) down-regulation of cell-cell adhesion and activation of mesenchymal

differentiation (Slug), and (4) initiation of a mesenchymal fate (vimentin). We observed strong expression of E-cadherin in the dental and oral epithelium at early stages of odontogenesis (Fig. 3A). At later stages of regression, the presence of E-cadherin was decreased uniformly in the DL, while remaining

high in the rest of the oral epithelium (Figs. 3B-3D and data not shown). In the lamina, high levels of MMP2 were observed only on the DL side facing the tooth anlagen at E56 (Fig. 3E). The elevation of MMP2 expression continued throughout DL degradation, particularly in the islets of cells around the degrading lamina (Figs. 3F-3H). Prior to overt degradation of the DL, we observed only a few Slug-positive cells at E56 (Figs. 3I-3L) situated on the side facing the tooth and corresponding to the acidophilic cells (Figs. 3K, 3L). The number of Slug-positive cells increased with age and disintegration level, associated with small islets away from the lamina (Fig. 3L). c-Myb was previously observed during the formation and migration of neural crest cells (Karafiat *et al.*, 2005). During DL development, the area of c-Myb-positive cells overlapped with MMP2 and Slug positivity (Figs. 3M-3P).

Changes in expression of E-cadherin, MMP2, Slug, and c-Myb appeared to point to EMT (Appendix Table 2). Further, we performed double staining for epithelial (cytokeratin) and mesenchymal (vimentin) cytoskeletal proteins during lamina disintegration (Fig. 4). Both were reported in cultured cells during induced EMT (Boyer *et al.*, 1989). In our sections, we saw strong expression of cytokeratin in the DL cells and weak expression in a few cells already disconnected from the body of the lamina (Figs. 4B, 4C, 4E). A few cells at the edge of DL, at the site of lamina disintegration, were shown to be positive for cytokeratin and vimentin (Figs. 4D, 4F). Interestingly, only cells on the aboral side of the lamina, in the migration direction observed by DiI, were positive for both cytokeratin and vimentin.

DISCUSSION

The present study was designed to uncover the developmental processes acting during DL regression in a diphyodont mammal. As the lamina degenerated, lamina cells facing the tooth enlarged, became rounded, contained acidophilic cytoplasm, and formed circular structures disconnected from the lamina. Similar to the pig lamina cells, an acidophilic appearance, cellular hypertrophy, and changes in cell polarization and shape have previously been described in cardiac endothelial cells during EMT (Boyer *et al.*, 1999) and during wound healing in the palatal mucosa (Fejerskov, 1972).

The breakdown of the basement membrane resulted in a movement of cells out of the lamina, as shown by our DiI labeling experiments, and seems to be the main mechanism involved in the epithelial cell mass reduction during lamina degradation. The laminin expression highlighted numerous small blood vessels around this side of the lamina. Notably, the first signs of lamina degradation correlated with the appearance of these blood vessels. The close temporal and spatial relationship between the initiation of angiogenesis in the adjacent mesenchyme and degradation of DL indicates that such vessels may play a role in loss of the lamina. One possibility is that the blood vessels might stimulate transformation of DL cells. A regulatory loop between angiogenesis and EMT has previously been described during carcinogenesis (Thiery *et al.*, 2009).

Importantly, not all of the lamina undergoes degradation in a diphyodont species at the same time and speed during prenatal

development, since part of the lamina is required for production of the next generation of teeth. In the middle of gestation, a set of proliferating cells is therefore found at the tip of the extending lamina, where the second generation of teeth buds, while the superficial part of lamina close to the oral epithelium already exhibits signs of degradation (Stembirek *et al.*, 2010). What protects this deep part of the lamina from degradation is a challenging problem that we intend to investigate in the future.

Some apoptotic cells were observed in the disintegrating lamina, but these were found mostly at sites connecting the lamina with the outer enamel epithelium, where only remnants of the lamina were located, rather than in the main body of the lamina. In human dentition, TUNEL-positive cells were also rare in the DL (Hatakeyama *et al.*, 2000). This indicates that cell death may play a role in clearing up those cells that failed to migrate away, rather than driving the loss of the lamina.

The epithelial lamina cells adjacent to the tooth start to move out of the lamina, triggered by loss of the basement membrane on this side, with down-regulation of E-cadherin and up-regulation of Slug, c-Myb, and MMP2. Once the cells have broken out of the lamina, they appear to activate the production of the mesenchymal cytoskeletal filament vimentin and deactivate epithelial cytokeratin, indicating EMT (Boyer *et al.*, 1989). Vimentin also regulates the induction of migration associated with EMT *via* up-regulation of Slug (Ivaska, 2011). A few cells showed localization of both vimentin and cytokeratin in non-overlapping regions of the same cell, indicating cells in the process of transformation. Similar asymmetrical expression was shown in primary mesenchymal cells and carcinoma cells (Franke *et al.*, 1982; Boyer *et al.*, 1989). These dual-positive cells were situated on the aboral part of the lamina, where Slug expression was observed.

The breakdown of the DL shares several similarities with the palatal seam during secondary palate development (compared in Appendix Table 3) and Hertwig's epithelial root sheath (HERS). Apoptosis, EMT, and migration have all been considered responsible for HERS breakdown (Suzuki *et al.*, 2002; Zeichner-David *et al.*, 2003; Huang *et al.*, 2009).

Analysis of our data has shown that regression starts on the side nearest the tooth. This indicates that a signal from the tooth or surrounding mesenchyme next to the lamina may induce the lamina to regress, or that signals from the oral side can prevent DL regression. In the snake, Bmps, Shh, and Wnts have all been implicated as having a role in the development of the permanent DL, with overexpression of Wnt signaling leading to increased elongation of the lamina (Handrigan and Richman, 2010). Overexpression of Wnt signaling in mice leads to multiple teeth developing from the molar placode, although these additional teeth appear to form by budding off from each other, rather than sequentially from a DL (Jarvinen *et al.*, 2006).

In summary, we have shown that, in the pig, loss of the lamina is due to migration of cells away from the lamina and a transformation to mesenchyme, with some loss of cells by apoptosis. The uncovering of further details can help to clarify the evolutionary routes toward mammalian diphyodonty. Understanding how tooth number is controlled is an important step in the modulation of this process. Failure of a second tooth

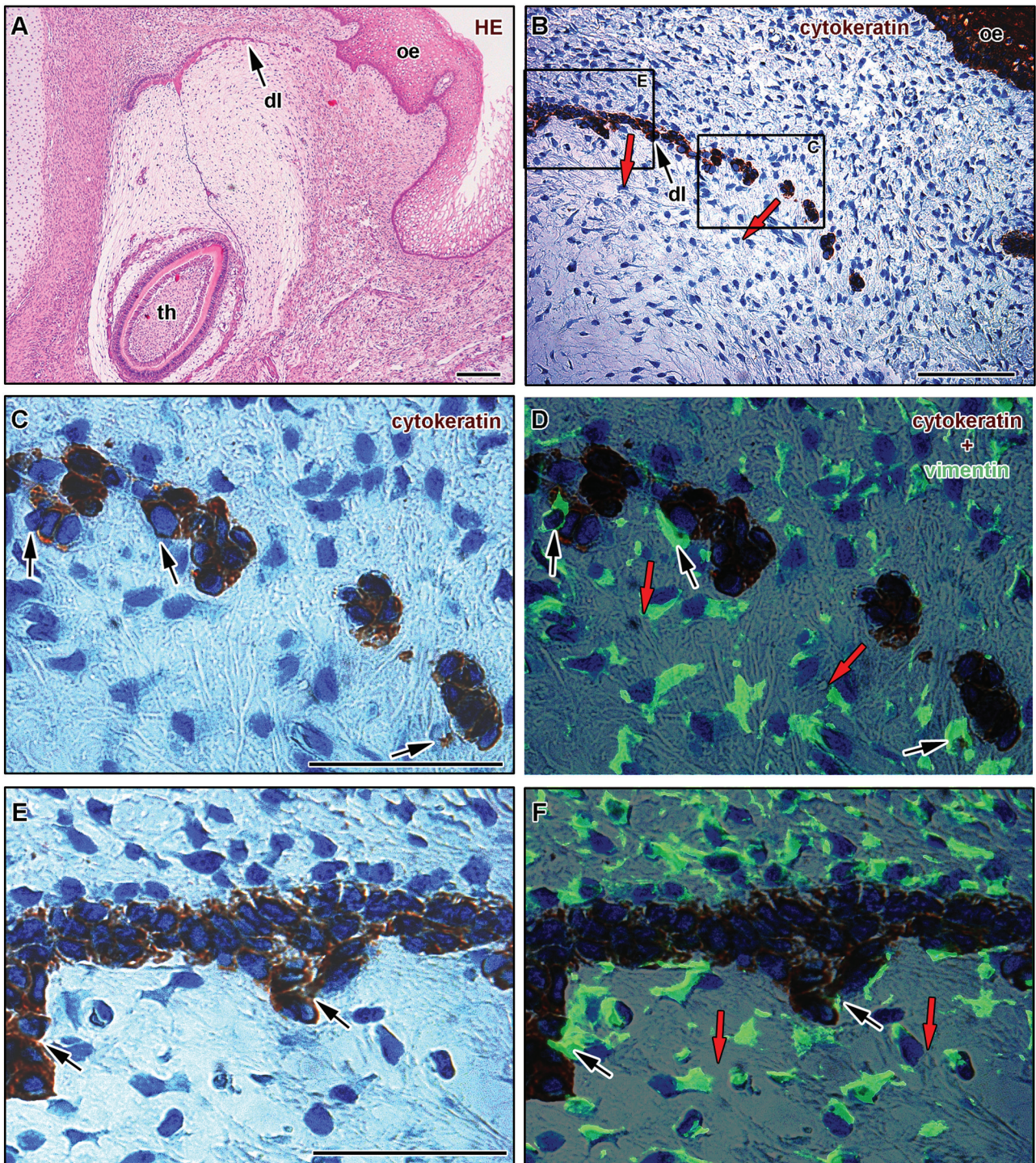


Figure 4. Double staining of cytoskeletal intermediate filaments indicating an EMT. **(A)** The area of the dental lamina that exhibited a high level of regression (arrow) was used for double labeling of filaments. Alternative section stained with hematoxylin-eosin. **(B)** Epithelial cytokeratin was detected in the oral epithelium (oe) and disintegrating dental lamina (dl). Immunohistochemical reactions were visualized with diaminobenzidine (brown cells), and slides were counterstained with hematoxylin to contrast negative cells in blue. **(C,E)** Higher power view of 2 parts of the lamina (as shown boxed in B) stained for cytokeratin. **(D, F)** Mesenchymal vimentin filaments were labeled by FITC (in green) on the same slides, and pictures were overlaid for analysis of the overlap. Cells facing the future direction of migration (red arrows) were found to express both proteins (black arrows). The vimentin staining did not extend throughout the cytoplasm of these dental lamina cells, but appeared in clusters at the cell periphery, while cytokeratin levels were reduced. Scale bar = 100 μ m.

generation to form is a relatively common defect (Matalova *et al.*, 2008). According to our data, one cause of such a defect might be premature lamina degradation. If the signals responsible for degradation of the lamina can be controlled, it might be possible to sustain the DL and generate additional tooth generations to replace lost, missing, or damaged teeth. It is therefore important to address what triggers the DL to regress in diphyodont species, and what prevents its regression in polyphyodont species.

ACKNOWLEDGMENTS

This work was supported by GAASCR (grant KJB601110910). The laboratory runs under IRP IPAG No. AVOZ 5045015. International cooperation between the laboratories in London and Brno was supported by an International Joint grant from the Royal Society (JP080875). The author(s) declare no potential conflicts of interest with respect to the authorship and/or publication of this article.

REFERENCES

- Ahlstrom JD, Erickson CA (2009). The neural crest epithelial-mesenchymal transition in 4D: a 'tail' of multiple non-obligatory cellular mechanisms. *Development* 136:1801-1812.
- Baum B, Settleman J, Quinlan MP (2008). Transitions between epithelial and mesenchymal states in development and disease. *Semin Cell Dev Biol* 19:294-308.
- Boyer AS, Erickson CP, Runyan RB (1999). Epithelial-mesenchymal transformation in the embryonic heart is mediated through distinct pertussis toxin-sensitive and TGFbeta signal transduction mechanisms. *Dev Dyn* 214:81-91.
- Boyer B, Tucker GC, Valles AM, Franke WW, Thiery JP (1989). Rearrangements of desmosomal and cytoskeletal proteins during the transition from epithelial to fibroblastoid organization in cultured rat bladder carcinoma cells. *J Cell Biol* 109(4 Pt 1):1495-1509.
- Buchtová M, Handrigan GR, Tucker AS, Lozanoff S, Town L, Fu K, *et al.* (2008). Initiation and patterning of the snake dentition are dependent on Sonic hedgehog signaling. *Dev Biol* 319:132-145.
- Eversole LR (1999). Malignant epithelial odontogenic tumors. *Semin Diagn Pathol* 16:317-324.
- Fejerskov O (1972). Excision wounds in palatal epithelium in guinea pigs. *Scand J Dent Res* 80:139-154.
- Franke WW, Grund C, Kuhn C, Jackson BW, Illmensee K (1982). Formation of cytoskeletal elements during mouse embryogenesis. III. Primary mesenchymal cells and the first appearance of vimentin filaments. *Differentiation* 23:43-59.
- Fraser GJ, Smith MM (2011). Evolution of developmental pattern for vertebrate dentitions: an oro-pharyngeal specific mechanism. *J Exp Zool B Mol Dev Evol* 316(B):99-112.
- Handrigan GR, Richman JM (2010). A network of Wnt, hedgehog and BMP signaling pathways regulates tooth replacement in snakes. *Dev Biol* 348:130-141.
- Hatakeyama S, Tomichi N, Ohara-Nemoto Y, Satoh M (2000). The immunohistochemical localization of Fas and Fas ligand in jaw bone and tooth germ of human fetuses. *Calcif Tissue Int* 66:330-337.
- Huang GT, Gronthos S, Shi S (2009). Mesenchymal stem cells derived from dental tissues vs. those from other sources: their biology and role in regenerative medicine. *J Dent Res* 88:792-806.
- Ivaska J (2011). Vimentin: central hub in EMT induction? *Small GTPases* 2:51-53.
- Jarvinen E, Salazar-Ciudad I, Birchmeier W, Taketo MM, Jernvall J, Thesleff I (2006). Continuous tooth generation in mouse is induced by activated epithelial Wnt/beta-catenin signaling. *Proc Natl Acad Sci USA* 103:18627-18632.
- Jarvinen E, Tummers M, Thesleff I (2009). The role of the dental lamina in mammalian tooth replacement. *J Exp Zool B Mol Dev Evol* 312(B): 281-291.
- Jin JZ, Ding J (2006). Analysis of cell migration, transdifferentiation and apoptosis during mouse secondary palate fusion. *Development* 133:3341-3347.
- Karafiát V, Dvorakova M, Krejci E, Kralova J, Pajer P, Snajdr P, *et al.* (2005). Transcription factor c-Myb is involved in the regulation of the epithelial-mesenchymal transition in the avian neural crest. *Cell Mol Life Sci* 62:2516-2525.
- Kindaichi K (1980). An electron microscopic study of cell death in molar tooth germ epithelia of mouse embryos. *Arch Histol Jpn* 43:289-304.
- Matalova E, Antonarakis GS, Sharpe PT, Tucker AS (2005). Cell lineage of primary and secondary enamel knots. *Dev Dyn* 233:754-759.
- Matalova E, Fleischmannova J, Sharpe PT, Tucker AS (2008). Tooth agenesis: from molecular genetics to molecular dentistry. *J Dent Res* 87:617-623.
- Moskow BS, Bloom A (1983). Embryogenesis of the gingival cyst. *J Clin Periodontol* 10:119-130.
- Prindull G, Zipori D (2004). Environmental guidance of normal and tumor cell plasticity: epithelial mesenchymal transitions as a paradigm. *Blood* 103:2892-2899.
- Sasaki C, Sato T, Kozawa Y (2001). Apoptosis in regressive deciduous tooth germs of *Suncus murinus* evaluated by the TUNEL method and electron microscopy. *Arch Oral Biol* 46:649-660.
- Stembirek J, Buchtová M, Kral T, Matalova E, Lozanoff S, Misek I (2010). Early morphogenesis of heterodont dentition in minipigs. *Eur J Oral Sci* 118:547-558.
- Suzuki M, Inoue T, Shimono M, Yamada S (2002). Behavior of epithelial root sheath during tooth root formation in porcine molars: TUNEL, TEM, and immunohistochemical studies. *Anat Embryol (Berl)* 206:13-20.
- Thiery JP, Acloque H, Huang RY, Nieto MA (2009). Epithelial-mesenchymal transitions in development and disease. *Cell* 139:871-890.
- Vahtokari A, Åberg T, Thesleff I (1996). Apoptosis in the developing tooth: association with an embryonic signaling center and suppression by EGF and FGF-4. *Development* 122:121-129.
- Zeichner-David M, Oishi K, Su Z, Zakartchenko V, Chen LS, Arzate H, *et al.* (2003). Role of Hertwig's epithelial root sheath cells in tooth root development. *Dev Dyn* 228:651-663.

Komentář k přiložené publikaci č. 3

PUTNOVA, Iveta, Hana DOSEDELOVA, Vitezslav BRYJA, Marie LANDOVA, Marcela BUCHTOVA a Jan STEMBIREK. Angled Growth of the Dental Lamina Is Accompanied by Asymmetrical Expression of the WNT Pathway Receptor Frizzled 6. *Frontiers in Physiology* [online]. 2017, 8, 29. ISSN 1664-042X. Dostupné z: doi:[10.3389/fphys.2017.00029](https://doi.org/10.3389/fphys.2017.00029)

IF = 3,394; kvartil Q1

V této publikaci jsme se zaměřili na protein Frizzled 6 (FZD 6), který patří k membránovým receptorům kanonické i nekanonické signální WNT dráhy, která je odpovědná za regulaci proliferace buněk, buněčné adheze a/nebo migrace buněk a zároveň je klíčová i pro odontogenezi nebo karcinogenezi (Logan a Nusse, 2004). V buňkách ameloblastomu bylo popsáno narušení této dráhy (Siar et al., 2012), což může potenciálně souviset s tvorbou karcinogenních buněk v ameloblastomu (Kim et al., 2021).

U FZD6 byla v literatuře popsána zodpovědnost za buněčnou polaritu buněk během embryogeneze, např. při vývoji neurální trubice nebo vlasového folikulu (Borelo et al., 1999, Logan a Nusse, 2004, Chang et al., 2016), dosud však nebylo známo, zda hraje roli i při degradaci zubní lišty.

Výsledky našich experimentů na prasečím biomodelu prokazují asymetrickou expresi FZD6 v zubní liště, a to po celou dobu od počátku jejího vývoje až po regresi. Během růstu lišty jsme prokázali silnější expresi tohoto proteinu především na její labiální straně, tedy ve směru růstu dentální lišty. Během regrese zubní lišty byly buňky s pozitivním FZD6 signálem v povrchové části lišty, právě v místě, kde degradující buňky zubní lišty procházejí epitelo-mezenchymální transformací nebo migrují. Možné změny v expresi FZD6 během odontogeneze by tak mohly být klíčové při pozdějším vzniku odontogenních tumorů, což však vyžaduje další výzkum.



Angled Growth of the Dental Lamina Is Accompanied by Asymmetrical Expression of the WNT Pathway Receptor Frizzled 6

Iveta Putnová^{1,2}, Hana Dosedělová^{1,2}, Vitezslav Bryja³, Marie Landová¹, Marcela Buchtová^{1,3*} and Jan Štebánek^{1,4}

¹ Laboratory of Molecular Morphogenesis, Institute of Animal Physiology and Genetics, Academy of Sciences, Brno, Czechia,

² Department of Anatomy, Histology and Embryology, University of Veterinary and Pharmaceutical Sciences, Brno, Czechia,

³ Department of Animal Physiology and Immunology, Institute of Experimental Biology, Masaryk University, Brno, Czechia,

⁴ Department of Maxillofacial Surgery, University Hospital Ostrava, Ostrava, Czechia

OPEN ACCESS

Edited by:

Claudio Cantù,
University of Zurich, Switzerland

Reviewed by:

Jean-Christophe Farges,
Claude Bernard University Lyon 1,
France

Michel Goldberg,
French Institute of Health and Medical
Research (Inserm), France

Catherine Chaussain,
Paris Descartes University, France

*Correspondence:

Marcela Buchtova
buchtova@iach.cz

Specialty section:

This article was submitted to
Craniofacial Biology and Dental
Research,
a section of the journal
Frontiers in Physiology

Received: 09 October 2016

Accepted: 11 January 2017

Published: 31 January 2017

Citation:

Putnová I, Dosedělová H, Bryja V,
Landová M, Buchtová M and
Štebánek J (2017) Angled Growth of
the Dental Lamina Is Accompanied by
Asymmetrical Expression of the WNT
Pathway Receptor Frizzled 6.
Front. Physiol. 8:29.
doi: 10.3389/fphys.2017.00029

Frizzled 6 (FZD6) belongs to a family of proteins that serve as receptors in the WNT signaling pathway. FZD6 plays an important role in the establishment of planar cell polarity in many embryonic processes such as convergent extension during gastrulation, neural tube closure, or hair patterning. Based on its role during hair development, we hypothesized that FZD6 may have similar expression pattern and function in the dental lamina, which is also a distinct epithelial protrusion growing characteristically angled into the mesenchyme. Diphyodont minipig was selected as a model species because its dentition closely resemble human ones with successional generation of teeth initiated from the dental lamina. We revealed asymmetrical expression of FZD6 in the dental lamina of early as well as late stages during its regression with stronger expression located on the labial side of the dental lamina. During lamina regression, FZD6-positive cells were found in its superficial part and the signal coincided with the upregulation of molecules involved in epithelial-mesenchymal transition and increased migratory potential of epithelial cells. FZD6-expression was also turned on during differentiation of cells producing hard tissues, in which mature odontoblasts, ameloblasts, or surrounding osteoblasts were FZD6-positive. On the other hand, the tip of successional lamina and its lingual part, in which progenitor cells are located, exhibited FZD6-negativity. In conclusion, asymmetrical expression of FZD6 correlates with the growth directionality and side-specific morphological differences in the dental lamina of diphyodont species. Based on observed expression pattern, we propose that the dental lamina is other epithelial tissue, where planar cell polarity signaling is involved during its asymmetrical growth.

Keywords: FZD6, successional dental lamina, WNT signaling, planar cell polarity (PCP), odontoblast, ameloblast, osteoblast, epithelial remnants

INTRODUCTION

Tooth development is a complex process that is dependent on reciprocal and strictly regulated interactions between the ectoderm-derived epithelium and cranial neural crest-derived mesenchyme (Thesleff et al., 1995). Numerous regulatory genes associated with all stages of tooth formation (patterning, morphogenesis, cytodifferentiation, and mineralization) belong

to evolutionarily conserved signaling pathways. They are necessary for individual steps of odontogenesis and are regulated by a precise timing mechanism (Thesleff, 2003; Mitsiadis and Luder, 2011). The WNT signaling pathway has previously been demonstrated to play an important role in mouse as well as human tooth development (Sarkar and Sharpe, 1999; Sarkar et al., 2000; Handrigan and Richman, 2010). FZD members belongs to a family of proteins that serve as receptors in WNT signaling pathways (Fischer et al., 2007; Dijksterhuis et al., 2016; Wang et al., 2016). Their functions include activation of the FZD/ β -catenin, FZD/ Ca^{+2} and FZD/planar cell polarity signaling pathways (Schulte and Bryja, 2007). To date, 10 FZD proteins have been described in mammals (Schulte and Bryja, 2007; Dijksterhuis et al., 2016). While the expression of several ligands of WNT signaling during odontogenesis has been well-described (Cai et al., 2011; Lin et al., 2011; Wang et al., 2014), little attention has been paid to the expression of individual receptors. Here, we focus on FZD6, which is involved in PCP (planar cell polarity) signaling and is required for the transmission of polarity signals across the plasma membrane in epidermal cells (Wang et al., 2006).

Cellular communication mediated by WNT and FZD has been shown to be essential for proper embryonic development of invertebrates as well as vertebrates. FZD induction has been found in several developmental processes such as the polarized cell movements required for convergent extension during gastrulation in frog and fish (Borello et al., 1999), neural induction and patterning, cell proliferation, cell specification, stem cell differentiation, axonal outgrowth and guidance, and synaptogenesis (Logan and Nusse, 2004; Chien et al., 2009; Wang et al., 2010). Besides these early patterning processes, FZD3 and FZD6 have been reported redundantly to control neural tube closure and planar orientation of hair bundles on a subset of auditory and vestibular sensory cells. In the inner ear, these two proteins are located on the lateral faces of sensory and auxiliary cells in a pattern that correlates with the axis of planar polarity (Wang et al., 2006). The polarity of FZD6 localization with respect to the asymmetric position of the kinocilium is reversed between vestibular hair cells in the cristae of the semicircular canals and auditory hair cells in the organ of Corti (Wang et al., 2006). FZD6 controls macroscopic hair patterning in the mouse and is also expressed in the skin and hair follicles (Guo et al., 2004; Wang et al., 2010; Chang et al., 2016).

Mutations in PCP genes lead to a wide range of developmental defects, including a shortened body axis, a widened neural plate, and neural tube defects (NTDs; Simons and Mlodzik, 2008). In the case of targeted deletion of the *Fzd6* gene, stereotyped whorls on the hind feet, variable whorls and tufts on the head and disorientation of hairs on the torso are evident (Guo et al., 2004). In the *Fzd6*^{-/-} mouse, the orientations of the earliest born hair follicles are uncorrelated, but over time the follicles reorient to create patterns, which are typical for different body regions and are characterized by a high degree of local arrangement (Wang et al., 2010). Fifty percent of male newborns, but not female *Fzd6*^{-/-} mice, displayed abnormal claw morphology. The claws are easily lost with age or under increased mechanical stress. The claw disappears or become rudimentary on the hind

limbs at the age of 2–3 months. The reason for the significant misbalance between sexes is unknown but it could be due to the more aggressive behavior of males (Fröjmark et al., 2011). Similarly in humans, loss-of-function mutations caused recessive nail dysplasia (Fröjmark et al., 2011; Naz et al., 2012). While several ectodermal derivatives have been found to be affected in transgenic mouse lines or humans with defective FZD6, to date, no tooth phenotype has been described.

Here, we analyzed the expression of FZD6, a transmembrane protein of the WNT family, that is known to regulate the number of epithelial differentiation-related genes. During human odontogenesis, *Fzd6* was shown to exhibit weak mRNA expression in the dental epithelium of incisors and molars at 8 and 12 weeks of gestation (Wang et al., 2014). Later during 15 week, *Fzd6* was observed in the inner and outer enamel epithelium and in the surrounding mesenchymal cells (Wang et al., 2014). However, the distribution of FZD6 on protein level has not been analyzed yet. We focused on premolar development in diphyodont dentition during early as well as late mineralization stages of odontogenesis to determine the distribution of its expression throughout development. Labio-lingual differences during the initiation and regression of dental lamina were analyzed to uncover signaling involved in asymmetrical morphology and growth of the lamina. Therefore, the main aim of our study was to describe the expression pattern of FZD6 at the protein level during early odontogenesis in the minipig dentition with a special focus on the asymmetric distribution of FZD6 in the dental lamina during its angled growth and regression. Furthermore, changes in FZD6-positivity in odontoblasts and ameloblasts during their differentiation were determined.

MATERIALS AND METHODS

Embryonic Material

Selected developmental stages of the minipig (E29, E30, E36, E56, E67) were used to analyse the expression of FZD6 during odontogenesis. Minipig embryos and fetuses were obtained from Liběchov animal facility (Liběchov, Czech Republic). The day after insemination was established as day 1 of gestation. Staged embryos and fetuses were obtained by hysterectomy. All samples were fixed in 4% neutral formaldehyde and decalcified in 12.5% EDTA in 4% PFA until the mandibular bones of embryos were soft enough for further processing. Sections were stained with Haematoxylin-Eosin and alternative slides were used for immunohistochemical labeling. All procedures were conducted following a protocol approved by the Laboratory Animal Science Committee of the Institute of Animal Physiology and Genetics, Academy of Sciences (approval no. 020/2010, Liběchov, Czech Republic).

Immunohistochemical Analysis

For detection of FZD6-positivity, we performed immunohistochemical labeling. After deparaffinization and rehydration, antigen retrieval was performed in a water bath (97°C) in citrate buffer (pH = 6) for 20 min. Blocking serum was applied to the sections for 20 min and slides were incubated

for 1 h at room temperature with primary FZD6 antibody (cat. no. G260, Antibodies online, 1:200 dilution). The secondary antibody was applied for 30 min. Streptavidin-FITC complex (1:250 dilution, cat. no. 554060, BD Pharmingen, Franklin Lakes, USA) was used for visualization of FZD6-positive cells (30 min). DAPI (cat. no. P36935, Invitrogen, Oregon, USA) or DRAQ5 (1:500 dilution, cat. no. 62254, Thermo Scientific, USA) were applied for the counterstaining. The photos taken under a fluorescence microscope Leica DM LB2 (Leica Microsystems, Germany) were merged together in Adobe Photoshop 7.0 (USA). High power images were taken on confocal microscope Leica SP5 using 40x (air) objectives (Leica Microsystems, Germany) with Leica Application Suite software.

RESULTS AND DISCUSSION

Asymmetrical Expression of FZD6 at Early Stages of Odontogenesis

PCP components are often localized asymmetrically in different types of cells. The Frizzled family was found to be required for producing the correct orientation of cuticular bristles and hairs (Guo et al., 2004). This process is referred to as tissue or planar polarity (Gubb and García-Bellido, 1982; Vinson et al., 1989). Such polarization is often precisely coordinated relative to the axes of a tissue or organ, but the mechanisms underlying this regulation are still poorly understood. As exact coordination of tissue polarity in the labio-lingual axis is necessary to direct the angled growth of dental lamina into the mesenchyme, we wondered whether protein expression FZD6 can be associated with morphological side-related differences in the dental lamina. Indeed, we observed significant differences in the level of FZD6-positivity in distinct areas of the dental lamina at all stages of minipig odontogenesis. Already at the epithelial thickening stage, a strong FZD6 signal was apparent on the labial side of the oral epithelium and in the dental epithelium, especially in its basal layer (Figure 1A). The signal became weaker toward its lingual side. Distinct expression was also obvious in the mesenchyme surrounding the epithelial thickening, where more FZD6-positivity was noticeable in the labial area (Figure 1A). Later, during dental lamina growth into the mesenchyme, stronger expression was observed also on the labial side of the oral dental interface in comparison with the lingual area (Figures 1B,C,C'). At the dental bud stage, FZD6 was only weakly expressed inside the tooth anlagen (Figures 1D,D') while FZD6-immunopositivity was detected in the dental lamina connecting the tooth to the oral epithelium, where stronger expression was located on the labial side (Figures 1D,D').

At the cap stage (Figure 1E), distinct expression was found throughout all thicknesses of the oral epithelium and in the dental lamina, but was not apparent inside the tooth anlagen. The signal spread into the cervical loop area during the early bell stage (Figure 1F). Almost no signal was visible in the stellate reticulum (Figure 1F). The dental papilla and surrounding mesenchyme were FZD6-negative. FZD6-signal was abundant in the basal layer of the oral epithelium at all analyzed stages and became localized to the superficial area of membrane in more differentiated superficial layers of the epithelium (Figure 1).

It is known that FZD6 is transducing signals in non-canonical WNT pathway and *Wnt5a* is one of its representative, which signals upstream of PCP pathway in mammals (Moon et al., 1993; Kilian et al., 2003). It was shown that WNT5a regulates tooth growth, cusp patterning and odontoblast differentiation in developing mouse molars and incisors (Lin et al., 2011). Previously, WNT5a expression was found not only in the dental mesenchyme but also in the dental epithelium in mouse during E14–E17 (Cai et al., 2011). However, we detected FZD6 even at very early stages of epithelial thickening and in the surrounding mesenchyme, and therefore another WNT ligand probably activates signaling at these early stages, which will be necessary to further analyse in future.

FZD can also mediate canonical signaling with activation of β -catenin. WNT3a is strongly expressed in the inner enamel epithelium of humans during the bell stage (Wang et al., 2014). In mice, *Wnt3a* is expressed in the enamel knot at the cap stage (Millar et al., 2003). These expression patterns do not seem to correlate with our observations of a strong signal located in the superficial part of the tooth anlagen whereas deeper parts including enamel knots and cervical loops were FZD6-negative (Figure 1).

FZD6 was also distributed in distinct areas of the mesenchyme surrounding epithelial thickenings during the early stages of odontogenesis; however, mesenchymal expression was downregulated and only small spots were visible on the mesenchymal cell surface at older stages. On the other hand, FZD6 was mostly expressed in the epithelium with uniform expression throughout the whole thickness of the oral epithelium. This finding is consistent with observations in FZD6 knockout mice, where numerous genes encoding keratins, keratin-associated proteins and transglutaminases and their substrates were significantly downregulated (Cui et al., 2013). Therefore, the mesenchymal expression pattern is dissimilar to the epithelial signal indicating distinct role of FZD signaling in the epithelium in contrast to the mesenchyme.

FZD6 Expression in the Successional Dental Lamina

During later stages of odontogenesis, the dental lamina protruded deeply into the mesenchyme and morphological changes were obvious in its superficial part (Figure 2). In the most superficial area, cells connecting the lamina to the oral epithelium were FZD6-positive (Figures 2A,B, 3A,A',B,B'). Expression in superficial cells even increased following disconnection of the lamina from the oral epithelium (Figures 2C, 3D,D',E,E'). Cells on the labial side separating from the lamina were strongly FZD6-positive similar to the stalk of very flat cells connecting the dental lamina to the tooth (Figures 2A–C). On the other hand, the apical tip of the successional lamina was FZD6-negative (Figures 2A–D, 3C,C',E,F'). Therefore, there are significant differences in FZD6 expression through the dental lamina with higher expression maintained in its superficial layers.

While, the most distal tip of the successional dental lamina was FZD6-negative, β -catenin was previously described in the tip and lingual side of the dental lamina in snake and alligator (Wu et al., 2013) and transcription factor *Lef1* (Wnt/ β -catenin pathway target gene) in corn snake and python dental lamina (Handrigan

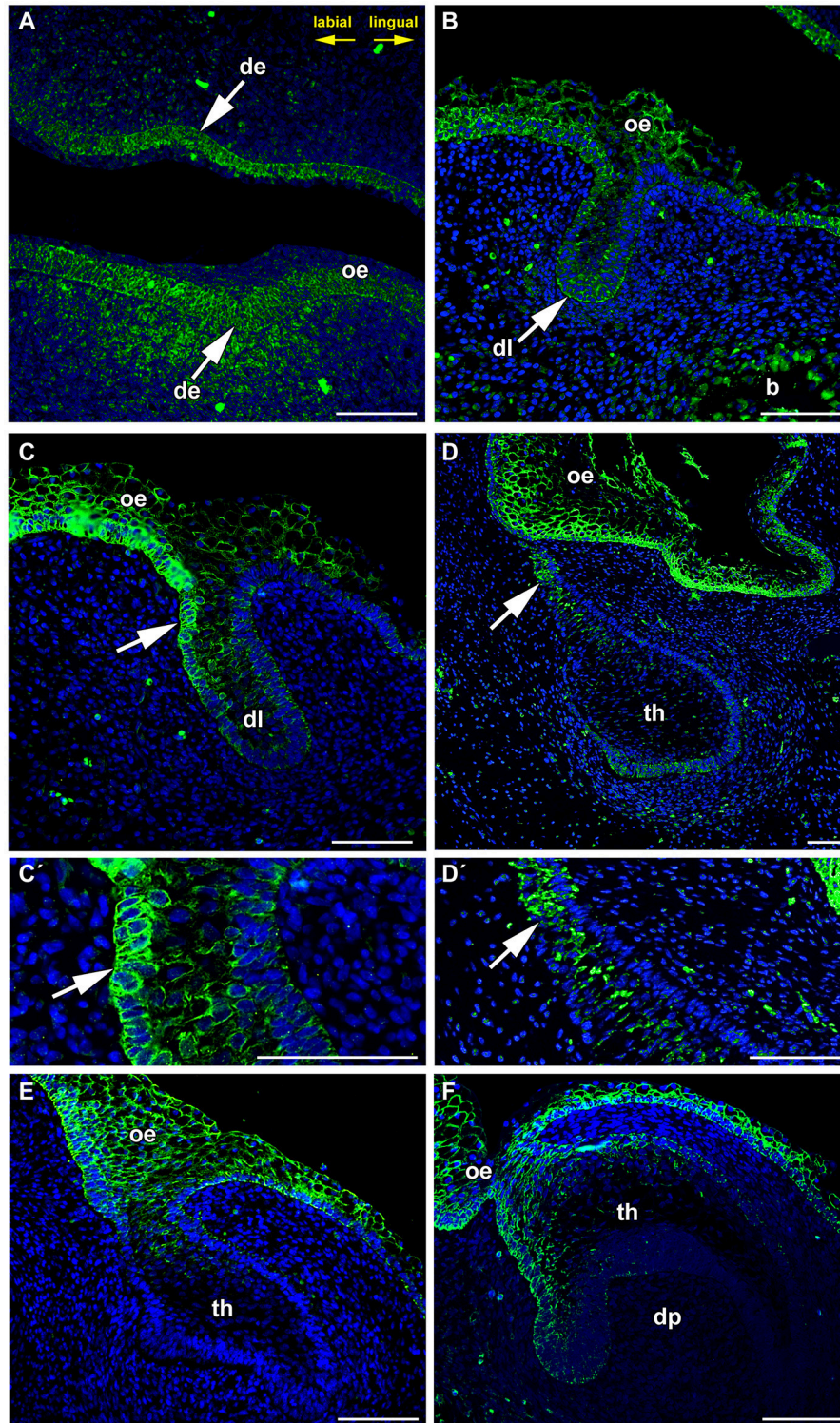


FIGURE 1 | FZD6 expression is asymmetrical in the dental lamina. (A) At epithelial thickening stage, the oral epithelium and surrounding mesenchyme are FZD6-positive. **(B,C,C'** in detail) Later, FZD6-positive signal is located on the labial side (arrow) of the protruding dental lamina. **(D,D'** in detail) At dental bud stage, stronger FZD6-immunopositivity (arrow) was detected on the labial side of dental germ. **(E,F)** At bell stage, the labial cervical loop is more positive than the lingual one. Almost no signal was visible in the stellate reticulum. The dental papilla and surrounding mesenchyme were FZD6-negative. b, bone; de, dental epithelium; dl, dental lamina; dp, dental papilla; oe, oral epithelium; th, tooth. Scale bar = 100 μ m.

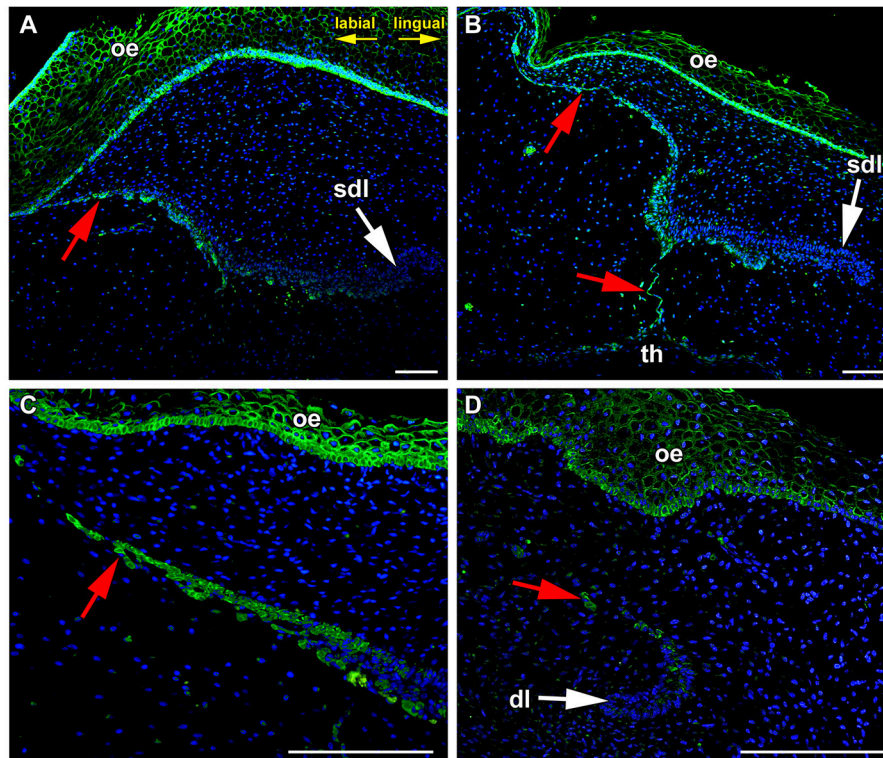


FIGURE 2 | The tip of growing successional dental lamina is FZD6-negative. (A) In the most superficial area, flat cells connecting the lamina to the oral epithelium were FZD6-positive. (B) Cells on the labial side separating from the lamina were also FZD6-positive similarly to the stalk of very flat cells connecting the dental lamina to the tooth. However, the apical tip of the successional lamina was FZD6-negative. (C) When dental lamina disconnected from the oral epithelium, the stronger positivity of FZD6 was evident in the superficial fragments and epithelial clusters of cells. (D) Rudimentary interdental lamina exhibited only weak FZD6 expression. dl, dental lamina; oe, oral epithelium; sdl, successional dental lamina; th, tooth; red arrow, epithelial remnants. Scale bar = 100 μm .

and Richman, 2010; Gaete and Tucker, 2013). WNT ligands that signal through β -catenin are involved in stem/progenitor self-renewal and maintenance of cells in a proliferative and undifferentiated state while non-canonical signaling promotes their differentiation (Liu et al., 2009; Grumolato et al., 2010). As non-canonical signaling is known to inhibit WNT/ β -catenin canonical signaling (Topol et al., 2003; Mikels and Nusse, 2006), this asymmetrical expression of non-canonical and canonical WNT molecules and the balance among them is critical for the regulation of dental progenitor cell lines similar to that shown in other systems (Grigoryan et al., 2008). Based on our evidence, FZD6 is not expressed in the areas of dental lamina with high cell proliferation or proposed localization of progenitor cells. Therefore, canonical and non-canonical WNT signaling exhibits distinct asymmetrical expression pattern through the lamina, which seems to be aligned with side-specific differences during successional dental lamina formation.

FZD6 Was Strongly Expressed in the Epithelial Remnants and Pearls during Dental Lamina Regression

The minipig similar to human has a diphyodont type of dentition, where only two generation of teeth are initiated.

During embryonic period, the dental lamina undergoes major morphological changes and becomes thinner and disconnected from the oral epithelium. Cells are elongated in the superficial area of the dental lamina (Buchtová et al., 2012). Furthermore, they are elongated in the area of the dental stalk connecting the tooth anlagen to the dental lamina. After the dental lamina had disconnected from the oral epithelium, stronger expression of FZD6 was evident in the superficial epithelial cells. In deeper parts of the lamina, the expression of FZD6 was apparent on the side facing the tooth, which undergoes regression (Figure 2C). There were also differences in the level of expression along the jaw axis. In the area between teeth, rudimentary interdental lamina exhibited only weak FZD6 expression located in the most superficial area (Figure 2D).

Later during dental lamina regression, the dental lamina become fragmented, and only occasional epithelial islands remain in the superficial area (Figure 4A). Some of these fragments undergo further morphological changes and epithelial pearls become visible along the jaw (Buchtová et al., 2012). Expression was also found in the epithelial clusters during the process of pearl formation (Figure 4C) as well as in the basal layer of already formed pearls (Figure 4B), while the central area was negative (Figure 4D).

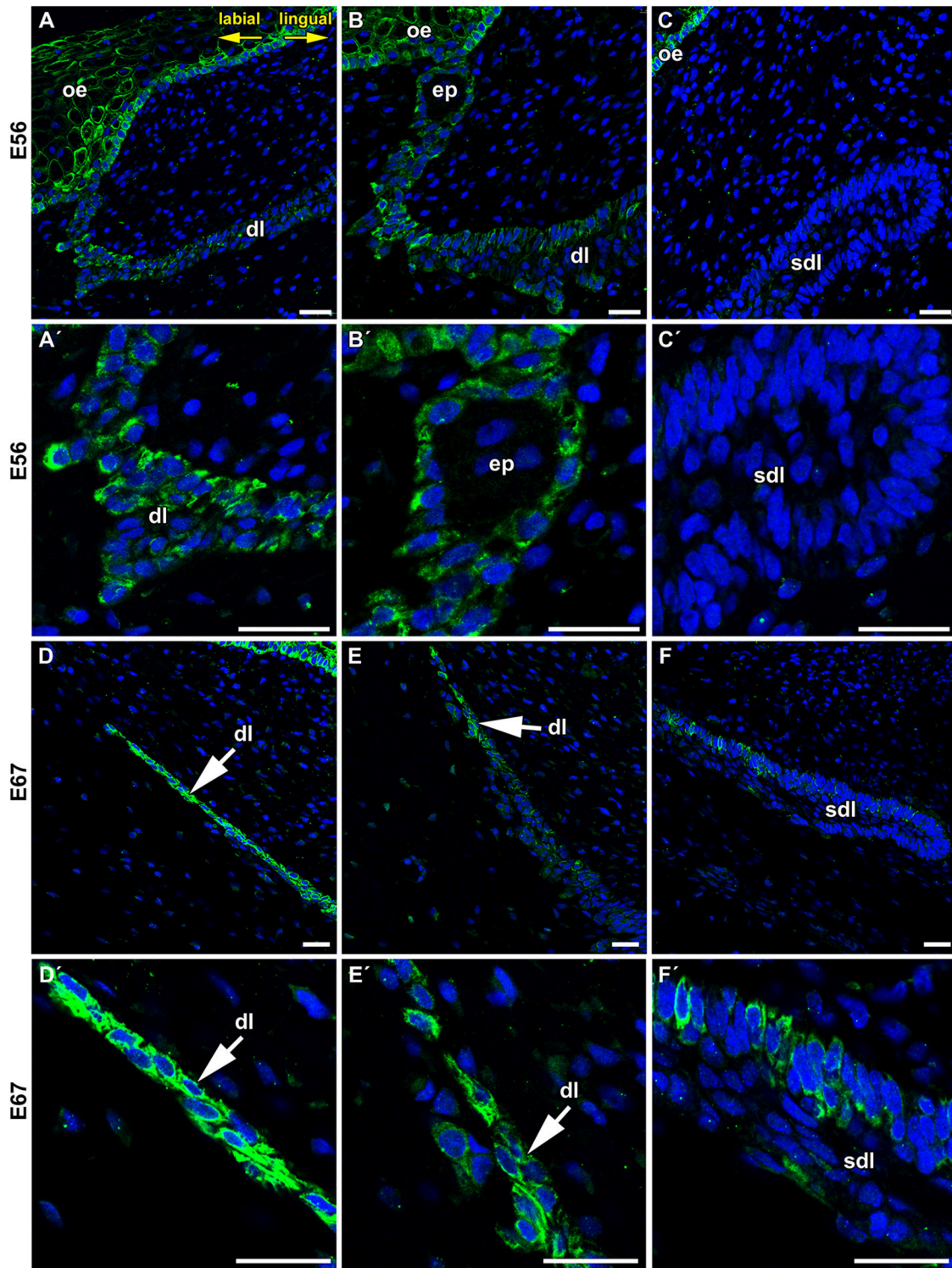


FIGURE 3 | Details of FZD6 expression in the dental lamina. (A,A',B,B') Stronger expression of FZD6 was observed in the superficial area of the dental lamina, which was still connected to the oral epithelium. **(C,C')** No FZD6 expression was found in deeper successional dental lamina while spotted pattern of expression was observed in surrounding mesenchymal cells. **(D,D')** Later in development, superficial part was disconnected from the oral epithelium and cells exhibited strong FZD6-positivity. **(E,E')** Expression was gradually lost in the central part of the lamina. **(F,F')** The tip of the successional lamina was negative similar to younger stage, only few positive cells were found in more superficial position. dl, dental lamina; ep, epithelial pearl; oe, oral epithelium; sdl, successional dental lamina. Scale bar = 25 μ m.

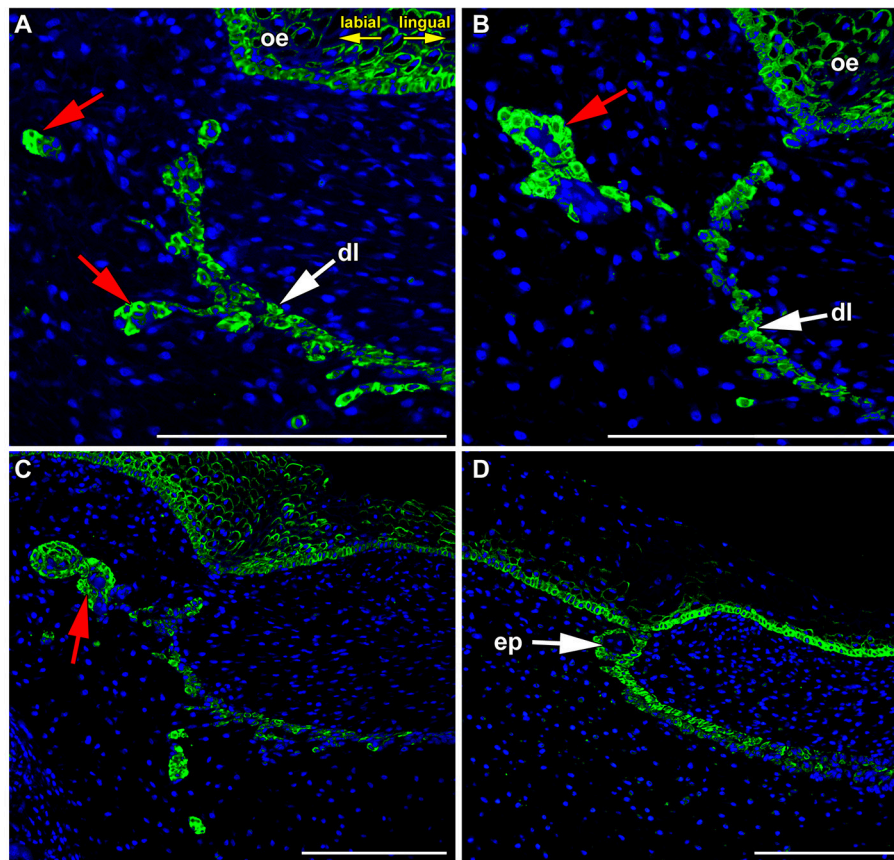


FIGURE 4 | FZD6 expression in epithelial remnants and pearls. (A,B) Localized and cytoplasmic expression of FZD6 was found in epithelial remnants. **(C)** The expression was found in the epithelial clusters during process of pearl formation as well as in the basal layer of already formed pearls **(D)**, while their central area was negative. ep, epithelial pearl; red arrow, epithelial remnants. Scale bar = 100 μm .

Interestingly, distinct expression was obvious especially in the basal layers of the lamina epithelium facing the tooth where clusters of elongated cells were moving out of the dental lamina. The expression of FZD6 during lamina regression coincides with the upregulation of molecules involved in epithelial-mesenchymal transition of epithelial cells (Buchtová et al., 2012). Our observations that cells moving from the dental lamina are FZD6-positive is consistent with the previously known role of PCP proteins in notochord or somite cell elongation during their convergent extension (Keller et al., 2000; Keller, 2002; Seifert and Mlodzik, 2007) as well as regulation of cell polarity and directed motility during gastrulation in frogs and fish, and neural tube and eyelid closure in mammals (Wang et al., 2006; Seifert and Mlodzik, 2007).

Frizzled 6 in Differentiation of Hard-Tissue Producing Cells

Both canonical and non-canonical WNT pathways were previously shown to be involved in the differentiation of hard-tissue producing cells (Millar et al., 2003; Lin et al., 2011; Sakisaka et al., 2015). WNT signaling was shown to promote the differentiation of dental follicle cells into the cementoblast

or osteoblast phenotype (Peng et al., 2010; Du et al., 2012; Sakisaka et al., 2015; Nemoto et al., 2016). Moreover, Wnt5a overexpression promotes the differentiation of dental papilla cells and increased the expression of mineralization-related genes (Peng et al., 2010).

In agreement with these findings, FZD6 expression was switched on during the differentiation of odontoblasts, ameloblasts, and osteoblasts in minipigs (Figure 5) at time when the production of hard tissues started. Differentiated and secretory ameloblasts were FZD6-positive while non-differentiated cells of the inner enamel epithelium were negative (Figures 5A,A'). A similar pattern was observed in the dental papilla where differentiated odontoblasts exhibiting dentin production were FZD6-positive (Figures 5A,A'). Almost no signal was found in the stellate reticulum or stratum intermedium (Figure 5A). On the other hand, the outer enamel epithelium was positive, especially the superficial clusters of cells during disruption of the enamel organ by blood vessels. FZD6 signal was also located in the structures surrounding teeth in the jaw such as alveolar bones, in which osteoblasts were positive (Figures 5B,B') along with the secretory area of salivary glands or their ducts (Figures 5C,C').

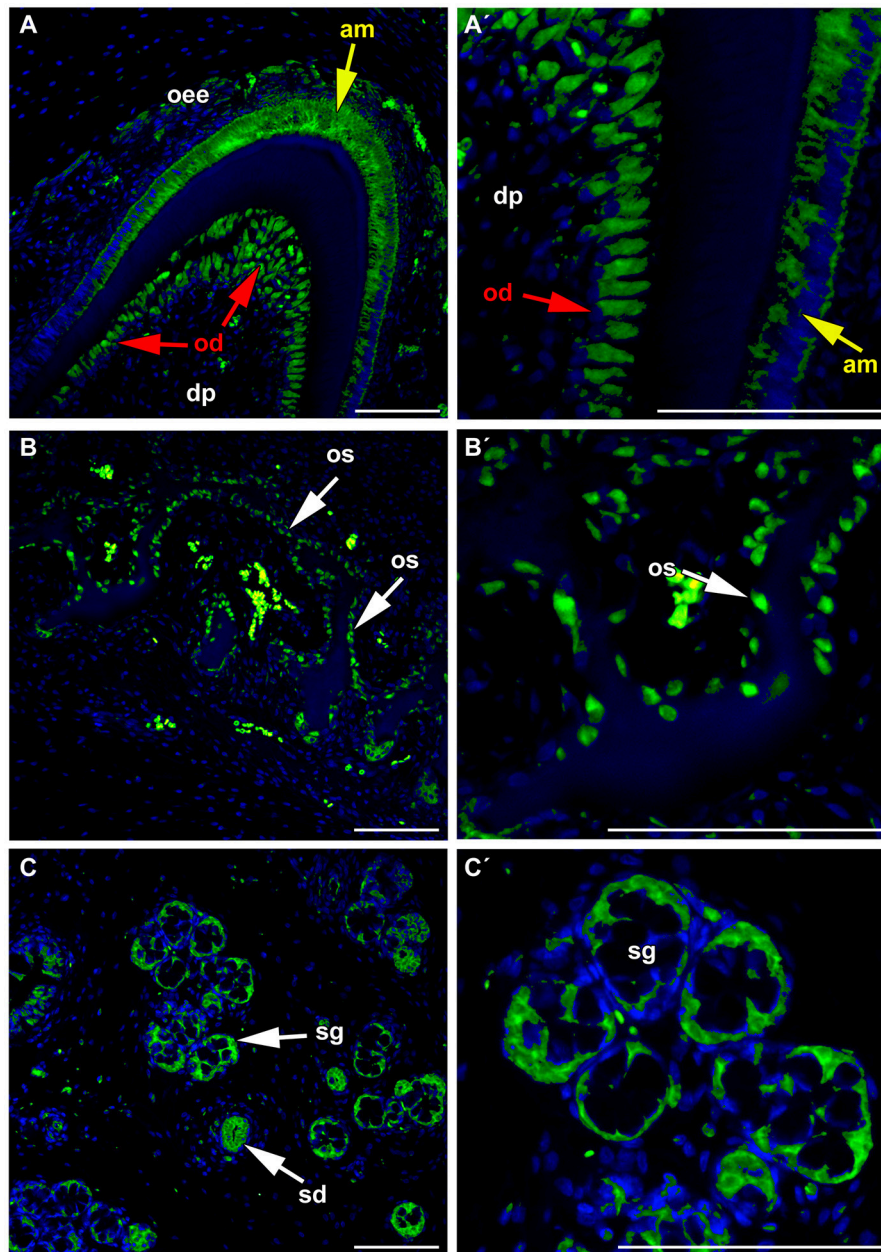
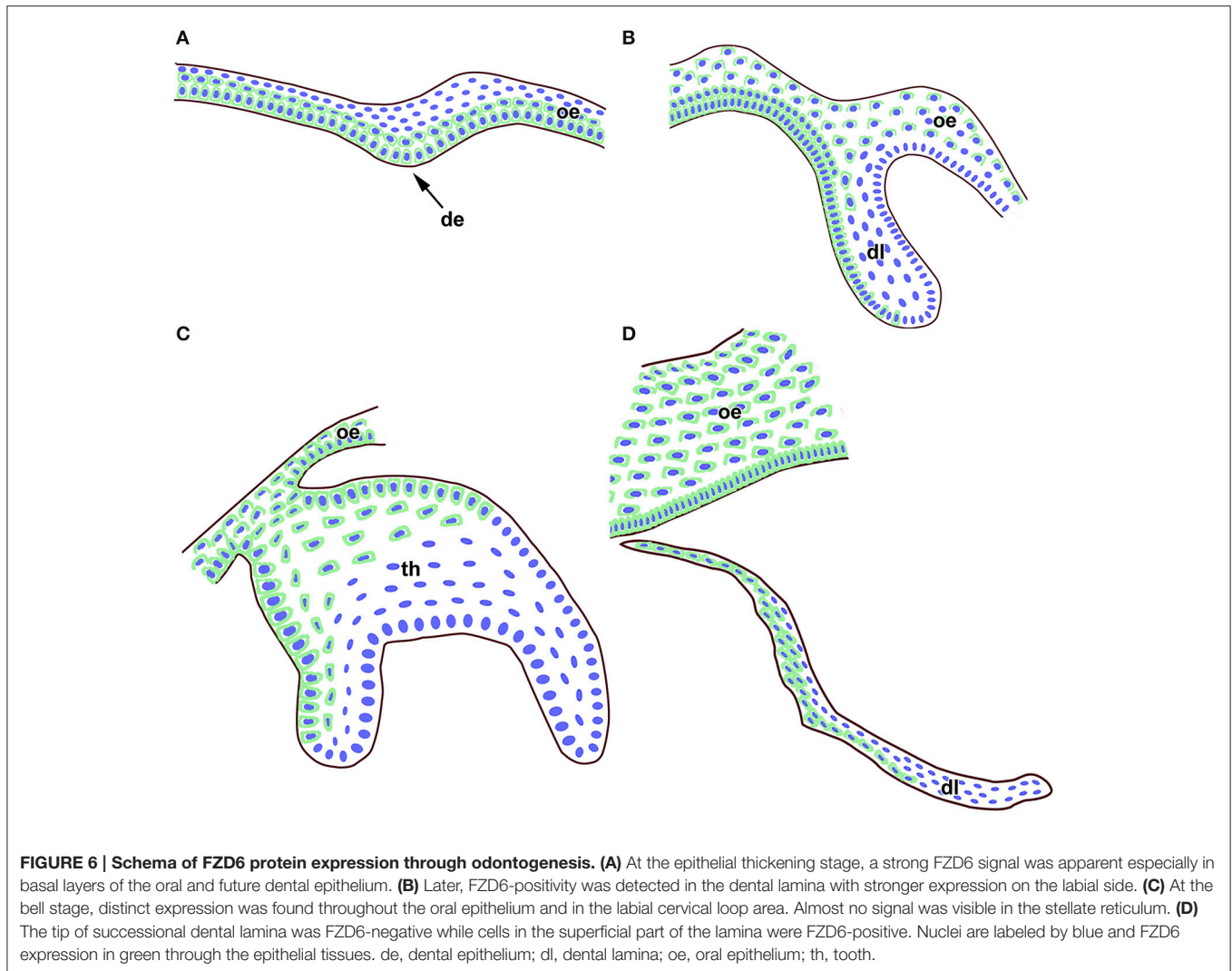


FIGURE 5 | FZD6 in differentiated ameloblasts and odontoblasts. (A,A') Differentiated and secretory ameloblasts were FZD6-positive while non-differentiated cells of the inner enamel epithelium were negative. Similar pattern was observed in the dental papilla where differentiated odontoblasts exhibiting dentin production were FZD6-positive. FZD6 signal was localized at different stages of ameloblasts differentiation after their elongation. **(B,B')** FZD6 signal was located also in the structures surrounding teeth such as alveolar bone where osteoblasts were positive and secretory cells of salivary gland or their ducts **(C,C')**. am, ameloblast; dp, dental papilla; od, odontoblast; oee, outer enamel epithelium; sg, salivary gland. Scale bar = 100 μm .

While the tooth phenotype of FZD6 mutant mice has not yet been described, *Wnt5a*-deficient mice exhibit delayed odontoblast differentiation (Lin et al., 2011). Abnormal morphology of ameloblasts and defective odontoblast differentiation with absence of predentin formation were also found in *Ror2* mutant mice (Lin et al., 2011) in which ROR2 can serve as an alternative WNT receptor (Oishi et al.,

2003). Odontoblasts in *Wnt5a*-deficient mice were shorter and thicker than in control animals. Similarly in *Ror2*-deficient mice, odontoblasts were polarized but appeared to be shorter in comparison to littermate control animals (Lin et al., 2011). While *Wnt5a* is expressed in the dental mesenchyme, its receptor is also expressed in the epithelium. It was proposed that another receptor must be involved in WNT5a-mediated signaling as



defects in tooth development in *Ror2* mutants occur much later than observed in *WNT5a*-deficient mice (Lin et al., 2011). Based on our observations, FZD6 could be one of these receptors.

Odontoblasts and ameloblasts are highly polarized cells with a characteristic morphology and arrangement of cellular compartments. In odontoblasts, FZD6 was expressed asymmetrically only on the side facing the dentin (Figures 5A,A'). In ameloblasts, FZD6 was observed on both sides of differentiated cells, and later, the signal showed a more uniform distribution through the cells. Differentiation of ameloblasts and odontoblasts is characterized by elongation of the cells and establishment of their polarity. Actin filament bundles exhibit a polarized distribution in rat ameloblasts and are abundant at the ameloblast junction area (Nishikawa and Kitamura, 1985, 1986). As actin cytoskeleton organization is downstream of the PCP signaling pathway, it is possible that FZD6 can be involved in the rearrangement of cellular polarity in the odontoblasts and ameloblasts during their differentiation.

CONCLUSIONS

In summary, FZD6 was expressed asymmetrically in the dental lamina at early as well as late stages of diphyodont dentition (Figure 6). We observed significant differences in the level of FZD6 expression in distinct areas of the dental lamina with stronger expression in the labial and superficial parts (Figure 6). The apical tip of the successional lamina was FZD6-negative. During dental lamina regression, labial cells separating from the lamina were strongly FZD6-positive similar to the stalk of very flat cells connecting the dental lamina to the tooth germ. On the other hand, FZD6 was not expressed in the areas of dental lamina with high cell proliferation or proposed localization of progenitor cells.

FZD6 expression was also switched on during the differentiation of odontoblasts, ameloblasts, and osteoblasts in minipigs at time when the production of hard tissues started. In odontoblasts, FZD6 was expressed asymmetrically only on

the side facing the dentin therefore it is possible that FZD6 can be involved in the establishment of cellular polarity in the odontoblasts during their differentiation. However, the exact role of FZD6 in the growth directionality of the lamina and differentiation of hard tissue producing cells has to be proven experimentally in future.

AUTHOR CONTRIBUTIONS

MB and VB designed the project. IP, HD, ML, and JS performed and interpreted experiments. IP, MB, and JS wrote

manuscript with contribution of VB. All authors approved the manuscript.

ACKNOWLEDGMENTS

This study was supported by the Czech Science Foundation (14-29273P to IP and JS) and Grant Agency of the University of Veterinary and Pharmaceutical Sciences Brno (108/2015/FVL to HD), Masaryk University (MUNI/A/0988/2016) and institutional support (RVO:67985904). This contribution is free of conflict of interest.

REFERENCES

- Borello, U., Buffa, V., Sonnino, C., Melchionna, R., Vivarelli, E., and Cossu, G. (1999). Differential expression of the Wnt putative receptors Frizzled during mouse somitogenesis. *Mech. Dev.* 89, 173–177. doi: 10.1016/S0925-4773(99)00205-1
- Buchtová, M., Stembírek, J., Glocová, K., Matalová, E., and Tucker, A. S. (2012). Early regression of the dental lamina underlies the development of diphyodont dentitions. *J. Dent. Res.* 91, 491–498. doi: 10.1177/0022034512442896
- Cai, J., Mutoh, N., Shin, J. O., Tani-Ishii, N., Ohshima, H., Cho, S. W., et al. (2011). Wnt5a plays a crucial role in determining tooth size during murine tooth development. *Cell Tissue Res.* 345, 367–377. doi: 10.1007/s00441-011-1224-4
- Chang, H., Smallwood, P. M., Williams, J., and Nathans, J. (2016). The spatio-temporal domains of Frizzled6 action in planar polarity control of hair follicle orientation. *Dev. Biol.* 409, 181–193. doi: 10.1016/j.ydbio.2015.10.027
- Chien, A. J., Conrad, W. H., and Moon, R. T. (2009). A Wnt survival guide: from flies to human disease. *J. Invest. Dermatol.* 129, 1614–1627. doi: 10.1038/jid.2008.445
- Cui, C. Y., Klar, J., Georgii-Hemming, P., Fröjmark, A. S., Baig, S. M., Schlessinger, D., et al. (2013). Frizzled6 deficiency disrupts the differentiation process of nail development. *J. Invest. Dermatol.* 133, 1990–1997. doi: 10.1038/jid.2013.84
- Dijksterhuis, J. P., Petersen, J., and Schulte, G. (2016). WNT/Frizzled signalling: receptor-ligand selectivity with focus on FZD-G protein signalling and its physiological relevance: IUPHAR Review 3. *Br. J. Pharmacol.* 171, 1195–1209. doi: 10.1111/bph.12364
- Du, Y., Ling, J., Wei, X., Ning, Y., Xie, N., Gu, H., et al. (2012). Wnt/β-catenin signaling participates in cementoblast/osteoblast differentiation of dental follicle cells. *Connect. Tissue Res.* 53, 390–397. doi: 10.3109/03008207.2012.668980
- Fischer, T., Guimera, J., Wurst, W., and Prakash, N. (2007). Distinct but redundant expression of the Frizzled Wnt receptor genes at signaling centers of the developing mouse brain. *Neuroscience* 147, 693–711. doi: 10.1016/j.neuroscience.2007.04.060
- Fröjmark, A. S., Schuster, J., Sobol, M., Entesarian, M., Kilander, M. B., Gabrikova, D., et al. (2011). Mutations in Frizzled 6 cause isolated autosomal-recessive nail dysplasia. *Am. J. Hum. Genet.* 88, 852–860. doi: 10.1016/j.ajhg.2011.05.013
- Gaete, M., and Tucker, A. S. (2013). Organized emergence of multiple-generations of teeth in snakes is dysregulated by activation of Wnt/β-catenin signalling. *PLoS ONE* 8:e74484. doi: 10.1371/journal.pone.0074484
- Grigoryan, T., Wend, P., Klaus, A., and Birchmeier, W. (2008). Deciphering the function of canonical Wnt signals in development and disease: conditional loss- and gain-of-function mutations of β-catenin in mice. *Genes Dev.* 22, 2308–2341. doi: 10.1101/gad.1686208
- Grumolato, L., Liu, G., Mong, P., Mudbhary, R., Biswas, R., Arroyave, R., et al. (2010). Canonical and noncanonical Wnts use a common mechanism to activate completely unrelated coreceptors. *Genes Dev.* 24, 2517–2530. doi: 10.1101/gad.1957710
- Gubb, D., and García-Bellido, A. (1982). A genetic analysis of the determination of cuticular polarity during development in *Drosophila melanogaster*. *J. Embryol. Exp. Morphol.* 68, 37–57.
- Guo, N., Hawkins, C., and Nathans, J. (2004). Frizzled6 controls hair patterning in mice. *Proc. Natl. Acad. Sci. U.S.A.* 101, 9277–9281. doi: 10.1073/pnas.0402802101
- Handrigan, G. R., and Richman, J. M. (2010). A network of Wnt, hedgehog and BMP signaling pathways regulates tooth replacement in snakes. *Dev. Biol.* 348, 130–141. doi: 10.1016/j.ydbio.2010.09.003
- Keller, R. (2002). Shaping the vertebrate body plan by polarized embryonic cell movements. *Science* 298, 1950–1954. doi: 10.1126/science.1079478
- Keller, R., Davidson, L., Edlund, A., Elul, T., Ezin, M., Shook, D., et al. (2000). Mechanisms of convergence and extension by cell intercalation. *Philos. Trans. R. Soc. Lond. B Biol. Sci.* 355, 897–922. doi: 10.1098/rstb.2000.0626
- Kilian, B., Mansukoski, H., Barbosa, F. C., Ulrich, F., Tada, M., and Heisenberg, C. P. (2003). The role of Ppt/Wnt5 in regulating cell shape and movement during zebrafish gastrulation. *Mech. Dev.* 120, 467–476. doi: 10.1016/S0925-4773(03)00004-2
- Lin, M., Li, L., Liu, C., Liu, H., He, F., Yan, F., et al. (2011). Wnt5a regulates growth, patterning, and odontoblast differentiation of developing mouse tooth. *Dev. Dyn.* 240, 432–440. doi: 10.1002/dvdy.22550
- Liu, G., Vijayakumar, S., Grumolato, L., Arroyave, R., Qiao, H., Akiri, G., et al. (2009). Canonical Wnts function as potent regulators of osteogenesis by human mesenchymal stem cells. *J. Cell Biol.* 185, 67–75. doi: 10.1083/jcb.200810137
- Logan, C. Y., and Nusse, R. (2004). The Wnt signaling pathway in development and disease. *Annu. Rev. Cell Dev. Biol.* 20, 781–810. doi: 10.1146/annurev.cellbio.20.010403.113126
- Mikels, A. J., and Nusse, R. (2006). Purified Wnt5a protein activates or inhibits β-catenin-TCF signaling depending on receptor context. *PLoS Biol.* 4:e115. doi: 10.1371/journal.pbio.0040115
- Millar, S. E., Koyama, E., Reddy, S. T., Andl, T., Gaddapara, T., Piddington, R., et al. (2003). Over- and ectopic expression of Wnt3 causes progressive loss of ameloblasts in postnatal mouse incisor teeth. *Connect. Tissue Res.* 44(Suppl. 1), 124–129. doi: 10.1080/03008200390152205
- Mitsiadis, T. A., and Luder, H. U. (2011). Genetic basis for tooth malformations: from mice to men and back again. *Clin. Genet.* 80, 319–329. doi: 10.1111/j.1399-0004.2011.01762.x
- Moon, R. T., Campbell, R. M., Christian, J. L., McGrew, L. L., Shih, J., and Fraser, S. (1993). Xwnt-5A: a maternal Wnt that affects morphogenetic movements after overexpression in embryos of *Xenopus laevis*. *Development* 119, 97–111.
- Naz, G., Pasternack, S. M., Perrin, C., Mattheisen, M., Refke, M., Khan, S., et al. (2012). FZD6 encoding the Wnt receptor frizzled 6 is mutated in autosomal-recessive nail dysplasia. *Br. J. Dermatol.* 166, 1088–1094. doi: 10.1111/j.1365-2133.2011.10800.x
- Nemoto, E., Sakisaka, Y., Tsuchiya, M., Tamura, M., Nakamura, T., Kanaya, S., et al. (2016). Wnt3a signaling induces murine dental follicle cells to differentiate into cementoblastic/osteoblastic cells via an osterix-dependent pathway. *J. Periodont. Res.* 51, 164–174. doi: 10.1111/jre.12294
- Nishikawa, S., and Kitamura, H. (1985). Three-dimensional network of microtubules in secretory ameloblasts of rat incisors. *Arch. Oral Biol.* 30, 1–11.
- Nishikawa, S., and Kitamura, H. (1986). Localization of actin during differentiation of the ameloblast, its related epithelial cells and odontoblasts in the rat incisor using NBD-phalloidin. *Differentiation* 30, 237–243.

- Oishi, I., Suzuki, H., Onishi, N., Takada, R., Kani, S., Ohkawara, B., et al. (2003). The receptor tyrosine kinase Ror2 is involved in non-canonical Wnt5a/JNK signalling pathway. *Genes Cells* 8, 645–654. doi: 10.1046/j.1365-2443.2003.00662.x
- Peng, L., Ren, L. B., Dong, G., Wang, C. L., Xu, P., Ye, L., et al. (2010). Wnt5a promotes differentiation of human dental papilla cells. *Int. Endod. J.* 43, 404–412. doi: 10.1111/j.1365-2591.2010.01693.x
- Sakisaka, Y., Tsuchiya, M., Nakamura, T., Tamura, M., Shimauchi, H., and Nemoto, E. (2015). Wnt5a attenuates Wnt3a-induced alkaline phosphatase expression in dental follicle cells. *Exp. Cell Res.* 336, 85–93. doi: 10.1016/j.yexcr.2015.06.013
- Sarkar, L., Cobourne, M., Naylor, S., Smalley, M., Dale, T., and Sharpe, P. T. (2000). Wnt/Shh interactions regulate ectodermal boundary formation during mammalian tooth development. *Proc. Natl. Acad. Sci. U.S.A.* 97, 4520–4524. doi: 10.1073/pnas.97.9.4520
- Sarkar, L., and Sharpe, P. T. (1999). Expression of Wnt signalling pathway genes during tooth development. *Mech. Dev.* 85, 197–200. doi: 10.1016/S0925-4773(99)00095-7
- Schulte, G., and Bryja, V. (2007). The Frizzled family of unconventional G-protein-coupled receptors. *Trends Pharmacol. Sci.* 28, 518–525. doi: 10.1016/j.tips.2007.09.001
- Seifert, J. R., and Mlodzik, M. (2007). Frizzled/PCP signalling: a conserved mechanism regulating cell polarity and directed motility. *Nat. Rev. Genet.* 8, 126–138. doi: 10.1038/nrg2042
- Simons, M., and Mlodzik, M. (2008). Planar cell polarity signaling: from fly development to human disease. *Annu. Rev. Genet.* 42, 517–540. doi: 10.1146/annurev.genet.42.110807.091432
- Thesleff, I. (2003). Epithelial-mesenchymal signalling regulating tooth morphogenesis. *J. Cell Sci.* 116, 1647–1648. doi: 10.1242/jcs.00410
- Thesleff, I., Vaahtokari, A., Kettunen, P., and Aberg, T. (1995). Epithelial-mesenchymal signaling during tooth development. *Connect. Tissue Res.* 32, 9–15. doi: 10.3109/03008209509013700
- Topol, L., Jiang, X., Choi, H., Garrett-Beal, L., Carolan, P. J., and Yang, Y. (2003). Wnt-5a inhibits the canonical Wnt pathway by promoting GSK-3-independent β -catenin degradation. *J. Cell Biol.* 162, 899–908. doi: 10.1083/jcb.200303158
- Vinson, C. R., Conover, S., and Adler, P. N. (1989). A Drosophila tissue polarity locus encodes a protein containing seven potential transmembrane domains. *Nature* 338, 263–264. doi: 10.1038/338263a0
- Wang, B., Li, H., Liu, Y., Lin, X., Lin, Y., Wang, Y., et al. (2014). Expression patterns of WNT/ β -CATENIN signaling molecules during human tooth development. *J. Mol. Histol.* 45, 487–496. doi: 10.1007/s10735-014-9572-5
- Wang, Y., Badea, T., and Nathans, J. (2006). Order from disorder: self-organization in mammalian hair patterning. *Proc. Natl. Acad. Sci. U.S.A.* 103, 19800–19805. doi: 10.1073/pnas.0609712104
- Wang, Y., Chang, H., and Nathans, J. (2010). When whorls collide: the development of hair patterns in frizzled 6 mutant mice. *Development* 137, 4091–4099. doi: 10.1242/dev.057455
- Wang, Y., Chang, H., Rattner, A., and Nathans, J. (2016). Frizzled receptors in development and disease. *Curr. Top. Dev. Biol.* 117, 113–139. doi: 10.1016/bs.ctdb.2015.11.028
- Wang, Y., Guo, N., and Nathans, J. (2006). The role of Frizzled3 and Frizzled6 in neural tube closure and in the planar polarity of inner-ear sensory hair cells. *J. Neurosci.* 26, 2147–2156. doi: 10.1523/JNEUROSCI.4698-05.2005
- Wu, P., Wu, X., Jiang, T. X., Elsey, R. M., Temple, B. L., Divers, S. J., et al. (2013). Specialized stem cell niche enables repetitive renewal of alligator teeth. *Proc. Natl. Acad. Sci. U.S.A.* 110, E2009–E2018. doi: 10.1073/pnas.1213202110

Conflict of Interest Statement: The authors declare that the research was conducted in the absence of any commercial or financial relationships that could be construed as a potential conflict of interest.

Copyright © 2017 Putnová, Dosedělová, Bryja, Landová, Buchtová and Štembírek. This is an open-access article distributed under the terms of the Creative Commons Attribution License (CC BY). The use, distribution or reproduction in other forums is permitted, provided the original author(s) or licensor are credited and that the original publication in this journal is cited, in accordance with accepted academic practice. No use, distribution or reproduction is permitted which does not comply with these terms.

Komentář k přiložené publikaci č. 4

FILUSOVA, Jana, Iveta PUTNOVA, Pavel HURNÍK, Zdenek DANEK, Ctirad MACHACEK, **Jan STEMBÍREK**, Marcela BUCHTOVA a Barbora Moldovan PUTNOVA. Alteration of primary cilia morphology and associated signalling in ameloblastoma. *Archives of Oral Biology* [online]. 2022, 142, 105499. ISSN 0003-9969. Dostupné z: doi:[10.1016/j.archoralbio.2022.105499](https://doi.org/10.1016/j.archoralbio.2022.105499)

IF = 2,64; kvartil Q3

Jednou z buněčných struktur, které mohou hrát roli v etiologii odontogenních tumorů, jsou primární cilie, respektive případná porucha jejich signalizace. Jedná se o buněčné výběžky – axonomy, které vycházejí z povrchu buňky do extracelulárního prostoru a fungují jako „buněčná anténa“ zachytávající biosignály z okolí buňky a předávající je do jejího nitra k dalšímu zpracování (Li et al., 2021). Tento proces je nutný k normálnímu fungování buňky, k udržování homeostázy, která souvisí s proliferací, diferenciací, migrací nebo třeba polaritou. Přítomnost primárních cilií v dentální liště s převážně rostro-kaudální orientací již byla popsána dříve, stejně jako fakt, že jejich počet v průběhu její degradace klesá (Hampl et al., 2017). Poruchy těchto struktur – ciliopatie – byly prokázány jednak v souvislosti s vývojem orofaciální oblasti a vznikem např. Bardet-Biedlova syndromu, Ellis–van Creveldova syndromu, Weyersovy akrofaciální dysostózy, kranioektodermální dysplazie nebo orofacioidigitálního syndromu (Hampl et al., 2017). Kromě těchto vývojových poruch byla porucha funkce cilií pozorována rovněž v procesu karcinogeneze u nádoru prsu, prostaty nebo rekta (Higgins et al., 2019).

Proto jsme se v této studii zaměřili na detekci abnormalit primárních cilií u ameloblastomů se zaměřením na jejich morfologii a počet, dále jsme pak analyzovali změny exprese v asociovaných genech (geny pro transportní proteiny IFT20, IFT80, IFT88, SHH receptor PTCH1 a transkripční faktor GLI1, který je efektozem SHH dráhy).

V souboru jsme analyzovali celkem devět ameloblastomů (subtypy plexiformní, folikulární a bazaloidní), které byly získány z Fakultní nemocnice Brno a Fakultní nemocnice Ostrava. Jako kontrolu jsme použili zdravou gingivu a zárodečné vaky zubů, které jsme získali při extrakci neprořezaných posledních stoliček.

Výsledky ukázaly rozdíly v distribuci a morfologii primárních řasinek u různých histologických podtypů ameloblastomů. Nejvyšší počet cilií byl nalezen v plexiformní formě ameloblastomu, menší počet byl přítomen ve folikulárním; ve zdravé kontrolní tkáni (gingiva) byl počet nejmenší.

Imunofluorescenční vyšetření SHH proteinu v ameloblastomu a ve vývojovém stadiu zvonku u primárních molárů lidských embryí (ED 56) ukázala stejnou míru exprese v obou tkáních; tento protein byl lokalizován v blízkosti primárních cilií. Zajímavostí bylo zvýšení exprese transkripčního faktoru GLI1 a PTCH1 v ameloblastomu, zatímco exprese transportních proteinů IFT20, IFT80, IFT88 zůstala oproti kontrolní tkáni beze změny. Při funkčním experimentu s inhibítorem SHH dráhy došlo k snížení exprese efektoru GLI1 a CCDND1, který působí jako regulátor buněčného cyklu, a k alteraci exprese transportních proteinů IFT20, IFT80, IFT88.

Tato studie, která zahrnovala komplexní hodnocení od popisné morfologie, přes imunofluorescenci a analýzu genové exprese až po funkční experiment s inhibítorem SHH dráhy, je příkladem vědecko–klinické spolupráce, která odhalila přítomnost poruch primárních cilií u ameloblastomu a změny v SHH dráze při její inhibici.

K plnému pochopení role těchto organel při iniciaci patologických procesů vedoucích ke vzniku a růstu odontogenních tumorů nám nicméně může pomoci jen další, podrobnější, výzkum se zaměřením na signalizaci SHH a ciliogenezi. Současně nám takovýto výzkum může otevřít cestu k další nechirurgické terapii tohoto typu nádorů.



Short Communication

Alteration of primary cilia morphology and associated signalling in ameloblastoma



Jana Filušová^a, Iveta Putnová^{a,b}, Pavel Hurník^{a,c,d}, Zdeněk Daněk^{e,f}, Ctirad Macháček^g, Jan Štembírek^{a,h}, Marcela Buchtová^{a,i}, Barbora Moldovan Putnová^{a,j,*}

^a Laboratory of Molecular Morphogenesis, Institute of Animal Physiology and Genetics, Czech Academy of Sciences, Brno, Czech Republic

^b Department of Anatomy, Histology and Embryology, University of Veterinary Sciences Brno, Brno, Czech Republic

^c Department of Clinical and Molecular Pathology and Medical Genetics, Faculty of Medicine and University Hospital Ostrava, Ostrava, Czech Republic

^d Department of Histology and Embryology, Medical Faculty, Masaryk University, Brno, Czech Republic

^e Department of Maxillofacial Surgery, University Hospital Brno and Faculty of Medicine, Masaryk University, Brno, Czech Republic

^f RECETOX, Faculty of Science, Masaryk University, Kotlarska 2, Brno, Czech Republic

^g Department of Pathology, University Hospital Brno and Faculty of Medicine, Masaryk University, Brno, Czech Republic

^h Department of Maxillofacial Surgery, University Hospital Ostrava, Ostrava, Czech Republic

ⁱ Department of Experimental Biology, Faculty of Science, Masaryk University, Brno, Czech Republic

^j Department of Pathological Morphology and Parasitology, University of Veterinary Sciences Brno, Brno, Czech Republic

ARTICLE INFO

Keywords:
Ameloblastoma
SHH
IFT
Primary cilia

ABSTRACT

Objectives: Primary cilium is a cellular organelle with growing significance confirmed in tumour biology. Primary cilia have been associated with fine tuning of numerous cell signalling pathways and the role of this structure in cancer initiation and progression is recently at the forefront of attention. Here, we investigated possible alterations in the occurrence of primary cilia and changes of associated signalling in ameloblastoma, which represents the most common odontogenic tumour.

Methods: We performed immunohistochemistry to assess the number and morphology of primary cilia in ameloblastoma tissues. The gene expression of key SHH pathway members was analysed by qPCR. As a functional experiment, we treated a primary ameloblastoma cell line by a SHH pathway inhibitor Sonidegib (LDE225).

Results: We uncovered differences in primary cilia distribution and appearance in histological subtypes of ameloblastoma with the highest number of ciliated cells in plexiform and follicular subtypes. SHH protein was located close to primary cilia in ameloblastoma epithelial cells and the expression of molecules downstream of SHH signalling was upregulated. Moreover, the inhibition of SHH pathway by Sonidegib caused downregulation of SHH effector gene *GLI1* and cell cycle regulator *CCND1* in ameloblastoma primary cell line. The inhibition of SHH signalling also altered the expression of molecules involved in intraflagellar transport.

Conclusions: In conclusion, our study uncovered alterations in number of ciliated cells and associated signalling in ameloblastoma, which indicate SHH inhibitors as potential therapeutic target to treat this disease.

1. Introduction

Primary cilia are solitary, microtubule-based organelles, which are found in most of vertebrate quiescent cells. They consist of an axoneme, projecting from the cell surface, membrane components, and a basal body, which anchors the primary cilium in plasmatic membrane (Sorokin, 1968). Their axoneme comprises of nine radial microtubule doublets, and lacks a central doublet, which is found in motile cilia (Satir &

Christensen, 2007; Satir et al., 2010). Although these organelles are unable to move, they play an important role in the cellular physiology during developmental processes of dental structures as well as related diseases (Berbari et al., 2009; Hampl et al., 2017). Their ciliary membrane contains a unique array of receptors that can detect various chemical and physical cues from the environment and relay them into intracellular signals (Alcedo et al., 1996). Up to now, associations between primary cilia and multiple signalling pathways have been

* Correspondence to: Laboratory of Molecular Morphogenesis, Institute of Animal Physiology and Genetics, Czech Academy of Sciences, Veverí 97, Brno, 602 00, Czech Republic.

E-mail address: bara.putnova@gmail.com (B. Moldovan Putnová).

<https://doi.org/10.1016/j.archoralbio.2022.105499>

Received 7 March 2022; Received in revised form 14 June 2022; Accepted 1 July 2022

Available online 4 July 2022

0003-9969/© 2022 The Authors. Published by Elsevier Ltd. This is an open access article under the CC BY license (<http://creativecommons.org/licenses/by/4.0/>).

demonstrated including Hedgehog (Rohatgi et al., 2007) or WNT pathways (Corbit et al., 2008), Receptor tyrosine kinases (RTKs) (Christensen et al., 2017) and G protein-coupled receptors (GPCRs) (Berbari et al., 2008).

Primary cilia appear to provide the spatial and temporal integration of multiple signalling pathways, which makes them an essential organelle in maintaining cellular homeostasis. In order for a primary cilium to respond properly to surrounding signals, its internal environment needs to maintain specific adaptive dynamics, which is regulated by the apparatus of intraflagellar transport (IFT) (Pazour et al., 2000). This process is driven by molecular motor proteins kinesin-2 and dynein-2 (Toropova et al., 2019; Zhao et al., 2012). The disruption of these motors or other IFT-related proteins thus leads to primary cilia defects and associated medical conditions, known collectively as ciliopathies (Li et al., 2004). Disorders or loss of primary cilia are also typical for certain types of tumors. Reduction of these organelles was noted in various carcinomas, such as breast cancer (Menzl et al., 2014), renal cancer (Basten et al., 2013), or pancreatic cancer (Seeley et al., 2009).

Here, we focus on the correlation of primary cilia disruption in ameloblastoma, which is an odontogenic tumor characteristic by upregulated expression of several genes associated with primary cilia and the Sonic Hedgehog signalling pathway (Gurgel et al., 2014). Ameloblastoma was reported to display an upregulation of *WNT1* expression, which is coordinated and coregulated with both cilia-related genes and Sonic Hedgehog signalling during odontogenesis (Hosoya et al., 2020; Liu et al., 2014). Moreover, SMO is the one of the most often mutated gene in ameloblastoma patients (Gultekin et al., 2018; Sweeney et al., 2014). Furthermore, a difference in the frequency of SMO mutation was found in various histological subtypes of ameloblastoma, where almost all plexiform types carried SMO mutation, while follicular type exhibited either SMO or BRAF mutations (Sweeney et al., 2014). Also, receptor *PTCH1* was found to be mutated in ameloblastoma patients (Shimura et al., 2020). Based on these facts, we proposed the disruption of ciliogenesis in ameloblastoma patients and analysed possible alterations in expression cilia-related genes such as *IFT20*, *IFT80*, *IFT88*, the Sonic Hedgehog receptor *PTCH1*, and its downstream transcription factor *GLI1*. Moreover, we focused on the morphology of primary cilia in ameloblastoma samples and analysed differences in primary cilia appearance in the epithelial component of this tumour.

2. Material and methods

2.1. Human tissues

Patient tissue samples were obtained from the Clinic of Oral and Maxillofacial Surgery of Faculty Hospital in Ostrava and from the Clinic of Oral and Maxillofacial Surgery of Faculty Hospital in Brno. We assessed 9 patients with ameloblastoma ($n = 3$ plexiform type; $n = 3$ follicular type; $n = 3$ basal cell type) and in total 6 patients with unrelated disease to obtain the control tissues (3 normal gingival tissue containing superficial lamina propria and gingival epithelium; 3 follicular sacs - dental sacs). Human embryonic tissue was obtained from Department of Pathology of Faculty Hospital Ostrava. All procedures were approved by the Hospital's Ethical Committees (Ethical approval number 472/2015, 469/2016).

2.2. Immunofluorescence and immunohistochemistry

For the immunofluorescent analysis of protein expression, the 5 μm sections were prepared. Sections were stained by Haematoxylin and Eosin and alternative sections were used for an immunofluorescent analysis of protein expression. Following proteins were evaluated using these primary antibodies: Anti-acetylated-alpha Tubulin (Lys40) in dilution 1:100 (Cat. No. 32-2700, Thermo Fisher Scientific, USA); Anti-Pericentrin antibody - Centrosome Marker in dilution 1:100 (Cat. No.

ab4448, Abcam, UK); Anti-Sonic Hedgehog antibody in dilution 1:50 (EP1190Y, Cat. No. 53281, Abcam, UK). DRAQ5™ in dilution 1:500 (Cat. No. 62251, Thermo Fisher Scientific, USA) was used to counterstain the nuclei. As a secondary antibody Alexa Fluor 488 was used in dilution 1:200 (Cat. No. A11008, Thermo Fisher Scientific, USA) and Alexa Fluor 565 in dilution 1:200 (Cat. No. A11004 Thermo Fisher Scientific, USA). In all cases, antigen retrieval was performed in citric acid, pH6 (20 min, hot bath 90 °C). The tissue sections were observed under the confocal microscope Leica TCS SP8 (Leica Microsystems, Germany) and edited in Adobe Photoshop 2021 (Adobe, USA). To determine the proliferation index, the tissue sections were prepared in the same way as described above. As a primary antibody rabbit monoclonal anti-Ki-67 antibody was used (Cat. No. RBK027, Zytomed Systems, Germany), 3,3'-Diaminobenzidine (DAB; Cat. No. K3468, Dako, USA) was used as a chromogenic substrate and Hematoxylin was applied to counterstain nuclei.

2.3. Analyses of primary cilia occurrence

The percentage of ciliated cells was counted in follicular, plexiform and basal cell type of ameloblastoma while using Image J (NIH, USA). Only the epithelial neoplastic cells were included in our analyses. Physiological gingiva was used as a control tissue. We counted only cells with a visible centrosome and cells in the division were excluded from analyses. Statistical significance was evaluated in GraphPad (GraphPad Software Inc., San Diego, CA, USA).

2.4. Isolation of RNA from FFPE samples

The total RNA was isolated from the formalin fixed paraffin embedded tissue blocks by RNeasy FFPE kit (Cat. No. 73504, Qiagen, Hilde, Germany) and transcribed into cDNA by gb Reverse Transcription Kit (Cat. No. 3012, Generi Biotech, Hradec Králové, Czech Republic).

All used tissue blocks were obtained from the Department of Pathology of University Hospital Ostrava (ethical approvals No. 472/2015, 469/2016).

2.5. Ameloblastoma cell cultures

Primary cell culture was established from plexiform ameloblastoma of a 39-year-old male patient, the tumour was localized in the mandibular region. The study was approved by the Ethics Committee of the University Hospital Brno, Czech Republic (No. 08-120619/EK, 2019). Tissue was dissected and proteolytic dissociation was performed in 1 mg/ml (300 U/ml) of Collagenase IV (cat. No. 4188, Warthington, Germany) in MEM α medium with no nucleosides (Gibco™, cat No. 12561056), which was supplemented with 10% FBS, at 37 °C for 16 h.

The dissociation solution was replaced by growth medium (RnT Prime, Epithelial Culture Medium, cat. No. CnT-PR, CELLnTEC) supplemented with penicillin/streptomycin, without a FBS supplementation. The cells were seeded to the 12-well culture plates in the concentration 20.000 cells/cm² and allowed to adhere to the culture dishes during 12 h of incubation at 37 °C in a humidified atmosphere containing 5% CO₂. The culture medium was replaced every 24 h. In the 40% confluence, the cells were stained by immunofluorescence for Cytokeratin and Vimentin to verify their origin and they were treated with Sonidegib (NVP-LDE225, Cat. No. S2151, Selleckchem, Houston, USA) in the 0.1 μM and 0.5 μM concentrations, or in vehicle (DMSO) as a control for 24 h. Each concentration was used on 3 replicates. Total RNA was isolated from cells using RNeasy Plus Mini Kit (cat No. 74136, Qiagen, USA).

2.6. Gene expression analyses by qPCR

The previously isolated mRNA was transcribed to the cDNA using Elite Reverse Transcription Kit (Cat. No. 3012, Generi Biotech, Hradec

Králové, Czech Republic).

qPCR gene expression analysis (TaqMan™ Gene Expression Assays, ThermoFisher Scientific, USA) was performed on the paraffin block samples and also on the samples obtained from the cell cultures. Following genes were examined: *CCND1* (ID: Hs00765553_m1), *GLI1* (ID: Hs00171790_m1), *PTCH1* (ID: Hs00181117_m1), *SHH* (ID: Hs00179843_m1), *IFT20* (ID: Hs015776074_m1), *IFT80* (ID: Hs00398803_m1), *IFT88* (ID: Hs00197926_m1) and *GAPDH* (ID:

HS02758991-m1) as a housekeeping reference gene. The qPCR was performed on Light Cycler 96 (Roche, Mannheim, Germany) during 40 cycles of 95 °C/15 s and 60 °C/1 min

In case of cell cultures, average of 3 technical replicates were generated for each of 4 biological replicates and these values were used for statistical analysis. Gene expression levels were calculated using delta-delta CT analysis with normalization to the level of housekeeping gene *GAPDH*. Obtained data were compared to the control (not treated)

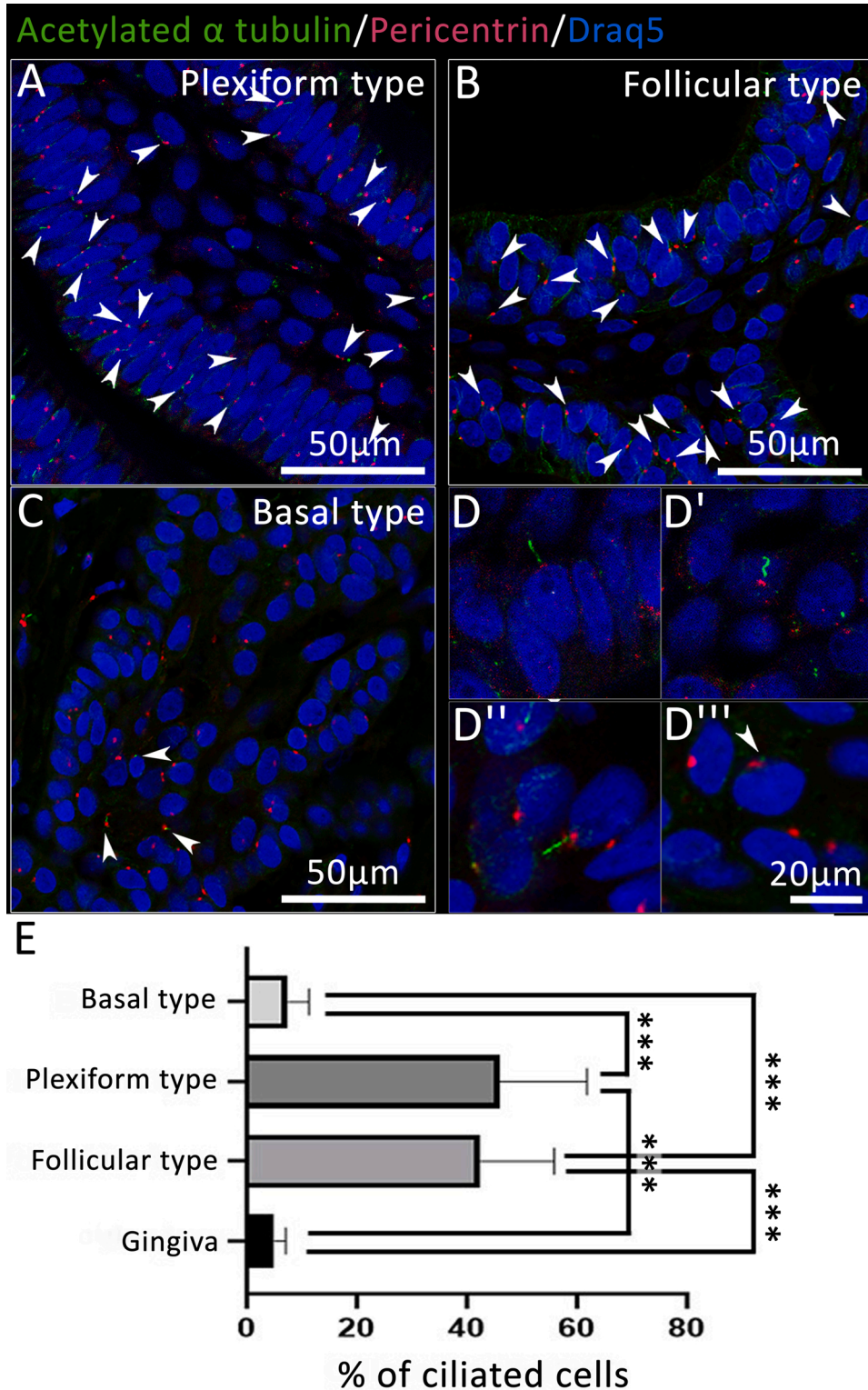


Fig. 1. Primary cilia morphology and occurrence in ameloblastoma.

The appearance of primary cilia is different in the plexiform (A) and follicular (B) histological subtypes (A, B) in comparison to basal subtype (C). Primary cilia are in ameloblastoma tissues often long, irregular, and variably curved (D-D'). The primary cilia in basal subtype of ameloblastoma are shorter compared to the other two histological forms, plexiform and follicular subtypes (D).

(E) The analyses of the percentage of ciliated cells display differences in primary cilia occurrence in gingiva and three histological subtypes of ameloblastoma. The number of ciliated cells was higher in plexiform and follicular histological subtype in comparison to basal cell subtype. The number of cells counted: 3626 (for plexiform and follicular subtypes), 1500 (for basal cell subtype) and 1184 (for gingiva); * ** (p < 0.0001).

cells, and the level of mRNA expression of control cells was set up as a value 1. The unpaired two-tailed Student's *t*-test was performed in GraphPad (GraphPad Software Inc., San Diego, CA, USA), and the differences in expression were considered to be significant at $p < 0.05$.

3. Results

3.1. Primary cilia morphology in ameloblastoma tissues

Follicular, plexiform and basal cell subtypes of ameloblastoma were selected for our analyses. The primary cilia were found to be abundant in plexiform and follicular ameloblastoma (Fig. 1A, B) while rare cilia were dispersed in the basal subtype (Fig. 1C). The morphology of primary cilia was altered with the presence of curved, S-shaped or extremely elongated cilia (Fig. 1D-D). The appearance of ciliated cells in the plexiform and follicular histological subtypes of ameloblastoma was significantly higher than in normal gingiva (Fig. 1E). Only the basal cell histological subtype of ameloblastoma did not exhibit significantly higher number of ciliated cells compared to the normal gingiva (Fig. 1E). Therefore, the evaluation of occurrence of ciliated cells uncovered

statistically significant differences among the ameloblastoma histological subtypes.

Because primary cilia are not present on dividing cells (as the centriole is needed during the replication), we wanted to clarify the possibility, if the lack of primary cilia in basal type of ameloblastoma is due to higher proliferation activity. However, the Ki-67 index analysis did not reveal statistically significant differences in the proliferation among individual ameloblastoma subtypes (Fig. 2).

3.2. Primary cilia associated Hh signalling is upregulated in ameloblastoma

SHH protein was found to be located asymmetrically in cytoplasm of ameloblastoma cells (Fig. 3A, B). SHH signal was located mostly in a close proximity to the primary cilia (Fig. 3A, B). The expression pattern suggests the accumulation of this protein in the area surrounding the transitional zone of primary cilia. There were not differences in the distribution of SHH signal in plexiform, follicular or basal subtypes and all subtypes displayed polarized expression of this protein in epithelial cells.

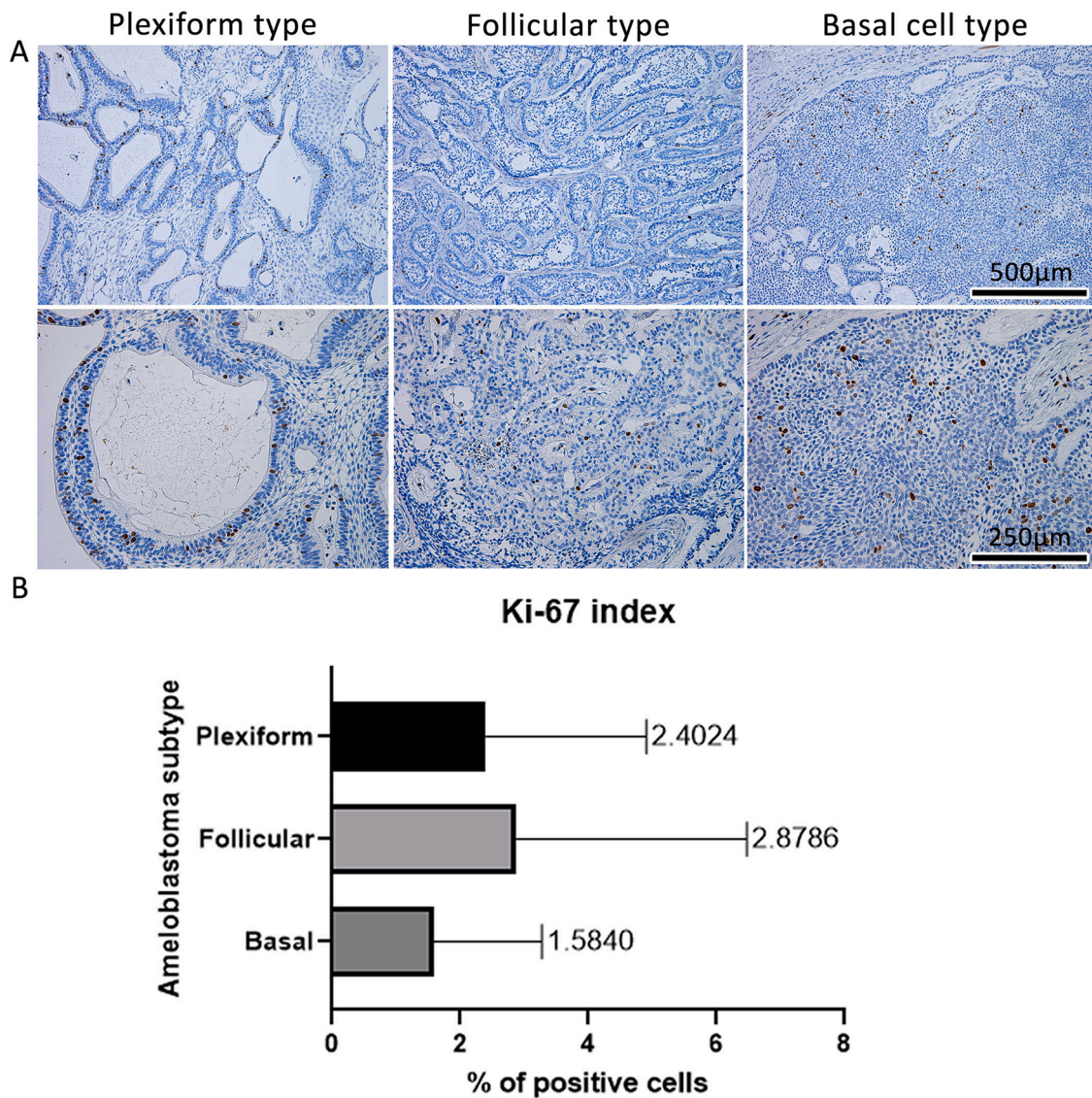


Fig. 2. Ki-67 index of a types of ameloblastoma.

(A) The positive cells were counted in the “hot spot” areas of neoplastic tissue. (B) There is no statistically significant difference among the histological subtypes. The data were obtained by evaluating 3 tissue samples from each histological subtype.

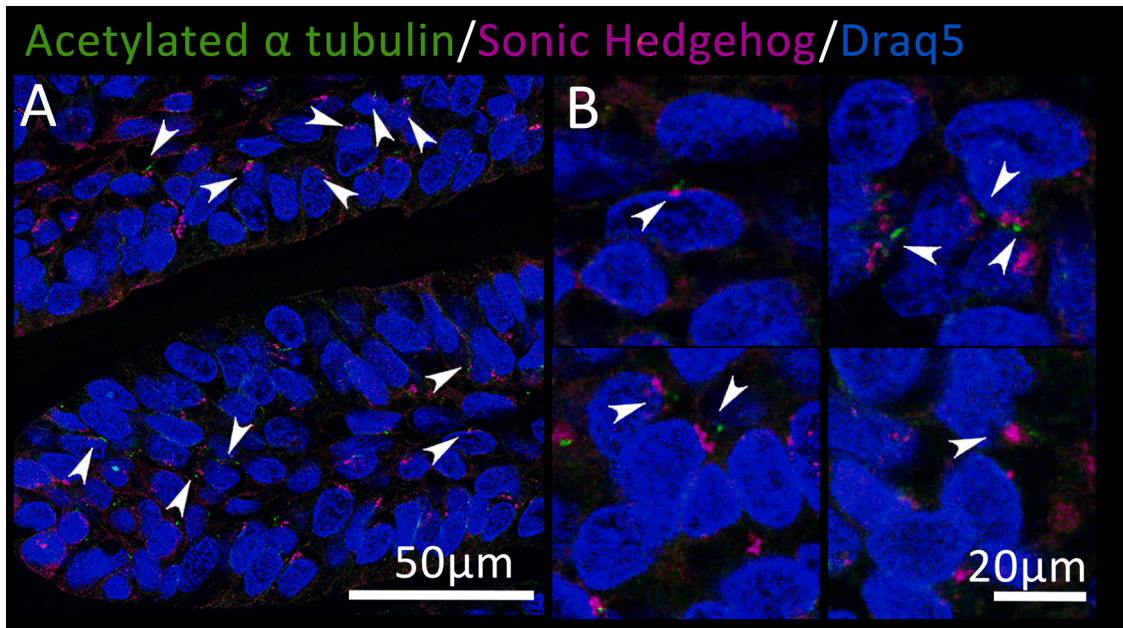


Fig. 3. Sonic hedgehog protein expression in ameloblastoma tissues. Immunohistochemical analyses of SHH protein (purple) expression revealed its localization mostly in the close proximity of primary cilia (green) in ameloblastoma epithelial cells. Nuclei are counterstained by Draq5 (blue). Scale bar – 20 µm.

We also asked if there are some similarities in primary cilia appearance and SHH protein expression between ameloblastoma and ameloblasts in embryonic tissues. Immunofluorescence detection of primary cilia by acetylated-alpha tubulin in human molar ameloblasts at a bell stage in embryonic day 56 (ED56) uncovered very similar

expression pattern in embryonic tissue to ameloblastoma epithelium (Fig. 4B). Expression of SHH in the human embryonic tooth was also comparable to epithelial cells in the ameloblastoma (Fig. 4C).

Next, we evaluated possible changes in gene expression of SHH signalling members (Fig. 5A) in ameloblastoma tissues where mRNA

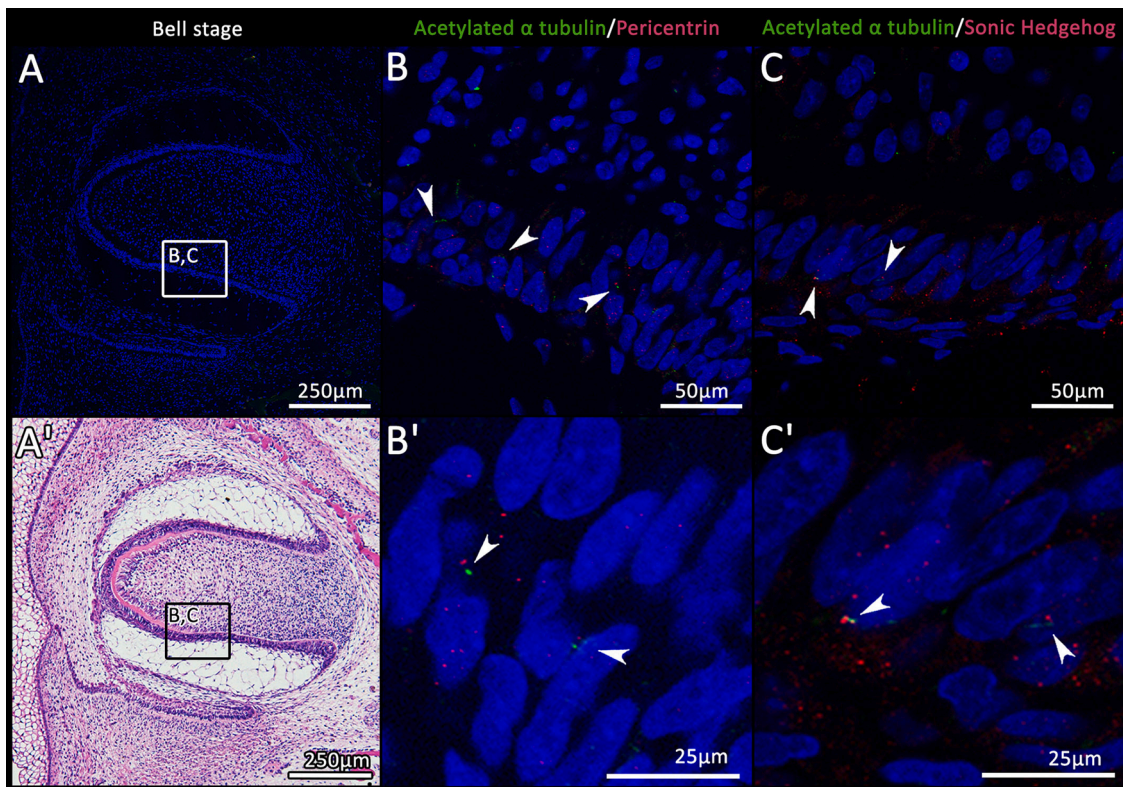


Fig. 4. Primary cilia and Sonic Hedgehog expression in a molar of human embryo (ED56). (A, A ') Transversal sections through human molar tooth at bell stage stained by DRAQ5 (A) and Haematoxylin and Eosin (A '). (B, B ') The primary cilia are sparsely located in the palisading layer of ameloblasts. There is a variation in the cilia length and their orientation seems to be randomized in this early stage of their differentiation. (C, C ') The Sonic Hedgehog signal is often located in the close proximity to the primary cilia. Nuclei are counterstained with DAPI.

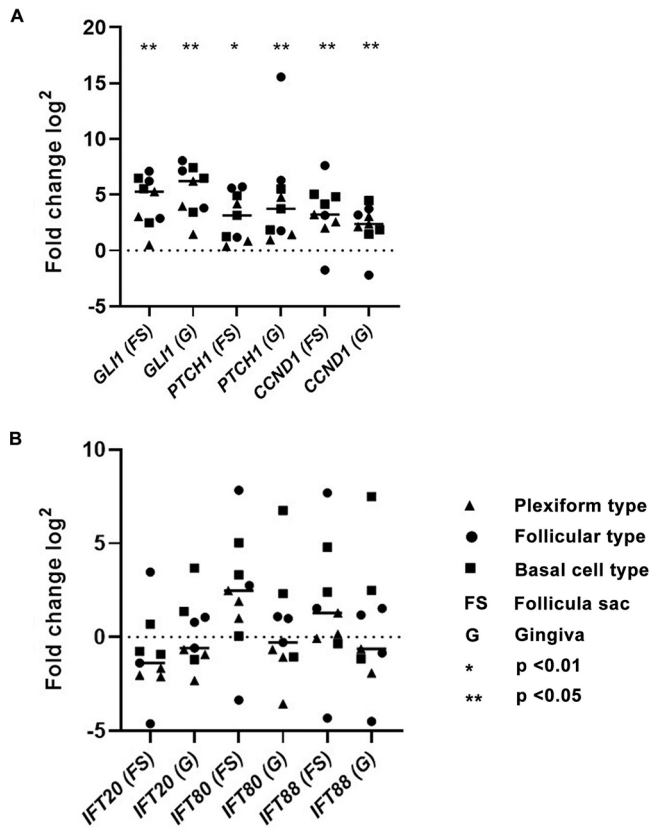


Fig. 5. Gene expression analysis of SHH signalling pathway members and molecules of intraflagellar transport in ameloblastoma tissues.

Two types of tissue were used as controls: follicular sac (FS) and normal gingiva (G). (A) SHH pathway members (*GLI1* and *PTCH1*) were statistically significantly upregulated in ameloblastoma tissues isolated from paraffin-embedded samples. Moreover, *CCND1* was significantly upregulated. There was no statistically significant difference when comparing results using two different control tissues.

(B) The gene expression of intraflagellar transport molecules (*IFT20*, *IFT80* and *IFT88*) were not found to be significantly changed in comparison to control gingiva.

The plexiform ameloblastomas are depicted as triangles, follicular as dots and basal cell ameloblastomas as squares.

The expression levels of control tissues were set up as 1; all the values are displayed in logarithm form (0 on the x axis shows control expression values).

was isolated from paraffin embedded samples. The expression of transcription factor *GLI1*, which is effector of SHH pathway and the receptor *PTCH1* was upregulated in ameloblastoma samples in comparison to control gingiva and follicular sac (Fig. 5A). No statistically significant differences were observed among individual histological subtypes.

As SHH pathway is able to stimulate proliferation, we also evaluated gene expression of *CCND1*, coding Cyclin D1, known regulator of cell cycle (Todd et al., 2002). Expression of *CCND1* was upregulated in all types of ameloblastoma tissues compared to the normal gingiva and follicular sac (Fig. 5A). There were not significant differences in *CCND1* expression when comparing plexiform, follicular or basal subtypes (Fig. 5A).

The expression of genes coding intraflagellar transport proteins *IFT20*, *IFT80* and *IFT88* was not changed from their expression in normal gingiva and follicular sac (Fig. 5B). Samples of basal cell subtype of ameloblastoma exhibited higher expression of all analysed intraflagellar proteins (*IFT20*, *IFT80* and *IFT88*), however this difference was not statistically significant when compared to plexiform and follicular types (Fig. 5B). The results did not reveal statistically significant differences when they were compared to different type of control tissues (follicular

sac or gingiva) (Fig. 5).

3.3. Effect of Hedgehog pathway inhibition on ameloblastoma cell line

Freshly dissected ameloblastoma tissue of patient mandible was used to establish primary cell line. Cells were treated with SHH inhibitor Sonidegib while using two different concentrations (0.1 μ M and 0.5 μ M) for 24 h and the effect on selected members of SHH pathway or primary cilia signalling was evaluated. A downregulation of SHH effector *GLI1* was observed at both used concentrations (Fig. 6A). However, statistically significant change in comparison to control was found only when using higher concentration of Sonidegib (Fig. 6A). The expression of SHH receptor *PTCH1* was not significantly affected by Sonidegib at any of used concentrations (Fig. 6B).

As increased SHH signalling inhibitors negatively regulate the proliferation of oral tumours (Freitas et al., 2020), we also evaluated the effect of Sonidegib on Cyclin D1 expression in our ameloblastoma cell line. We observed a downregulation of *CCND1* expression after treatment with higher concentration of Sonidegib (0.5 μ M), however this change was not statistically significant in comparison to control (Fig. 6C).

Next, we wanted to determine the effect of SHH inhibitor on expression of intraflagellar transport molecules (Fig. 7). The expression of *IFT20* was statistically significantly upregulated after Sonidegib treatment when compared to cultures grown just in the medium (Fig. 7A). There were no statistically significant changes in *IFT80* expression in comparison to controls (Fig. 7B). The expression of *IFT88* was significantly downregulated in comparison to control medium (Fig. 7C) when using higher concentration of Sonidegib (0.5 μ M).

4. Discussion

Ameloblastoma is probably one of the most controversial neoplasms of the facial region. Ameloblastomas do not belong among the most common lesions of the jaw, but they are the most common odontogenic neoplasm in human (Philipsen & Reichart, 2006; Reichart et al., 1995). Ameloblastomas are benign lesion, but they expand intensively into surrounding tissues and the recurrence after a surgical excision is very high, even when „clean margins“ are confirmed (Yang et al., 2017).

The pathogenesis of this neoplasm is still not well understood. As a tumour of epithelial origin, they were proposed to arise from remnants of dental lamina and the tumour itself resembles various stages resembling odontogenesis (Heikinheimo et al., 2015; Melrose, 1999).

Here, we focused on primary cilia appearance in ameloblastoma and evaluated possible differences among their histological subtypes. Up to our best knowledge, there is no described evidence of a difference in the biological behaviour, in terms of local recurrence or progression, between various histological subtypes of ameloblastoma. However, our analyses uncovered higher abundance of ciliary cells with elongated cilia in the most common subtypes of ameloblastoma, plexiform and follicular types. Differences in primary cilia size or number have been previously noticed in many types of tumours such as breast cancer, renal cancer or pancreatic cancer (Basten et al., 2013; Schraml et al., 2009; Seeley et al., 2009; Yuan et al., 2010). However, in most of these cases, the reduction of primary cilia or their shortening was determined while cilia elongation or their increased number is uncommon event in tumour biology (Liu, Kiseleva, & Golemis, 2018). Even though, primary cilia have been found on almost all cell types of human body, they are not present on the cell for the whole cell cycle (Plotnikova et al., 2009).

One possible explanation of these differences can be generally very slow progression of ameloblastoma. As primary cilia are detectable just in non-dividing cells, ameloblastoma epithelium is fulfilled by these cells, which is in contrast to the fast-dividing cells in tumours such as pancreatic or breast carcinoma (Menzl et al., 2014; Seeley et al., 2009).

Interestingly, the basal subtype of ameloblastoma did not exhibit difference in the number of ciliated cells in comparison to gingiva. Basal

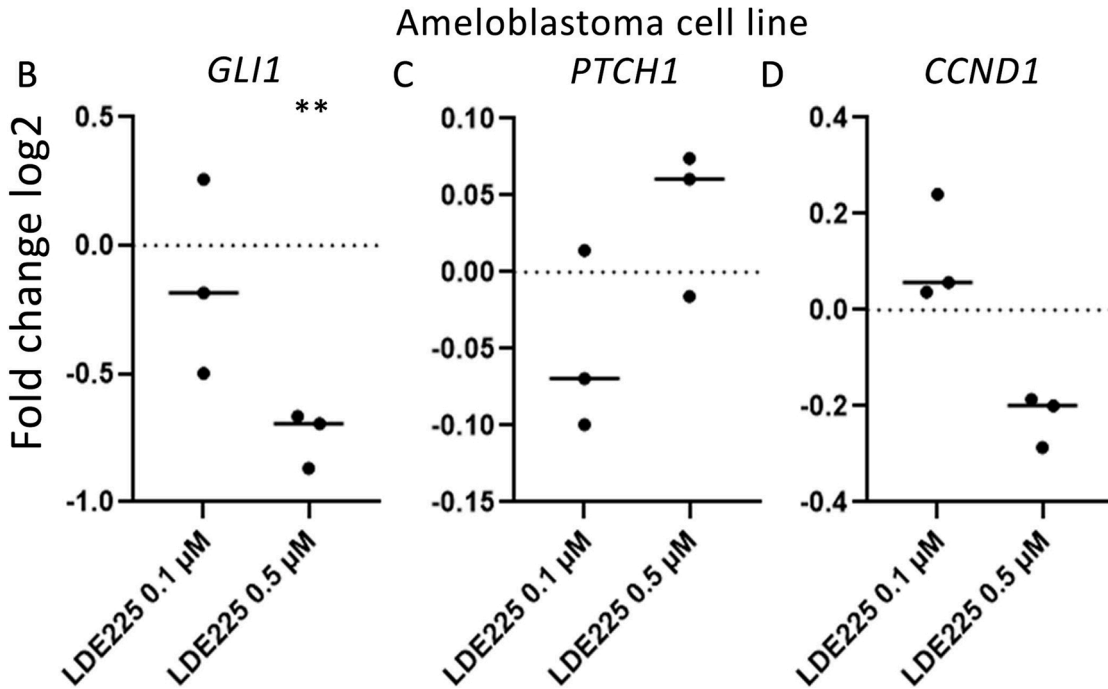
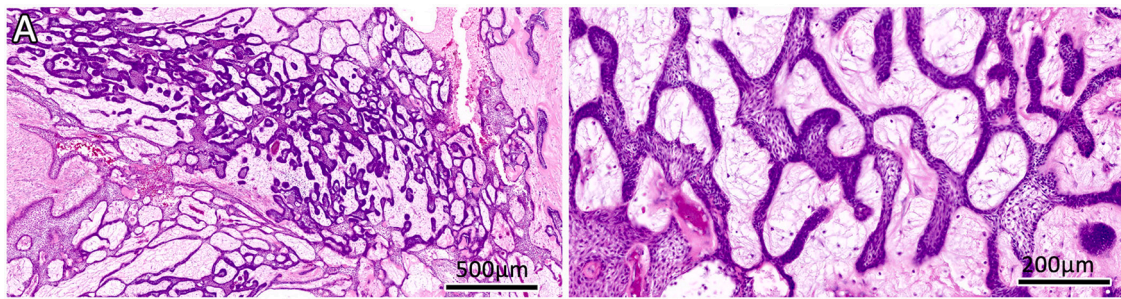


Fig. 6. Gene expression analysis of *GLI1*, *PTCH1* and *CCND1* in primary ameloblastoma cell line.

Cell cultures were treated by Sonidegib (LDE225) for 24 h in concentrations 0.1 μM and 0.5 μM. (A) Tissue used for the primary cell culture was collected from plexiform ameloblastoma type; Haematoxylin and Eosin staining. (B) There was statistically significant upregulation of *GLI1* expression in cultures treated with SHH inhibitor Sonidegib. (C) No changes in *PTCH1* expression were observed when compared Sonidegib treated cultures to untreated control cells. (D) *CCND1* expression was slightly decreased in the cells treated by Sonidegib in concentration 0.5 μM but these changes did not exhibit statistical significance.

The expression levels of control tissues were set up as 1; all the values are displayed in logarithm form (0 on the x axis shows control expression values).

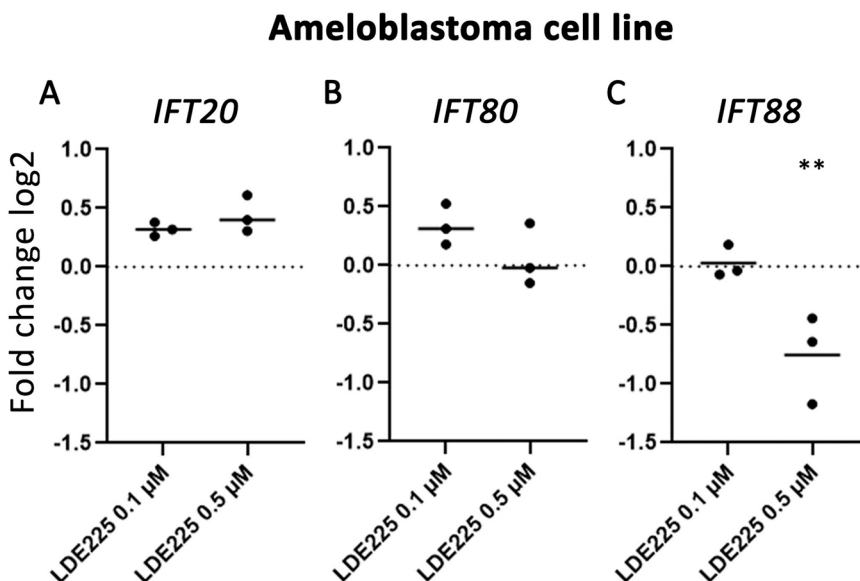


Fig. 7. Gene expression analysis of *IFT20*, *IFT80* and *IFT88* in primary ameloblastoma cell line.

Cell cultures were treated by Sonidegib (LDE225) for 24 h in concentrations 0.1 μM and 0.5 μM. (A) There was upregulation of *IFT20* expression after Sonidegib treatment, which was statistically significant when using lower Sonidegib concentration. (B) Expression levels of *IFT80* did not display any statistically significant changes. (C) There was statistically significant downregulation of *IFT88* expression in cultures treated by 0.5 μM Sonidegib.

The expression levels of control tissues were set up as 1; all the values are displayed in logarithm form (0 on the x axis shows control expression values).

cell ameloblastoma is very rare cancer in human population (Sridhar et al., 2015; Wright & Vered, 2017). It is probable that because of this low incidence, there has not been up to now recognised any significant difference in the biological behaviour of this subtype when compared to the more common variants such as plexiform or follicular types. Our findings demonstrate a variability in ameloblastoma pathogenesis and uncovered differences in cell behaviour, which indicate necessity to evaluate individual histological subtypes separately as different processes may be involved in initiation and progression of these tumour subtypes.

The essential function of primary cilia to Hedgehog pathway signalling was uncovered almost two decades ago (Huangfu et al., 2003). The primary cilium is crucial to respond to the SHH ligands in mammalian cells (Bangs & Anderson, 2017). The expression of SHH protein has been previously investigated in ameloblastoma on the protein level, where ameloblastoma epithelial cells were found to be highly positive by immunohistochemistry detection (Kumamoto et al., 2004; Zhang et al., 2006). However, the information about its localisation in the cells was missing. Using immunofluorescent labelling of SHH protein allowed us to uncover its polarized expression in the epithelial cells of ameloblastoma concentrating in close proximity to the primary cilium.

On the RNA level, we found a high expression of SHH effector *GLI1* as well as its receptor *PTCH1* in ameloblastoma tissues. Previously, high expression of *PTCH1* receptor was detected in several stages through tooth development (Hardcastle et al., 1998) and in ameloblastoma samples when protein expression was detected by immunohistochemistry (Barreto et al., 2002; Kumamoto et al., 2004). Increased level of *PTCH1* and *GLI1* was detected also in laser capture dissected ameloblastoma tissues (DeVilliers et al., 2011) and our data further support these findings. We also evaluated possible differences in expression of SHH signalling members among ameloblastoma subtypes and have not found significant variability in *GLI1* and *PTCH1* expression regardless of there was a significant difference in the number of ciliated cells in subtypes.

As intraflagellar transport molecules (IFT20, IFT80, IFT88) are key for primary cilia function, we evaluated their expression and surprisingly, we have not found significant differences in their expression when compared to a normal gingiva or follicular sac. On the other hand, samples of basal cell subtype displayed tendency to exhibit higher expression in all three analysed intraflagellar transport molecules in contrast to plexiform and follicular subtypes. As primary cilia function is affected by cell dynamic and cell cycle progression, we evaluated *CCND1* expression as marker of increased cell proliferation. Increased *CCND1* expression was previously determined in several cancer types leading to dysregulation in CDK activity and rapid cell growth (Qie & Diehl, 2016). Significantly increased expression of *CCND1* was found in all ameloblastoma tissues, however no difference was determined between individual histological subtypes, which would explain differences in IFT molecules expression. This differential response of basal cell subtype will need further experimental clarification in future.

Treatment of the ameloblastoma primary cell line by Hedgehog signalling inhibitor Sonidegib (LDE225; SMO inhibitor) lead to downregulation of *GLI1* expression. These results are corresponding to experiments performed on basal cell carcinoma, medulloblastoma or prostate cancer (Dummer et al., 2020; Rodon et al., 2014; Ross et al., 2017). No significant changes were observed in the expression level of receptor *PTCH1* in our study after the treatment with Sonidegib for 24 h. As this is very short timepoint, back loop regulation on receptor level has not been probably initiated yet.

Even though these data are not statistically significant, there was a trend towards downregulation of *CCND1* in treated cells while using higher concentration of Sonidegib. Similarly, the association between SHH signalling and cell proliferation was found in ameloblastoma cells using AM-1 cells (Kanda et al., 2013). AM-1 cell line also express *SHH* and *PTCH1*, and their growth was suppressed by using SHH antibody or cyclopamine (pan-inhibitor of SHH signalling). Their results also

indicated an anti-apoptotic role of SHH signalling in the growth of ameloblastoma cells (Kanda et al., 2013). All these mentioned facts are suggesting that blockage of Hh pathway in ameloblastoma cells leads to their lower proliferation ability and indicate clinical potential of SHH inhibitors to slow down ameloblastoma growth in patient.

Interestingly, after the Sonidegib treatment, there was upregulation of *IFT20* expression on the mRNA level while *IFT88* expression was downregulated compared to not treated cells used as a control. Why there is differential respond of IFT molecules to SHH inhibition in ameloblastoma cell line, it is difficult to explain as there is only sporadic information about the role of individual IFT molecules in solid cancers and no information at all about their role in ameloblastoma. Moreover, IFT molecules can play role not just in primary cilia function and signalling, but also in regulation of cell migration independently of the primary cilium. For example, IFT20 was found to regulate cell polarity during collective cancer cell invasion in colorectal cancer (Aoki et al., 2019) and breast cancer (Yang et al., 2021). Uncovering specific roles of individual IFT molecules in cellular processes will be necessary to follow first and special attention should be paid to differences between ciliated and non-ciliated tumour types.

5. Conclusions

In contrast to most of tumour types, primary cilia are well formed and elongated in ameloblastoma epithelial cells. However, there are some differences among histological subtypes and our analyses uncovered lower number of ciliated cells in basal cell subtype of ameloblastoma. Moreover, we found alterations in SHH signalling and SMO inhibitor Sonidegib affected not just downstream Hh signalling, but also the expression of intraflagellar transport molecules. However, further uncovering of interplay between the Sonic Hedgehog signalling and ciliogenesis in odontogenetic tumours will be crucial for understanding the role of these organelles in initiation of pathological processes leading to neoplasia growth, which can open new avenues for future therapies.

Author Contributions

Study design: BMP, MB. Performed experiments, data analyses, contributed to material: JF, IP, CM, PH, ZD, JS. Original draft writing, literature search: JF, BMP, MB, IP. Final manuscript inspection: BMP, MB. Grant support: MB, ZD. All authors contributed to the article and approved the submitted version.

Funding

This research was supported by the Ministry of Health of the Czech Republic (grant NV20–08–00205) and by Ministry of Health of the Czech Republic – conceptual development of research organization (FNBr, 65269705).

CRedit authorship Contribution statement

Study design: BMP, MB Performed experiments, data analyses, contributed to material: JF, IP, CM, PH, ZD, JS Original draft writing, literature search: JF, BMP, MB, IP Final manuscript inspection: BMP, MB Grant support: Ministry of Health of the Czech Republic (grant NV20–08–00205 and conceptual development of research organization FNBr, 65269705).

Declaration of Competing Interest

The authors declare that they have no known competing financial interests or personal relationships that could have appeared to influence the work reported in this paper.

Acknowledgments

Authors would like to thank to Lucie Vrlíková and Denisa Lusková for histological processing of tissues.

References

- Alcedo, J., Ayzenzon, M., Von Ohlen, T., Noll, M., & Hooper, J. E. (1996). The *Drosophila* smoothened gene encodes a seven-pass membrane protein, a putative receptor for the hedgehog signal. *Cell*, *86*(2), 221–232. [https://doi.org/10.1016/s0092-8674\(00\)80094-x](https://doi.org/10.1016/s0092-8674(00)80094-x)
- Aoki, T., Nishita, M., Sonoda, J., Ikeda, T., Kakeji, Y., & Minami, Y. (2019). Intraflagellar transport 20 promotes collective cancer cell invasion by regulating polarized organization of Golgi-associated microtubules. *Cancer Sci*. <https://doi.org/10.1111/cas.13970>
- Bangs, F., & Anderson, K. V. (2017). Primary cilia and mammalian hedgehog signaling. *Cold Spring Harbor Perspectives in Biology*, *9*(5). <https://doi.org/10.1101/cshperspect.a028175>
- Barreto, D. C., Bale, A. E., De Marco, L., & Gomez, R. S. (2002). Immunolocalization of PTCH protein in odontogenic cysts and tumors. *Journal of Dental Research*, *81*(11), 757–760. <https://doi.org/10.1177/0810757>
- Basten, S. G., Willekers, S., Vermaat, J. S., Slaats, G. G., Voest, E. E., van Diest, P. J., & Giles, R. H. (2013). Reduced cilia frequencies in human renal cell carcinomas versus neighboring parenchymal tissue. *Cilia*, *2*(1), 2. <https://doi.org/10.1186/2046-2530-2-2>
- Berbari, N. F., Lewis, J. S., Bishop, G. A., Askwith, C. C., & Mykytyn, K. (2008). Bardet-Biedl syndrome proteins are required for the localization of G protein-coupled receptors to primary cilia. *Proceedings of the National Academy of Sciences United States A*, *105*(11), 4242–4246. <https://doi.org/10.1073/pnas.0711027105>
- Berbari, N. F., O'Connor, A. K., Haycraft, C. J., & Yoder, B. K. (2009). The primary cilium as a complex signaling center. *Current Biology*, *19*(13), R526–535. <https://doi.org/10.1016/j.cub.2009.05.025>
- Christensen, S. T., Morthorst, S. K., Mogensen, J. B., & Pedersen, L. B. (2017). Primary cilia and coordination of receptor tyrosine kinase (RTK) and transforming growth factor beta (TGF-beta) signaling. *Cold Spring Harbor Perspectives in Medicine*, *9*(6). <https://doi.org/10.1101/cshperspect.a028167>
- Corbit, K. C., Shyer, A. E., Dowdle, W. E., Gauden, J., Singla, V., Chen, M. H., & Reiter, J. F. (2013). Kif3a constrains beta-catenin-dependent Wnt signalling through dual ciliary and non-ciliary mechanisms. *Nature Cell Biology*, *10*(1), 70–76. <https://doi.org/10.1038/ncb1670>
- DeVilliers, P., Suggs, C., Simmons, D., Murrach, V., & Wright, J. T. (2011). Microgenomics of ameloblastoma. *Journal of Dental Research*, *90*(4), 463–469. <https://doi.org/10.1177/0022034510391791>
- Dummer, R., Liu, L., Squitieri, N., Gutzmer, R., & Lear, J. (2020). Expression of Glioma-associated oncogene homolog 1 as biomarker with sonidegib in advanced basal cell carcinoma. *Oncotarget*, *11*(37), 3473–3483. <https://doi.org/10.18632/oncotarget.27735>
- Freitas, R. D., Dias, R. B., Vidal, M. T. A., Valverde, L. de F., Costa, R. G. A., Damasceno, A. K. A., ... Gurgel Rocha, C. A. (2020). Inhibition of CAL27 Oral Squamous Carcinoma Cell by Targeting Hedgehog Pathway With Vismodegib or Itraconazole. *Front Oncol*. <https://doi.org/10.3389/fonc.2020.563838>
- Gultekin, S. E., Aziz, R., Heydt, C., Senguven, B., Zoller, J., Safi, A. F., & Buettner, R. (2018). The landscape of genetic alterations in ameloblastomas relates to clinical features. *Virchows Archive*, *472*(5), 807–814. <https://doi.org/10.1007/s00428-018-2305-5>
- Gurgel, C.A., Buim, M.E., Carvalho, K.C., Sales, C.B., Reis, M.G., de Souza, R.O., Ramos, E.A. (2014). Transcriptional profiles of SHH pathway genes in keratocystic odontogenic tumor and ameloblastoma. *J Oral Pathol Med*, *43*(8), 619–626. <https://doi.org/10.1111/jop.12180>
- Hampel, M., Cela, P., Szabo-Rogers, H. L., Kunova Bosakova, M., Dosedelova, H., Krejci, P., & Buchtova, M. (2017). Role of Primary Cilia in Odontogenesis. *Journal of Dental Research*, *96*(9), 965–974. <https://doi.org/10.1177/0022034517713688>
- Hardcastle, Z., Mo, R., Hui, C. C., & Sharpe, P. T. (1998). The Shh signalling pathway in tooth development: Defects in Gli2 and Gli3 mutants. *Development*, *125*(15), 2803–2811. <https://doi.org/10.1242/dev.125.15.2803>
- Heikinheimo, K., Kurppa, K. J., Laiho, A., Peltonen, S., Bernal, A., Bouattour, A., & Morgan, P. R. (2015). Early dental epithelial transcription factors distinguish ameloblastoma from keratocystic odontogenic tumor. *Journal of Dental Research*, *94*(1), 101–111. <https://doi.org/10.1177/0022034514556815>
- Hosoya, A., Shalehin, N., Takebe, H., Shimo, T., & Irie, K. (2020). Sonic hedgehog signaling and tooth development. *International Journal of Molecular Sciences*, *21*(5). <https://doi.org/10.3390/ijms21051587>
- Huangfu, D., Liu, A., Rakeman, A. S., Murcia, N. S., Niswander, L., & Anderson, K. V. (2003). Hedgehog signalling in the mouse requires intraflagellar transport proteins. *Nature*, *426*(6962), 83–87. <https://doi.org/10.1038/nature02061>
- Kanda, S., Mitsuyasu, T., Nakao, Y., Kawano, S., Goto, Y., Matsubara, R., & Nakamura, S. (2013). Anti-apoptotic role of the sonic hedgehog signaling pathway in the proliferation of ameloblastoma. *Int J Oncol*. <https://doi.org/10.3892/ijo.2013.2010>
- Kumamoto, H., Ohki, K., & Ooya, K. (2004). Expression of Sonic hedgehog (SHH) signaling molecules in ameloblastomas. *Journal of Oral Pathology & Medicine*, *33*(3), 185–190. <https://doi.org/10.1111/j.0904-2512.2004.00070.x>
- Li, J. B., Gerdes, J. M., Haycraft, C. J., Fan, Y., Teslovich, T. M., May-Simera, H., & Dutcher, S. K. (2004). Comparative genomics identifies a flagellar and basal body proteome that includes the BBS5 human disease gene. *Cell*, *117*(4), 541–552. [https://doi.org/10.1016/s0092-8674\(04\)00450-7](https://doi.org/10.1016/s0092-8674(04)00450-7)
- Liu, B., Chen, S., Cheng, D., Jing, W., & Helms, J. A. (2014). Primary cilia integrate hedgehog and Wnt signaling during tooth development. *Journal of Dental Research*, *93*(5), 475–482. <https://doi.org/10.1177/0022034514528211>
- Liu, H., Kiseleva, A. A., & Golemis, E. A. (2018). Ciliary signalling in cancer. *Nat Rev Cancer*. <https://doi.org/10.1038/s41568-018-0023-6>
- Melrose, R. J. (1999). Benign epithelial odontogenic tumors. *Seminars in Diagnostic Pathology*, *16*(4), 271–287. (<http://www.ncbi.nlm.nih.gov/pubmed/10587269>).
- Menzl, I., Lebeau, L., Pandey, R., Hassounah, N. B., Li, F. W., Nagle, R., & McDermott, K. M. (2014). Loss of primary cilia occurs early in breast cancer development. *Cilia*, *3*, 7. <https://doi.org/10.1186/2046-2530-3-7>
- Pazour, G. J., Dickert, B. L., Vucica, Y., Seeley, E. S., Rosenbaum, J. L., Witman, G. B., & Cole, D. G. (2000). Chlamydomonas IFT88 and its mouse homologue, polycystic kidney disease gene tg737, are required for assembly of cilia and flagella. *Journal of Cell Biology*, *151*(3), 709–718. <https://doi.org/10.1083/jcb.151.3.709>
- Philipsen, H. P., & Reichart, P. A. (2006). Classification of odontogenic tumours. A historical review. *Journal of Oral Pathology & Medicine*, *35*(9), 525–529. <https://doi.org/10.1111/j.1600-0714.2006.00470.x>
- Plotnikova, O. V., Pugacheva, E. N., & Golemis, E. A. (2009). Primary cilia and the cell cycle. *Methods Cell Biology*, *94*, 137–160. [https://doi.org/10.1016/S0091-679X\(08\)94007-3](https://doi.org/10.1016/S0091-679X(08)94007-3)
- Qie, S., & Diehl, J. A. (2016). Cyclin D1, cancer progression, and opportunities in cancer treatment. *Journal of Molecular Medicine (Berlin)*, *94*(12), 1313–1326. <https://doi.org/10.1007/s00109-016-1475-3>
- Reichart, P. A., Philipsen, H. P., & Sonner, S. (1995). Ameloblastoma: Biological profile of 3677 cases. *European Journal of Cancer Part B: Oral Oncology*, *31B*(2), 86–99. <http://www.ncbi.nlm.nih.gov/pubmed/7633291>
- Rodon, J., Tawbi, H.A., Thomas, A.L., Stoller, R.G., Turttschi, C.P., Baselga, J., Mita, A.C. (2014). A phase I, multicenter, open-label, first-in-human, dose-escalation study of the oral smoothened inhibitor Sonidegib (LDE225) in patients with advanced solid tumors. *Clin Cancer Res*, *20*(7), 1900–1909. <https://doi.org/10.1158/1078-0432.CCR-13-1710>
- Rohatgi, R., Milenkovic, L., & Scott, M. P. (2007). Patched1 regulates hedgehog signaling at the primary cilium. *Science*, *317*(5836), 372–376. <https://doi.org/10.1126/science.1139740>
- Ross, A. E., Hughes, R. M., Glavaris, S., Ghabili, K., He, P., Anders, N. M., & Antonarakis, E. S. (2017). Pharmacodynamic and pharmacokinetic neoadjuvant study of hedgehog pathway inhibitor Sonidegib (LDE-225) in men with high-risk localized prostate cancer undergoing prostatectomy. *Oncotarget*, *8*(61), 104182–104192. <https://doi.org/10.18632/oncotarget.22115>
- Satir, P., & Christensen, S. T. (2007). Overview of structure and function of mammalian cilia. *Annual Review of Physics*, *69*, 377–400. <https://doi.org/10.1146/annurev.physiol.69.040705.141236>
- Satir, P., Pedersen, L. B., & Christensen, S. T. (2010). The primary cilium at a glance. *Journal of Cell Science*, *123*(Pt 4), 499–503. <https://doi.org/10.1242/jcs.050377>
- Schraml, P., Frew, I. J., Thoma, C. R., Boysen, G., Struckmann, K., Krek, W., & Moch, H. (2009). Sporadic clear cell renal cell carcinoma but not the papillary type is characterized by severely reduced frequency of primary cilia. *Modern Pathology*, *22*(1), 31–36. <https://doi.org/10.1038/modpathol.2008.132>
- Seeley, E. S., Carriere, C., Goetze, T., Longnecker, D. S., & Korc, M. (2009). Pancreatic cancer and precursor pancreatic intraepithelial neoplasia lesions are devoid of primary cilia. *Cancer Research*, *69*(2), 422–430. <https://doi.org/10.1158/0008-5472.CAN-08-1290>
- Shimura, M., Nakashiro, K. I., Sawatani, Y., Hasegawa, T., Kamimura, R., Izumi, S., & Kawamata, H. (2020). Whole exome sequencing of SMO, BRAF, PTCH1 and GNAS in odontogenic diseases. *In Vivo*, *34*(6), 3233–3240. <https://doi.org/10.21873/in vivo.12159>
- Sorokin, S. P. (1968). Reconstructions of centriole formation and ciliogenesis in mammalian lungs. *Journal of Cell Science*, *3*(2), 207–230. <https://doi.org/10.1242/jcs.3.2.207>
- Sridhar, M., Bhaskar Reddy, L. R., Kharat, S., Mahesh, B. S., Gandhi, L., Mahendra, A., & Grewal, P. (2015). Basal cell ameloblastoma: A rare histological variant of an uncommon tumor. *Nigerian Journal of Surgery*, *21*(1), 66–69. <https://doi.org/10.4103/1117-6806.152730>
- Sweeney, R. T., McClary, A. C., Myers, B. R., Biscocho, J., Neahring, L., Kwei, K. A., & West, R. B. (2014). Identification of recurrent SMO and BRAF mutations in ameloblastomas. *Nature Genetics*, *46*(7), 722–725. <https://doi.org/10.1038/ng.2986>
- Toropova, K., Zalyte, R., Mukhopadhyay, A. G., Mladenov, M., Carter, A. P., & Roberts, A. J. (2019). Structure of the dynein-2 complex and its assembly with intraflagellar transport trains. *Nature Structural & Molecular Biology*, *26*(9), 823–829. <https://doi.org/10.1038/s41594-019-0286-y>
- Wright, J. M., & Vered, M. (2017). Update from the 4th edition of the world health organization classification of head and neck tumours: Odontogenic and maxillofacial bone tumors. *Head & Neck Pathology*, *11*(1), 68–77. <https://doi.org/10.1007/s12105-017-0794-1>
- Yang, H., Zhang, F., Long, H., Lin, Y., Liano, J., Xia, H., & Huang, K. (2021). IFT20 Mediates the Transport of Cell Migration Regulators From the Trans-Golgi Network to the Plasma Membrane in Breast Cancer Cells. *Front Cell Dev Biol*. <https://doi.org/10.3389/fcell.2021.632198>
- Yang, R., Liu, Z., Gokavrapu, S., Peng, C., Ji, T., & Cao, W. (2017). Recurrence and cancerization of ameloblastoma: multivariate analysis of 87 recurrent craniofacial ameloblastoma to assess risk factors associated with early recurrence and secondary ameloblastic carcinoma. *Chinese Journal of Cancer Research*, *29*(3), 189–195. <https://doi.org/10.21147/j.issn.1000-9604.2017.03.04>

- Yuan, K., Frolova, N., Xie, Y., Wang, D., Cook, L., Kwon, Y. J., & Frost, A. R. (2010). Primary cilia are decreased in breast cancer: analysis of a collection of human breast cancer cell lines and tissues. *Journal of Histochemistry and Cytochemistry*, 58(10), 857–870. <https://doi.org/10.1369/jhc.2010.955856>
- Zhang, L., Chen, X. M., Sun, Z. J., Bian, Z., Fan, M. W., & Chen, Z. (2006). Epithelial expression of SHH signaling pathway in odontogenic tumors. *Oral Oncology*, 42(4), 398–408. <https://doi.org/10.1016/j.oraloncology.2005.09.008>
- Zhao, C., Omori, Y., Brodowska, K., Kovach, P., & Malicki, J. (2012). Kinesin-2 family in vertebrate ciliogenesis. *Proc Natl Acad Sci United States A*, 109(7), 2388–2393. <https://doi.org/10.1073/pnas.1116035109>

Experimentální chirurgie v oblasti temporomandibulárního kloubu

Temporomandibulární kloub (TMK) spojuje kloubní výběžek dolní čelisti se spánkovou kostí lebky. Od okolních struktur je oddělen pomocí kloubního pouzdra a kloubním diskem rozdělen na horní kloubní prostor, který umožňuje translační pohyby, a dolní kloubní prostor, který umožňuje naopak rotační pohyby (Shu et al., 2022).

Povrch kloubních ploch je tvořen kombinací hyalinní a vazivové chrupavky s omezenou regenerační aktivitou, které umožňují kompenzovat velké tlaky při žvýkání (Ottaria et al., 2018). Nadměrný pohyb nebo změna směru pohybu kloubní hlavičky významně ovlivňuje kloubní funkci (Zemen, 1999). Právě při hypermobilitě čelistního kloubu dochází při otvírání úst k tzv. „přeskakování“ kloubní hlavičky společně s kloubním diskem přes kloubní hrbolek (*tuberculum articulare*), čímž dochází k jeho traumatizaci (Machoň, 2005). U člověka se hypermobilita projevuje „vyskakovaním“ čelisti při širokém otvírání úst, „lupnutím“ během otevíracího pohybu a v některých případech i bolestivostí (Taskesen et al., 2020).

V současnosti je známo, že přítomnost krve v kloubu např. po jeho poranění a fixaci (nepohyblivosti) může vést k vazivovému nebo dokonce až kostnímu srůstu a tím ke snížení dynamiky jeho pohybu (Hase, 2002). V tomto případě se ukazuje jako důležitý fenomén přítomnost vlastní krve, která může iniciovat vznik a vývoj vazivových srůstů v kloubu, a tím příznivě snížit jeho nadměrnou pohyblivost při současném zachování funkčnosti.

V klinické praxi se u hypermobility TMK, pokud selže konzervativní terapie, využívá aplikace autologní krve do kloubu jako jedna z možných terapeutických metod (**Obr.2**). Léčebný postup spočívá v odběru plné krve z předloktí a její následné aplikaci intra- a periartikulárně. Je nutno dodat, že některá pracoviště doplňují vlastní aplikaci o mezičelistní fixaci (Abrahamsson et al., 2020), kterou ale na našem pracovišti neděláme. Nicméně z vlastní praxe máme dobré zkušenosti s limitováním otvírání úst a příjmem pouze tekuté stravy týden po výkonu. Princip působení aplikace autologní krve do kloubu a jeho okolí na snížení hypermobility v TMK však dosud není zcela jasný.



Obr. 2: **Vlevo:** odběr plné krve z pravé horní končetiny. **Vpravo:** peri- a intraartikulární aplikace krve do levého čelistního kloubu.

Pro bližší zkoumání účinků aplikované autologní krve na vznik srůstů limitujících pohyblivost TMK byl vybrán experimentální biomodel v podobě prasete domácího, jehož TMK je svojí anatomickou strukturou velmi podobný lidskému (Stembírek et al., 2012, Kyllar et al., 2014). Do čelistního kloubu prasete domácího jsme aplikovali autologní krev a následně sledovali změny, které po aplikaci nastanou. V rámci tohoto experimentu se nám podařilo prokázat resorpci krve z kloubní štěrbiny 14 dní po aplikaci. Po měsíci byla kloubní štěrbina bez nálezu zánětlivých změn či srůstů (Stembírek et al., 2013). Tento výsledek naznačuje, že účinek možná nespočívá ani tak v předpokládaném vzniku vazivových srůstů, ale spíše ve vytvoření hematomu, který limituje pohyblivost kloubu kvůli bolestivosti, případně díky srůstům v okolí samotného kloubu spíše než v jeho vnitřních prostorech. Limitací tohoto výzkumu je fakt, že u prasete není možné limitovat dva týdny po zákroku otevírání čelisti, které se v klinické praxi, jak už jsme uvedli výše, ukazuje jako pozitivní faktor.

Dalším příkladem kloubního onemocnění může být degradace kloubní chrupavky na základě makrotraumatu (např. úraz) nebo systémového degenerativního onemocnění. Jelikož chrupavka není schopna regenerace, postupně dochází k její degradaci, což se klinicky může projevat bolestí, „vrzotem“ či omezenou hybností postiženého kloubu (Zemen, 1999, Štembírek et al., 2018). Klinická terapie takového onemocnění je v současné době buď pouze symptomatická, protože současná medicína dosud nedisponuje prostředky k regeneraci kloubní chrupavky, nebo chirurgická, spočívající v artrocentéze, artroskopii nebo otevřené chirurgii (Ferri et al, 2018).

I když se objevují publikace o intraartikulární aplikaci preparátu na podporu regenerace chrupavky v podobě např. plazmy bohaté na destičky (PRP; Liu et al., 2022) nebo dokonce pomocí kmenových buněk (Gong et al., 2022), princip jejich účinku není plně znám.

Cílem naší další studie proto bylo experimentální sledování předpokládané regenerace měkkých a tvrdých tkání čelistního kloubu po aplikaci kmenových buněk pocházejících z lidské tukové tkáně do čelistního kloubu imunodeficientního králíka (Putnová et al., 2019). Cílem bylo ověření hypotézy, že přítomnost faktorů přítomných v kmenových buňkách (byť lidských) může stimulovat rychlejší regeneraci traumatu v TMK. Jako experimentální zvíře byl v tomto případě zvolen králík domácí pro jeho snadnější dostupnost, jednodušší chov a nižší náklady na experiment ve srovnání s prasetem. Čelistní kloub králíka je morfologicky relativně podobný lidskému kloubu, je v něm tedy přítomen kloubní disk, který, stejně jako u člověka, dělí čelistní kloub na dva prostory. Jednoznačnou nevýhodou pro experimentální použití tohoto zvířecího modelu byl výrazně menší rozměr kloubu, který si vyžádal nutnost otevřeného přístupu pro aplikaci kmenových buněk (Kyllar et al., 2014). Experiment s použitím lidských kmenových buněk z tukové tkáně člověka aplikovaných do poškozeného TMK imunodeficientního králíka neodhalil rychlejší regeneraci chrupavky, nicméně pozorována byla silnější angiogeneze v okolních měkkých tkáních ve srovnání s kontrolní skupinou.

Komentář k přiložené publikaci č. 5

Jan STEMBIREK, Michal KYLLAR, Iveta PUTNOVA, Ladislav STEHLIK a Marcela BUCHTOVA.

The pig as an experimental model for clinical craniofacial research. *Laboratory Animals* [online]. 2012, **46**(4), 269–279. ISSN 0023-6772. Dostupné z: doi:[10.1258/la.2012.012062](https://doi.org/10.1258/la.2012.012062)

IF = 1,257; Kvartil Q2

Cílem této studie bylo zhodnotit základní anatomické struktury oblasti hlavy u prasete domácího (*Sus scrofa f. domestica*) v souvislosti s jeho možným využitím v experimentálním výzkumu. Studie spočívala v naskenování hlav prasečích kadaverů pomocí CT a MRI a v následné preparaci významných struktur orofaciální oblasti, které mohou být u člověka postiženy patologickými procesy. Jednou ze struktur, které se ukázaly být velmi podobné lidským, byl čelistní kloub. U prasete, stejně jako u člověka, je přítomna kloubní jamka s kloubní hlavicí, ale také kloubní disk, který rozděluje kloubní prostor na dvě části. Velikost kloubu se liší podle stáří zvoleného experimentálního jedince. Nevýhodou je jeho horší dostupnost v souvislosti se silnější vrstvou okolních měkkých tkání ve srovnání s člověkem, což komplikuje aplikaci krve nebo jiných terapeutických látek do čelistního kloubu a vyžaduje otevřený přístup až na synovii kloubu. Významný rozdíl mezi lidským a prasečím čelistním kloubem jsme našli pouze v distální části, kde jamka kvůli menšímu mastoidnímu výběžku není ohraničena.

Výsledky naší studie nám potvrdily, že kromě primátů je možné i prase domácí považovat za zvířecí model, jehož čelistní kloub může být s úspěchem využit při experimentech v tkáňovém inženýrství nebo při nácviku nových chirurgických postupů.

Review Article

The pig as an experimental model for clinical craniofacial research

J Štembírek^{1,2}, M Kyllar³, I Putnová³, L Stehlík⁴ and M Buchtová^{1,3}

¹Institute of Animal Physiology and Genetics, v.v.i., Academy of Sciences of Czech Republic, Brno, Czech Republic; ²Department of Oral and Maxillofacial Surgery, University Hospital Ostrava, Czech Republic; ³Department of Anatomy, Histology and Embryology, Faculty of Veterinary Medicine, University of Veterinary and Pharmaceutical Sciences Brno, Brno, Czech Republic; ⁴Department of Diagnostic Imaging, Small Animals Clinics, Faculty of Veterinary Medicine, University of Veterinary and Pharmaceutical Sciences Brno, Brno, Czech Republic

Corresponding author: M Buchtová, Institute of Animal Physiology and Genetics, v.v.i., Academy of Sciences of the Czech Republic, Veverí 97, 602 00 Brno, Czech Republic. Email: buchtova@iach.cz

Abstract

The pig represents a useful, large experimental model for biomedical research. Recently, it has been used in different areas of biomedical research. The aim of this study was to review the basic anatomical structures of the head region in the pig in relation to their use in current research. Attention was focused on the areas that are frequently affected by pathological processes in humans: the oral cavity with teeth, salivary gland, orbit, nasal cavity and paranasal sinuses, maxilla, mandible and temporomandibular joint. Not all of the structures have an equal morphology in the pig and human, and these morphological dissimilarities must be taken into account before choosing the pig as an experimental model for regenerative medicine.

Keywords: Pig, experimental animal model, oral cavity, teeth, maxilla, mandible

Laboratory Animals 2012; **46**: 269–279. DOI: 10.1258/la.2012.012062

History of using the pig as an experimental model

The pig, one of the first species to be domesticated, represents one of the most important livestock species with nearly 500 different breeds with a worldwide distribution.¹ Recently, the pig became a very frequent and favourite biomedical model.^{2–11} It could possibly represent a significant source of organs for future transplantations. Minipigs are considered as an experimental model in many biomedical fields due to their apparent similarity to the human in terms of anatomy, as well as for economic advantages and ethical reasons. Because of the physiological similarities, the transfer of results acquired in pigs to human conditions is more exact compared with other experimental animals such as the mouse, rat or rabbit. The history of using pigs as an animal model suitable for research is also much older. The first symposium devoted exclusively to the basis for and the extent of the utilization of pigs in biomedical research was held at the Pacific Northwest Laboratory, Richland, Washington, in 1965.⁵

Many different pig breeds carrying human diseases and symptoms such as diabetes mellitus and melanomas have been established.^{8,12,13} Pigs and minipigs have become firmly established as the main research models in some

areas of biomedical and pharmacological research because of their anatomical similarities to humans (e.g. body size, skin, cardiovascular system and urinary system), their functional similarities (gastrointestinal system and immune system) and because of the availability of disease models (e.g. arteriosclerosis, metabolic syndrome, gastric ulcer and wound healing).¹⁴ Recently, the minipig was used as a model for testing the toxicity of new medicines and chemicals. It is necessary to test new pharmaceuticals intended for use in humans on non-rodent species. The most common choices are dogs or, in limited numbers, primates. Pigs and minipigs have been identified as being suitable to take the role of non-rodent species in the toxicity testing of pharmaceutical products because of their haematological and cardiovascular similarities to humans. The RETHINK project recently focused on the evaluation of the potential impact of toxicity testing in the minipig as an alternative approach.^{15,16} Therefore, it is evident that the pig can be a more useful experimental animal model in many aspects compared to the other animals (mice, rats, rabbits or dogs) that are routinely used.

This study aimed to summarize the clinically most important anatomical structures of the craniofacial region, to compare their morphology in the pig with corresponding structures in the human and to review a possible use of the pig model in craniofacial research.

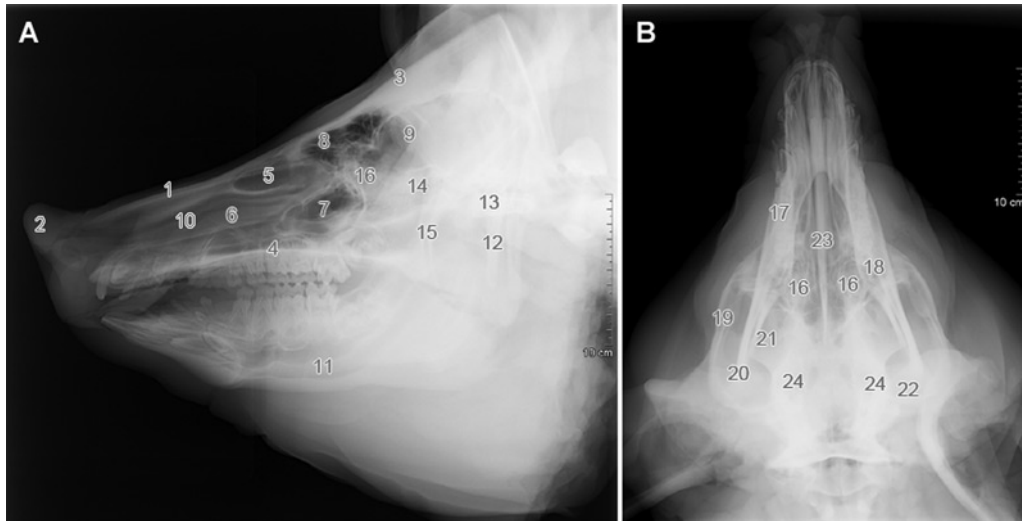


Figure 1 Radiography of pig head. 1: os nasale, 2: os rostrale, 3: os frontale, 4: palatum durum, 5: concha nasalis dorsalis (sinus conchae dorsalis), 6: concha nasalis ventralis, 7: sinus maxillaris, 8: sinus frontalis rostralis, 9: sinus frontalis caudalis, 10: meatus nasi medius, 11: canalis mandibulae, 12: processus paracondylaris, 13: pars basilaris ossis occipitalis, 14: sinus sphenoidalis, 15: processus pterygoideus, 16: labyrinthus ethmoidalis, 17: corpus mandibulae, 18: angulus mandibulae, 19: arcus zygomaticus, 20: condylus mandibulae, 21: processus condylaris mandibulae, 22: squama ossis temporalis, 23: vomer (septum nasi), 24: bulla tympanica

Clinical relevance of the pig model to human oral cavity diseases

In contrast to humans, where the oral cavity is nearly oval-shaped, the oral cavity of the pig is narrow and long, and does not differ between breeds (Figure 1). The labia are short and less movable, which reduces the ability of the pig to fully open the oral cavity compared to other species. Such an anatomical layout of the labia and oral cavity makes intubation for anaesthesia complicated. For clinicians, it is important to notice that the pig cannot breathe with an open mouth and the nasal airways have to be left free during intubation for respiration. The intubation technique requires training and experience as the long oral cavity makes this difficult.

The external nose of the pig, supported by rostral bone, is fused with the upper lip to form the rostrum (Figures 1 and 2). A thick layer of fat – *panniculus adiposus buccae* – underlies the cheeks, and the buccal mucosa is smooth without papillae. This solid layer makes access to caudal cheek structures more difficult and must be taken into account when a surgical approach is planned. Furthermore, X-ray imaging of caudal areas is almost impossible (Figure 1).

The hard palate is covered by the oral mucosa with prominent palatal ridges – *rugae palatinae* (Figure 4). Palatal ridges (20–23) are printed on to the bony surface of the hard palate – the maxillary and palatal bones – while in humans they are only situated on the anterior part of the palatal mucosa, without any prints on the supporting bone.¹⁷ The soft palate of the pig contains two tonsils – *tonsillae veli palatini*. The tonsils in the lateral wall of the oropharynx, which are present in other domestic species, are not developed in the pig. In contrast to humans, the *frenulum linguae* of the pig is bifurcated (data not shown).

The oral mucosa of the pig provides a suitable model for studying the biological processes that regulate scarless

wound healing in order to find novel approaches for preventing scar formation. The histological structure of the palatal mucosa shows the same pattern as that of humans.¹⁸ Furthermore, oral scarless healing was shown to resemble fetal skin, with rapid and transient inflammatory reactions in contrast to the adult skin, and it showed molecular responses during healing.^{19,20} Uncovering the molecular pathways involved in scar formation and processes of the pig oral mucosa healing without their formation might allow them to be used in the development of new clinical techniques and in the discovery of molecules suppressing scar formation after surgical treatments.

The oral mucosa of the pig can also be used to improve clinically effective delivery systems for DNA and RNAi technologies.³ These days, interest in delivering drugs through the buccal mucosa has increased, but a major limitation in buccal drug delivery is the low permeability of the epithelium. Therefore, knowing the effect of drug applications on individual layers of the oral mucosa is very critical.^{21–23} The porcine snout and buccal mucosa have been successfully used as a model for human treatment in penetration studies.^{7,21} Finally, there is a need in reconstructive surgery for flaps lined by non-keratinizing stratified squamous epithelium or mucous membrane in human medicine.²⁴ Pig buccal mucosa flaps were prefabricated in the skin and found to be significantly enlarged after 1 week of incubation. These procedures can be used for nasal or oral reconstructions.²⁴

The porcine tongue, which is long and firmly attached to the floor of the oral cavity by a double frenulum, possesses a similar histological structure as in humans. It was recently used as a model for investigating surgical techniques for reducing tongue volume by cold ablation (coblation).^{25–27} Coblation is a radiofrequency method used for the volumetric reduction of soft tissues in patients with obstructive sleep apnoea syndrome.²⁸ As significant lesions often

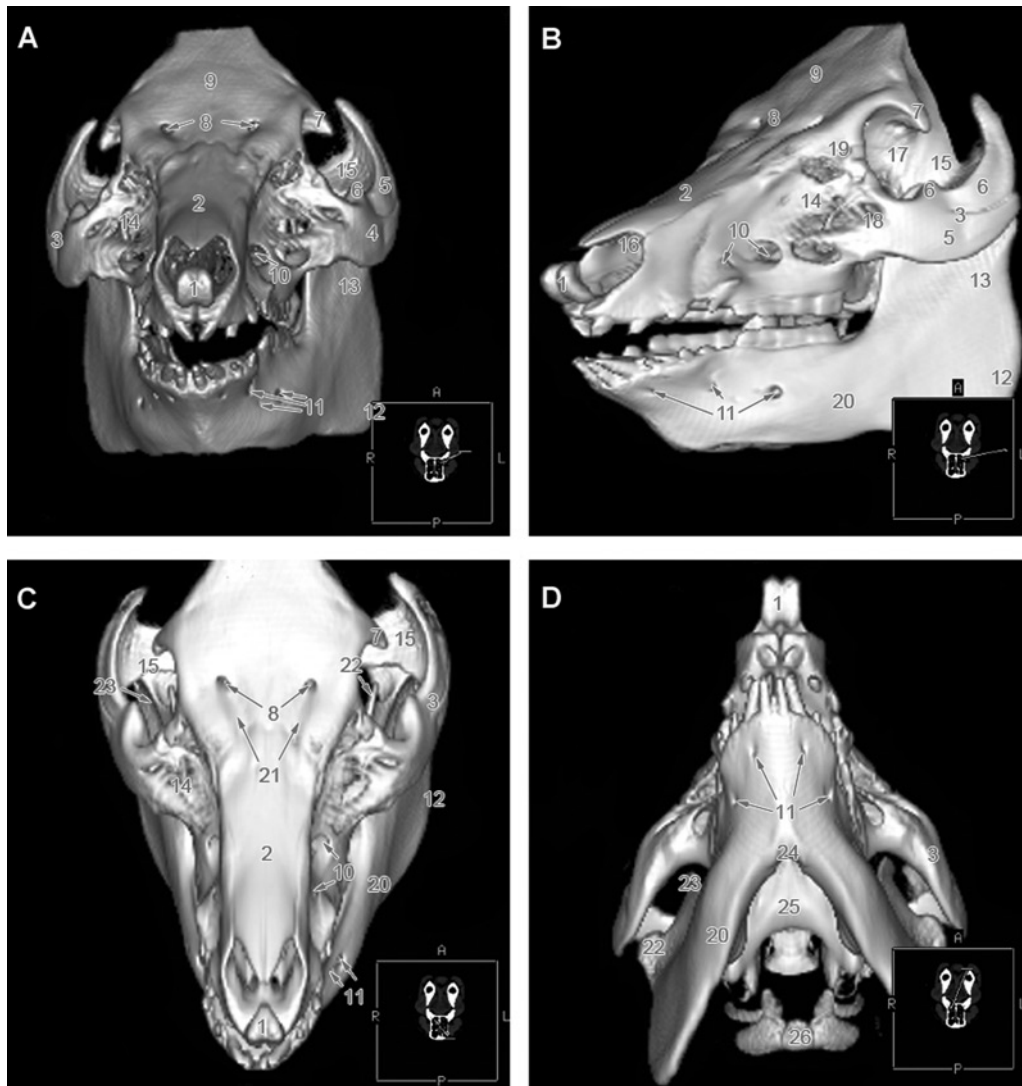


Figure 2 3D reconstruction of CT in pig. 1: os rostrale, 2: os nasale, 3: arcus zygomaticus, 4: processus temporalis ossis zygomatici, 5: processus zygomaticus ossis temporalis, 6: processus frontalis ossis zygomatici, 7: processus zygomaticus ossis frontalis, 8: foramen supraorbitale, 9: os frontale, 10: foramen infraorbitale, 11: foramina mentalia, 12: angulus mandibulae, 13: ramus mandibulae, 14: maxilla, 15: fossa temporalis, 16: incisura nasoincisiva, 17: orbita, 18: os zygomaticum, 19: os lacrimale, 20: corpus mandibulae, 21: sulcus supraorbitalis, 22: processus coronoideus mandibulae, 23: processus condylaris mandibulae, 24: angulus mentalis, 25: basis cranii, 26: os hyoideum

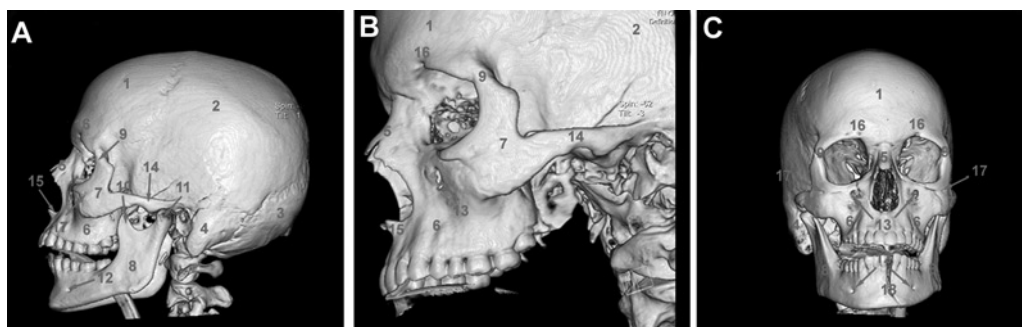


Figure 3 3D reconstruction of CT in human. 1: os frontale, 2: os parietale, 3: os occipitale, 4: processus mastoideus ossis temporalis, 5: os nasale, 6: maxilla, 7: os zygomaticum, 8: angulus mandibulae, 9: sutura zygomaticofrontalis, 10: processus coronoideus mandibulae, 11: processus condylaris mandibulae, 12: foramen mentale, 13: foramen infraorbitale, 14: arcus zygomaticotemporalis, 15: spina nasalis anterior, 16: foramen supraorbitale, 17: foramen zygomaticofaciale, 18: fractura mandibulae

develop after this procedure, surgical approaches were tested on the porcine tongue in order to determine the

process of lesion/scar formation and to develop further improvements in this surgical technique.

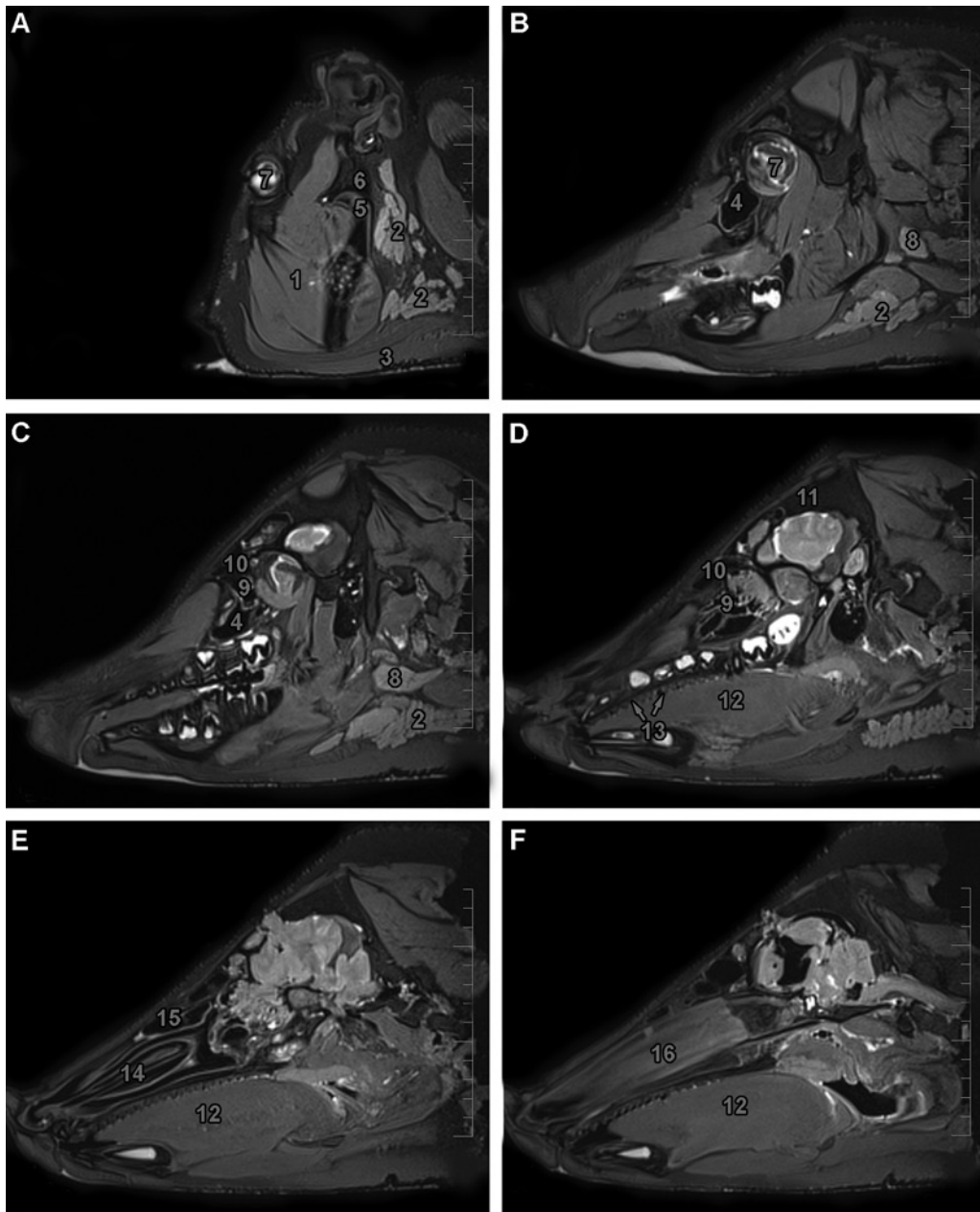


Figure 4 MRI of pig head (sagittal plane). 1: m. masseter, 2: gl. parotis, 3: m. cutaneus faciei, 4: sinus maxillaris, 5: condylus mandibulae, 6: articulatio temporomandibularis, 7: bulbus oculi, 8: gl. submandibularis, 9: labyrinthus ethmoidalis, 10: sinus frontalis (pars rostralis), 11: sinus frontalis (pars caudalis), 12: tongue, 13: rugae palatinae, 14: concha nasalis ventralis, 15: sinus conchae dorsalis, 16: septum nasi

Clinical relevance of the pig model to human salivary gland diseases

The same types of major salivary glands are found in humans as in the pig: the parotid gland and the submandibular and sublingual glands (Figure 4). Minor salivary glands are localized throughout the oral cavity in the buccal, labial, palatal and lingual regions. In contrast to humans, pig buccal glands are arranged into two lines: dorsal and ventral.

The parotid gland (*glandula parotis*) in the pig is a large and distinctly triangular structure covered by fatty tissue (Figure 4). The parotid duct perforates the buccinator

muscle at the level of the upper fourth premolar to the first molar tooth and opens into the vestibule on the *papilla parotidea*.

The mandibular gland (*glandula mandibularis*) is covered by the parotid gland (Figure 4). The duct follows the intermandibular space beneath the mylohyoideus muscle and opens into the oral cavity at the *frenulum linguae* or on the *caruncula sublingualis*.

There are two sublingual salivary glands in the pig. The monostomatic sublingual gland (*glandula sublingualis monostomatica seu major*) forms several ducts that unite into the major sublingual duct (*ductus sublingualis major*), which opens into the oral cavity in the same opening as

the *ductus mandibularis*. The polystomatic sublingual gland (*glandula sublingualis polystomatica seu minor*) is much larger and conveys secretions through small openings into the sublingual recessus.

The salivary glands in rodent models are well described and often used. However, they exhibit several specifics that hinder their use by many researchers. These limitations include the small volume of the salivary glands, the thin diameters of the gland ducts and also the short lifespan of these animals.²⁹ Therefore, the pig is a more suitable model for these studies due to the similar size of their salivary glands and because pigs share many morphological and physiological characteristics with human glands, including the ductal system and their structure. Pigs are also widely used for salivary gland research because their saliva flow rate is very similar to that in humans.^{29,30} Furthermore, the histological structure of the submandibular gland is characterized by a parenchyma of mixed acini and serous acini in both the human and pig.³¹ Typical serous acini of the parotid gland have also been found to be microscopically and histochemically similar.³²

Investigators and clinicians have been paying attention to salivary glands due to the fact that these structures are very often affected in patients with head and neck carcinoma, which is treated by ionizing radiation.³³ Studying radiation-induced structural and functional changes in salivary glands is important for human oncology treatment.^{34,35} The similarity between porcine and human physiology and the availability of slaughterhouse tissues suggests the use of porcine parotid cells as a model for amylase secretion.³⁶ Also, localized gene transfer to salivary glands has great potential for the treatment of salivary gland, systemic, oral and upper gastrointestinal tract diseases. Numerous studies on rodents have shown that salivary glands can secrete transgenic secretory proteins into either the saliva or bloodstream.^{30,37} However, there are still many unsolved questions regarding this problem, so minipig salivary glands, given their volume and morphological similarities to human salivary glands, may be useful as a large animal model for preclinical gene transfer experiments.^{38,39}

Clinical relevance of the pig model to human dental diseases

The pig has been used as a dental model for a long time as they share the bunodont and brachyodont type of dentition with the same pattern of enamel mineralization.^{40,41} Furthermore, both humans and pigs have diphyodont and normodont dentition with four types of teeth in the permanent dentition, each with a specific size and shape (Figures 2 and 4). The dental formula of deciduous dentition in the pig is 3i 1c 3p in all dental quadrants and 3I 1C 4(3)P 3M for permanent dentition;²⁹ in some cases, the first premolar is markedly smaller than the other teeth or it can be absent, as also seen in some other domestic animals where the presence of these teeth is rather rare. This tooth is often called 'dens lupinus'.

While humans are born edentulous, and the first deciduous teeth erupt at approximately 6 to 10 months after

birth, newborn piglets usually have eight erupted teeth.⁴² They are the third incisor and canine in all dental quadrants. These teeth are called 'needle teeth' and are often cut off because they can injure the mammary gland of the sow. Deciduous dentition in the pig is complete at 6 to 8 months of age and the permanent teeth erupt from 4 to 24 months after birth.

Recently, significant attention was paid to the possibilities of tooth replacement in humans. The regeneration of a functional tooth is one of the most promising therapeutic strategies for the replacement of lost or damaged teeth.⁴³ With the enhancement in tissue engineering and stem cell biology, several possible options for tooth replacement have been developed. Current research is focused on improvements in artificial dental implantations followed by periodontal apparatus recovery or the *de novo* production of biological teeth from embryonic or postnatal tooth buds.⁴⁴⁻⁴⁸

From a clinical perspective, the most important part of the tooth is the root, which forms the support for the (natural or artificial) crown, as the crown alone cannot fulfil normal tooth functions without a viable root.⁴⁹ Stem cells from human apical papillae or periodontal ligament stem cells have been successfully used to form the root/periodontal complex of porcelain crowns in the minipig.⁴⁹

Dental implants were tested for their stability and healing process in minipig maxillae using different types of dental implants, coatings and rate of osseointegration in different age groups.⁵⁰⁻⁵² Recently, growth factors such as bone morphogenetic protein (BMP) and collagen were shown to support the healing and osseointegration process after dental implantation.⁵³⁻⁵⁵ The pig mandible was shown to be less suitable than the maxilla for testing dental implants for two main reasons. Firstly, there is the superficial position of the large inferior alveolar canal. During insertion of the implant, penetration of the superior wall of the inferior alveolar canal is likely in pigs and must be taken into account. Secondly, the canines (especially in male pigs) fill a major part of the mandibular bone. In cases where there is a problem with these teeth, it is too complicated to extract them without ruining the complex structure of the bone. Therefore, proper implantation in the pig mandible is more difficult and the rate of successfully implanted teeth was only reported to be about 60%.⁵⁴

Tooth components of pigs on normal and low phosphorus diets were compared⁵⁶ and the effect of tooth extraction on bone mineralization apposition was analysed.^{57,58} As porcine alveolar bone shows a similar bone mineral density and bone mineral content to human alveolar bone,⁵⁹ it can be used as a model for human implantation techniques or dietary effects on tooth mineralization.

Periodontal diseases are ranked among the most frequent health problems in humans. At present, there is no ideal therapeutic approach for the management of periodontitis or for achieving optimal periodontal tissue regeneration.⁶⁰ From the clinical aspect, the loss of periodontal supporting tissue caused by inflammatory periodontal disease is the main complication.⁶¹ Similar symptoms were observed in a pig after the age of 6 months – swollen gingiva, plaque and calculus formation, 1–2 mm red collarettes on marginal

gingiva and bleeding on probing. The inflammatory process in periodontal tissues in pigs was similar to that seen in human periodontal diseases;²⁹ thus, the ability of culture cells replanted from alveolar bone and the periodontium to form new periodontal tissues was investigated in pigs.⁶¹ Cultured cells were found to contribute to the formation of new cementum, bone and attachment tissues and they prevented epithelial downgrowth during wound healing.⁶¹ Furthermore, the possibility of using autologous periodontal ligament stem cells (PDLSCs) to treat periodontal defects in a porcine model of periodontitis was studied.⁶⁰ Autologous PDLSCs were obtained from teeth extracted from minipigs. Cells were cultured *in vitro* and transplanted into areas with alveolar bone and periodontal defects. The PDLSCs were shown to regenerate the periodontal tissues, indicating the possibility of using stem cells for the treatment of periodontitis.^{60,62,63}

Clinical relevance of the pig model to human nasal cavity diseases

The nasal cavity of the pig is very long and narrow (Figure 4). The bony roof of the nasal cavity is almost complete rostrally on account of the long nasal and rostral bones.

Paranasal sinuses in the pig are separated into two main complexes (maxillary and frontal) and another two small sinuses (sphenoid and lacrimal). The maxillary sinus projects into the lacrimal and zygomatic bones (Figure 4). Caudally, the maxillary sinus extends to a transverse level, passing through the last molar tooth. The frontal sinus (*sinus frontalis*) represents the largest cavity and excavates the frontal, parietal, occipital and temporal bones (Figure 4). The rostral medial frontal sinus also communicates rostrally with the dorsal nasal concha and extends rostrally into the caudal part of the nasal bone and caudally to the level of the medial wall of the orbit. The lacrimal sinus (*sinus lacrimonalis*) is an excavation into the lacrimal bone, and is sometimes considered to be part of the rostral medial frontal sinus. The sphenoid sinus (*sinus sphenoidal*) is a paired sinus (right and left side) divided by a septum (*septum sinuum sphenoidalium*) that excavates into the pre-sphenoid, basisphenoid and temporal bones.

Discovering the pharmacokinetics of drugs administered to the nasal cavity is the aim of many experimental studies. The interest in delivering drugs through the nasal mucosa (mucus and mucociliary clearance, enzymatic degradation, immunological factors, blood flow and the deposition of drugs in the nasal cavity) of experimental animals is important for researching non-invasive treatments in humans.^{64,65} The pig model was used to study the effects of the systemic administration of the nitric oxide synthesis inhibitor on the vasculature of the pig nasal mucosa,⁶⁶ and to test different vasodilators (capsaicin, resisiferatoxin) on the nasal mucosa and superficial skin.⁶⁷ Furthermore, the airway cell biology of the pig is similar to that of humans, therefore recombinant adeno-associated virus (rAAV)-mediated gene therapy was used in the lungs for the treatment of cystic fibrosis.^{68,69}

Nasal polyps develop from the respiratory mucosa. However, the inflammatory conditions in the nasal mucosa that may play an important role in the aetiology and pathogenesis of nasal polyp formation are not fully understood.⁷⁰ The nasal mucosa of the pig can be used as an experimental model in the study of *Streptococcus* infection, for which aspects of the pathogenesis of infection still remain unclear,^{71,72} for the laser therapy of structural deformities in the nasal septum^{73,74} and for the closure of oronasal fistulas and for nasal septal cartilaginous surgery.⁷⁵⁻⁷⁷ Furthermore, porcine paranasal sinuses serve as a model for the experimental treatment of fungal sinusitis or rhinosinusitis in both human and veterinary medicine.^{78,79}

The pig was tested and found to be a suitable animal model for creating and closing oronasal communications.⁸⁰ Furthermore, whether or not these defects could be closed using biodegradable materials was also analysed.⁸¹ Although bone formation in maxillary sinus rafting or dental implants is routinely used in humans, surgeons cannot take histological samples to gain a better understanding.⁸² However, a detailed analysis is possible in the pig, which offers new opportunities for studying these processes in *in vivo* models. More recent studies focused on testing the effect of bone-substitution materials on *de novo* bone formations, where the porcine model is a valuable model for the preclinical testing of new materials.⁸³ On the other hand, the excessive thickness of the cortical bone restricts the use of pigs for the modified Caldwell-Luc procedure and the pig is not the best model for training in this method.⁸⁴

Clinical relevance of the pig model to human maxillary bone diseases

The maxilla is the main bone of the upper jaw that carries the upper premolar and molar teeth (Figure 2). The facial surface is smoothly concave. The infraorbital opening (*foramen infraorbitale*) is located near the centre of the bone (occasionally there might be two openings). Caudally, a facial crest (*crista facialis*) extends on to the zygomatic process and continues as a crest across the zygomatic bone. The infraorbital canal (*canalis infraorbitalis*) extends longitudinally in a rostral direction from the maxillary foramen to the infraorbital foramen (Figure 2). The canal is wide and compressed dorsoventrally and its roof serves as the floor of the maxillary sinus. The maxillary foramen is located just medial to the zygomatic process.

Bone pillars or buttresses are areas with thicker bone tissue supporting the maxillofacial region. In both humans and dogs, they represent clinically important structures regarding the management of craniofacial fractures.⁸⁵ The buttresses can be identified by transillumination of the skull (Figure 5). In humans, they are divided into three main areas: the medial (nasomaxillary) buttress, the lateral buttress (zygomaticomaxillary) and the posterior (pterygomaxillary) buttress, similar to the pig (Figure 5). The lateral buttress is the most prominent and seems to play a major role in supporting the upper jaw of the pig.

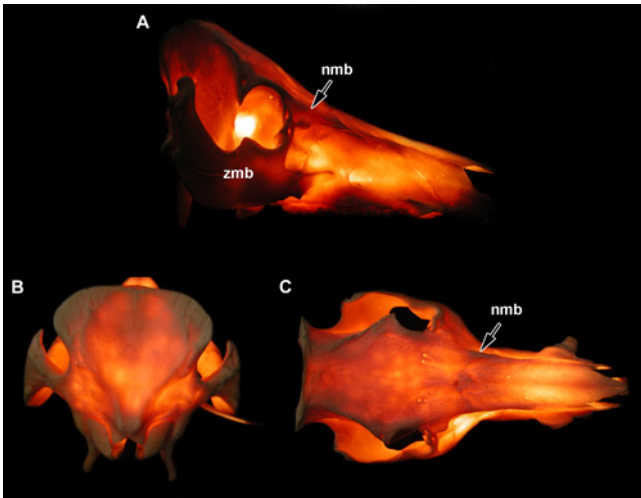


Figure 5 Transillumination of the pig skull. (A) lateral view, (B) caudal view, (C) dorsal view. The buttresses formed by thick bony tissue are illustrated as dark areas of the skull. Maxillary bone is supported by nasomaxillary (nmb) and zygomaxillary (zmb) buttresses

Similar to the dog and in contrast to humans, the pig does not have a bony support around its entire orbit, but its caudal part is supported by the orbital ligament. Therefore, the zygomatic arch bridges and transmits all forces and, therefore, it is reinforced by thick and dorsally protruding bony tissue.

Regarding bone anatomy, morphology, healing and remodelling, the pig is considered to be closely representative of humans and therefore a suitable species of choice.⁸⁶ Pigs have a denser trabecular network⁸⁷ but the structure of the lamellar bone is similar to that in humans.⁸⁸ When compared to the bone composition of various different species, porcine bone has been shown to have similarities to human bone in terms of bone mineral density and bone mineral concentration.⁵⁹ Also, the bone remodelling processes are similar, as well as the mechanical parameters during trabecular and intracortical BMU-based remodelling.^{87,88} A comparison of the regeneration rate of bone in dogs, pigs and humans⁸⁹ revealed that pigs have a more similar rate of bone regeneration to humans than to dogs (dog, 1.5–2.0 mm/day; pig, 1.2–1.5 mm/day; human, 1.0–1.5 mm/day). In addition, in a study of the effects of fluoride on cortical bone remodelling in growing pigs, the results showed that pigs have a similar cortical bone mineralization rate to humans.⁹⁰

Due to these similarities, a pig model was recently used to study bone formation after maxillary distraction.⁹ This surgical procedure is mainly recommended for children with cleft palates where the upper teeth are situated behind the lower teeth. The Le Fort I device was tested for its stability and the pig was established as a useful model for studying the healing mechanism during distraction osteogenesis.⁹

Experiments in the minipig may also help in designing internal non-bioresorbable and bioresorbable distraction devices. The pig maxilla can be used in tissue-engineering approaches for coordinated autologous tooth and bone reconstruction, and it also provides a basis for future

improvements in this technique for eventual clinical use in humans.^{91,92}

As the maxillary bone is a very thick and massive bone, recent studies of distraction osteogenesis used a more easily accessible bone: the frontal bone.^{92–94} Temporal and parietal bone segments were used to evaluate the optimal timing and long-term effects of fixation techniques on a growing cranium *in utero*.⁹⁵ The testing of new material, for example coralline hydroxyapatite and an expanded polytetrafluoroethylene membrane, was used in the treatment of calvarian defects⁹⁶ and the implantation of biodegradable miniplates.⁹² Furthermore, platelet rich plasma (PRP) was tested in peri-implant bone regeneration and the pig was shown to be a suitable animal model for such a purpose.⁹⁷

Clinical relevance of the pig model to human orbital diseases

The orbit of the pig is relatively small compared with humans (Figures 2 and 3). The infraorbital margin is formed by the lacrimal and zygomatic bone (*os lacrimale et zygomaticum*), and the supraorbital margin by the frontal bone (*os frontale*). Its bony margin is deficient caudolaterally, and this space is filled with the orbital ligament (*ligamentum orbitale*), which connects the *processus zygomaticus ossis frontalis* with the *processus frontalis ossis zygomatici* (Figure 2).

The adult pig can effectively serve as a model for resident training in lateral canthotomy or as a dummy orbit for the teaching and training of diagnostic and eye surgery procedures.^{98,99} To date, there is no precise method for controlling and monitoring expansion to induce normal growth in the developing facial skeleton, but the pig orbit is suitable for stimulating normal orbital growth in the neonatal facial skeleton.¹⁰⁰ Another application of the pig orbit is in laser surgery for the detection of temperature distributions in orbital tissues during and immediately after the application of CO₂ and Nd:YAG laser irradiation to muscle tissue adjacent to the optic nerve.^{99,101}

Moreover, the pig orbit is also an excellent experimental model for the development and testing of alloplastic materials that could be used in orbit reconstruction after trauma, tumours or developmental abnormalities. These materials would degrade slowly and have osteoconductive properties to allow their replacement and remodelling by osseous tissue. These properties should be tested in a pig model in order to determine their uses in human medicine.^{102–104}

Clinical relevance of the pig model to human mandible diseases

The mandible or the lower jaw consists of the body (*corpus mandibulae*) and massive ramus (*ramus mandibulae*) in pigs. A pair of medial mental foramina is situated dorsally to the mandibular angle. On the lateral surface, the lateral mental foramina usually number from three to five; this is in contrast to humans, where only one mental foramen

opens up between the first and second premolars (Figures 2 and 3). Moreover, thick bone tissue is situated between the tooth roots and mandibular canal in humans (the wisdom teeth are sometimes exceptions to this), whereas in the pig the tooth roots are in direct contact with the canal.

It must also be pointed out that the presence of multiple mental foramina in pigs makes local anaesthesia more difficult than with humans. Only large, local infiltration anaesthesia is possible, with no possibility of selectively anaesthetizing specific nerves, therefore making this an imprecise procedure. Furthermore, the thick layer of fatty tissue covering the ramus mandible can make access to this area difficult.

Current strategies for jaw reconstruction require multiple surgeries to replace bone and teeth. The pig mandibles serve to help improve tissue engineering approaches for coordinated autologous tooth and mandible reconstructions and as a model for providing a basis for future improvements in these techniques for eventual clinical use in humans.¹⁰⁵⁻¹⁰⁷ Pigs are suitable experimental animal models for studying the blood supply in the mandibular cortex and the design of osteosynthetic plates and screws.^{108,109} The pig mandible is also necessary for understanding the mechanisms and molecular events that regulate bone formation during distraction osteogenesis.¹¹⁰⁻¹¹² Moreover, the pig mandible helps in testing endoscopic procedures for the placement and activation of a distraction device for mandibular advancement,¹¹³ and for the endoscopic resection of mandibular angles.¹¹⁴

Stem-cell-based tissue engineering is currently viewed as a very promising method for bone regeneration,¹¹⁵ and the pig can be a very useful model. Stem cells of miniature pigs were isolated from deciduous teeth, the ilium or bone marrow and engrafted on to the critically sized bone defects generated in pig mandible models.^{11,105,106,116-119} The results indicated that these cells were able to engraft and regenerate bone in order to repair mandibular defects. A further step will be to transfer the acquired results to human clinical trials.

Clinical relevance of the pig model to human temporomandibular joint diseases

The morphology of the pig temporomandibular joint (TMJ) closely resembles that of humans,¹²⁰ including its internal structures, such as the articular disc, and its attachments.¹²¹ The pig TMJ is a simple incongruent joint, similar to that of humans (Figure 4). Except for the small mastoid eminence (*processus mastoideus*), there are no caudal borders to the mandibular fossa. The retroarticular process (*processus retroarticularis*) is not formed in the pig.

Human disorders of the TMJ are represented by a wide spectrum of morphological and functional changes that can affect not only the TMJ but also masticators and other areas of the face. This disorder is showing an increasing trend in humans, perhaps due to the influence of psychological stress in the present population. The presence of long-term tenseness and emotional stress is considered to be the main aetiological factor. These tissues are difficult

to visualize dynamically and therefore the *in vivo* processes are poorly understood.

The pig was recently proposed as the best non-primate model for human TMJ disorders; it has been used for direct measurements of TMJ tissue deformation and load during biting.^{122,123} The pig can also be useful in tissue engineering of the articular disc as the topographical biochemical and biomechanical parameters of its disc are most similar to the disc in humans^{124,125} or in the development of new therapies for degenerative TMJ diseases and post-traumatic conditions.¹²⁶

Furthermore, the invasive arthroscopic surgery of the TMJ is technically demanding and requires the acquisition of adequate arthroscopic skills that can hardly be obtained from patients alone. Thus, the pig TMJ serves as a reliable educational model for arthroscopic surgery and its further refinement in the TMJ.¹²⁷

Current applications for clinicians

The completion of pig genome sequencing has opened up the pig model for use with modern molecular methods.¹ In recent times, the pig has not just been used as an animal model for surgical treatment, but also for the possibility of targeting diseases via gene therapy.³ Bone regeneration was found to be enhanced in minipigs after BMP-2 gene delivery using liposomal vectors,^{128,129} adenovirus-mediated transfer¹³⁰ or the gene delivery was combined with collagen carrier.¹²⁸ Moreover, the protein can be also directly provided on hyaluronan-based hydrogel mixed with hydroxyapatite nanoparticles¹³¹ to improve the healing of cranial defects. As the formation of new bone is also accompanied by angiogenesis,¹³² the using of growth factors represent an ideal method for the cranial reconstruction and the possibility to repair a large-scale skull defect¹³³ Furthermore, mesenchymal stem cell transplantation can be used to reconstruct orofacial tissue.¹³⁴ Therefore, we hope that our recent study will open up the pig model to further applications by surgeons, as well as veterinary researchers.

ACKNOWLEDGEMENTS

This work was supported by the Czech Science Foundation (grant 304/08/P289). The lab runs under IRP IPAG No. AVOZ 5045015.

REFERENCES

- 1 Rothschild MF. Porcine genomics delivers new tools and results: this little piggy did more than just go to market. *Genet Res* 2004;**83**:1-6
- 2 Bermejo A, Gonzalez O, Gonzalez JM. The pig as an animal model for experimentation on the temporomandibular articular complex. *Oral Surg Oral Med Oral Pathol* 1993;**75**:18-23
- 3 Blagbrough IS, Zara C. Animal models for target diseases in gene therapy—using DNA and siRNA delivery strategies. *Pharm Res* 2009;**26**:1-18
- 4 Bustad LK. Pigs in the laboratory. *Sci Am* 1966;**214**:94-100
- 5 Bustad LK, McClellan RO. Use of pigs in biomedical research. *Nature* 1965;**208**:531-5

- 6 Bustad LK, McClellan RO. Swine in biomedical research. *Science* 1966;**152**:1526–30
- 7 Jacobi U, Toll R, Audring H, Sterry W, Lademann J. The porcine snout – an *in vitro* model for human lips? *Exp Dermatol* 2005;**14**:96–102
- 8 Millikan LE, Boylon JL, Hook RR, Manning PJ. Melanoma in Sinclair swine: a new animal model. *J Invest Dermatol* 1974;**62**:20–30
- 9 Papadaki ME, Troulis MJ, Glowacki J, Kaban LB. A minipig model of maxillary distraction osteogenesis. *J Oral Maxillofac Surg* 2010;**68**:2783–91
- 10 Sasaki R, Watanabe Y, Yamato M, Aoki S, Okano T, Ando T. Surgical anatomy of the swine face. *Lab Anim* 2010;**44**:359–63
- 11 Zheng Y, Liu Y, Zhang C, et al. Stem cells from deciduous tooth repair mandibular defect in swine. *J Dent Res* 2009;**88**:249–54
- 12 Horak V, Fortyn K, Hruban V, Klaudy J. Hereditary melanoblastoma in miniature pigs and its successful therapy by devitalization technique. *Cell Mol Biol* 1999;**45**:1119–29
- 13 Larsen MO, Rolin B. Use of the Gottingen minipig as a model of diabetes, with special focus on type 1 diabetes research. *ILAR J* 2004;**45**:303–13
- 14 van der Laan JW, Brightwell J, McAnulty P, Ratky J, Stark C. Regulatory acceptability of the minipig in the development of pharmaceuticals, chemicals and other products. *J Pharmacol Toxicol* 2010;**62**:184–95
- 15 Forster R, Bode G, Ellegaard L, van der Laan JW. The RETHINK project: minipigs as models for the toxicity testing of new medicines and chemicals: an impact assessment. *J Pharmacol Toxicol* 2010;**62**:158–9
- 16 Forster R, Bode G, Ellegaard L, van der Laan JW. The RETHINK project on minipigs in the toxicity testing of new medicines and chemicals: conclusions and recommendations. *J Pharmacol Toxicol* 2010;**62**:236–42
- 17 Hauser G, Daponte A, Roberts MJ. Palatal rugae. *J Anat* 1989;**165**:237–49
- 18 Wong JW, Gallant-Behm C, Wiebe C, et al. Wound healing in oral mucosa results in reduced scar formation as compared with skin: evidence from the red Duroc pig model and humans. *Wound Repair Regen* 2009;**17**:717–29
- 19 Mak K, Manji A, Gallant-Behm C, et al. Scarless healing of oral mucosa is characterized by faster resolution of inflammation and control of myofibroblast action compared to skin wounds in the red Duroc pig model. *J Dermatol Sci* 2009;**56**:168–80
- 20 Larjava H, Wiebe C, Gallant-Behm C, Hart DA, Heino J, Hakkinen L. Exploring scarless healing of oral soft tissues. *J Can Dent Assoc* 2011;**77**:b18
- 21 Campisi G, Paderni C, Saccone R, et al. Carbamazepine transbuccal delivery: the histo-morphological features of reconstituted human oral epithelium and buccal porcine mucosae in the transmucosal permeation. *Int J Immunopath Pharmacol* 2008;**21**:903–10
- 22 De Caro V, Giandalia G, Siragusa MG, Paderni C, Campisi G, Giannola LI. Evaluation of galantamine transbuccal absorption by reconstituted human oral epithelium and porcine tissue as buccal mucosa models: part I. *Eur J Pharm Biopharm* 2008;**70**:869–73
- 23 Sudhakar Y, Bandyopadhyay AK. Novel buccal adhesive tablets using *Aloe vera L* and *Sinapis alba* – a promising option for improved bioavailability of diltiazem hydrochloride. *PDA J Pharm Sci Tech* 2008;**62**:97–110
- 24 Carls FR, Jackson IT, Behl AK, Lebeda R, Webster H. Prefabrication of mucosa-lined flaps: a preliminary study in the pig model. *Plast Reconstr Surg* 1998;**101**:1022–8
- 25 Ge NN, Schalch P, Senders CW. The macroscopic and microscopic effects of radiofrequency injury in the porcine tongue: a pilot study. *Otolaryngol Head Neck Surg* 2009;**141**:408–12
- 26 Powell NB, Riley RW, Troell RJ, Blumen MB, Guilleminault C. Radiofrequency volumetric reduction of the tongue. A porcine pilot study for the treatment of obstructive sleep apnea syndrome. *Chest* 1997;**111**:1348–55
- 27 Salinas NL, Barrera JE. Coblation lesion formation in a porcine tongue model. *Otolaryngol Head Neck Surg* 2010;**143**:448–53
- 28 Li KK, Powell N, Riley R. Radiofrequency thermal ablation therapy for obstructive sleep apnea. *Oral Maxillofac S Clin* 2002;**14**:359–63
- 29 Wang S, Liu Y, Fang D, Shi S. The miniature pig: a useful large animal model for dental and orofacial research. *Oral Dis* 2007;**13**:530–7
- 30 Shan Z, Li J, Zheng C, et al. Increased fluid secretion after adenoviral-mediated transfer of the human aquaporin-1 cDNA to irradiated miniature pig parotid glands. *Mol Ther* 2005;**11**:444–51
- 31 Zhang X, Li J, Liu XY, Sun YL, Zhang CM, Wang SL. Morphological characteristics of submandibular glands of miniature pig. *Chinese Med J-Peking* 2005;**118**:1368–73
- 32 Wang SL, Li J, Zhu XZ, Sun K, Liu XY, Zhang YG. Sialographic characterization of the normal parotid gland of the miniature pig. *Dentomaxillofac Rad* 1998;**27**:178–81
- 33 Gosselin TK, Pavilonis H. Head and neck cancer: managing xerostomia and other treatment induced side effects. *ORL Head Neck Nurs* 2002;**20**:15–22
- 34 Radfar L, Sirois DA. Structural and functional injury in minipig salivary glands following fractionated exposure to 70 Gy of ionizing radiation: an animal model for human radiation-induced salivary gland injury. *Oral Surg Oral Med Oral Pathol* 2003;**96**:267–74
- 35 Xu J, Yan X, Gao R, et al. Effect of irradiation on microvascular endothelial cells of parotid glands in the miniature pig. *Int J Radiat Oncol* 2010;**78**:897–903
- 36 Brooks JC, Brooks M, Piskrowski J, Watson JD. Amylase secretion by cultured porcine parotid cells. *Arch Oral Biol* 1995;**40**:425–32
- 37 Yan X, Voutetakis A, Zheng C, et al. Sorting of transgenic secretory proteins in miniature pig parotid glands following adenoviral-mediated gene transfer. *J Gene Med* 2007;**9**:779–87
- 38 Hai B, Yan X, Voutetakis A, et al. Long-term transduction of miniature pig parotid glands using serotype 2 adeno-associated viral vectors. *J Gene Med* 2009;**11**:506–14
- 39 Li J, Zheng C, Zhang X, et al. Developing a convenient large animal model for gene transfer to salivary glands *in vivo*. *J Gene Med* 2004;**6**:55–63
- 40 Cooper WE. A microchemical, microradiographic and histological investigation of amelogenesis in the pig. *Arch Oral Biol* 1968;**13**:27–48
- 41 Fejerskov O. Human dentition and experimental animals. *J Dent Res* 1979;**58**(Spec Issue B):725–34
- 42 Putnova I, Odehnalova S, Horak V, et al. Comparative morphology of normal and cleft minipigs demonstrates dual origin of incisors. *Arch Oral Biol* 2011;**56**:1624–34
- 43 Yen AH, Sharpe PT. Regeneration of teeth using stem cell-based tissue engineering. *Expert Opin Biol Ther* 2006;**6**:9–16
- 44 Honda MJ, Fong H, Iwatsuki S, Sumita Y, Sarikaya M. Tooth-forming potential in embryonic and postnatal tooth bud cells. *Med Mol Morph* 2008;**41**:183–92
- 45 Honda MJ, Sumita Y, Kagami H, Ueda M. Histological and immunohistochemical studies of tissue engineered odontogenesis. *Arch Histol Cytol* 2005;**68**:89–101
- 46 Young CS, Terada S, Vacanti JP, Honda M, Bartlett JD, Yelick PC. Tissue engineering of complex tooth structures on biodegradable polymer scaffolds. *J Dent Res* 2002;**81**:695–700
- 47 Ohazama A, Modino SA, Miletich I, Sharpe PT. Stem-cell-based tissue engineering of murine teeth. *J Dent Res* 2004;**83**:518–22
- 48 Iwatsuki S, Honda MJ, Harada H, Ueda M. Cell proliferation in teeth reconstructed from dispersed cells of embryonic tooth germs in a three-dimensional scaffold. *Eur J Oral Sci* 2006;**114**:310–17
- 49 Sonoyama W, Liu Y, Fang D, et al. Mesenchymal stem cell-mediated functional tooth regeneration in swine. *PLoS One* 2006;**1**:e79
- 50 Nkenke E, Fenner M, Vairaktaris EG, Neukam FW, Radespiel-Troger M. Immediate versus delayed loading of dental implants in the maxillae of minipigs. Part II: histomorphometric analysis. *Int J Oral Max Impl* 2005;**20**:540–6
- 51 Nkenke E, Lehner B, Fenner M, et al. Immediate versus delayed loading of dental implants in the maxillae of minipigs: follow-up of implant stability and implant failures. *Int J Oral Max Impl* 2005;**20**:39–47
- 52 Fenner M, Vairaktaris E, Stockmann P, Schlegel KA, Neukam FW, Nkenke E. Influence of residual alveolar bone height on implant stability in the maxilla: an experimental animal study. *Clin Oral Implan Res* 2009;**20**:751–5
- 53 Stadlinger B, Pilling E, Huhle M, et al. Suitability of differently designed matrix-based implant surface coatings: an animal study on bone formation. *J Biomed Mater Res* 2008;**87**:516–24
- 54 Stadlinger B, Pilling E, Huhle M, et al. Evaluation of osseointegration of dental implants coated with collagen, chondroitin sulphate and BMP-4: an animal study. *Int J Oral Max Surg* 2008;**37**:54–9
- 55 Stadlinger B, Pilling E, Mai R, et al. Effect of biological implant surface coatings on bone formation, applying collagen, proteoglycans, glycosaminoglycans and growth factors. *J Mater Sci* 2008;**19**:1043–9

- 56 McClure FJ, King CT, Derr J, Wilk AL. Major components of the primary and secondary dentition of miniature and duroc swine fed normal vs low phosphorus diets. *Arch Oral Biol* 1966;**11**:253-66
- 57 Yeh K, Popowics T, Rafferty K, Herring S, Egbert M. The effects of tooth extraction on alveolar bone biomechanics in the miniature pig, *Sus scrofa*. *Arch Oral Biol* 2010;**55**:663-9
- 58 Yeh KD, Popowics TE. The impact of occlusal function on structural adaptation in alveolar bone of the growing pig, *Sus scrofa*. *Arch Oral Biol* 2010;**56**:79-89
- 59 Aerssens J, Boonen S, Lowet G, Dequeker J. Interspecies differences in bone composition, density, and quality: potential implications for *in vivo* bone research. *Endocrinology* 1998;**139**:663-70
- 60 Liu Y, Zheng Y, Ding G, et al. Periodontal ligament stem cell-mediated treatment for periodontitis in miniature swine. *Stem Cells* 2008;**26**:1065-73
- 61 Lang H, Schuler N, Nolden R. Attachment formation following replantation of cultured cells into periodontal defects - a study in minipigs. *J Dent Res* 1998;**77**:393-405
- 62 Ding G, Liu Y, Wang W, et al. Allogeneic periodontal ligament stem cell therapy for periodontitis in swine. *Stem Cells* 2011;**28**:1829-38
- 63 Park JY, Jeon SH, Choung PH. Efficacy of periodontal stem cell transplantation in the treatment of advanced periodontitis. *Cell Transplant* 2011;**20**:271-85
- 64 Gizuraron S. The relevance of nasal physiology to the design of drug absorption studies. *Adv Drug Deliver Rev* 1993;**11**:329-47
- 65 Illum L. Nasal delivery. The use of animal models to predict performance in man. *J Drug Target* 1996;**3**:427-42
- 66 Rinder J, Lundberg JM. Nasal vasoconstriction and decongestant effects of nitric oxide synthase inhibition in the pig. *Acta Physiol Scand* 1996;**157**:233-44
- 67 Rinder J, Szallasi A, Lundberg JM. Capsaicin-, resiniferatoxin-, and lactic acid-evoked vascular effects in the pig nasal mucosa *in vivo* with reference to characterization of the vanilloid receptor. *Pharmacol Toxicol* 1996;**78**:327-35
- 68 Liu X, Luo M, Guo C, Yan Z, Wang Y, Engelhardt JF. Comparative biology of rAAV transduction in ferret, pig and human airway epithelia. *Gene Ther* 2007;**14**:1543-8
- 69 Liu X, Luo M, Zhang L, Ding W, Yan Z, Engelhardt JF. Bioelectric properties of chloride channels in human, pig, ferret, and mouse airway epithelia. *Am J Resp Cell Mol* 2007;**36**:313-23
- 70 Shin SH, Park JY, Jeon CH, Choi JK, Lee SH. Quantitative analysis of eotaxin and RANTES messenger RNA in nasal polyps: association of tissue and nasal eosinophils. *Laryngoscope* 2000;**110**:1353-7
- 71 Madsen LW, Aalbaek B, Nielsen OL, Jensen HE. Aerogenous infection of microbiologically defined minipigs with *Streptococcus suis* serotype 2. A new model. *APMIS* 2001;**109**:412-18
- 72 Madsen LW, Nielsen B, Aalbaek B, Jensen HE, Nielsen JP, Riising HJ. Experimental infection of conventional pigs with *Streptococcus suis* serotype 2 by aerosolic exposure. *Acta Vet Scand* 2001;**42**:303-6
- 73 Lacroix JS, Stjarne P, Anggard A, Lundberg JM. Sympathetic vascular control of the pig nasal mucosa: (I) Increased resistance and capacitance vessel responses upon stimulation with irregular bursts compared to continuous impulses. *Acta Physiol Scand* 1988;**132**:83-90
- 74 Protsenko DE, Zemek A, Wong BJ. Temperature dependent change in equilibrium elastic modulus after thermally induced stress relaxation in porcine septal cartilage. *Laser Surg Med* 2008;**40**:202-10
- 75 Kirschner RE, Cabiling DS, Slemp AE, Siddiqi F, LaRossa DD, Losee JE. Repair of oronasal fistulae with acellular dermal matrices. *Plast Reconstr Surg* 2006;**118**:1431-40
- 76 Silverman RP, Bonasser L, Passaretti D, Randolph MA, Yaremchuk MJ. Adhesion of tissue-engineered cartilage to native cartilage. *Plast Reconstr Surg* 2000;**105**:1393-8
- 77 Wong BJ, Chao KK, Kim HK, et al. The porcine and lagomorph septal cartilages: models for tissue engineering and morphologic cartilage research. *Am J Rhinol* 2001;**15**:109-16
- 78 Benninger MS, McFarlin K, Hamilton DR, et al. Ultrasonographic evaluation of sinusitis during microgravity in a novel animal model. *Arch Otolaryngol* 2010;**136**:1094-8
- 79 Schumacher S, Stahl J, Baumer W, Kietzmann M. The use of an *in vitro*-cultured porcine nasal mucosa model for the biocompatibility assessment of biodegradable magnesium. *Altern Lab Anim* 2011;**39**:261-71
- 80 Liu Y, Springer IN, Zimmermann CE, et al. Missing osteogenic effect of expanded autogenous osteoblast-like cells in a minipig model of sinus augmentation with simultaneous dental implant installation. *Clin Oral Implan Res* 2008;**19**:497-504
- 81 van Minnen B, Stegenga B, Zuidema J, et al. An animal model for oroantral communications: a pilot study with Gottingen minipigs. *Lab Anim* 2005;**39**:280-3
- 82 Roldan JC, Knueppel H, Schmidt C, Jepsen S, Zimmermann C, Terheyden H. Single-stage sinus augmentation with cancellous iliac bone and anorganic bovine bone in the presence of platelet-rich plasma in the miniature pig. *Clin Oral Implan Res* 2008;**19**:373-8
- 83 Schlegel KA, Rupprecht S, Petrovic L, et al. Preclinical animal model for *de novo* bone formation in human maxillary sinus. *Oral Surg Oral Med Oral Pathol* 2009;**108**:e37-44
- 84 Estaca E, Cabezas J, Uson J, Sanchez-Margallo F, Morell E, Latorre R. Maxillary sinus-floor elevation: an animal model. *Clin Oral Implan Res* 2008;**19**:1044-8
- 85 Johnson AL, Houlton JEF, Vannini R. *Principles of Fracture Management in the Dog and Cat*. Davos Platz: AO Publishing, 2005
- 86 Thorwarth M, Rupprecht S, Falk S, Felszeghy E, Wiltfang J, Schlegel KA. Expression of bone matrix proteins during *de novo* bone formation using a bovine collagen and platelet-rich plasma (PRP) - an immunohistochemical analysis. *Biomaterials* 2005;**26**:2575-84
- 87 Mosekilde L, Weisbrode SE, Safran JA, et al. Calcium-restricted ovariectomized Sinclair S-1 minipigs: an animal model of osteopenia and trabecular plate perforation. *Bone* 1993;**14**:379-82
- 88 Mosekilde L, Kragstrup J, Richards A. Compressive strength, ash weight, and volume of vertebral trabecular bone in experimental fluorosis in pigs. *Calcified Tissue Int* 1987;**40**:318-22
- 89 Laiblin C, Jaeschke G. Clinical chemistry examinations of bone and muscle metabolism under stress in the Gottingen miniature pig - an experimental study. *Berl Munch Tierarztl* 1979;**92**:124-8
- 90 Kragstrup J, Richards A, Fejerskov O. Effects of fluoride on cortical bone remodeling in the growing domestic pig. *Bone* 1989;**10**:421-4
- 91 Gateno J, Seymour-Dempsey K, Teichgraber JF, Lalani Z, Yanez R, Xia JJ. Prototype testing for a new bioabsorbable Le Fort III distraction device: a pilot study. *J Oral Maxillofac Surg* 2004;**62**:1517-23
- 92 Wiltfang J, Merten HA, Schultze-Mosgau S, Schrell U, Wenzel D, Kessler P. Biodegradable miniplates (LactoSorb): long-term results in infant minipigs and clinical results. *J Craniofac Surg* 2000;**11**:239-43
- 93 Lethaus B, Tudor C, Bumiller L, Birkholz T, Wiltfang J, Kessler P. Guided bone regeneration: dynamic procedures versus static shielding in an animal model. *J Biomed Mater Res* 2010;**95**:126-30
- 94 Tudor C, Bumiller L, Birkholz T, Stockmann P, Wiltfang J, Kessler P. Static and dynamic periosteal elevation: a pilot study in a pig model. *Int J Oral Maxillofac Surg* 2010;**39**:897-903
- 95 Sims CD, Butler PE, Casanova R, Randolph MA, Ahn DK, Yaremchuk MJ. Surgical model to assess the effects and optimal timing of craniofacial fixation. *J Craniofac Surg* 1996;**7**:412-16
- 96 Reedy BK, Pan F, Kim WS, Gannon FH, Krasinskas A, Bartlett SP. Properties of coralline hydroxyapatite and expanded polytetrafluoroethylene membrane in the immature craniofacial skeleton. *Plast Reconstr Surg* 1999;**103**:20-6
- 97 Schlegel KA, Zimmermann R, Thorwarth M, et al. Sinus floor elevation using autogenous bone or bone substitute combined with platelet-rich plasma. *Oral Surg Oral Med Oral Pathol* 2007;**104**:e15-25
- 98 Suner S, Simmons W, Savitt DL. A porcine model for instruction of lateral canthotomy. *Acad Emerg Med* 2000;**7**:837-8
- 99 Uhlig CE, Gerding H. A dummy orbit for training in diagnostic procedures and laser surgery with enucleated eyes. *Am J Ophthalmol* 1998;**126**:464-6
- 100 Reedy BK, Pan F, Kim WS, Bartlett SP. The direct effect of intraorbital pressure on orbital growth in the anophthalmic piglet. *Plast Reconstr Surg* 1999;**104**:713-18
- 101 Chedid MK, Handy FF, Wilkinson DA, Kennerdell JS, Maroon JC. Temperature distributions in porcine orbital tissues following the use of CO₂ and Nd:YAG lasers. *Ophthalm Surg Las* 1993;**24**:100-4
- 102 Ahn DK, Sims CD, Randolph MA, et al. Craniofacial skeletal fixation using biodegradable plates and cyanoacrylate glue. *Plast Reconstr Surg* 1997;**99**:1508-15
- 103 Rohner D, Huttmacher DW, Cheng TK, Oberholzer M, Hammer B. *In vivo* efficacy of bone-marrow-coated polycaprolactone scaffolds for

- the reconstruction of orbital defects in the pig. *J Biomed Mater Res* 2003;**66**:574–80
- 104 Nabavi CB, Liu E, Tao JP. The effect of tissue wrapping on the expansion of hydrophilic orbital implants. *Ophthalm Plast Rec* 2011;**27**:327–9
- 105 Abukawa H, Shin M, Williams WB, Vacanti JP, Kaban LB, Troulis MJ. Reconstruction of mandibular defects with autologous tissue-engineered bone. *J Oral Maxillofac Surg* 2004;**62**:601–6
- 106 Abukawa H, Zhang W, Young CS, et al. Reconstructing mandibular defects using autologous tissue-engineered tooth and bone constructs. *J Oral Maxillofac Surg* 2009;**67**:335–47
- 107 Carstens MH, Chin M, Li XJ. In situ osteogenesis: regeneration of 10-cm mandibular defect in porcine model using recombinant human bone morphogenetic protein-2 (rhBMP-2) and Helistat absorbable collagen sponge. *J Craniofac Surg* 2005;**16**:1033–42
- 108 Saka B, Wree A, Anders L, Gundlach KK. Experimental and comparative study of the blood supply to the mandibular cortex in Gottingen minipigs and in man. *J Craniomaxillofac Surg* 2002;**30**:219–25
- 109 Saka B, Wree A, Henkel KO, Anders L, Gundlach KK. Blood supply of the mandibular cortex: an experimental study in Gottingen minipigs with special reference to the condyle. *J Craniomaxillofac Surg* 2002;**30**:41–5
- 110 Glowacki J, Shusterman EM, Troulis M, Holmes R, Perrott D, Kaban LB. Distraction osteogenesis of the porcine mandible: histomorphometric evaluation of bone. *Plast Reconstr Surg* 2004;**113**:566–73
- 111 Schmoker RR. Mandibular reconstruction using a special plate. Animal experiments and clinical application. *J Maxillofac Surg* 1983;**11**:99–106
- 112 Yates KE, Troulis MJ, Kaban LB, Glowacki J. IGF-I, TGF-beta, and BMP-4 are expressed during distraction osteogenesis of the pig mandible. *Int J Oral Maxillofac Surg* 2002;**31**:173–8
- 113 Troulis MJ, Nahlieli O, Castano F, Kaban LB. Minimally invasive orthognathic surgery: endoscopic vertical ramus osteotomy. *Int J Oral Maxillofac Surg* 2000;**29**:239–42
- 114 Ma S, Fang RH. Endoscopic mandibular angle surgery: a swine model. *Ann Plas Surg* 1994;**33**:473–5
- 115 Petite H, Viateau V, Bensaid W, et al. Tissue-engineered bone regeneration. *Nat Biotechnol* 2000;**18**:959–63
- 116 Miura M, Miura Y, Sonoyama W, Yamaza T, Gronthos S, Shi S. Bone marrow-derived mesenchymal stem cells for regenerative medicine in craniofacial region. *Oral Dis* 2006;**12**:514–22
- 117 von Wilmsky C, Schwarz S, Kerl JM, et al. Reconstruction of a mandibular defect with autogenous, autoclaved bone grafts and tissue engineering: an *in vivo* pilot study. *J Biomed Mater Res* 2010;**93**:1510–18
- 118 Zhang W, Abukawa H, Troulis MJ, Kaban LB, Vacanti JP, Yelick PC. Tissue engineered hybrid tooth-bone constructs. *Methods* 2009;**47**:122–8
- 119 Kuo TF, Lin HC, Yang KC, et al. Bone marrow combined with dental bud cells promotes tooth regeneration in miniature pig model. *Artif Organs* 2011;**35**:113–21
- 120 Herring SW, Scapino RP. Physiology of feeding in miniature pigs. *J Morph* 1973;**141**:427–60
- 121 Strom D, Holm S, Clemensson E, Haraldson T, Carlsson GE. Gross anatomy of the mandibular joint and masticatory muscles in the domestic pig (*Sus scrofa*). *Arch Oral Biol* 1986;**31**:763–8
- 122 Nickel J, Spilker R, Iwasaki L, et al. Static and dynamic mechanics of the temporomandibular joint: plowing forces, joint load and tissue stress. *Orthod Craniofac Res* 2009;**12**:159–67
- 123 Sindelar BJ, Herring SW. Soft tissue mechanics of the temporomandibular joint. *Cells Tissues Organs* 2005;**180**:36–43
- 124 Kalpakci KN, Willard VP, Wong ME, Athanasiou KA. An interspecies comparison of the temporomandibular joint disc. *J Dent Res* 2011;**90**:193–8
- 125 Kalpakci KN, Kim EJ, Athanasiou KA. Assessment of growth factor treatment on fibrochondrocyte and chondrocyte co-cultures for TMJ fibrocartilage engineering. *Acta Biomater* 2011;**7**:1710–18
- 126 Lin YY, Tanaka N, Ohkuma S, et al. The mandibular cartilage metabolism is altered by damaged subchondral bone from traumatic impact loading. *Ann Biomed Eng* 2009;**37**:1358–67
- 127 Kaduk WM, Koppe T. Metric analysis of the upper space of the temporomandibular joint (TMJ) in pigs (*Sus scrofa domestica*) for evaluation of the pig as a model for arthroscopic TMJ surgery. *Ann Anat* 2007;**189**:367–70
- 128 Lutz R, Park J, Felszeghy E, Wiltfang J, Nkenke E, Schlegel KA. Bone regeneration after topical BMP-2-gene delivery in circumferential peri-implant bone defects. *Clin Oral Implan Res* 2008;**19**:590–9
- 129 Park J, Lutz R, Felszeghy E, et al. The effect on bone regeneration of a liposomal vector to deliver BMP-2 gene to bone grafts in peri-implant bone defects. *Biomaterials* 2007;**28**:2772–82
- 130 Chang SC, Wei FC, Chuang H, et al. *Ex vivo* gene therapy in autologous critical-size craniofacial bone regeneration. *Plast Reconstr Surg* 2003;**112**:1841–50
- 131 Docherty-Skogh AC, Bergman K, Waern MJ, et al. Bone morphogenetic protein-2 delivered by hyaluronan-based hydrogel induces massive bone formation and healing of cranial defects in minipigs. *Plast Reconstr Surg* 2010;**125**:1383–92
- 132 Zhang F, Qiu T, Wu X, et al. Sustained BMP signaling in osteoblasts stimulates bone formation by promoting angiogenesis and osteoblast differentiation. *J Bone Miner Res* 2009;**24**:1224–33
- 133 Chang SC, Lin TM, Chung HY, et al. Large-scale bicortical skull bone regeneration using *ex vivo* replication-defective adenoviral-mediated bone morphogenetic protein-2 gene-transferred bone marrow stromal cells and composite biomaterials. *Neurosurgery* 2009;**65**:75–81
- 134 Fang D, Seo BM, Liu Y, et al. Transplantation of mesenchymal stem cells is an optimal approach for plastic surgery. *Stem Cells* 2007;**25**:1021–8

(Accepted 25 May 2012)

Komentář k přiložené publikaci č. 6

Jan STEMBIREK*(corresponding author), Eva MATALOVA, Marcela BUCHTOVA, Vladimír MACHON a Ivan MISEK. Investigation of an autologous blood treatment strategy for temporomandibular joint hypermobility in a pig model. *International Journal of Oral and Maxillofacial Surgery* [online]. 2013, **42**(3), 369–375. ISSN 0901-5027. Dostupné z: doi:[10.1016/j.ijom.2012.07.001](https://doi.org/10.1016/j.ijom.2012.07.001)

IF = 1,359; Kvartil Q2

Cílem projektu bylo získat informace o osudu autologní krve aplikované do čelistního kloubu s cílem omezit jeho mobilitu, protože v literatuře se jako princip této terapie uvádí vznik aseptického zánětu vedoucího k tvorbě adhezí mezi kloubním diskem, kloubním pouzdem a kloubní jamkou. Výsledkem vzniku těchto adhezí by měla být právě menší pohyblivost kloubu.

Jako experimentální model bylo použito 12 prasat domácích (*Sus scrofa f. domestica*), u kterých jsme v celkové anestezii intraartikulárně a do okolí TMK aplikovali jejich autologní krev. Aplikace byla prováděna vzhledem k relativně hlubokému uložení kloubu (Stembirek et al., 2012) pomocí otevřeného přístupu. Druhostranný kloub sloužil jako kontrolní. Zvířata byla následně po 1 hodině, 1, 2 a 4 týdnech po aplikaci humaně utracena, celé hlavy byly vyšetřeny na magnetické rezonanci a následně byly čelistní klouby (tzn. jamka, disk i hlavice) vypreparovány a histopatologicky zpracovány. Naše výsledky ukázaly přítomnost krve ve formě sraženin v distálních částech horní kloubní štěrbině 1 hodinu a 1 týden po aplikaci. Ještě 2 týdny po léčbě byly stále patrné malé krevní sraženiny v distální části kloubního prostoru, po 4 týdnech od operace v horní kloubní štěrbině již nebyly patrné žádné zbytky krve. Co je však vzhledem k vysvětlení mechanismu působení popisovanému v literatuře ještě důležitější, nebyly pozorovány žádné zánětlivé změny nebo srůsty. Podobný experiment provedl Gulses a jeho tým s tím rozdílem, že aplikoval šestnácti prasatům autologní krev bez otevřeného přístupu a do druhého čelistního kloubu aplikoval fyziologický roztok (Gulses et al., 2013). Vzorky odebíral za 4 týdny a analyzoval pouze retrodiskální tkáň a laterální část pouzdra. V jejich experimentu pak našli u kloubu po aplikaci autologní krve regenerativní změny a zánětlivý infiltrát s lymfocyty a makrofágy, s destrukcí kolagenních vláken a zvýšenou fibrotickou aktivitou v retrodiskální tkáni a laterální části synovie. Podobné změny pozorovali i u kloubu po aplikaci fyziologického roztoku, ale se statisticky menším rozsahem fibrózy.

Výsledky obou studií naznačují, že aplikace autologní krve nemá vliv na tvorbu adhezí přímo v kloubní štěrbině, ale postihuje měkké tkáně, jako jsou retrodiskální tkáň nebo laterální část pouzdra. Je tak možné zvážit i možnost pouze periartikulární aplikace, která vytvoří hematoma okolo kloubního pouzdra a svalů, které se na něj upínají; v takovém případě by mohlo docházet ke snížení rozsahu otevírání úst ne na základě intraartikulárních srůstů, ale spíše na základě vzniklého sterilního zánětu v okolí kloubu, který vede ke vzniku vazivových srůstů limitujících jeho pohyblivost.

Investigation of an autologous blood treatment strategy for temporomandibular joint hypermobility in a pig model

**J. Stembirek^{1,2,3}, E. Matalova^{1,4},
 M. Buchtova^{1,4}, V. Machon⁵, I. Misek¹**

¹Institute of Animal Physiology and Genetics CAS, v.v.i., Brno, Czech Republic; ²Department of Oral and Maxillofacial Surgery, University Hospital Ostrava, Czech Republic; ³Faculty of Medicine, Masaryk University, Brno, Czech Republic; ⁴Faculty of Veterinary Medicine, University of Veterinary and Pharmaceutical Sciences, Brno, Czech Republic; ⁵Department of Oral and Maxillofacial Surgery, Charles University, Prague, Czech Republic

J. Stembirek, E. Matalova, M. Buchtova, V. Machon, I. Misek: Investigation of an autologous blood treatment strategy for temporomandibular joint hypermobility in a pig model. Int. J. Oral Maxillofac. Surg. 2013; 42: 369–375. Published by Elsevier Ltd on behalf of International Association of Oral and Maxillofacial Surgeons.

Abstract. Many different surgical and non-surgical techniques are used for the treatment of temporomandibular joint (TMJ) hypermobility. One of these methods is autologous blood injection into the TMJ. The fate of the autologous blood used for treatment of recurring condylar dislocation is still not completely understood. The authors used 12 pigs (*Sus scrota f. domestica*) as a model species for autologous blood delivery into the TMJ. Blood injection was followed by histopathological analysis at different times after treatment (1 h, 1, 2 and 4 weeks). Samples were examined by magnetic resonance imaging, macroscopic and histological methods. The deposition of the remaining blood was observed in the form of clots in the distal parts of the upper joint cavity 1 h and 1 week after treatment. 2 weeks after treatment, small blood clots were still apparent in the distal part of the upper joint cavity. 4 weeks after surgery, no remnants of blood, changes or adhesions were apparent inside the TMJ. No morphological or histological changes were observed in the TMJ after the injection of autologous blood suggesting another mechanism is involved in the hypermobility treatment.

Keywords: temporomandibular joint; pig; autologous blood; hypermobility.

Accepted for publication 10 July 2012
 Available online 4 August 2012

The temporomandibular joint (TMJ) provides the junction between the jaw (mandibular condyle) and the neurocranium (temporal bone). Condyle dislocation (or hypermobility) of TMJ is one of the most frequent TMJ disorders in humans.¹ In the case of hypermobility, the condyle reaches a position in front of the articular tubercle at wide mouth opening, which can be caused by abnormalities in the shape of the joints, by ligament looseness or by reduced muscle tension.²

The treatment of TMJ hypermobility includes surgical or non-surgical approaches. Surgical procedures can be divided into two categories; those that limit the range of condylar movement, and those that remove the blocking factor that prevents the condyle from returning.^{3–6} Non-surgical treatment includes a soft diet, pharmacotherapy, physical therapy, stress reduction, movement limitation and occlusal splint therapy. Joint movement reduction can be caused by the injection of

different substances such as autologous blood or sclerosing solutions into the upper joint cavity.^{2,7,8} Although there are many clinical studies about a high success rate of autologous blood injection into TMJ,^{2,3,7,9,10} the effect and the detailed mechanism of this therapy are not well understood.

It has been proposed that autologous blood in the TMJ may result in joint degeneration and/or formation of adhesions inside the joint. There is a lack of

studies examining in detail the mechanisms of the effect of autologous blood injection into the TMJ. This type of study can only be carried out using a suitable animal model (human-like size, with similar structure and motion of TMJ) paired with subsequent histological evaluations.

Several studies have been performed to understand the joint pathology and different approaches have been tested for their treatment. A sheep model was used for the evaluation of histopathological changes after intracapsular condylar fracture, the fate of auricular cartilage graft in the surgical treatment of TMJ ankylosis, intraarticular scarring and ankylosis management.^{11–13} Blood was injected into the rabbit TMJ.¹⁴ The rabbit and sheep condyles are adapted to a herbivorous diet so are more rounded than those of humans,¹⁴ which causes greater mobility in the transverse plane and limited mouth opening.

In contrast, pigs are omnivorous like humans and therefore the structure of their TMJ resembles that of humans. Their diarthrodial synovial TMJ consists of an articular pit, articular disc and articular condyle surrounded by a ligamentous capsule. The articular disc, as in humans, divides the joint into two compartments described as two articulations: the meniscotemporal (suprameniscal) joint permitting translational movements, and the condylomeniscal (inframemiscal) joint, which permits rotational movements.

The disc has a biconcave shape; the fossa is shallow, and the condyle is elliptic.^{15,16} The masticator muscle arrangement is similar to that in humans, therefore moderate translation movements are allowed in all planes; the major movement is provided by rotation of the joint condyle.^{15,17}

Based on these morphological similarities, the authors selected the pig as a model organism for this study, which aims to confirm or disprove the hypothesis that aseptic inflammation and subsequent formation of lesions and adhesions are responsible for the therapeutic effect of autologous blood used for TMJ hypermobility treatment.

Materials and methods

12 pigs (*Sus scrofa f. domestica*) aged 2 years were obtained from the breeding unit of the Institute of Animal Physiology and Genetics, Academy of Science of the Czech Republic in Libečov. Animals were divided into four groups of three animals, none of which had any previous history of TMJ hypermobility. The first group was killed 1 h after treatment, the second group 1 week, the third group 2 weeks and the fourth group 4 weeks after autologous blood injection. The animals were housed in separate breeding boxes under conventional conditions and provided with water and food ad libitum. The experimental procedure was approved

by the Animal Research Committee of IAPG CAS, v.v.i. (Nr. 67985904).

All surgical procedures were performed in the aseptic conditions of an operating theatre with disinfectant applied over the operating field. All animals were premedicated with ketamine (22 mg/kg) and atropine (0.04 mg/kg) and anaesthetized with thiopental (15 mg/kg) prior to intubation. Anaesthesia was maintained with inhaled isoflurane (1.5%). The animals were mechanically ventilated with an initial tidal volume of 10 ml/kg and a respiratory rate of 15 breaths per min. The tidal volume was adjusted to maintain an arterial $PaCO_2$ of 35–40 mmHg during the experiment. Hydration was maintained using lactated Ringer's solution delivered through a cannulated dorsal auricular vein. Body temperature was maintained at 38.0–39.0 °C using a circulating hot water heating pad. Both heart rate and oxygen saturation levels were monitored throughout all surgical procedures.

The lateral approach was carried out from the lateral side of the articular capsule. A small incision was made above the lateral part of the left condyle, approximately 1 cm below the external auditory meatus during a wide mandible opening. The first 20-gauge needle was inserted towards the posterior aspect of the condyle in the posterior part of the superior joint cavity in the anterior-medial direction, before being withdrawn slightly (about 1 mm) to

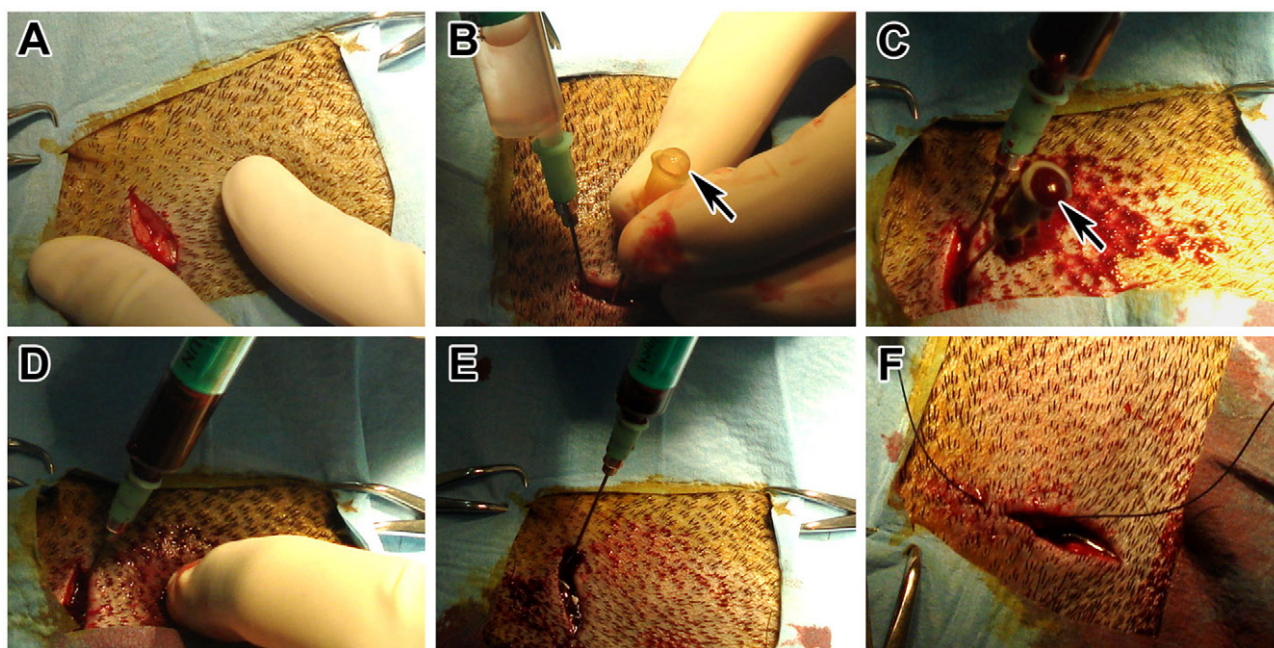


Fig. 1. Surgical approach in the pig. (A) Small incision and preparation through the skin and adipose layer. (B) Arthrocentesis with saline solution, black arrow shows positive return of irritant. (C) Recheck of arthrocentesis with autologous blood, black arrow shows positive return of autologous blood. (D) Injection of autologous blood into left upper joint cavity. (E) Injection of autologous blood around left TMJ. (F) Skin suture.

prevent subchondral application and saline solution was injected. During the saline solution application, no protrusive movement of the mandible was observed and the correct position of the needle therefore had to be checked by arthrocentesis with saline solution. The second 20-gauge needle was inserted approximately 0.5–1 cm before the first needle at the same horizontal level but in the posterior-medial direction. After this procedure, successful arthrocentesis with saline solution was performed in all cases. The next step was collecting blood from the jugular vein and injecting 1.0 ml of this blood into the superior joint cavity and 0.5 ml around the articular capsule, followed by wound suture (Fig. 1). The left TMJ served as the experimental joint for blood application and the right TMJ was left without treatment as the control tissue. As it would be difficult to maintain pigs in a sterile environment after the procedure, antibiotics (amoxicillin Bioventa 15% inj. ad us.vet, 15 ml/kg and day, divided into two doses) were administered to prevent infection.

The experimental pigs were killed by intravenous injection of thiopental at four different time intervals after successful autologous blood delivery (1 h, 1, 2 and 4 weeks after treatment). The whole heads were placed on ice and immediately transported for examination by 3T nuclear magnetic resonance imaging (MRI; Siemens Ltd., Siemens Magnetom Trio 3T) at the Institute of Clinical and Experimental Medicine (Prague, Czech Republic). After this analysis, both TMJs were dissected, fixed in 10% paraformaldehyde and examined using a stereoscopic microscope (Leica, Germany). After 10 days in paraformaldehyde, decalcification was performed in Livrea's solution (4% HNO₃, 0.15% CrO₃) for approximately 1 month, after which the specimens were embedded in paraffin, cut into 5 µm sagittal histological sections, and split over four parallel slides. Haematoxylin–eosin (HE) was used as the primary staining for the histological analysis, elastic fibres were visualized by Orcein, reticular fibres were stained with Gömori, and Van Gieson staining was used for the detection of collagen fibres.

Results

In the samples taken 1 h and 1 week after treatment, macroscopic examination revealed deposition of the remaining blood in the form of clots in distal parts of the upper joint cavity. No alterations on the articular surface were observed. 2 weeks after treatment, small blood clots were still apparent in the distal part of the

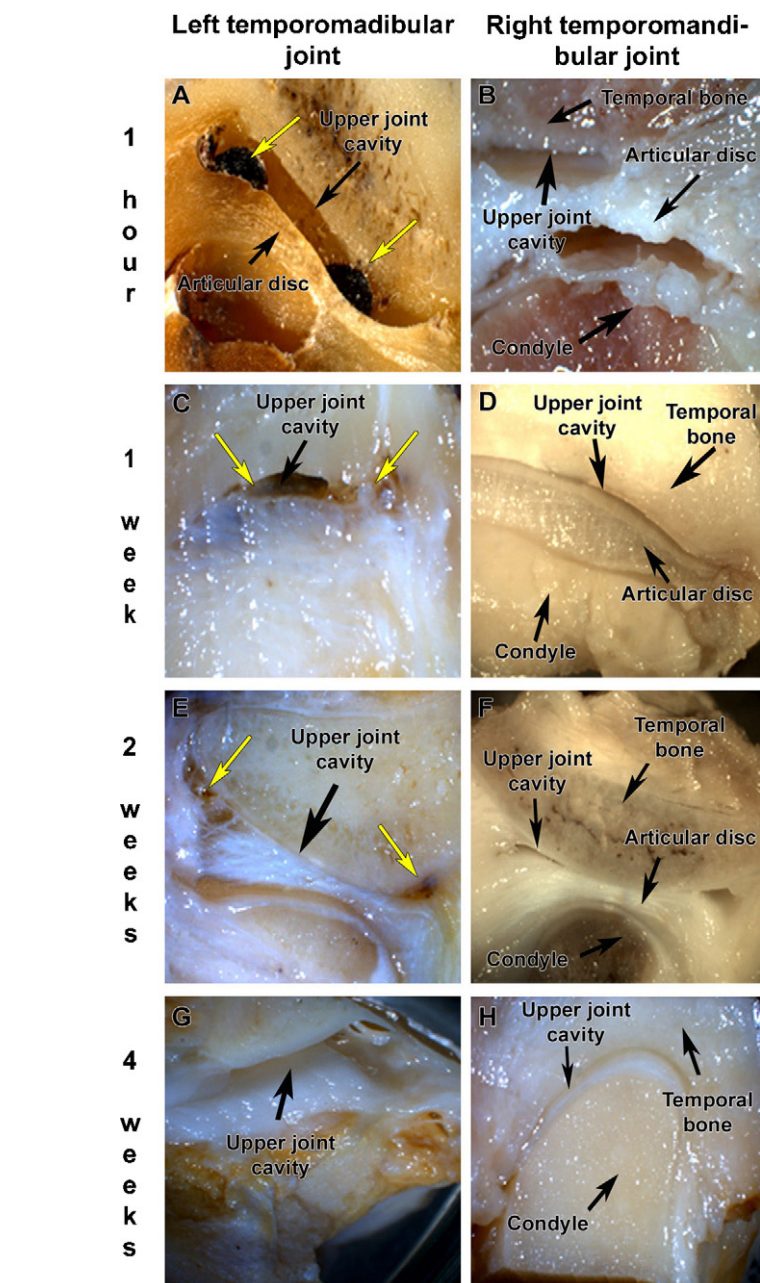


Fig. 2. Macroscopic view of pig TMJ after treatment. (A) Macroscopic view of left TMJ 1 h after treatment, yellow arrows shows visible clots in the upper joint cavity. (B) Macroscopic view of right control TMJ at same stage with physiological anatomical structure. (C) Macroscopic view of left TMJ 1 week after treatment, yellow arrows show remaining blood clots in the distal and central parts of the upper joint cavity. (D) Macroscopic view of right control TMJ 1 week after treatment with physiological anatomical structure. (E) Macroscopic view of left TMJ 2 weeks after treatment, yellow arrows show remaining small blood clots in the distal part of the upper joint cavity. (F) Macroscopic view of right control TMJ 2 weeks after treatment, there are not apparent morphological changes. (G) Macroscopic view of left TMJ 4 weeks after treatment. The upper joint cavity remained with smooth surfaces and without changes or adhesions. (H) Macroscopic view of right control TMJ 4 weeks after treatment. There joint surfaces are still smooth without changes.

upper joint cavity. 4 weeks after surgery, no remnants of blood, changes or adhesions were apparent inside the TMJ (Fig. 2).

In MRI, the injection injury caused by the needle was visible in the articular disc and surface of the temporal bone 1 h after surgery. There were no apparent morphological

changes in the nuclear magnetic resonance (NMR) images when comparing the control and experimental joints (Fig. 3).

Regarding histological analysis, no inflammatory or non-inflammatory morphological lesions were observed at any time after the treatment. The superior and inferior articular spaces showed no sign of joint exudation. The surface of the synovium was covered with small finger-like projections (villi) with no morphological lesions. The fibrous articular discs (menisci) formed fibrocartilage pads containing bundles of elastic and collagen fibres between opposing surfaces of the joint. Fibroblasts were rare and were dispersed among fibres. Articular cartilage covering the condyle of the mandible and temporal bone was formed of hyaline cartilage with no apparent erosion or pathological defects (Fig. 4). The middle and deep layers of cartilage were organized into columns of chondrocytes with normal appearance.

Selective histological staining for different types of fibres demonstrated non-fragmented fibres in their typical arrangement. The menisci, peripheral surfaces of the joints and the fibrous tissue of the joint capsule showed no dystrophic or inflammatory lesions (Fig. 4).

Discussion

Autologous blood injection is a simple treatment for TMJ hypermobility in humans. The major advantage of TMJ autologous blood injection is that it is minimally invasive, and being a non-surgical technique it is more acceptable and comfortable for patients. This method does not require surgical incision, tissue dissection, bone preparation or general anaesthesia, and eliminates postoperative complications such as facial nerve injuries, infection and oedema. The disadvantages of the technique are that the needle is advanced without visualization and there is therefore a risk of incorrect application of the autologous blood. Needle insertion can damage the surrounding tissues and cause bleeding in and around the joint.

Schulz was the first to report the treatment of human patients using autologous blood for recurrent condyle dislocation.¹⁸ He injected autologous blood twice a week for 3 weeks and used intermaxillary fixation for jaw immobilization. 10 of 16 patients were asymptomatic after 1 year. Jacobi-Hermanns et al. injected autologous blood once into the affected side and used intermaxillary fixation for 2 weeks.³ This approach was successful in 94% of condyle dislocations. Hasson and

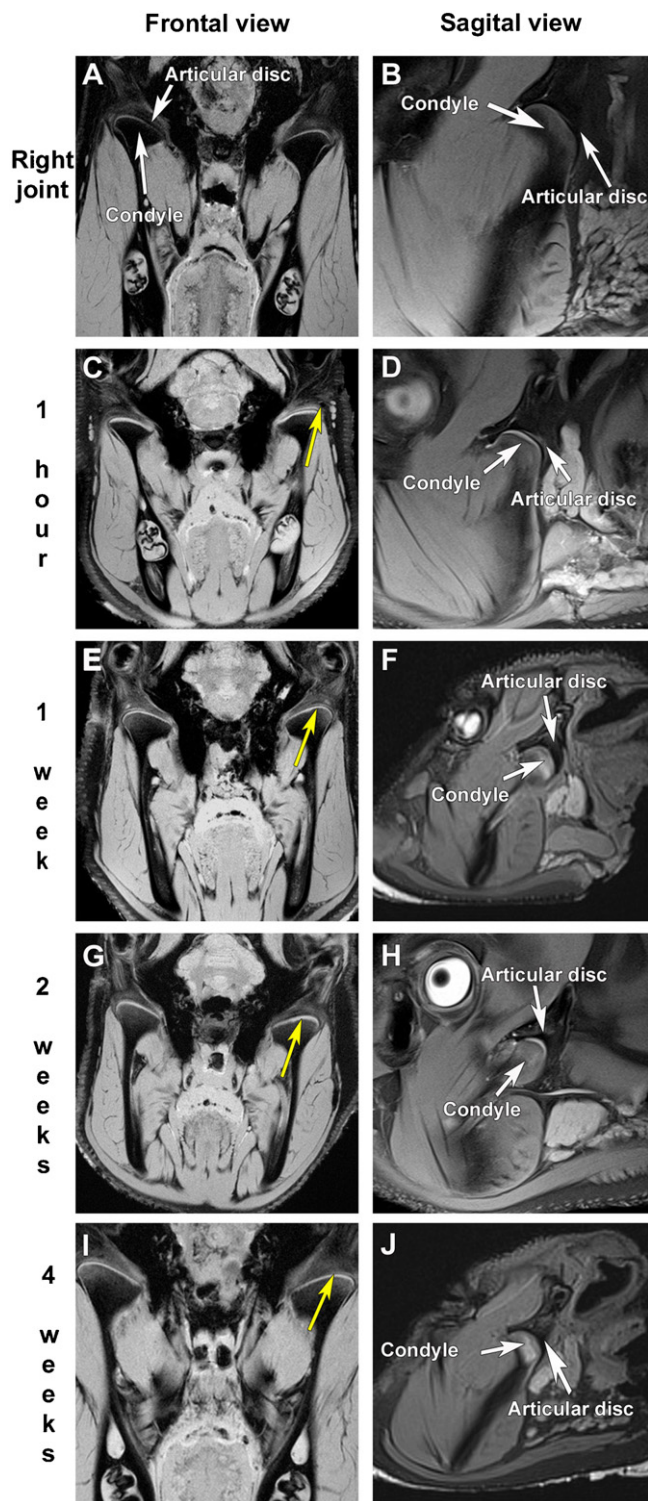


Fig. 3. NMR analysis of TMJ after blood treatment. (A) Frontal view of pigs head with both TMJs. (B) Sagittal view of physiological TMJ. (C) Frontal view of both TMJs 1 h after treatment, yellow arrow shows damage of articular disc and temporal bone surface caused by needle. (D) Sagittal view of left TMJ 1 h after treatment with no apparent evidence of blood and damage. (E) Frontal view of both TMJs 1 week after treatment, yellow arrow shows left TMJ but there is no evidence of blood. (F) Sagittal view of left TMJ 1 week after treatment. (G) Frontal view of both TMJs 2 weeks after treatment, yellow arrow shows left TMJ with no apparent changes and blood rests. (H) Sagittal view of left TMJ 2 weeks after treatment with no apparent morphological changes. (I) Frontal view of both TMJs 4 weeks after treatment, yellow arrow shows left TMJ with no apparent changes. (J) Sagittal view of left TMJ 4 weeks after treatment. (For interpretation of the references to colour in this figure legend, the reader is referred to the web version of the article.)

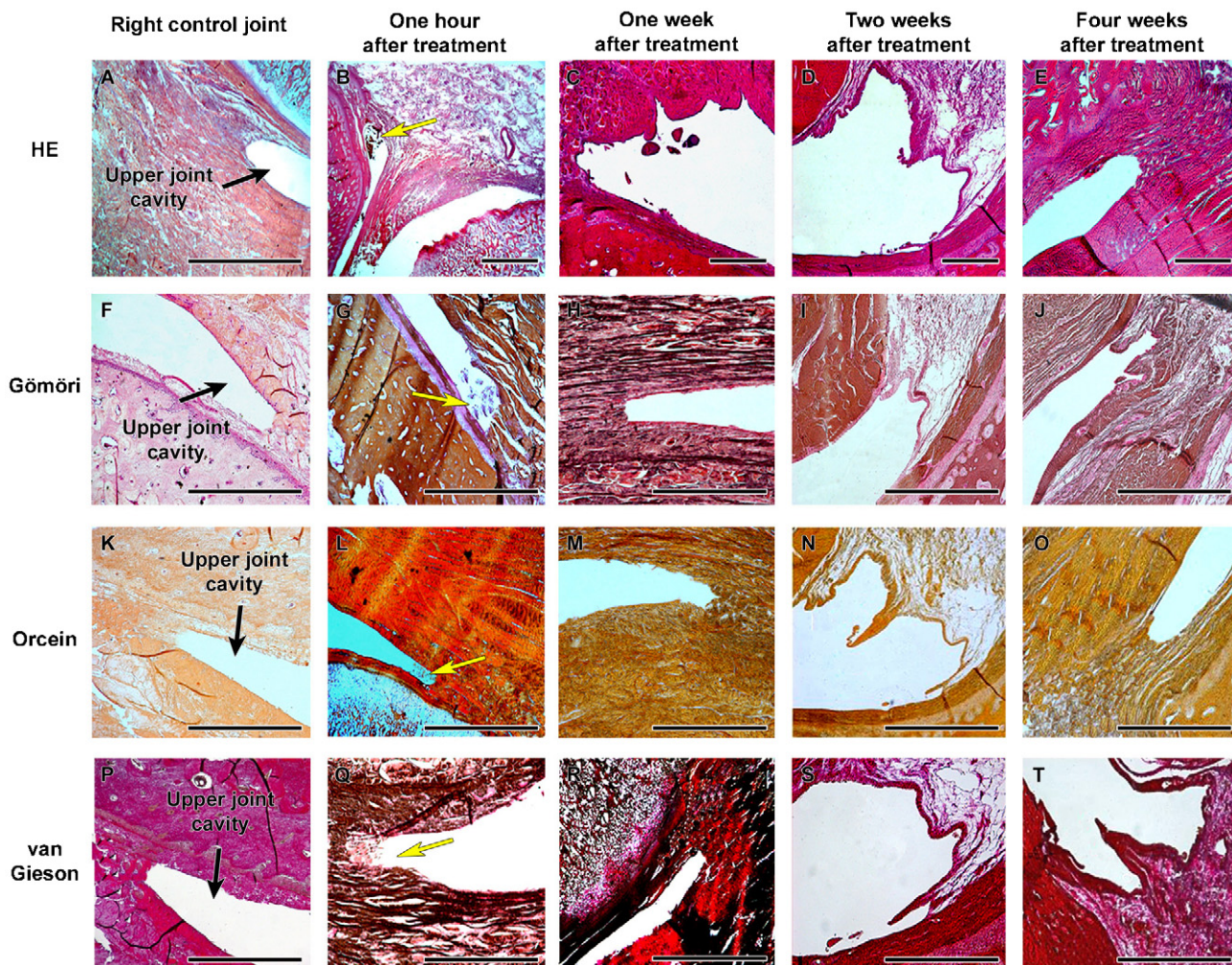


Fig. 4. Microscopic structure of pig TMJ after blood treatment. (A) Right control TMJ stained with HE, (F) with Gömöri for reticular fibres visualization, (K) with Orcein for elastic fibres and (P) with van Gieson for collagen fibres. There are characteristic smooth surfaces in the upper joint cavity. (B, G, L, O) Left treated TMJ collected 1 h after treatment. Yellow arrow shows blood clots in the distal part of cavity, there are no other morphological changes. (C, H, M, R) Left treated TMJ 1 week after treatment; there is no apparent blood or other changes. (D, J, N, S) Left TMJ 2 weeks after treatment. Special staining demonstrated non-fragmented fibres with their characteristic arrangement in the joint without obvious microscopic changes. Scale bar 200 μ m.

Nahlieli reported four patients who received one injection of autologous blood and were then instructed to restrict their mandibular movement for 7 days.² Dislocation of condyles did not reoccur, and all patients presented normal mouth opening at follow-up inspections. Kato et al. reported autologous blood injection as a method for treatment of TMJ hypermobility in an 84-year-old woman with subsequent mandible fixation for 1 month. The result was favourable, and no ankylosis occurred.⁹ Machon et al. treated 25 patients diagnosed with chronic recurrent TMJ dislocation.⁷ The patients were treated by bilateral injections of autologous blood into the upper joint space and around the TMJ capsules. 80% of patients did not require any further treatment during the following year.

Based on clinical data, the presence of autologous blood in the TMJ (injury, surgery) and subsequent immobility may result in adhesion or in development of ankylosis. These studies also reported limited mouth opening in patients with a history of TMJ injury or degenerative diseases.^{19–22} Despite the fact that autologous blood injection is used as a routine therapy in humans, it remains unclear what happens in unaffected TMJs after injection. The injection of autologous blood into the knee joint in rabbit and dogs led to joint changes under pathological conditions such as traumatic bleeding, haemophilic bleeding or rheumatoid arthritis.^{23–26} Oxidative stress (injury, arthritis, infection) at the molecular level was shown to contribute to formation of cross-linked proteins that

may serve as an initial scaffold for the development of adhesion under pathological conditions.²⁷ Some authors suggest that exposure of cartilage to blood alters chondrocyte metabolism, which might lead to unknown alterations and cartilage destruction, plus changes in matrix integrity that may result in lasting joint damage.^{23,24,26} Others suggest that such exposure has only a temporary effect and that a single episode of intra-articular bleeding only leads to reversible cartilage damage.^{25,28,29}

One possible explanation for the effect of autologous blood is an aseptic inflammation resulting in scar and fibrous tissue formation between the surfaces of the articular disc and articular socket, causing a reduction in the extent of condylar movement.^{2,9} No destructive changes to the bony

components of the joint controlled by X-ray have been observed in humans.^{2,9,10}

Until now, experiments involving autologous blood injection into unaffected TMJ in animals have only been performed on rabbits. Candrl et al. used 8 white rabbits for bilateral autologous blood injection into the TMJ. After injection, the mandibles were fixed by orthodontic brackets and elastics for 24 h and the animals killed after 1 month. There was no evidence of degeneration in the joint and no adhesions were found.¹⁴

In the present study on a pig model, the authors have not found any lesions or morphological changes, which could be responsible for the beneficial results of autologous blood injection reported elsewhere. They cannot confirm that injection of autologous blood into the TMJ has any effect based on inflammatory changes. There were some disadvantages of the pig model that should be taken into account when using it for TMJ disease research. The surgery had to be carried out under general anaesthesia. In comparison to experiments on rabbit or dog knee joints, which provide easy access for needle penetration due to the thin layer of subcutaneous tissue, the pig TMJ is situated under a large amount of subcutaneous and adipose tissue and a small skin incision is therefore necessary. The correct needle position could not be confirmed by protrusive movement of the mandible, meaning that in the pig, unlike humans, a double arthrocentesis with saline solution was necessary.

In conclusion, a methodical approach for autologous blood treatment of the TMJ and pathohistological evaluation of specimens in pigs has been demonstrated. Although the human TMJ is unique, the size of the articular structures in the pig, the shape and microscopic characteristics of the meniscus and further similarities favour it as a model species.^{15–17} Although the injection of autologous blood into the TMJ is a relatively successful treatment in humans, elucidating the effect remains to be determined. The present experiment showed no structural changes in the joints and did not confirm the theory of aseptic inflammation resulting in the formation of adhesions inside the joint. This information can be extended by a detailed cellular and molecular analysis, which may help to explain the therapeutic effect in humans.

Funding

This study was funded by Ministry of Education, Youth and Sport of the CR (Project FRVS G4145512008) and SVC

1M0528 Craniofacial Medical Research using animal models runs under the project of the Ministry of Health (OK 10/II – NT 1 1420-612010).

Competing interests

The authors report no conflicts of interest.

Ethical approval

The experimental procedure was approved by the Animal Research Committee of IAPG CAS, v.v.i. (Nr. 67985904).

References

- Antczak-Bouckoms AA. Epidemiology of research for temporomandibular disorders. *J Orofac Pain* 1995;**9**:226–34.
- Hasson O, Nahlieli O. Autologous blood injection for treatment of recurrent temporomandibular joint dislocation. *Oral Surg Oral Med Oral Pathol Oral Radiol Endod* 2001;**92**:390–3.
- Jacobi-Hermanns E, Wagner G, Tetsch P. Investigations on recurrent condyle dislocation in patients with temporomandibular joint dysfunction: a therapeutical concept. *Int J Oral Surg* 1981;**10**:318–23.
- Poirier F, Blanchereau C, Francfort E, Agostini P, Petavy A, Khorshid M, et al. Surgical treatment of temporomandibular joint: apropos of 94 cases. *Rev Stomatol Chir Maxillofac* 2006;**107**:436–40.
- Shibata T, Yamashita T, Nakajima N, Ueda M, Ishijima T, Shigezumi M, et al. Treatment of habitual temporomandibular joint dislocation with miniplate eminoplasty: a report of nine cases. *J Oral Rehabil* 2002;**29**:890–4.
- Tasanen A, Lamberg MA. Closed condylotomy in the treatment of recurrent dislocation of the mandibular condyle. *Int J Oral Surg* 1978;**7**:1–6.
- Machon V, Abramowicz S, Paska J, Dolwick MF. Autologous blood injection for the treatment of chronic recurrent temporomandibular joint dislocation. *J Oral Maxillofac Surg* 2009;**67**:114–9.
- Matsushita K, Abe T, Fujiwara T. OK-432 (Picibanil) sclerotherapy for recurrent dislocation of the temporomandibular joint in elderly edentulous patients: case reports. *Br J Oral Maxillofac Surg* 2007;**45**(September (6)):511–3. [Epub 2006 Oct 23].
- Kato T, Shimoyama T, Nasu D, Kaneko T, Horie N, Kudo I. Autologous blood injection into the articular cavity for the treatment of recurrent temporomandibular joint dislocation: a case report. *J Oral Sci* 2007;**49**:237–9.
- Pinto AS, McVeigh KP, Bainton R. The use of autologous blood and adjunctive 'face lift' bandage in the management of recurrent TMJ dislocation. *Br J Oral Maxillofac Surg* 2009;**47**(4):323–4.
- Shimizu M, Kurita K, Matsuura H, Ishimaru JI, Goss AN. The role of muscle grafts in temporomandibular joint ankylosis: short-term experimental study in sheep. *Int J Oral Maxillofac Surg* 2006;**35**(September (9)):842–9. Epub 2006 May 26.
- Long X, Goss AN. A sheep model of intra-capsular condylar fracture. *J Oral Maxillofac Surg* 2007;**65**(June (6)):1102–8.
- Takaishi M, Kurita K, Matsuura H, Goss AN. Effect of auricular cartilage graft in the surgical treatment of temporomandibular joint ankylosis: an animal study using sheep. *J Oral Maxillofac Surg* 2007;**65**(February (2)):198–204.
- Candrl C, Yüce S, Yildm S, Sert H. Histopathologic evaluation of autologous blood injection to the temporomandibular joint. *Craniofac Surg* 2011;**22**(November (6)):2202–4.
- Bermejo A, Gonzalez O, Gonzalez JM. The pig as an animal-model for experimentation on the temporomandibular articular complex. *Oral Surg Oral Med Oral Pathol Oral Radiol Endod* 1993;**75**:18–23.
- Detamore MS, Hegde JN, Wagle RR, Almarza AJ, Montufar-Solis D, Duke PJ, et al. Cell type and distribution in the porcine temporomandibular joint disc. *J Oral Maxillofac Surg* 2006;**64**:243–8.
- Helland MM. Anatomy and function of the temporomandibular joint. *J Orthop Sports Phys Ther* 1980;**1**:145–52.
- Schulz S. Evaluation of periarticular autotransfusion for therapy of recurrent dislocations of the temporomandibular joint. *Dtsch Stomatol* 1973;**23**:94–8.
- Campos PS, Macedo Sobrinho JB, Crusoe-Rebello IM, Pena N, Dantas JA, Mariz AC, et al. Temporomandibular joint disc adhesion without mouthopening limitation. *J Oral Maxillofac Surg* 2008;**66**:551–4.
- Hase M. Adhesions in the temporomandibular joint: formation and significance. *Aust Dent J* 2002;**47**:163–9.
- Kim YK, Im JH, Chung H, Yun PY. Clinical application of ultrathin arthroscopy in the temporomandibular joint for treatment of closed lock patients. *J Oral Maxillofac Surg* 2009;**67**:1039–45.
- Zhang S, Liu X, Yang C, Cai X, Chen M, Haddad MS, et al. Intraarticular adhesions of the temporomandibular joint: relation between arthroscopic findings and clinical symptoms. *BMC Musculoskeletal Disorders* 2009;**10**:70.
- Hooiveld M, Roosendaal G, Wenting M, van den Berg M, Bijlsma J, Lafeber F. Short-term exposure of cartilage to blood results in chondrocyte apoptosis. *Am J Pathol* 2003;**162**:943–51.
- Hooiveld MJ, Roosendaal G, Jacobs KM, Vianen ME, van den Berg HM, Bijlsma JW, et al. Initiation of degenerative joint damage by experimental bleeding combined with loading of the joint: a possible mechanism of hemophilic arthropathy. *Arthritis Rheum* 2004;**50**:2024–31.

25. Roosendaal G, TeKoppele JM, Vianen ME, van den Berg HM, Lafeber FP, Bijlsma JW. Blood-induced joint damage: a canine in vivo study. *Arthritis Rheum* 1999;**42**: 1033–9.
26. Hooiveld M, Roosendaal G, Vianen M, van den Berg M, Bijlsma J, Lafeber F. Blood-induced joint damage: longterm effects in vitro and in vivo. *J Rheumatol* 2003;**30**:339–44.
27. Dijkgraaf LC, Zardeneta G, Cordewener FW, Liem RS, Schmitz JP, de Bont LG, et al. Crosslinking of fibrinogen and fibronectin by free radicals: a possible initial step in adhesion formation in osteoarthritis of the temporomandibular joint. *J Oral Maxillofac Surg* 2003;**61**:101–11.
28. Safran MR, Johnston-Jones K, Kabo JM, Meals RA. The effect of experimental hemarthrosis on joint stiffness and synovial histology in a rabbit model. *Clin Orthop* 1994;**303**:280–8.
29. Tan AH, Mitra AK, Chang PC, Tay BK, Nag HL, Sim CS. Assessment of blood-induced cartilage damage in rabbit knees using scanning electron microscopy. *J Orthop Surg (Hong Kong)* 2004;**12**:199–204.

Address:

Jan Stembirek

Institute of Animal Physiology and Genetics
v.v.i.Academy of Sciences of the Czech Republic
Veveri 97

602 00 Brno

Czech Republic

Tel: +420 777 136 039

E-mail: stembirek@iach.cz

Komentář k přiložené publikaci č. 7

Michal KYLLAR, Barbora PUTNOVA, Vladimír JEKL, Ladislav STEHLIK, Marcela BUCHTOVA a **Jan STEMBIREK**. Diagnostic imaging modalities and surgical anatomy of the temporomandibular joint in rabbits. *Laboratory Animals* [online]. 2018, **52**(1), 38–50. ISSN 0023-6772. Dostupné z: doi:[10.1177/0023677217702178](https://doi.org/10.1177/0023677217702178)

IF = 1,117; kvartil Q2

Králík (*Oryctolagus cuniculus f. domesticus*) je jako modelový druh v rámci výzkumu oblasti čelistního kloubu používán relativně často. V morfologii králičího a lidského TMK však existují významné rozdíly, které je třeba před použitím tohoto modelu pro experimentální výzkum vzít v úvahu. V této studii jsme si kladli za cíl podobnosti a rozdíly ve struktuře králičího a lidského TMK podrobně zmapovat a popsat pro účely dalšího výzkumu v této oblasti.

Jedním z rozdílů je kompletní laterální kostěné překrytí králičího čelistního kloubu jařmovým obloukem, což komplikuje chirurgický přístup. Nejvýraznějším morfologickým rozdílem mezi králičím a lidským čelistním kloubem je však tvar kloubního výběžku, který je u králíka více oploštěný a krátkým krčkem spojený s větví dolní čelisti. V retrodiskální oblasti není v oblasti kloubní jamky vytvořena kost, ale je krytá pouze tenkou vrstvou temporálního svalu a podkožní tkáň. Z tohoto důvodu je pro chirurgickou intervenci do čelistního kloubu nutné zvolit přístup z dorzální části. Vzhledem k odlišnému anatomickému umístění pak u králíků není třeba uvažovat o strukturách, jako je lícni nerv, maxilární arterie a průšní žláza.

Mandibulární kondylus králíka je pokryt sekundární chrupavkou a vazivovou tkání podobně jako u lidí. V případě použití králíka jako zvířecího modelu je také důležité zvážit hloubku experimentálních defektů vytvořených v kondylární chrupavce. Na základě zjištěných parametrů jsme pro další výzkum v oblasti defektů chrupavky a kostí doporučili u králíka hloubku defektu méně než 150 µm pro chrupavky a více než 220 µm pro subchondrální defekty. Na rozdíl od lidí je králičí chrupavka nejtlustší ve střední oblasti, nikoliv v postero-superiorní oblasti. V uspořádání chrupavčitých buněk pak mezi lidskými a králičími chrupavkami TMK nejsou žádné významné rozdíly.

Mezi lidským a králičím kloubním diskem významné rozdíly nacházíme. Zatímco lidský disk je popsán jako hustá vláknitá fibrochrupavčitá tkáň s buňkami podobnými chondrocytům, králičí disk obsahuje dobře diferencovanou chrupavčitou tkáň.

Vzhledem k výše jmenovaným rozdílům v utváření králičího a lidského čelistního kloubu se tak králík sice nejvíce jako vhodný model pro zkoumání či zdokonalování chirurgických postupů, nicméně pro snadnou manipulaci a nízké náklady na chov může být (při respektování a zvažování všech morfologických rozdílů) úspěšně použit jako výzkumný model pro experimenty v tkáňovém inženýrství.

Diagnostic imaging modalities and surgical anatomy of the temporomandibular joint in rabbits

Michal Kyllar^{1,2}, Barbora Putnová^{3,4}, Vladimír Jekl⁵,
Ladislav Stehlík⁶, Marcela Buchtová³ and Jan Štembírek^{3,7}

Laboratory Animals
 2018, Vol. 52(1) 38–50
 © The Author(s) 2017
 Reprints and permissions:
 sagepub.co.uk/
 journalsPermissions.nav
 DOI: 10.1177/0023677217702178
 journals.sagepub.com/home/lan



Abstract

The temporomandibular joint (TMJ) is a condylar synovial joint that, together with the masticatory muscles, controls mandibular movement during mastication. The rabbit is often used as a model species for studying the mechanisms of TMJ diseases, and in regenerative research. However, there are significant differences between rabbit and human TMJs that should be taken into account before using this model for experimental research. Here, we use several analytical approaches (radiography, computed tomography and magnetic resonance imaging) to enable a detailed description and analysis of the rabbit TMJ morphology. Moreover, possible surgical approaches have been introduced with a focus on available access into the rabbit TMJ cavity, which relate our findings to clinical usage.

Keywords

animal model, feeding, jaw, rabbit, temporomandibular joint (TMJ)

Date received: 24 September 2016; accepted: 3 March 2017

The temporomandibular joint (TMJ, *articulatio temporomandibularis*) is a multi-component structure that, together with the masticatory muscles, controls mandibular movement during mastication. It consists of the condylar process of the mandibular ramus (*ramus mandibulae*), mandibular fossa of the temporal bone (*fossa mandibularis ossis temporalis*), a thin articular disc (*discus articularis*), and a loose joint capsule reinforced with fibrous lateral ligaments.¹ The structure and function of this incongruent, condylar synovial joint (hinge sliding joint) are unique among the diarthrodial joints.²

There are many diseases and traumas affecting the TMJ. While many studies have provided detailed information about the development, anatomy and aetiopathogenesis of TMJ diseases, there is a lack of comprehensive understanding of the mechanism initiating these diseases. Many of the symptoms are difficult or impossible to treat using current methods, highlighting the need for extensive research in this field. The use of animal models for such research is indispensable.³ Due to physiological and anatomical differences between the human TMJ and those of experimental animals, no one animal model can provide a full understanding that could be directly related to humans.⁴ In

addition, many other variables, such as gender, age, size and depth/age of the defect, postoperative treatment, etc., need to be considered when designing experiments. Therefore, an investigator faces the challenging task of choosing the most suitable model and treatment protocol in order to answer a specific question. Discrepancies

¹Department of Anatomy, Histology and Embryology, Faculty of Veterinary Medicine, University of Veterinary and Pharmaceutical Sciences Brno, Brno, Czech Republic

²Companion Care, Broadstairs, UK

³Institute of Animal Physiology and Genetics, v.v.i., Academy of Sciences of Czech Republic, Brno, Czech Republic

⁴Department of Pathological Morphology and Parasitology, University of Veterinary and Pharmaceutical Sciences Brno, Brno, Czech Republic

⁵Avian and Exotic Animal Clinic, University of Veterinary and Pharmaceutical Sciences Brno, Brno, Czech Republic

⁶Department of Diagnostic Imaging, Small Animals Clinics, Faculty of Veterinary Medicine, University of Veterinary and Pharmaceutical Sciences Brno, Brno, Czech Republic

⁷Department of Oral and Maxillofacial Surgery, University Hospital Ostrava, Czech Republic

Corresponding author:

Marcela Buchtová, Institute of Animal Physiology and Genetics CAS, v.v.i., Veverí 97, Brno, 602 00, Czech Republic.
 Email: buchtova@iach.cz

in the results of clinical studies focused on treatment modalities for TMJ dysfunction make it obvious that animal models are needed to define and control experimental variables.⁵ Although no one animal model can exactly duplicate the human condition, a number of authors have argued that, despite its prognathism, the pig, *Sus scrofa*, is the best non-primate model for modelling the human TMJ form and function.^{6–9} Although large animal models such as the pig may resemble humans more closely than smaller animals, they are usually neither practical nor economically feasible for conducting initial experiments in large animals.¹⁰

One of the smaller animal models frequently utilized in research is the rabbit. Rabbits are easy to handle and inexpensive to maintain in cages, making them convenient animals for use in experimental studies. Rabbits are often used in studies to test dental implants,^{11–14} to test bone grafts following the extraction of cheek teeth,¹⁵ and to investigate the influence of biomaterials on the bone healing process around the tooth sockets.^{16,17} Studies on the effect of tooth loss on the histochemical composition of TMJ cartilage and disc¹⁸ and on the histology of the condyle¹⁹ have been performed. Surgical alterations of the rabbit TMJ for investigation of discectomy effects^{20,21} and implantation of disc replacements have also been reported.²² However, although the rabbit has been routinely used as an experimental animal model, very little information is available about the anatomy of its TMJ, and its coverage in veterinary textbooks is even more cursory.²³ The best description of the rabbit TMJ²⁴ is unfortunately not easily accessible to English-speaking researchers; and other descriptions of rabbit TMJs are contradictory, particularly with respect to their nomenclature.²⁵

Considering the lack of complete information about the anatomical and histopathological characteristics of the rabbit TMJ, the purpose of this investigation was to (1) provide an overall description of a rabbit TMJ with an emphasis on gross anatomy and its comparison to a human TMJ; (2) describe the appearance of the anatomical structures on radiographs, computed tomography (CT) and magnetic resonance imaging (MRI) scans, and discuss the advantages and disadvantages of individual techniques for TMJ studies; and (3) relate our findings to clinical usage and describe achievable surgical approaches into a rabbit TMJ.

Materials and methods

Animals

Twelve clinically normal eight-month-old outbred male New Zealand white specific pathogen-free rabbits (*Oryctolagus cuniculus*, strain Hsdlf:NZW; Harlan

Laboratories Inc, Belton, UK) were used in this study. The weight of the animals ranged from 2.92 to 3.15 kg (mean 3.03 ± 0.2 kg). The animals were fully developed and were free of any pathological processes. All the rabbits were housed individually in an animal care facility under controlled conditions, and were handled and euthanized according to the agreement of the Branch Commission for Animal Welfare of the Ministry of Agriculture of the Czech Republic (project PP52-2013 UVPS).

Diagnostic imaging

The rabbit heads were radiographed using a Gierth X-ray machine (Gierth HF 200A; Gierth X-Ray International GmbH, Riesa, Germany). Radiographs were captured on computed radiography cassettes. The focal length was set to 100 cm and the exposure values were 50 kV, 200 mA, and 150 ms (30 mAs). The images were stored in a digital imaging and communications in medicine (DICOM) format using a computed radiography system (FCR Capsula XL; Fuji, Tokyo, Japan). The image resolution was 1760×2140 pixels.

Native transverse CT scans of each rabbit's head were obtained using a multidetector CT scanner (LightSpeed 16; GE Medical Systems, Milwaukee, WI, USA). The scanning protocol was 80 kV, with an automatic mA setting, a tube rotation time of one second, a slice thickness of 1.25 mm, a spiral pitch factor of 0.9 and a high frequency convolution kernel (proprietary name: bone). All the scans were obtained using the helical mode. Radiographic and CT analyses were performed at the Department of Diagnostic Imaging, Small Animals Clinic, Faculty of Veterinary Medicine (Brno, Czech Republic).

MRI analysis (Bruker Avance 9.4T, Bruker BioSpec; Bruker, Ettlingen, Germany) of the rabbit heads was conducted at the Institute of Scientific Instruments of the Czech Academy of Sciences (Brno, Czech Republic). Images were acquired in sagittal and transverse planes with fast spin echo (FSE) sequences. The heads were positioned in ventral recumbency during the scanning procedure. FSE T1-weighted transverse MR images were obtained with the following parameters: FLASH, AVG = 6, TE = 3.7 ms, TR = 369 ms, matrices = 512×512 . Acquisition time 14.5 min and RARE, AVG = 6, TE = 25 ms, TR = 3500 ms, matrices = 512×256 , RARE factor = 8.

Dissection procedure

Palpable anatomical landmarks were identified prior to dissection using a rabbit skull model as a reference. Anatomical dissections of the TMJ were performed using a stratigraphic approach, and each dissected

layer was photographed using a Nikon D 5100 camera (Nikon Europe BV, Amsterdam, The Netherlands). The key anatomical structures were identified and indicated on the photographs.

Histological evaluation

The harvested mandibular condyles (*condyles mandibulares*), including the articular cartilage, were fixed for three days in 10% buffered formaldehyde and decalcified in 12.5% EDTA solution (pH = 8), which was prepared as a mixture of 0.5 mmol/L EDTA, 4% buffered formaldehyde and PBS buffer (pH = 7.4). The tissue samples were left in this decalcification solution in an incubator at a temperature of 37°C for 11 months. Following the decalcification, the samples were processed for histological analysis using a standard procedure – they were washed in water (overnight) and dehydrated in an increasing alcohol series (30% for 3 h; 50% for 3 h; 70% overnight; 80% for 2 h; 95% for 2 h; 100% for 1 h). Then, the samples were soaked in xylene for 5 h, run through three paraffin baths (for 1 h in each of them) and embedded in paraffin blocks.

Five micrometre paraffin sections were stained with haematoxylin and eosin (H&E), Alcian blue (AB) and Masson's trichrome.²⁶ The staining protocols used in this study were modified in the following steps: after

staining in Mayer's haematoxylin, staining in acid-alcohol was not differentiated but was left in warm water for 5 min. In the case of the AB staining, H&E was used for a counterstaining. In the case of the Masson's trichrome, Weigert's haematoxylin (Diapath SpA, Martinengo BG, Italy) was used, then the sections were differentiated in acid-alcohol, stained with Fuchsin Ponceau acc. Masson (Diapath SpA), differentiated in 1% phosphotungstic acid and stained with a light green (Diapath SpA).

Morphometric assessment

Morphometric assessment was carried out on the dissected and macerated skulls (Figure 1). TMJ width (TMJW) was determined by measuring the distance between the medial aspect of the zygomatic process of the temporal bone (*processus zygomaticus ossis temporalis*) and the squama of the temporal bone. TMJ length (TMJL) was measured as the distance between the rostral aspect of the zygomatic process of the temporal bone and the most caudal projection of the zygomatic arch (*arcus zygomaticus*). Condylar width (CW) was measured at its widest point.

Furthermore, a surface projection of the TMJ on the rabbit skull was established by using an axis of the zygomatic arch and the line connecting the caudal aspect of the zygomatic process of the frontal bone

Table 1. Origins and insertions of muscles connected with temporomandibular joint (TMJ) function.

Muscle	Subdivision	Origin	Insertion
Musculus masseter	Pars superficialis	Arcus zygomaticus – rostral portion	Angulus mandibulae
	Pars profunda rostralis	Arcus zygomaticus – medially on caudal portion	Caudal corpus mandibulae to the level of angulus mandibulae
	Pars profunda caudalis	Arcus zygomaticus – medially on caudal portion	Angulus mandibulae to distal part of ramus mandibulae
Musculus temporalis superficialis		Os temporale and os parietale	Lateral and proximal aspect of the processus coronoides mandibulae
Musculus temporalis profundus	Pars medialis	Os temporale within the orbit	Rostral ridge of the coronoid process
	Pars lateralis	Os temporale	Proximal ridge and medial aspect of the coronoid process
Musculus pterygoideus medialis		Os pterygoideum/fossa pterygoidea	Medial aspect of the ramus mandibulae distally, angulus mandibulae and corpus mandibulae caudally
Musculus digastricus		Processus jugularis of the occipital bone	Rostral extent of the angulus mandibulae

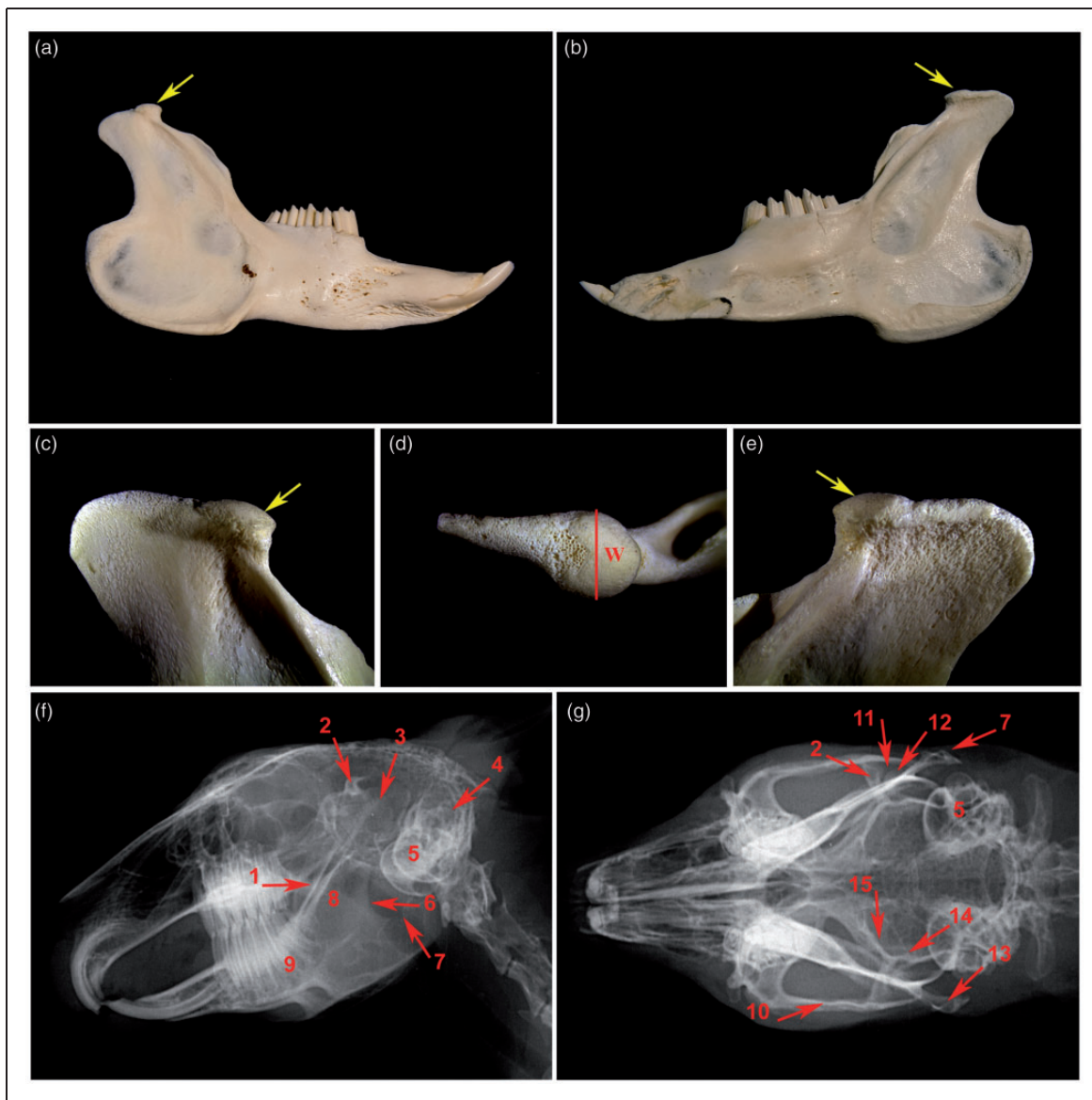


Figure 1. Mandible of the rabbit. (a) Lateral view of the rabbit mandible. (b) Medial view of the rabbit mandible. (c) Detail of lateral aspect of the mandibular caput (arrow) (d) Detail of dorsal aspect of the mandibular caput. (e) Detail of medial aspect of the mandibular caput. (f, g) Radiographs of rabbit skull. 1: cranial aspect of the ramus mandibulae, 2: processus zygomaticus ossis temporalis, 3: processus condylaris mandibulae, 4: meatus acusticus externus, 5: bulla tympani, 6: caudal aspect of the ramus mandibulae, 7: processus angularis, 8: ramus mandibulae, 9: corpus mandibulae, 10: arcus zygomaticus, 11: spatium articulare of the temporomandibular joint [TMJ], 12: condylus mandibulae, 13: processus caudalis arcus zygomatici, 14: os temporale, 15: os presphenoidale, w: TMJ width (TMJW).

(*processus zygomaticus ossis frontalis*) and ear canal (*meatus acusticus externus*).

Histological samples of the head of the mandible (*caput mandibulae*) were stained using AB and were used for measurements of the cartilage thickness. Photodocumentation was taken using a DMC2900 camera (Leica, Wetzlar, Germany), and the thickness of the hyaline cartilage was measured using the AxioVision 40 version 4.8.2.0 software (Carl Zeiss MicroImaging GmbH, Munich, Germany). The

acquired data were processed using the Statistica software (StatSoft, Tulsa, OK, USA).

Results

The TMJ is a complex congruent joint in a rabbit (Figure 1), in which the convex surface of the mandibular condyle articulates with the concave articular surface of the temporal bone (*facies articularis squama ossis temporalis*) located ventrally on the zygomatic

process of the temporal bone. The articular disc is formed within the joint despite the joint being congruent in rabbits.

Radiography

Lateral skull radiographs clearly displayed the bony structures of the facial area. It was not possible to visualize the bones of the TMJ in detail due to the superimposition of the adjacent bones and masticatory muscles, therefore only some of the structures were identified (Figure 1). Radiographs gave a clear picture of the location of the zygomatic process of the temporal bone overlying the less discernible mandibular condyle followed by an overlap of the caudal process of the zygomatic arch (*processus caudalis arcus zygomaticus*). The bony part of the ear external opening and tympanic bulla (*bulla tympani*) were located caudally (Figure 1f).

A dorsoventral radiographic view of the rabbit skull showed the TMJ in even greater detail, allowing easy identification of the TMJ articular space (*spatium articulare*), the coronoid process of the mandible (*processus coronoideus mandibulae*), the mandibular ramus and the wall of the temporal bone (*squama ossis temporalis*) with the tympanic bulla (Figure 1g).

The cross-section of the line connecting the ear canal and caudal process of the supraorbital margin (*processus caudalis margo supraorbitalis*) and the line connecting the caudal processes of the zygomatic arch was located above the joint space of the TMJ in all the skulls under investigation.

Computed tomography

All TMJ structures identified on the radiographs were identifiable on the CT images; however, a more detailed morphology was visible in the transverse or sagittal CT slices (Figure 2). The articular surface of the temporal bone, which superimposed with the zygomatic arch in the lateral view on the radiograph, was discernible on the CT images (Figure 2). This surface was composed of a transversally elongated shallow articular tubercle of the temporal bone (*tuberculum articulare ossis temporalis*) and a shallow triangular mandibular fossa of the temporal bone, which was positioned sagittally and caudally. In the dorsal view, the articular surface of the mandibular condyle descended in a dorsolateral to ventromedial direction. The articular surface was also located rostrally on the mandibular condyle in the shape of a convex triangle, with the base situated rostrally and the apex caudally (Figure 2). Apart from a small flat and indistinct mastoid eminence (*processus mastoideus*), there were no caudal borders

to the mandibular fossa. The retroarticular process (*processus retroarticularis*) was missing in the rabbits. Only the anterior–superior aspect of the mandibular condyle was in contact with the articular surface of the temporal bone, interposing the central part of the articular disc (Figure 2). Most of the muscular tissues were recognizable on the CT images, including the temporal, masseter (*musculus masseter*) and pterygoid (*musculus pterygoideus*) muscles (Figure 2).

Magnetic resonance imaging

The soft tissues of the TMJ, including the surrounding muscles, were well delineated on the MRI scans. The oval articular disc was transversally positioned (Figure 3). The TMJ capsule was attached to the borders of the articular surfaces. The articular disc was connected to the medial and lateral aspects of the joint capsule.

There are five main masticatory muscles in a rabbit (Table 1);^{24,27} however, only four were identified on the MR images. The masseter muscle consisted of three heads (Figure 4). The superficial head, or *pars superficialis*, originated from a point two-thirds of the way along the anterior portion of the lower border of the zygomatic arch (Figure 4), and was inserted into the mandibular angle (*angulus mandibulae*). The deep head, or *pars profunda*, originated one-third of the way along the medial–posterior part as well as from the medial portion of the zygomatic arch (Figure 4). It was inserted into the masseteric fossa (*fossa masseterica*) and subdivided into a rostral and a caudal part, which were indistinct on the MR images (Figure 3). During mastication, these two heads differed in function.

The superficial temporal muscle (*musculus temporalis superficialis*) tendon slid in the muscular groove (*sulcus muscularis*) dorsally over the TMJ. The medial aspect of the condylar process of the mandible (*processus condylaris ossis mandibularis*) and the mandibular ramus were the sites of attachment of the deep temporal muscle (*musculus temporalis profundus*) and both the pterygoid muscles (Figure 3, Table 1). The deep temporal muscle in the rabbits was further divided into the medial and lateral heads, which however were not discernible on the MR images.

Surgical anatomy

The superficial projection of the TMJ could be located by palpating the osseous part of the ear canal and caudal process of the supraorbital margin as well as the laterally located zygomatic arch (Figure 5). The cross-section of the axis of the zygomatic arch and the line connecting the supraorbital margin and

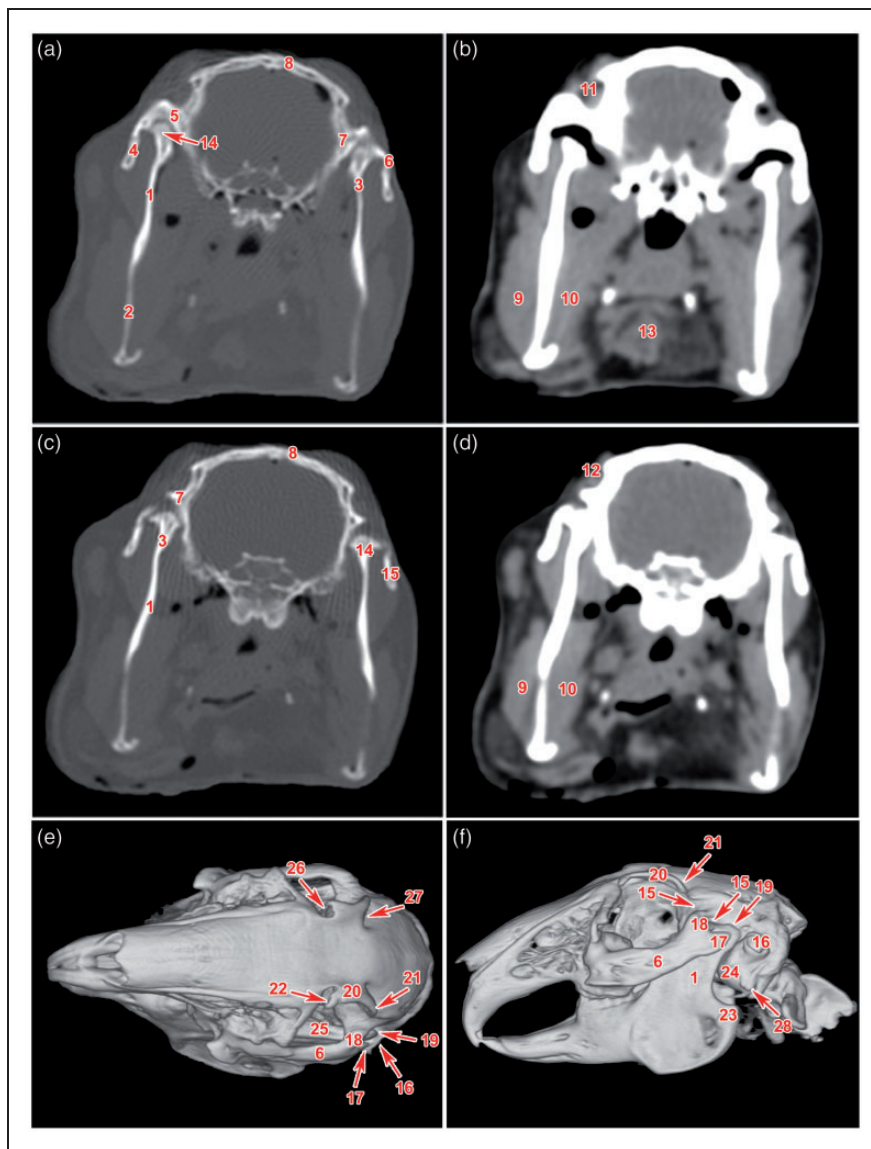


Figure 2. [a–f] Transverse and three-dimensional computed tomography images of the rabbit skull with focus on TMJ. 1: ramus mandibulae, 2: corpus mandibulae, 3: collum mandibulae, 4: arcus zygomaticus – processus temporalis ossis zygomatici, 5: arcus zygomaticus – processus zygomaticus ossis temporalis, 6: arcus zygomaticus, 7: os temporale, 8: os frontale, 9: musculus massetericus, 10: musculus pterygoideus medialis, 11: musculus temporalis superficialis, 12: sulcus muscularis (musculus temporalis), 13: tongue, 14: condylus mandibulae, 15: condylus mandibulae, 16: porus acusticus externus, 17: processus caudalis arcus zygomatici, 18: processus zygomaticus ossis temporalis, 19: processus condylaris, 20: margo supraorbitalis, 21: processus caudalis margo supraorbitalis, 22: processus rostralis margo supraorbitalis, 23: processus angularis mandibulae, 24: bulla tympani, 25: processus coronoideus mandibulae, 26: incisura supraorbitalis rostralis, 27: incisura supraorbitalis caudalis, 28: processus mastoideus.

the ear canal was located just above the TMJ space (Figure 5).

The TMJ was bordered dorsally by the zygomatic process of the temporal bone, medially by the squamous part of the temporal bone, and laterally by the zygomatic arch composed of the zygomatic process of the temporal bone and the temporal process of the zygomatic bone, which was projecting caudally into

the caudal process of the zygomatic arch beyond the borders of the mandibular ramus. The TMJ was caudally and ventrally opened and surrounded by soft tissues. The dorsal aspect of the TMJ was covered by the musculotendinous origin of the superficial temporal muscle, which was directed rostrally over the zygomatic process of the temporal bone in the muscular groove (Figure 5) and attached rostrally from the TMJ on the

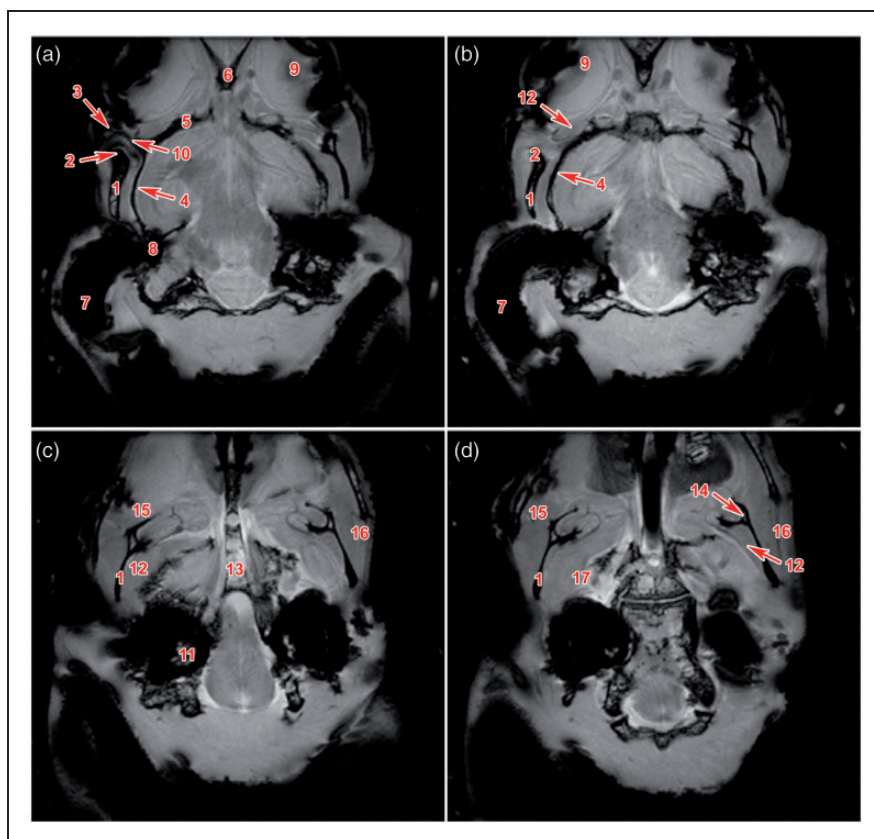


Figure 3. [a–d] Magnetic resonance imaging of the rabbit head in a transversal plane with focus on TMJ. 1: ramus mandibulae, 2: condylus mandibulae, 3: processus zygomaticus ossis temporalis, 4: os temporale, 5: os presphenoidale, 6: ala ossis presphenoidalis, 7: auris externa, 8: auris media, 9: bulbus oculi, 10: discus articularis, 11: bulla tympani, 12: musculus temporalis, 13: processus pterygoideus, 14: foramen mandibulae, 15: musculus masseter, 16: musculus zygomaticomandibularis, 17: musculus pterygoideus medialis.

indistinct coronoid process (*processus coronoideus*). The TMJ was bounded medially by the deep temporal muscle, which originated from the squamous part of the temporal bone and sphenoid bone (*ossis sphenoidalis*) and attached medially on the coronoid process and mandibular ramus. The condylar process of the mandible was covered caudolaterally only by the superficial fascia and by the skin, and was therefore easily palpable (Figure 5). The rostrolateral aspect of the zygomatic arch served as the origin of the masseter muscle – its superficial part originated from the base of the zygomatic arch and its deep part originated from the caudal process of the zygomatic arch (Figures 4 and 5).

The TMJ was surrounded by a thin capsule consisting of fibrous tissue and synovial lining. The capsule stretched from the edge of the mandibular fossa to the neck of the mandible (*collum mandibulae*) and as far caudally as the caudal process of the zygomatic arch. The articular space was divided into superior discotemporal and inferior discomandibular spaces. No large vessels or nerves were located in close proximity to

the rabbit TMJ. The lacrimal gland was located rostrally and dorsally adjacent to the TMJ.

The interposed articular disc exhibited a biconcave morphology and concave surface proximally and distally (Figure 5). Its central area was thinner and the disc was attached to the joint capsule medially and laterally.

Histological analysis of the TMJ

Individual areas of the TMJ, such as the mandibular head, mandibular fossa and fibrocartilaginous disc, exhibited differences in microscopic structure (Figure 6). The mandibular head was composed of two types of cartilage – hyaline cartilage and fibrocartilage. Collagen fibres of the fibrocartilage were arranged parallel to the surface. The fibrocartilage passed into the hyaline cartilage in a highly cellular zone of small flattened chondrocytes, which represents the resting zone of the cartilage. Chondrocytes in the hypertrophic zone were arranged in columns which were transversally orientated to the surface (Figure 6). The calcified cartilage zone was wide, especially in

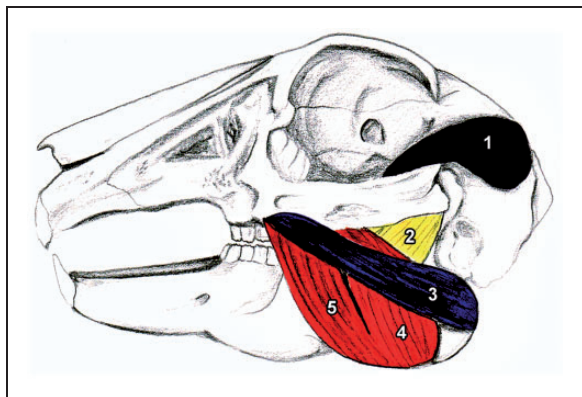


Figure 4. Masticatory muscle attachments in the rabbit. 1: musculus temporalis superficialis, 2: musculus masseter pars profunda caudalis, 3: musculus masseter pars superficialis (part 1), 4: musculus masseter pars superficialis (part 2), 5: musculus masseter pars profunda rostralis.

younger animals, and passed into the subchondral bone at a depth of about 200 μm under the surface. Trabecular bone contained a large amount of chondro-osseous tissue (Figure 6).

The articular disc was fibrocartilaginous (Figure 6) and revealed dense interwoven collagen fibres oriented predominantly mediolaterally on the periphery of the disc, whereas the crimped collagen fibres of the intermediate zone were directed rostrocaudally (Figure 6).

Morphometric assessment of rabbit TMJ

The cross-section of the line tangential to the dorsal aspect of the zygomatic arch and the line connecting the ear canal and the caudal process of the supraorbital margin was located above the TMJ in all the rabbits under investigation. The TMJ was roughly oval in shape, with an average width of 5 ± 0.02 mm and an average length of 15 ± 0.22 mm. The width of the mandibular condyle was 3 ± 0.09 mm.

Morphometric analysis of the cartilage thickness in the mandibular head area was carried out on histological sections, revealing differences in cartilage thickness in the rostral and caudal areas. The average thickness of the hyaline component was 196 μm rostrally, 209 μm medially and 169 μm caudally (Figure 6a,b). The thickness of the fibrous component also varied significantly – it was the thickest caudally and the thinnest rostrally.

Discussion

The TMJ is unique to mammals, but its morphology and function vary enormously among orders and species. Currently, the most commonly used model species

for studying TMJ diseases are rats, rabbits, pigs, and ruminant ungulates. Each of these animal groups has distinctive TMJ adaptations. With the exception of pigs, these species show less loading of the jaw joints during chewing than humans.²⁸

There are morphological differences between human and rabbit TMJs. One difference is the complete shielding of the rabbit TMJ by the zygomatic arch laterally and by the condylar process of the mandible caudally in rabbits. Therefore, the entire joint is covered by the overhanging zygomatic flange. On the other hand, the bone arrangement on the medial side is similar to that in humans. The most striking morphological difference between rabbit and human TMJs is, however, the shape of the articular surface of the condyle and of the retro-discal area. Rabbits have no postglenoid wall. Instead, a prominent condylar process rises above the level of the TMJ, leaving the posterior aspect of the TMJ unprotected by bone and covered only by a thin layer of temporal muscle and subcutaneous tissue. For this reason, resection of the condylar process is necessary for surgical intervention in the TMJ using the posterior approach. That the bony shield is missing has consequences for posterior disc attachments, where the disc is not rigidly anchored to the bone. In humans, the temporal and condylar attachments are separated by a delicate venous plexus, and the whole area is sheltered by a postglenoid process. This area was proposed as a space for disc attachments.²⁹ The equivalent space in the rabbit TMJ is filled by the condylar process of the mandible and the temporal muscle attached to this process. The general structure of the rabbit TMJ allows only a limited range of movements, such as hinge joint movements (e.g. opening and closing) and protrusive/retrusive movements.

The anatomy and location of the rabbit TMJ make its evaluation by radiography a challenge due to the limited visualization of craniofacial structures. The superimposition of several bones and some soft tissues disguises the clear pattern of the delicate structures of the skull. Only frontal sinuses and the facial skeleton are clearly discernible due to their superficial character. Different radiographic views have been suggested to improve visualization of the rabbit TMJ.^{25,27} Another study that suggested the use of different angles of projection for the visualization of the rabbit TMJ have reported a satisfactory assessment of the joint components and space in the rabbit when using a rostrocaudal view and a 10–20 degree rotation in a lateral direction.²⁷

Any mini-invasive treatment (injection or arthrocentesis) requiring TMJ access must always take into account the surrounding anatomical structures. In humans, these include the ear canal, facial nerve, skull base, superficial temporal vein, maxillary artery

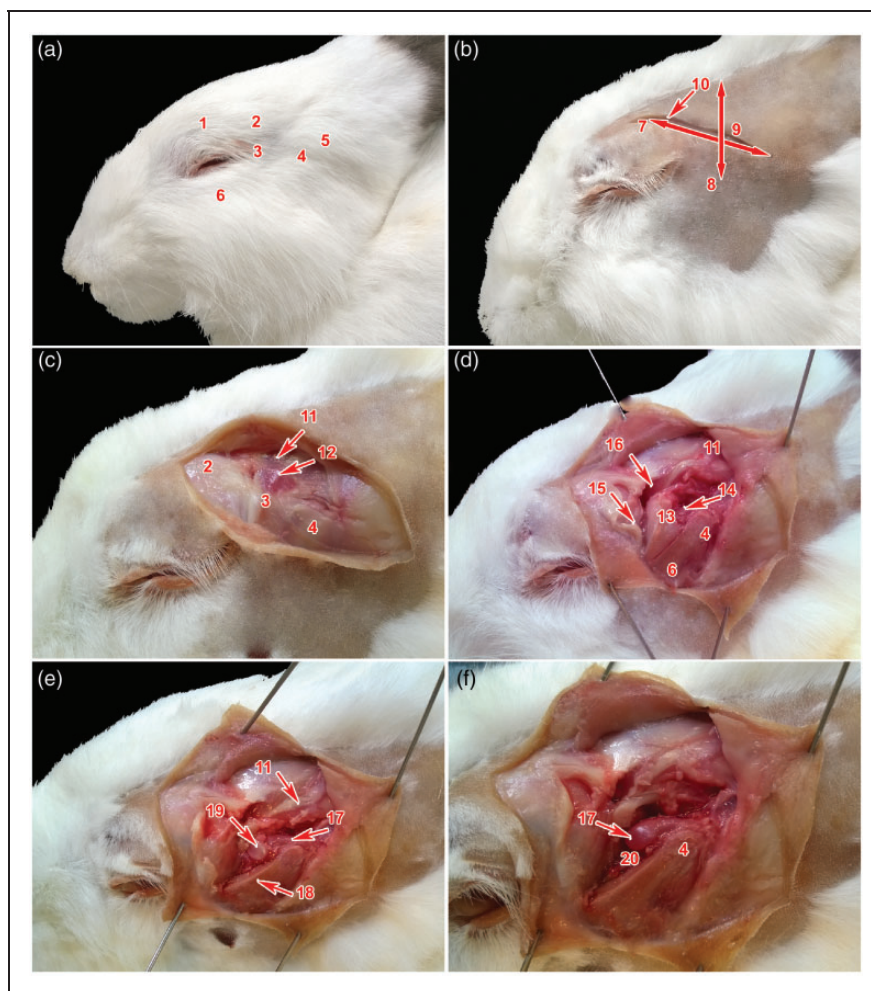


Figure 5. [a–f] Dissection of the temporomandibular joint in the rabbit. 1: margo supraorbitalis, 2: processus caudalis margo supraorbitalis, 3: ligamentum orbitale, 4: processus caudalis arcus zygomatici, 5: meatus acusticus externus, 6: arcus zygomaticus, 7: line connecting processus caudalis margo supraorbitalis and meatus acusticus externus, 8: line connecting contralateral processus caudalis arcus zygomatici, 9: intersection of the lines defines surface projection of the temporomandibular joint, 10: incision connecting margo supraorbitalis and meatus acusticus externus, 11: musculus temporalis, 12: capsula articularis of the temporomandibular joint, 13: processus zygomaticus ossis temporalis, 14: processus condylaris mandibulae, 15: ligamentum orbitale transacted, 16: sulcus muscoli temporalis, 17: condylus mandibulae/facies articularis, 18: removed processus zygomaticus ossis temporalis, 19: discus articularis, 20: cavum articulare after the removal of the discus articularis.

and parotid glands. In rabbits, structures such as the facial nerve, maxillary artery and parotid gland, do not need to be considered due to the different anatomical location of its TMJ. To perform a mini-invasive procedure in a rabbit, open surgery exposing the joint capsule is necessary and special care has to be taken with respect to the joint position. Whereas the joint is located posteriorly to the muscular prominence in humans, it is positioned anteriorly in rabbits.³⁰ Therefore, the best approach for any mini-invasive surgery in a rabbit TMJ should be from a dorsal aspect of the TMJ. An incision should be made halfway through

the line connecting the caudal process of the supra-orbital margin and the base of the ear.

The condyle of a rabbit is covered by secondary cartilage and fibrous tissue as in humans.³¹ It is also important to consider the depth of experimental defects created in the condylar cartilage before using the rabbit as an animal model. We proposed a depth of less than 150 μm for a cartilage defect and more than 220 μm for a subchondral defect. Unlike humans, the rabbit cartilage is thickest in the middle area and not in the poster-osuperior region. The densest part of the human TMJ cartilage is 480 μm .³² This fact should be taken into

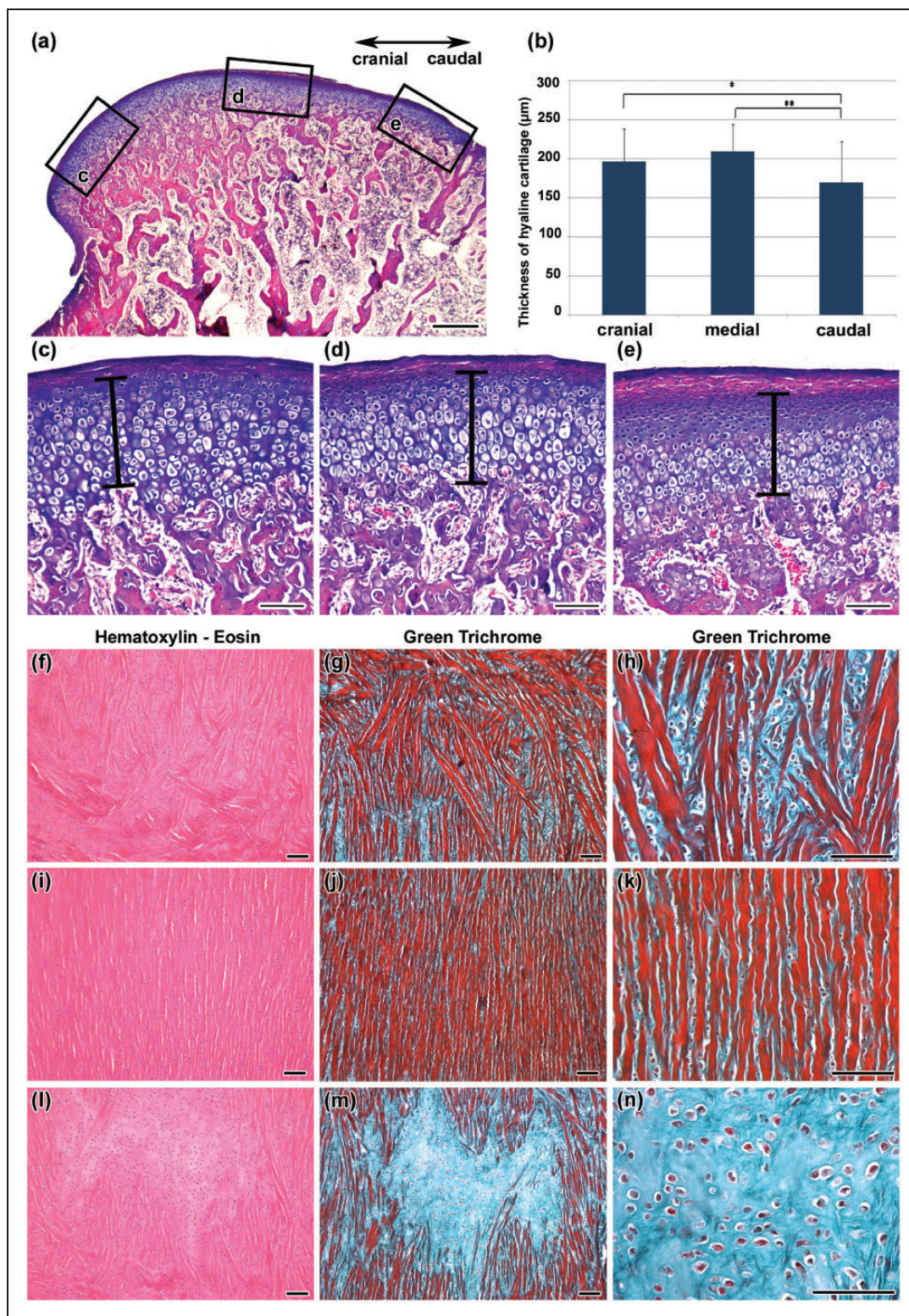


Figure 6. Microscopic analysis of the rabbit temporomandibular joint (TMJ). (a–e) Sagittal sections of caput mandibulae in the rabbit. Alcian blue, haematoxylin and eosin stainings of an eight-month-old animal. (b) Graph of hyaline cartilage thickness. We observed statistically significant differences in cartilage thickness between individual areas of caput mandibulae. $*P < 0.05$, $**0.00 < P < 0.01$. (c) Detail view of the cranial part of caput mandibulae. (d) Detail of the caudal part of caput mandibulae. (e) Detail of the caudal part of caput mandibulae. (f–h) Horizontal sections of articular disc. (f–h) Transitional area from disc to the capsule. (i–k) Most of the disc is formed by fibrocartilage. (l–n) Central area of the disc is mostly formed by cartilage. Scale bar in Figure A = 500 µm, scale bars in Figures B–N = 100 µm.

consideration when selecting tools for the preparation of experimental defects. With regard to the arrangement of cartilaginous cells, there are no significant differences between human and rabbit TMJ cartilages.³³ However, there are significant differences between human and rabbit TMJ discs. Whereas the human disc is described as dense fibrous tissue, or fibrocartilaginous plate, where the chondrocyte-like cells should not be referred to as chondrocytes,³⁴ the rabbit disc contains well-differentiated cartilaginous tissue. These chondrocytes are arranged between fibrous stripes, and islets of this cartilaginous tissue are present in the central area of the disc. It is worth noting that the cartilaginous tissue is found in young animals. Nevertheless, for a deeper understanding of the origin of these cells further immunohistochemical investigation will be necessary.

To identify the exact area for local injection into the rabbit TMJ it is possible to use the connection of the palpable reference points of the bony ear canal and caudal process of the supraorbital margin and the intersection of that line with a line tangential to the dorsal aspect of the zygomatic arch. The needle should be inserted at this point with its bevel pointing towards and parallel with the zygomatic arch. However, this approach may penetrate the tendon of the temporal muscle overlying the joint, which can cause sample contamination or possible tendinitis. Therefore, in cases in which a non-contaminated sample has to be collected, an open surgical approach above the TMJ is the only viable option. The incision should be performed sagittally above the TMJ along the line connecting the caudal process of the supraorbital margin and the base of the ear and by retracting the tendon of the temporal muscle laterally. A practical execution is however relatively difficult due to the size of the joint and also to the risk of cartilage damage. Unlike in humans, it is not possible to rely on the 'clap' of the needle on the fossa during its insertion. From our point of view, tilting the needle perpendicularly to the joint surface and performing a lateral perforation as in humans seems to be the best solution. The maximum dip of the needle insertion should be about 2–3 mm.

An arthrocentesis in a rabbit model is obviously even more difficult to perform and may also require open surgery. Due to the differences between rabbit and human TMJs, the rabbit TMJ is not really a suitable educational model for practicing arthroscopic surgery. Rabbit TMJ can however be used as a research model: while performing a surgical intervention, anatomical differences should be taken into account. Moreover, due to the very small size of the articular disc, the rabbit TMJ is not suitable for performing procedures such as arthroscopies, discopexis or discectomy.³⁵

Declaration of Conflicting Interests

The author(s) declared no potential conflicts of interest with respect to the research, authorship, and/or publication of this article.

Funding

The author(s) disclosed receipt of the following financial support for the research, authorship, and/or publication of this article: This study was supported by the Grant Agency of the Czech Republic (14-37368G to MB lab, 14-29273P to JS) and the Ministry of Health, Czech Republic (MH CZ-DRO-FNOs/2013).

References

1. Siessere S, Vitti M, Semprini M, et al. Macroscopic and microscopic aspects of the temporomandibular joint related to its clinical implication. *Micron* 2008; 39: 852–858.
2. Koolstra JH. Dynamics of the human masticatory system. *Crit Rev Oral Biol Med* 2002; 13: 366–376.
3. Neyt JG, Buckwalter JA and Carroll NC. Use of animal models in musculoskeletal research. *Iowa Orthop J* 1998; 18: 118–123.
4. Herring SW. TMJ anatomy and animal models. *J Musculoskelet Neuronal Interact* 2003; 3: 391–394; discussion 406–407.
5. Greene CS, Mohl ND, McNeill C, Clark GT and Truelove EL. Temporomandibular disorders and science: a response to the critics. *Am J Orthod Dentofacial Orthop* 1999; 116: 430–431.
6. Meister R, Berg R and Berg P. [Topographic and applied anatomy of the temporomandibular joint (articulatio temporomandibularis) of various domestic animals with special reference to the resection possibilities of the discus articularis. 4. Swine (*Sus scrofa domestica*)]. *Z Exp Chir* 1973; 6: 437–448.
7. Bermejo A, Gonzalez O and Gonzalez JM. The pig as an animal model for experimentation on the temporomandibular articular complex. *Oral Surg Oral Med Oral Pathol* 1993; 75: 18–23.
8. Strom D, Holm S, Clemensson E, Haraldson T and Carlsson GE. Gross anatomy of the mandibular joint and masticatory muscles in the domestic pig (*Sus scrofa*). *Arch Oral Biol* 1986; 31: 763–768.
9. Stembirek J, Kyllar M, Putnova I, Stehlik L and Buchtova M. The pig as an experimental model for clinical craniofacial research. *Lab Anim* 2012; 46: 269–279.
10. Sprinz RA. A note on the mandibular intra-articular disc in the joints of Marsupialia and Monotremata. *Proc Zool Soc Lond* 1965; 144: 327–337.
11. Rahmani M, Shimada E, Rokni S, et al. Osteotome sinus elevation and simultaneous placement of porous-surfaced dental implants: a morphometric study in rabbits. *Clin Oral Implants Res* 2005; 16: 692–699.
12. Kim YS, Kim SH, Kim KH, et al. Rabbit maxillary sinus augmentation model with simultaneous implant placement: differential responses to the graft materials. *J Periodontal Implant Sci* 2012; 42: 204–211.

13. Munhoz EA, Bodanezi A, Cestari TM, Taga R, de Carvalho PS and Ferreira O Jr. Long-term rabbits bone response to titanium implants in the presence of inorganic bovine-derived graft. *J Biomater Appl* 2012; 27: 91–98.
14. Guo Z, Iku S, Mu L, et al. Implantation with new three-dimensional porous titanium web for treatment of parietal bone defect in rabbit. *Artificial Organs* 2013; 37: 623–628.
15. Manso JE, Mourao CF, Pinheiro FA, Ferreira ML, Silva PC and Schanaider A. Molars extraction for bone graft study in rabbits. *Acta Cir Bras* 2011; 26(Suppl 2): 66–69.
16. Fisher JP, Lalani Z, Bossano CM, et al. Effect of biomaterial properties on bone healing in a rabbit tooth extraction socket model. *J Biomed Mater Res A* 2004; 68: 428–438.
17. Marei MK, Nouh SR, Saad MM and Ismail NS. Preservation and regeneration of alveolar bone by tissue-engineered implants. *Tissue Eng* 2005; 11: 751–767.
18. Huang Q, Opstelten D, Samman N and Tideman H. Experimentally induced unilateral tooth loss: histochemical studies of the temporomandibular joint. *J Dent Res* 2002; 81: 209–213.
19. Im JH, Kim SG, Oh JS, Lim SC and Ha JM. Influence of unilateral tooth loss in the temporomandibular joint and masseter muscle of rabbits. *Oral Surg Oral Med Oral Pathol Oral Radiol* 2012; 114: 9–16.
20. Sato S, Goto S, Koeda S and Motegi K. Changes of the elastic fibre network of the rabbit temporomandibular joint following discectomy. *J Oral Rehabil* 2002; 29: 847–852.
21. Dimitroulis G and Slavin J. The effects of unilateral discectomy and condylectomy on the contralateral intact rabbit craniomandibular joint. *J Oral Maxillofac Surg* 2006; 64: 1261–1266.
22. Feinberg SE and McDonnell EJ. The use of a collagen sheet as a disc replacement in the rabbit temporomandibular joint. *J Oral Maxillofac Surg* 1995; 53: 535–542; discussion 43.
23. Sahler LG, Morris TW, Katzberg RW and Tallents RH. Microangiography of the rabbit temporomandibular joint in the open and closed jaw positions. *J Oral Maxillofac Surg* 1990; 48: 831–834.
24. Barone R. *Anatomie comparée des mammifères domestiques. Arthrologie et myologie*. Paris: Vigot, 1989.
25. King AM, Cranfield F, Hall J, Hammond G and Sullivan M. Radiographic anatomy of the rabbit skull with particular reference to the tympanic bulla and temporomandibular joint. *Part 1: Lateral and long axis rotational angles*. *Vet J* 2010; 186: 232–243.
26. Bancroft JD and Cook HC. *Manual of histological techniques and their diagnostic application*. Edinburgh: Churchill Livingstone, 1994.
27. King AM, Cranfield F, Hall J, Hammond G and Sullivan M. Radiographic anatomy of the rabbit skull, with particular reference to the tympanic bulla and temporomandibular joint. *Part 2: Ventral and dorsal rotational angles*. *Vet J* 2010; 186: 244–251.
28. Herring SW. Masticatory muscles and the skull: a comparative perspective. *Arch Oral Biol* 2007; 52: 296–299.
29. Luder H-U. *Postnatal development, aging, and degeneration of the temporomandibular joint in humans, monkeys and rats*. Craniofacial Growth Series, Vol 32. Ann Arbor, MI: Center for Human Growth and Development, University of Michigan, 1996.
30. Kuruvilla VE and Prasad K. Arthrocentesis in TMJ internal derangement: a prospective study. *J Maxillofac Oral Surg* 2012; 11: 53–56.
31. Mizoguchi I, Takahashi I, Nakamura M, et al. An immunohistochemical study of regional differences in the distribution of type I and type II collagens in rat mandibular condylar cartilage. *Arch Oral Biol* 1996; 41: 863–869.
32. Bibb CA, Pullinger AG and Baldioceda F. The relationship of undifferentiated mesenchymal cells to TMJ articular tissue thickness. *J Dent Res* 1992; 71: 1816–1821.
33. Wang L, Lazebnik M and Detamore MS. Hyaline cartilage cells outperform mandibular condylar cartilage cells in a TMJ fibrocartilage tissue engineering application. *Osteoarthritis Cartilage* 2009; 17: 346–353.
34. Detamore MS and Athanasiou KA. Structure and function of the temporomandibular joint disc: implications for tissue engineering. *J Oral Maxillofac Surg* 2003; 61: 494–506.
35. Al-Moraissi EA. Open versus arthroscopic surgery for the management of internal derangement of the temporomandibular joint: a meta-analysis of the literature. *Int J Oral Maxillofac Surg* 2015; 44: 763–770.

Résumé

L'articulation temporo-mandibulaire (ATM) est une articulation synoviale condylienne qui, avec les muscles masticatoires, contrôle le mouvement mandibulaire lors de la mastication. Le lapin est souvent utilisé en tant qu'espèce modèle pour étudier les mécanismes des maladies de l'ATM ainsi qu'en recherche régénérative. Il existe toutefois des différences significatives entre l'ATM du lapin et celle de l'humain, qui devraient être prises en compte avant d'utiliser ce modèle pour la recherche expérimentale. Nous utilisons ici plusieurs approches analytiques (radiographie, balayage CT et IRM) pour permettre une description et une analyse détaillées de la morphologie de l'articulation temporo-mandibulaire du lapin. Des approches chirurgicales possibles qui relient nos découvertes à l'utilisation clinique sont également présentées en mettant l'accent sur l'accès disponible dans la cavité de l'ATM du lapin.

Abstract

Das Kiefergelenk ist ein kondyläres Synovialgelenk, dass zusammen mit Kaumuskeln die Unterkieferbewegung beim Kauen kontrolliert. Das Kaninchen wird häufig als Modell zur Untersuchung von Krankheiten des Kiefergelenks und in der regenerativen Forschung verwendet. Es bestehen jedoch wesentliche Unterschiede zwischen dem Kiefergelenk von Kaninchen und Mensch, die vor einer Nutzung dieses Modells für experimentelle Forschung berücksichtigt werden müssen. Anhand verschiedener Analyseverfahren (Radiografie, CT und MRI) ermöglichen wir hier eine detaillierte Beschreibung und Analyse der Kiefergelenkmorphologie des Kaninchens. Zudem werden mögliche chirurgische Verfahren mit Schwerpunkt auf verfügbarem Zugang zur Kiefergelenkhöhle des Kaninchens vorgestellt, die unsere Erkenntnisse mit klinischem Einsatz verbinden.

Resumen

La articulación temporomandibular (TMJ) es una articulación sinovial condilar que, junto con los músculos masticatorios, controla el movimiento durante la masticación. El conejo suele utilizarse como especie modelo para estudiar los mecanismos de los trastornos de TMJ y para la investigación regenerativa. No obstante, existen diferencias significativas entre la TMJ en humanos y en conejos que deberían tenerse en cuenta antes de utilizar este modelo para la investigación experimental. En este estudio utilizamos varios métodos analíticos (radiografía, CT y MRI) para conseguir una descripción y un análisis precisos de la morfología de la articulación temporomandibular. Asimismo, se introducen métodos quirúrgicos posibles con un foco en el acceso disponible a la cavidad de TMJ del conejo, uniendo de este modo nuestras conclusiones al uso clínico.

Komentář k přiložené publikaci č. 8

Barbora PUTNOVA, Pavel HURNIK, Vladimír JEKL, Dusan ZIAK, Vladimír MACHON, Misa SKORIC, Jiri STRANSKY a Jan STEMBIREK **(corresponding author)**. Effect of human adipose-derived regenerative cells on temporomandibular joint healing in immunodeficient rabbits. *Acta Veterinaria Brno* [online]. 2019, **88**(1), 49–56. ISSN 0001-7213. Dostupné z: doi:[10.2754/avb201988010049](https://doi.org/10.2754/avb201988010049)

IF = 0,566; kvartil Q3

Současná medicína hledá cestu k využití potenciálu kmenových buněk v regeneraci jednotlivých tkání. Jelikož embryonální kmenové buňky jsou z etického hlediska nedostupné, do popředí zájmu se dostávají mezenchymální kmenové buňky, u nichž není s odběrem ani etickou otázkou problém (Pagotto et al., 2021). Náš projekt se zabýval posouzením vlivu kmenových buněk na hojení léze temporomandibulárního kloubu a jejich možným využitím pro klinickou praxi.

Jako experimentální modelový organismus byl využit králík domácí (*Oryctolagus cuniculus f. domesticus*). Kmenové buňky, které měly sloužit jako zdroj faktorů ovlivňujících hojení, byly odebrány z lidské tukové tkáně. Po navození imunosuprese pomocí kortikoidů jsme u 17 králíků (9 v experimentální skupině, 8 v kontrolní skupině) v celkové anestezii vytvořili z otevřeného přístupu chirurgicky defekt v chrupavce a v kosti. U experimentální skupiny byla do horní kloubní štěrbině a do operační rány aplikována suspenze nediferencovaných lidských kmenových buněk z tukové tkáně (ASCs), zatímco u kontrolní skupiny došlo jen k proplachu fyziologickým roztokem. Zvířata byly humánně utracena po 11 a 28 dnech a oba čelistní klouby byly poté vypreparovány a histologicky zpracovány.

V oblasti rány vykazovala experimentální skupina po 11 dnech menší známky zánětlivého infiltrátu, byl zde patrný vyšší počet granulocytů a nekrotických změn. Po 28 dnech měly obě skupiny v měkkých tkáních stejné množství zánětlivého infiltrátu, ale u experimentální skupiny byl patrný vyšší stupeň angiogeneze.

V případě vyhodnocení reakce chrupavky vykazaly obě skupiny po 11 dnech experimentu srovnatelné známky nově vytvořené chrupavky. U experimentální skupiny byla patrná výraznější nekróza měkkých tkání, u jednoho kloubu došlo dokonce k resorpci chrupavky i kosti. Po 28 dnech bylo u kontrolní skupiny prokázáno větší množství nově

vytvořené chrupavky. Zajímavostí je, že v oblasti defektu kosti nebyl za 28 dní rozdíl v obou skupinách v množství osteoklastů ani osteoblastů. Přestože byly nalezeny určité náznaky zvýšeného hojení (výraznější angiogeneze v měkkých tkáních ve skupině, jíž byly aplikovány kmenové buňky), nepovažujeme celkově tento experiment s využitím mezidruhové aplikace kmenových buněk (byť po navození imunodeficiencie a s úmyslem využít těchto buněk pouze jako zdroje růstových faktorů) za příliš nadějný pro potenciální praktické využití. Vzhledem k tomu, že u králíka je poměrně obtížné (vzhledem k jeho fyziologii) získat dostatečné množství tukové tkáně pro odběr kmenových buněk z tuku, vhodnějším modelovým organismem by z tohoto pohledu mohlo být prase domácí.

Effect of human adipose-derived regenerative cells on temporomandibular joint healing in immunodeficient rabbits

Barbora Putnová¹, Pavel Hurník^{2,3}, Vladimír Jekl^{4,5}, Dušan Žiak², Vladimír Machoň⁶, Miša Škorič¹, Jiří Stránský⁷, Jan Štembírek⁷

¹University of Veterinary and Pharmaceutical Sciences Brno, Faculty of Veterinary Medicine, Department of Pathological Morphology and Parasitology, Brno, Czech Republic

²University Hospital Ostrava, Department of Pathology, Ostrava, Czech Republic

³University of Ostrava, Faculty of Medicine, Institute of Pathology, Ostrava, Czech Republic

⁴University of Veterinary and Pharmaceutical Sciences Brno, Faculty of Veterinary Medicine, Avian and Exotic Animal Clinic, Brno, Czech Republic

⁵Veterinary Clinic Jekl & Hauptman, Brno, Czech Republic

⁶General Hospital Prague, Department of Oral and Maxillofacial Surgery, Prague, Czech Republic

⁷University Hospital Ostrava, Department of Oral and Maxillofacial Surgery, Ostrava, Czech Republic

Received August 15, 2018

Accepted February 12, 2019

Abstract

Increasing research attention has focused on the use of stem cells (SCs) in regenerative and reparative medicine. Adipose-derived regenerative cells (ADRCs) are a relatively cheap and ethical source of SCs. Temporomandibular disorders (TMDs) have been reported with rising incidence over recent decades. The main aims of this study were to evaluate the effects of ADRCs application on the healing of both soft and hard temporomandibular joint (TMJ) tissues, and to assess the possible utilization of ADRCs in TMD treatment. We investigated the effects of human ADRCs on the healing of TMJ defects in immunodeficient rabbits. With no prior cultivation, ADRCs were applied to a surgically created defect in the cartilage of a rabbit TMJ. The healing process and inflammatory response were examined. Our results indicated that ADRCs supported repair processes in soft tissues. However, ADRC treatment induced a significant immune response in both soft and hard tissues, with hard tissues showing a higher level of bone remodelling. Non-differentiated ADRCs can be a promising tool for regenerative medicine of TMJ; however, deeper understanding of their effect on the cellular level is needed.

Joint regeneration, allotransplantation, animal model

The temporomandibular joint (TMJ) is a paired joint that connects the lower jaw to the temporal bone in mammals. A joint capsule attaches cranially to the temporal bone and caudally to the mandibular condyle neck, enclosing the entire articular system, including the condyle, articular disc, and fossa. This capsule is responsible for proprioception, articular structure nourishment, and prevention of joint dislocation (Berkovitz et al. 2009) The articular disc is located inside the TMJ, and divides it into two compartments that can be considered two individual joints: the meniscotemporal (suprameniscal) joint that enables translational movement, and the condylomeniscal (inframemiscal) joint that permits rotational movements. The articular surfaces comprise a hyaline/fibrocartilage composite with limited regenerative capacity. This joint structure is able to withstand the pressures occurring during mastication (Puricelli et al. 2012).

Regenerative cell therapy is currently the focus of extensive research, mostly involving the use of stem cells of various origins. Embryogenic stem cells are impractical for ethical reasons, therefore, attention is shifting to the use of adult stem cells or so-called tissue-specific stem cells, such as adipose-derived stem cells (ADSCs). The ADSCs can differentiate into other cell types, including endothelial cells and other cells that participate in angiogenesis

Address for correspondence:

MUDr. Jan Štembírek, Ph.D.
University Hospital Ostrava
17. listopadu 1790
708 52, Ostrava, Czech Republic

E-mail: stembirek@iach.cz
<http://actavet.vfu.cz/>

(Planat-Benard et al. 2004), as well as pancreatic endocrine cells that produce insulin, glucagon, and somatostatin (Timper et al. 2006). An *in vitro* study of rheumatoid arthritis reported that ADSCs exhibited immunomodulative effects, reducing the production of some proinflammatory cytokines and increasing production of the anti-inflammatory cytokine IL-10 and of antigen-specific regulatory T-lymphocytes (Gonzalez-Rey et al. 2010). However, the specific mechanisms underlying these processes remain unclear. The ADSCs can also accelerate neovascularisation. An investigation of skin healing in diabetic mice revealed that the ADSCs can increase expression of the vascular endothelial growth factor (VEGF) and the hypoxia-inducible factor 1-alpha (HIF-1 α) (Miranville et al. 2004; Gao et al. 2011). Another promising therapeutic use of ADSCs is in the treatment of ischaemia-caused pathologies (Moon et al. 2006). Experiments using bioactive glass or β -tricalcium phosphate scaffolds seeded with autologous ADSCs have been conducted to examine the role of ADSCs in healing jaw and skull injuries. The authors reported successful integration of the construct with the surrounding skeleton in 10 of 13 cases (Sandor et al. 2014).

While the stem cells' immunomodulative character and influence on tissue healing can be beneficial in reconstructive surgery and healing of problematic wounds, there is also a cancerogenic potential. It was shown that ADSCs co-cultivated with cancer cells can increase their multiplying (Yu et al. 2008). Notably, in breast cancer, both local and intravenous administration of ADSCs reportedly induces tumour cell proliferation and increases the risk of metastases (Muehlberg et al. 2009). Studies have also described the use of undifferentiated xenogenous ADSCs in the rabbit, for treatment of neural tissue (Lasso et al. 2015) or osteochondral defects (Jang et al. 2014).

In this study, we used a relatively cheap and ethically sourced heterogeneous population of cells from adipose tissue, termed human adipose-derived regenerative cells (ADRCs). These cells include ADSCs, endothelial cells, smooth muscle cells, haematopoietic cells, and other stromal cells. Compared to pure ADSCs, ADRCs are easier and less expensive to obtain, and are already used in clinical practise at our hospital. We used a rabbit model because this animal is easy to breed and is bigger than mice or rats, and thus more suitable for some types of studies, including investigations of the TMJ. The present study was designed to examine the suitability of direct application of unfiltered ADRCs in a rabbit model for TMJ research, as well as the effects of such xenogenous cells on the healing of TMJ defects.

Materials and Methods

Animals and immunosuppression

Seventeen 10-month-old male outbred New Zealand White SPF rabbits (strain CrI:KBL) were obtained from Charles River Laboratories, Inc. (Wilmington, USA). These rabbits were individually housed in wire-mesh cages at an animal care facility with controlled environmental conditions at the University of Veterinary and Pharmaceutical Sciences Brno, Czech Republic. The room temperature was maintained at 20–23 °C, with 40–55% relative humidity, and a 12-h light/dark cycle. The rabbits had free access to water, and were fed a complete pelleted diet and hay *ad libitum*. This study was performed in accordance with the ethical principles stated in the Declaration of Helsinki and approved by the Ethics Committee of the Faculty of Veterinary Medicine, University of Veterinary and Pharmaceutical Sciences Brno, approval No. 30307/2013-11. The animal housing, handling, and euthanasia were approved by the Branch Commission for Animal Welfare of the Ministry of Agriculture of the Czech Republic (project PP52-2013 UVPS).

After a three-week acclimatization period, the 17 rabbits were randomly divided into two groups: 9 in the experimental group and 8 in the control group. Prior to surgery, immunosuppression was induced in all rabbits via intramuscular administration of 2 mg/kg dexamethasone sodium phosphate (Dexamed, Medochemie Ltd, Limassol, Cyprus) three times at 6-h intervals (Jeklova et al. 2008). After surgery, all rabbits were administered 2 mg/kg of dexamethasone sodium phosphate 15 times at 2-day intervals (Jeklova et al. 2008).

Isolation of ADRCs

Adipose tissue was obtained from a single patient undergoing elective lipoplasty at the University Hospital Ostrava, with this patient's informed consent. The ADRCs were isolated from the adipose tissue using the Celution 800/CRS system (Cytori Therapeutics, Inc., San Diego, CA, USA). In this closed system process,

the adipose tissue was digested with Celase™ Reagent (Cytori Therapeutics, Inc., San Diego, CA, USA). Figure 1 shows the cell type proportions according to the manufacturer. The collection of adipose tissue from human volunteers was approved by the Ethics Committee of FN Ostrava (Approval No. 654/2014).

Experimental surgery

The animals were placed under total anaesthesia, and open surgery was performed. The incision was made in the parotidomasseteric region, approximately 3 cm cranioventrally from the auricle base. Using a rotational tool with a spherical head, we created two defects in the condyle. Into these defects, we added 1 ml human ADRCs in the experimental group, and 1 ml saline in the control group. Prior to the final suture, the wound was flushed with 0.5 ml human ADRC solution in the experimental group, and 0.5 ml saline in the control group (Plate III, Fig. 2).

Histological assessment

The animals were euthanized at two time points: 11 days (four from the experimental group, four from the control group) or 28 days (five from the experimental group, four from the control group) after the surgery. Joints were harvested together with the surrounding soft tissues. Samples were fixed in 10% buffered formaldehyde for 3 days, and then decalcified in EDTA solution with 4% formaldehyde for approximately one year. We prepared 5 µm thick paraffin sections, and then soft tissues were stained with haematoxylin and eosin, and hard tissues were stained with haematoxylin and eosin and Alcian blue. These histological sections were evaluated by two pathologists, with a focus on inflammatory and healing processes (Table 1). The validity of our results was verified using the STATISTICA software (StatSoft s.r.o., Pilsen, Czech Republic).

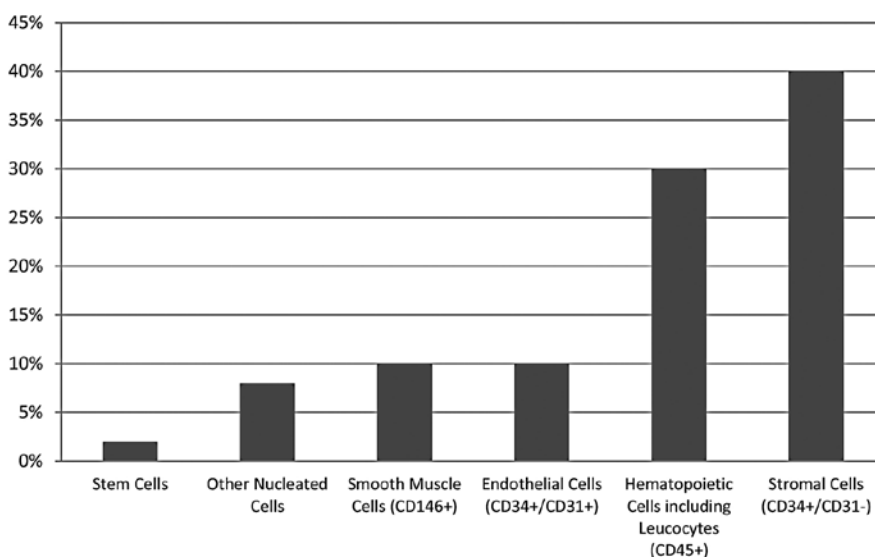


Fig. 1. Cell type proportions in the adipose-derived regenerative cells (ADRCs) isolated using the Celution 800/CRS system, according to the manufacturer (Cytori Therapeutics).

Results

Soft tissue healing after ADRC application

At 11 days after surgery, both the experimental and control groups showed notable inflammatory reactions in the soft tissues. Compared to the control group, the ADRC-treated group showed less pronounced inflammatory infiltrate around the area of suture. The ADRC-treated animals also showed higher occurrence of Langhans giant cells and eosinophilic granulocytes in the inflammatory infiltrate, and a higher degree of necrotic changes in the soft tissues. Moreover, compared to samples from the control group, samples from ADRC-treated animals showed lower proliferation of newly formed fibrovascular tissue.

Table 1. Tissue section features identified by microscopic evaluation.

Feature	Occurrence
Inflammatory infiltrate	+
Inflammatory infiltrate deep in the tissue	-
Langhans giant cells in the sutura	+
Langhans giant cells deep in the tissue	-
Fibrovascular tissue	+
Necrosis	-
Blood vessel proliferation in the site of sutura	+
Eosinophil granulocytes	-

+ present; - not present.

of cartilage and bone, which was microscopically confirmed (Plate III, Fig. 3). The experimental group showed a higher amount of osteoclasts than the control group (Fig. 4). Compared to the control group, the ADRC-treated group showed a thicker layer of fibrosis underlying the defect, a lower frequency of fibrovascular tissue.

At 28 days after surgery, both groups showed the same amount of inflammatory infiltrate. Compared to the control group, the ADRC-treated animals showed higher occurrence of Langhans giant cells and necrotic changes, and more proliferation of granulation tissue. On the other hand, the experimental group showed a slightly higher angiogenesis rate compared to the control group.

Hard tissue healing after ADRC application

At 11 days after surgery, the experimental and control groups showed similar degrees of newly formed cartilage. Compared to the control group, the ADRC-treated group showed more evidence of necrosis, as was observed in soft tissue. In one case, necrosis progressed to resorption

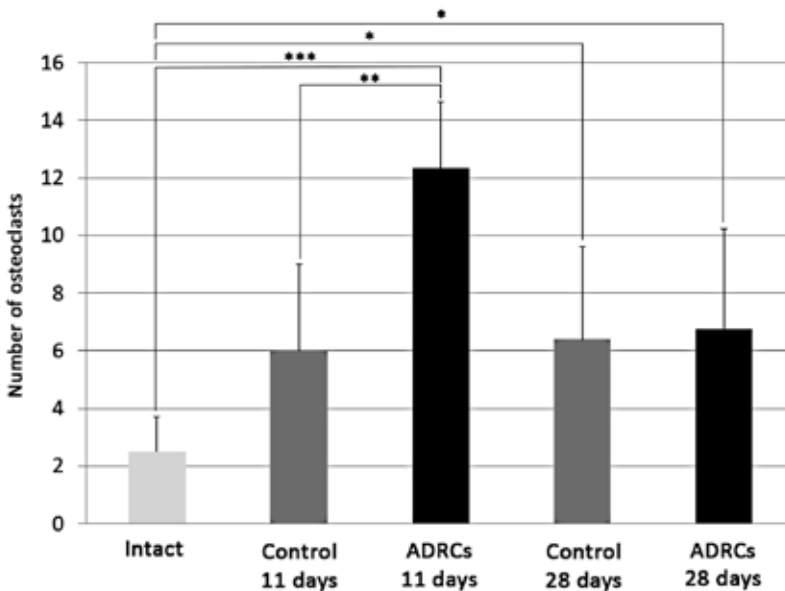


Fig. 4. Numbers of osteoclasts in the temporomandibular joint (TMJ) condyle during healing. Intact = normal rabbit TMJ condyle. ADRC - adipose-derived regenerative cell. Y axis shows the osteoclast-to-100 osteoblasts ratio (absolute value). Significance: * $P \leq 0.05$; ** $P \leq 0.01$; *** $P \leq 0.001$

At 28 days after surgery, the ADRC-treated animals showed a more pronounced inflammatory reaction in the hard tissues compared to the control group. Surprisingly, the control group exhibited more newly formed cartilage than the experimental group. The two groups did not significantly differ regarding the layer of the fibrosis underlying the defect, or the amount of osteoclasts (Fig. 4). Similarly, the groups did not significantly differ in the other investigated indicators, such as the distance of the osteoblast activity from the experimental defect.

Discussion

Among the widely used laboratory animals, the pig is the only omnivore having a TMJ condyle similar in size to humans, along with a similar dentition type and means of joint loading during mastication (Stembirek et al. 2012). However, the use of a pig model has several drawbacks, including the high cost, the time required for histological assessment of hard tissues, and the more complicated immunological preparation of animals for transplantation of heterologous biologic material. Rats and mice were not suitable for the present research due to the small size of their TMJ, and its morphological differences from the human TMJ. Carnivores, such as dogs and cats, were not considered due to ethical reasons. These factors led us to use rabbits as our animal model. The rabbit TMJ shares several important similarities with the human TMJ, and is larger than the rat or mouse TMJ. Moreover, the rabbit TMJ model has been successfully used in other studies (Ali and Sharawy 1996; Ahtiainen et al. 2013; Embree et al. 2016).

The morphological complexity of the TMJ limits the options for surgical resolution of serious TMJ dysfunctions and injuries. Any surgical intervention in this area is burdensome for the patient. Joint transplants often have a restricted service life, and full joint function is not always maintained. Cell therapy is considered a promising tool in regenerative medicine (Madeira et al. 2015; Mardones et al. 2015). Joint prostheses and scaffolds with stem cells are under development, which may facilitate the integration of implanted bone or other tissues, decrease GvHD (graft-versus-host disease), and improve healing (Murphy et al. 2013).

A previous study describes the use of ADSCs in a therapeutic method for treating inflammatory and degenerative TMJ disorders (Detamore and Athanasiou 2003). Adipose-derived stem cells are typically recruited to injury sites, where they assist in injured tissue repair and regeneration, and locally differentiate into smooth muscle or endothelial cells that can participate in angiogenesis and neovascularisation (Lin et al. 2010). Adipose-derived stem cells can also differentiate into other tissue-specific cells, such as adipocytes in adipose tissue or chondrocytes in cartilage. Since they exhibit good chondrogenic potential *in vitro* and can assist in cartilage repair, they are theoretically better candidates for treatment of degenerative or inflammatory disorders than current medications (Shen et al. 2015; Wu et al. 2015). Direct application of ADRCs is the preferred method of use, since it minimizes the surgical interference with the integrity of the damaged joint; an outpatient procedure, such as arthrocentesis or arthroscopy, would be sufficient. The ADRCs could potentially help with regeneration and repair processes, reduce inflammatory reactions, and directly integrate into the damaged tissue, contributing to its reconstruction.

In this study, we used ADRCs, which are heterogeneous cell population that includes stem cells. One previous study tested a suspension of non-differentiated SCs for TMJ regeneration in rabbits with osteoarthritis (Chen et al. 2013). The animals in one group were treated with autologous non-differentiated bone marrow stromal stem cells (BMSCs), while the second group was treated with chondrogenic differentiated BMSCs. The study results show that the non-differentiated SCs had a significantly smaller effect on joint

healing compared to the differentiated cells. Mapping of the BMSCs' fate revealed their survival in cartilage, subchondral bone, and synovial membrane for at least four weeks. The authors suggest that a suspension of autologous BMSCs can improve TMJ regeneration and slow the process of cartilage destruction in an osteoarthritic joint (Chen et al. 2013).

To our knowledge, no prior studies have investigated the application of human ADRCs in immunodeficient rabbits, or have described the effects of undifferentiated ADSCs in the TMJ region. Some authors consider successful differentiation to be a crucial step (Chen et al. 2013). In studies showing good results following the application of undifferentiated mesenchymal stem cells in joint osteoarthritis, the applied suspension has usually contained stem cells along with other factors that may have affected the results, such as platelet-rich plasma (Koh and Choi 2012). Prior reports also describe the use of undifferentiated xenogenous ADSCs in rabbits for treating neural tissue (Lasso et al. 2015) or osteochondral defects (Jang et al. 2014). These authors claim that even undifferentiated SCs can reduce the immune response and support better healing of defects. On the other hand, application of undifferentiated ADSCs during cornea xenotransplantation in rabbits did not influence the immune response or result in better graft integration. However, this treatment did increase inflammatory markers and neovascularisation (Fuentes-Julian et al. 2015). Most current data suggest that SCs can increase the proliferation of newly formed tissues. Accordingly, we found that prechondral fibrosis was more frequent in the experimental group, which may reflect an increased rate of repair processes in the treated joints (Murphy et al. 2013).

We considered the difference in osteoblast-to-osteoclast ratio to be a valid indication of bone remodelling and inflammatory response. This information can be easily obtained by light microscopy examination (Tanaka et al. 2005). We assumed that an increased number of osteoclasts signified a higher rate of bone remodelling. According to this assumption, the ADRC-treated animals showed a higher bone remodelling rate at 11 days after surgery compared to the control animals.

Prior studies have also suggested that SCs have benefits due to their immunomodulatory character (Bartholomew et al. 2002; Le Blanc et al. 2003; Tse et al. 2003; Gonzalez-Rey et al. 2010; Murphy et al. 2013). However, our present results indicated that ADRCs had the opposite effect, as evidenced by the more pronounced inflammatory reaction in ADRC-treated joints. It is possible that this effect may have stemmed from the use of heterologous cells.

Adipose-derived regenerative cells contain endothelial cells and ADSCs, and can reportedly induce neovascularisation due to increased VEGF expression in the treated tissue (Miranville et al. 2004; Zhu et al. 2010; Gao et al. 2011; Matsugami et al. 2014). Our results confirmed this expectation, with a higher number of vessels observed in soft tissues in the experimental group compared to the control group.

To prevent GvHD, we used an immunosuppressive protocol tested for rabbits (Jeklova et al. 2008). Despite this measure, we observed a higher than expected immunologic response to the heterologous cells in the experimental group. Our results did not confirm the previously described immunomodulative effects of ADRCs and ADSCs (Bartholomew et al. 2002; Le Blanc et al. 2003; Tse et al. 2003; Zhu et al. 2010). However, our present data do not enable us to determine whether this was due to the stem cells themselves or to the heterologous character of the ADRCs.

In conclusion, this study was designed to evaluate the potential of unprocessed ADRCs for TMD treatment. Adipose-derived regenerative cells have the advantages of being simple to use, requiring reduced time, providing increased comfort for the potential patient, and lowering the procedure costs. Our present results indicated that ADRC treatment promoted a slight increase of newly formed vessels in soft tissues, which can be considered a marker of improved reparative processes. Application of the ADRC suspension resulted in a stronger inflammatory reaction and a more pronounced foreign body reaction compared

to the control group. These observations can be explained by the fact that the applied ADRCs were heterogeneous, such that an immune-mediated reaction occurred despite immune suppressive therapy. Compared to controls, the ADRC-treated animals also showed a higher rate of bone remodelling. Overall, we conclude that ADRCs may be a promising tool for TMD treatment. Further studies are needed to better understand their effects on tissues *in vitro*.

Conflict of Interest

We have no conflicts of interest to disclose.

Acknowledgements

This work was supported by the Ministry of Health of the Czech Republic, RVO-FNOs/2013.

References

- Ahtiainen K, Mauno J, Ella V, Hagstrom J, Lindqvist C, Miettinen S, *et al.* 2013: Autologous adipose stem cells and polylactide discs in the replacement of the rabbit temporomandibular joint disc. *J R Soc Interface* **10**: 20130287
- Ali AM, Sharawy MM 1996: An immunohistochemical study of collagen types III, VI and IX in rabbit craniomandibular joint tissues following surgical induction of anterior disk displacement. *J Oral Pathol Med* **25**: 78-85
- Bartholomew A, Sturgeon C, Siatskas M, Ferrer K, McIntosh K, Patil S, *et al.* 2002: Mesenchymal stem cells suppress lymphocyte proliferation *in vitro* and prolong skin graft survival *in vivo*. *Exp Hematol* **30**: 42-48
- Berkovitz BK, Holland GR, Moxham BJ, Holland GR, Moxham BJ 2009: *Oral Anatomy, Histology and Embryology*. Mosby; 4th International edition, vol. 4
- Chen K, Man C, Zhang B, Hu J, Zhu SS 2013: Effect of *in vitro* chondrogenic differentiation of autologous mesenchymal stem cells on cartilage and subchondral cancellous bone repair in osteoarthritis of temporomandibular joint. *Int J Oral Maxillofac Surg* **42**: 240-248
- Detamore MS, Athanasiou KA 2003: Structure and function of the temporomandibular joint disc: implications for tissue engineering. *J Oral Maxillofac Surg* **61**: 494-506
- Embree MC, Chen M, Pylawka S, Kong D, Iwaoka GM, Kalajzic I, Yao H, Sun D, Sheu TJ, Koslovsky DA, Koch A, Mao JJ 2016: Exploiting endogenous fibrocartilage stem cells to regenerate cartilage and repair joint injury. *Nat Commun* **7**: 13073
- Fuentes-Julian S, Arnalich-Montiel F, Jaumandreu L, Leal M, Casado A, Garcia-Tunon I, Hernandez-Jimenez E, Lopez-Collazo E, De Miguel MP 2015: Adipose-derived mesenchymal stem cell administration does not improve corneal graft survival outcome. *PloS one* **10**: e0117945
- Gao W, Qiao X, Ma S, Cui L 2011: Adipose-derived stem cells accelerate neovascularization in ischaemic diabetic skin flap via expression of hypoxia-inducible factor-1alpha. *J Cell Mol Med* **15**: 2575-2585
- Gonzalez-Rey E, Gonzalez MA, Varela N, O'Valle F, Hernandez-Cortes P, Rico L, Büscher D, Delgado M 2010: Human adipose-derived mesenchymal stem cells reduce inflammatory and T cell responses and induce regulatory T cells *in vitro* in rheumatoid arthritis. *Ann Rheum Dis* **69**: 241-248
- Jang KM, Lee JH, Park CM, Song HR, Wang JH 2014: Xenotransplantation of human mesenchymal stem cells for repair of osteochondral defects in rabbits using osteochondral biphasic composite constructs. *Knee Surg Sports Traumatol Arthrosc* **22**: 1434-1444
- Jeklova E, Leva L, Jaglic Z, Faldyna M 2008: Dexamethasone-induced immunosuppression: a rabbit model. *Vet Immunol Immunopathol* **122**: 231-240
- Koh YG, Choi YJ 2012: Infrapatellar fat pad-derived mesenchymal stem cell therapy for knee osteoarthritis. *Knee* **19**: 902-907
- Lasso JM, Perez Cano R, Castro Y, Arenas L, Garcia J, Fernandez-Santos ME 2015: Xenotransplantation of human adipose-derived stem cells in the regeneration of a rabbit peripheral nerve. *J Plast Reconstr Aesthet Surg* **68**: e189-197
- Le Blanc K, Tammik L, Sundberg B, Haynesworth SE, Ringden O 2003: Mesenchymal stem cells inhibit and stimulate mixed lymphocyte cultures and mitogenic responses independently of the major histocompatibility complex. *Scand J Immunol* **57**: 11-20
- Lin CS, Xin ZC, Deng CH, Ning H, Lin G, Lue TF 2010: Defining adipose tissue-derived stem cells in tissue and in culture. *Histol Histopathol* **25**: 807-815
- Madeira C, Santhagunam A, Salgueiro JB, Cabral JM 2015: Advanced cell therapies for articular cartilage regeneration. *Trends Biotechnol* **33**: 35-42

- Mardones R, Jofre CM, Minguell JJ 2015: Cell therapy and tissue engineering approaches for cartilage repair and/or regeneration. *Int J Stem Cells* **8**: 48-53
- Matsugami H, Harada Y, Kurata Y, Yamamoto Y, Otsuki Y, Yaura H, Inoue Y, Morikawa K, Yoshida A, Shirayoshi Y, Suyama Y, Nakayama B, Iwaguro H, Yamamoto K, Hisatome I 2014: VEGF secretion by adipose tissue-derived regenerative cells is impaired under hyperglycemic conditions via glucose transporter activation and ROS increase. *Biomed Res Int* **35**: 397-405
- Miranville A, Heeschen C, Sengenès C, Curat CA, Busse R, Bouloumie A 2004: Improvement of postnatal neovascularization by human adipose tissue-derived stem cells. *Circulation* **110**: 349-355
- Moon MH, Kim SY, Kim YJ, Kim SJ, Lee JB, Bae YC, Sung SM, Jung JS 2006: Human adipose tissue-derived mesenchymal stem cells improve postnatal neovascularization in a mouse model of hindlimb ischemia. *Cell Physiol Biochem* **17**: 279-290
- Muehlberg FL, Song YH, Krohn A, Pinilla SP, Droll LH, Leng X, Seidensticker M, Rieke J, Altman AM, Devarajan E, Liu W, Arlinghaus RB, Alt EU 2009: Tissue-resident stem cells promote breast cancer growth and metastasis. *Carcinogenesis* **30**: 589-597
- Murphy MK, MacBarb RF, Wong ME, Athanasiou KA 2013: Temporomandibular disorders: a review of etiology, clinical management, and tissue engineering strategies. *Int J Oral Maxillofac Implants* **28**: e393-414
- Planat-Benard V, Silvestre JS, Cousin B, Andre M, Nibelink M, Tamarat R, Clergue M, Manneville C, Saillan-Barreau C, Duriez M, Tedgui A, Levy B, Pénicaud L, Casteilla L 2004: Plasticity of human adipose lineage cells toward endothelial cells: physiological and therapeutic perspectives. *Circulation* **109**: 656-663
- Prucelli E, Ponzoni D, Munaretto JC, Corsetti A, Leite MG 2012: Histomorphometric analysis of the temporal bone after change of direction of force vector of mandible: an experimental study in rabbits. *J Appl Oral Sci* **20**: 526-530
- Sandor GK, Numminen J, Wolff J, Thesleff T, Miettinen A, Tuovinen VJ, Mannerström B, Patrikoski M, Seppänen R, Miettinen S, Raitiaunen M, Öhman J 2014: Adipose stem cells used to reconstruct 13 cases with cranio-maxillofacial hard-tissue defects. *Stem Cells Transl Med* **3**: 530-540
- Shen J, Gao Q, Zhang Y, He Y 2015: Autologous platelet-rich plasma promotes proliferation and chondrogenic differentiation of adipose-derived stem cells. *Mol Med Rep* **11**: 1298-1303
- Stembirek J, Kyllar M, Putnova I, Stehlik L, Buchtova M 2012: The pig as an experimental model for clinical craniofacial research. *Lab Anim* **46**: 269-279
- Tanaka Y, Nakayamada S, Okada Y 2005: Osteoblasts and osteoclasts in bone remodeling and inflammation. *Curr Drug Targets Inflamm Allergy* **4**: 325-328
- Timper K, Sebock D, Eberhardt M, Linscheid P, Christ-Crain M, Keller U, Müller B, Zulewski H 2006: Human adipose tissue-derived mesenchymal stem cells differentiate into insulin, somatostatin, and glucagon expressing cells. *Biochem Biophys Res Commun* **341**: 1135-1140
- Tse WT, Pendleton JD, Beyer WM, Egalka MC, Guinan EC 2003: Suppression of allogeneic T-cell proliferation by human marrow stromal cells: implications in transplantation. *Transplantation* **75**: 389-397
- Wu SC, Hsiao HF, Ho ML, Hung YL, Chang JK, Wang GJ, Wang CZ 2015: Suppression of discoidin domain receptor 1 expression enhances the chondrogenesis of adipose-derived stem cells. *Am J Physiol Cell Physiol* **308**: C685-696
- Yu JM, Jun ES, Bae YC, Jung JS 2008: Mesenchymal stem cells derived from human adipose tissues favor tumor cell growth in vivo. *Stem Cells Dev* **17**: 463-473
- Zhu M, Zhou Z, Chen Y, Schreiber R, Ransom JT, Fraser JK, Hedrick MH, Pinkernell K, Kuo HC 2010: Supplementation of fat grafts with adipose-derived regenerative cells improves long-term graft retention. *Ann Plast Surg* **64**: 222-228

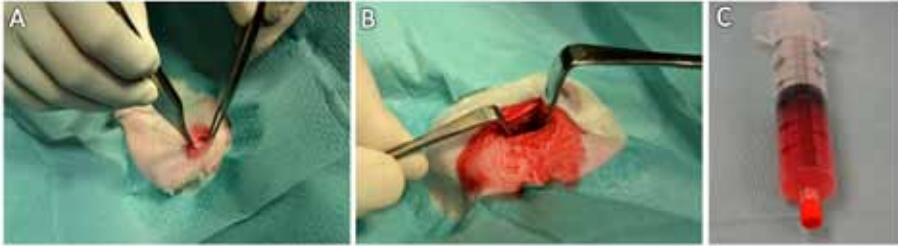


Fig. 2. Experimental surgery. (A) The incision was made in the parotidomasseteric region, approximately 3 cm cranioventrally from the auricle base (B) The temporomandibular joint (TMJ) was exposed. (C) The prepared adipose-derived regenerative cell suspension.

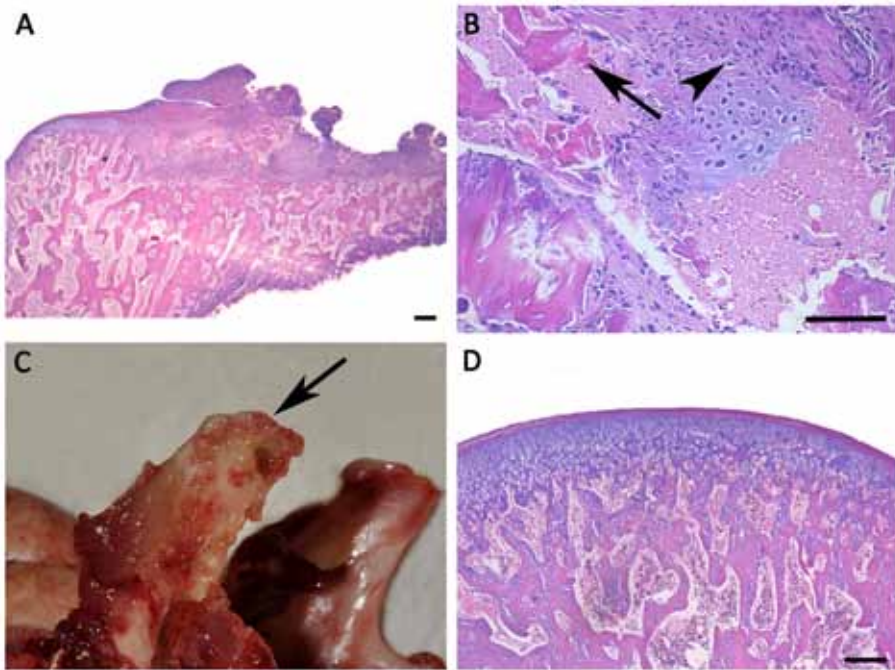
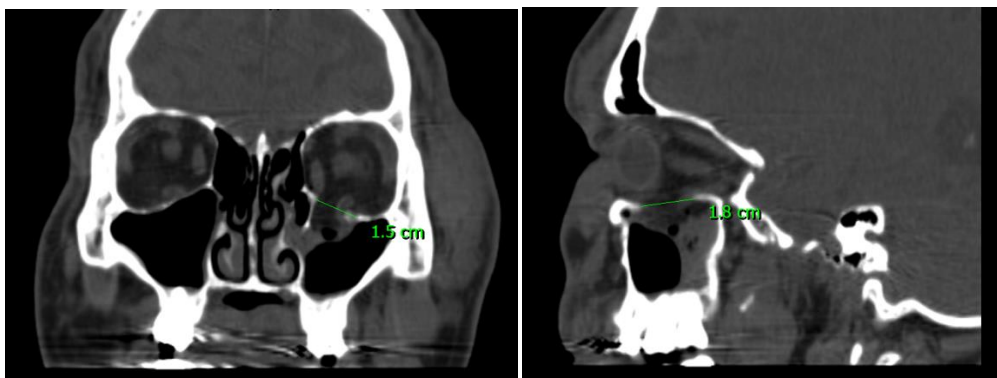


Fig. 3. Healing of hard tissues after adipose-derived regenerative cell (ADRC) application. (A) The loss of cartilage and bone resorption observed in one case. (B) Bone necrosis (arrow) and fibrosis formation (arrowhead). (C) Macroscopic appearance of the temporomandibular joint (TMJ) condyle shown in A. (D) Normal rabbit TMJ condyle surface presented for comparison. Scale bar, 100 μ m. Sections are stained with Alcian blue and haematoxylin-eosin.

Retromarginální zlomeniny očnice

Zlomeniny očnice se v rámci sdružených poranění obličejového skeletu nejrůznější etiologie vyskytují relativně často. Setkáváme se s nimi však i izolovaně, přičemž nejčastěji dochází k prolomení spodiny a/nebo mediální stěny očnice, které jsou k tomuto typu poranění z hlediska anatomického uspořádání nejvíce náchylné. Protože měkké tkáně vykazují větší pružnost než kostěné struktury, dochází k přenosu síly, její sumaci a prolomení nejslabší části, typicky tedy spodiny očnice. Po vyrovnání tlaku v orbitě se měkké tkáně vrací na základě elasticity do původní polohy, je zde však nebezpečí uskřinutí do kostního defektu, a tedy výhřezu měkkých tkání přes okraje kostního defektu (Warwar et al., 2000).

Typickým nálezem u retromarginálních zlomenin očnice (nebo také blowout zlomenina očnice) je různě velký kostěný defekt s možnou dislokací kostěných úlomků do maxilárního sinu, často doprovázený výše zmíněnou herniací měkkých tkání (**Obr.3**). Geometricky se většinou jedná o nepravidelnou elipsu různých velikostí, zasazenou do trojúhelníkovitě tvarované spodiny orbity. Tyto zlomeniny se liší také rozsahem výhřezu měkkých tkání očnice (Kovar et al., 2017).



Obr. 3: Vlevo: CT vyšetření s frontálním řezem pacienta s retromarginální zlomeninou očnice se zaznamenanou velikostí defektu v mediolaterálním směru. **Vpravo:** CT vyšetření se sagitálním řezem se zaznamenanou velikostí defektu v anterioposteriorním směru.

V současné době nejsou v odborné literatuře dostupná žádná jednoznačná doporučení, která by v běžné klinické praxi usnadňovala proces rozhodování mezi konzervativní a chirurgickou léčbou izolovaných retromarginálních zlomenin spodiny očnice u dospělých. Obecně doporučovanými kritérii pro chirurgickou intervenci jsou enoftalmus větší

než 2 mm nebo defekt větší než $1/3$ či $1/2$ spodiny orbity s přetrvávající herniací měkkých tkání a přítomnost pacientem subjektivně špatně snášené diplopie na podkladě poruchy postavení a motility očního bulbu (Harris et al., 1998, Harris, 2006, Rozsival, 2006, Gosse et al., 2010, Gosau et al., 2011, Hirjak et Machoň 2013, Boyette et al., 2015, Kovar et al., 2017, Lin et al., 2022, Oztuker et al., 2022).

Podle našich zkušeností však tato kritéria nejsou v běžné klinické praxi dostačující. Příkladem je obecně přeceňovaný enoftalmus, který je sice skutečně cenným diagnostickým kritériem, to však platí jen za předpokladu, že je přítomen – jeho nepřítomnost nemůže být považována za kontraindikaci k chirurgickému řešení. V běžné klinické praxi se navíc často stává, že je tento příznak zastřen rozvíjejícím se edémem měkkých tkání očnice, který naopak vede k exoftalmu (Timkovic et al., 2021). Problematika je dále komplikována nepravidelným tvarem orbity, který je jen stěží přesně identifikovatelný a měřitelný běžnými CT zobrazovacími technikami.

Naším cílem proto bylo identifikovat možná indikační kritéria pro rozhodování mezi konzervativní léčbou a chirurgickou revizí spojenou s rekonstrukcí izolovaných retromarginálních zlomenin spodiny očnice. Jako podklady pro tento výzkum nám sloužila data získaná pomocí CT a data z komplexního vyšetření pomocí panelu ortoptických metod. Na základě těchto údajů jsme navrhli skórovací systém indikující konzervativní a chirurgickou léčbu (podobně jako funguje Glasgow ComaScale hodnotící stav vědomí po traumatu hlavy). Jelikož z našich výsledků vyplývá, že poměr velikosti defektu k celkové velikosti spodiny je jeden ze dvou silných faktorů v našem skórovacím systému (druhým je elevace bulbu měřená na Lancasterově plátně), rádi bychom se v další fázi zaměřili na vývoj softwaru, který by dokázal provést automatickou 3D rekonstrukci očních a defektů u pacientů se zlomeninou očnice, u nichž neexistují CT snímky z dospělého věku před vznikem kostního defektu na spodině očnice.

Získané informace by se daly využít i v terapii, protože princip operací retromarginálních zlomenin očnice spočívá v repozici měkkých tkání zpět do očnice a v co nejpresnější rekonstrukci defektu pomocí různých materiálů (AlSubaie et al., 2022, Chattopadhyay et al., 2022; Murra – Douglass et al., 2022).

Jisté je, že tvar spodiny očnice a vzniklého traumatu je relativně složitý a vytvoření softwaru, který by nám ve virtuální rekonstrukci pomohl navrhnout individualizovaný tvar

orbitálního implantátu, který by byl poté například vyrobitelný 3D tiskem, by přínos do klinické praxe bezpochyby mít mohl. Takovýto postup je ovšem samozřejmě před klinickým využitím nutné ověřit na vhodném biomodelu. Dle našich poznatků by pro výzkum tohoto charakteru opět mohlo být vhodným biomodelem prase domácí, jehož očníce je relativně podobná lidské, přičemž dostupnost tohoto modelového organismu je výrazně jednodušší, než je tomu v případě primátů (Kyllar et al., 2016).

Komentář k přiložené publikaci č. 9

Michal KYLLAR, Jan STEMBIREK (*corresponding author*)*, Zdenek DANEK, Radek HODAN, Jiri STRANSKY, Vladimir MACHON a Rene FOLTAN. A porcine model: surgical anatomy of the orbit for maxillofacial surgery. *Laboratory Animals* [online]. 2016, **50**(2), 125–136. ISSN 0023-6772. Dostupné z: doi:[10.1177/0023677215577923](https://doi.org/10.1177/0023677215577923)

IF = 1,532; kvartil: VETERINARY SCIENCES Q1

Protože v literatuře byly dostupné pouze omezené informace týkající se anatomie očnice u prasete, rozhodli jsme se podrobně porovnat jednotlivé morfologické struktury prasečí a lidské očnice. Dalším cílem bylo zvážit praktické využití prasete jako biomodelu v experimentální chirurgii orbitálního regia.

Deset hlav prasečích kadaverů bylo vyšetřeno pomocí počítačové tomografie (CT) a magnetické rezonance (MRI) a následně byla provedena chirurgická preparace očnice. Pozornost byla zaměřena na struktury očnice (spodina, okraje a průběh nervů a svalů), které jsou při traumatech často postiženy.

Jedním ze závěrů naší studie bylo, že prasečí očnice je větší než lidská a má oválný tvar. Kostní část očnice je utvářena podobně jako u člověka, pouze ve ventrální části je očnice prasete otevřená do *fossa pterygopalatina* a laterálně chybí okraj úplně a je nahrazen svazkem vazivových vláken (*ligamentum orbitale*).

Tyto rozdíly však nejsou překážkou pro využití prasete jako vhodného biomodelu pro výzkumné účely nebo pro chirurgický výcvik přístupu do očnice. Přestože primáti jsou člověku anatomicky blíže, prase zůstává, zvláště když vezmeme v úvahu jeho dostupnost, stále velmi vhodným modelem pro tyto účely.

A porcine model: surgical anatomy of the orbit for maxillofacial surgery

Michal Kyllar^{1,2}, Jan Štembírek^{3,4}, Zdenek Danek⁵,
 Radek Hodan⁴, Jiří Stránský⁴, Vladimír Machoň⁶ and
 René Foltán⁶

Laboratory Animals
 2016, Vol. 50(2) 125–136
 © The Author(s) 2015
 Reprints and permissions:
 sagepub.co.uk/
 journalsPermissions.nav
 DOI: 10.1177/0023677215577923
 la.sagepub.com



Abstract

Due to its similarity to humans, the pig has proven to be a suitable biomodel for both research purposes and for training medical professionals, particularly in surgical specializations. For example, new implant materials have been tested on pig jaws and pigs have also been used in the development of new surgical techniques. For optimizing the effectiveness of such research or training, detailed data on the anatomy of their particular features are needed. At present, however, only limited information related to surgical and imaging anatomy of the facial and orbital areas of the pig and its comparison to human structures from the experimental surgery point of view is available in the literature. The aim of this study was to obtain such data and to compare the morphological structures of the porcine and human orbital regions and to lay down the foundation for practical use in experimental surgery. Ten pig heads were examined using computed tomography (CT) and magnetic resonance imaging (MRI) and, subsequently, a dissection of the orbit was carried out. Attention was focused on the structure of the orbit (floor, rim and nerves) frequently affected by pathological processes in humans (such as trauma, infection or tumours) and which consequently are frequently the subject of maxillofacial surgery. The porcine orbit is suitable for use in experimental medicine. However, if used in experiments, its anatomical peculiarities must be taken into consideration. Our study presents a foundation of basic knowledge for researchers who plan to use the pig as a biomedical model to investigate alternative treatments in the head region.

Keywords

pig, orbit, orbital surgery, animal biomodel

The pig has become popular as an experimental model for human systems in many biomedical fields due to its anatomical and physiological similarity to humans as well as for economic reasons. Because of the physiological similarities, the extrapolation of results acquired in pigs to human conditions gives more relevant results than those acquired from other experimental animals such as the mouse, rat or rabbit.¹ Experimental studies in terms of different surgical approaches to the facial skeleton have been performed in various model animals including rabbits, dogs, sheep or goats.^{2–8} A variety of animal models for implant biomaterial research have been described in a recent extensive literature review.⁹ In training and practising oral surgical procedures, pig heads are a well-established model.^{10–12}

¹Department of Anatomy, Histology and Embryology, Faculty of Veterinary Medicine, University of Veterinary and Pharmaceutical Sciences, Brno, Czech Republic

²Companion Care Animal Surgery, Broadstairs, Kent, UK

³Institute of Animal Physiology and Genetics, V.v.i., Academy of Sciences of Czech Republic, Brno, Czech Republic

⁴Department of Oral and Maxillofacial Surgery, University Hospital, Ostrava, Ostrava-Poruba, Czech Republic

⁵Department of Oral and Maxillofacial Surgery, University Hospital Brno, Brno, Czech Republic

⁶Department of Oral and Maxillofacial Surgery, University Hospital Prague, Prague, Czech Republic

Corresponding author:

Jan Štembírek, Institute of Animal Physiology and Genetics, V.v.i., Academy of Sciences of the Czech Republic Veverí 97, 602 00 Brno, Czech Republic.
 Email: stembirek@iach.cz



Figure 1. Morphometric assessment of the porcine orbit. Computed tomography 3D reconstruction of the porcine orbit.

OW: orbital width; OH: orbital height; a: line connecting processus zygomaticus ossis frontalis and processus frontalis ossis zygomatici.

However, only limited information has been obtained using modern imaging methods, or is available comparing the anatomy of the pig orbit to human structures from the perspective of experimental surgery. Compared with humans, the pig orbit is relatively small (Figure 1).

The eyelids, lacrimal system, orbit and conjunctiva together play an important role in the protection and function of the eye. Many diseases or trauma altering the structure or function of the eyelids, lacrimal system and/or the orbit can be detrimental to vision. Periorbital and facial injuries are mainly caused by assaults and falls and may at times involve the forehead.¹³ Such injuries necessitate cranial and orbital reconstructions to correct both aesthetic and functional defects.¹⁴ In order to achieve this, the surgeon needs to have a proper understanding of the human orbital structure, its relationship to both intra- and extracranial structures, and associated key surgical/anatomical landmarks. In general, the pig is a widely used animal model in medical research disciplines as it is very similar to humans in both physiological and individual anatomical aspects.^{1,15} However, little information is available about surgical procedures affecting the facial area and the orbit in animal models.¹⁶

The aim of this study was to describe the surgical anatomy, imaging and morphometric findings of the orbit required when planning surgery of maxillofacial aspects of the porcine orbital region. This information could be helpful both in the training of maxillofacial surgeons to enable them to perform trial surgeries on a cheap model similar to humans, and in the research of

new surgical methods that could be later extrapolated to humans.

Materials and methods

Ten heads of 24-month-old neutered male pigs were obtained from a slaughterhouse (Steinhauser, Tišnov, Czech Republic). All procedures were conducted following a protocol approved by the ethical committee of the university (VFU Brno, Czech Republic, No. 67985904). All the heads were fully developed and free of any obvious pathology in the facial area. The animals had no local or systemic illness likely to cause any pathological tissue alteration. The health status of the animals was inspected and confirmed by a certified veterinarian prior to and following the slaughter. Heads were examined by computed tomography (CT) and magnetic resonance imaging (MRI) and subsequently a dissection of the orbit was performed.

Diagnostic imaging

CT was performed using a single slice CT scanner (Synergy; GE Healthcare, Milwaukee, WI, USA). The following protocol was used: 120 kV, 100 mA, 3 mm slice thickness/3 mm spacing, DFOV 25 cm, standard reconstruction algorithm. MRI analysis (Magnetom Trio 3T; Siemens AG, Erlangen, Germany) of the pig heads was undertaken by the Institute for Clinical and Experimental Medicine, IKEM (Prague, Czech Republic). Forty-eight transverse and sagittal T1-weighted images were acquired using the above parameters.

Morphometric assessment of the orbit was carried out on the 3D reconstructed CT images and on the CT sagittal sections. Three measurements of the orbital rim and the orbit were collected. Aditus orbitae was assessed using orbital width (OW) and orbital height (OH). OW was measured from the most medial aspect of the orbital rim to the level of the imaginary line connecting laterally zygomatic process of the frontal bone with the frontal process of the zygomatic bone. OH was a line connecting the most proximal aspect of the supraorbital margin with the most distal aspect of the infraorbital margin (Figure 1, Table 1).

Orbital dissection

Dissection of the orbit was carried out using a stratigraphic approach based on surgical approaches used in human orbital surgery with adaptations to porcine anatomy. Each layer dissected was photographed for future description and comparison using a Nikon D 5100 camera (Nikon Europe BV, Amsterdam, The Netherlands). Detailed anatomic description of the

Table 1. Orbital rim measurements.

Head No	OW (mm)	OH (mm)
1	35	55
2	32	50
3	34	51
4	36	55
5	35	52
6	30	52
7	33	56
8	37	57
9	34	50
10	35	52
Mean	34.1	53
SD	2.02	2.53

OW: orbital width, OH: orbital height, SD: standard deviation.

images and dissected surgical approaches were carried out and served as a background for a comparison to human orbital anatomy and surgical approaches described in the literature.^{17,18}

Results

CT findings

The orbit of the pig is oval shaped and its longer axis vertically positioned, such that its average height is 53.0 mm and average width 34.1 mm.

Its infraorbital margin is formed by the lacrimal and zygomatic bones and the supraorbital margin of the frontal bone. Its bony margin is incomplete caudolaterally and is completed by the orbital ligament, which connects the processus zygomaticus ossis frontalis with the processus frontalis ossis zygomatici (Figure 1). The cavity is limited ventrally by a ridge on the frontal and lacrimal bones and is separated by a crest from the temporal fossa. The medial wall is perforated dorsally by the orbital opening of the canalis supraorbitalis and ventrally by the optic and ethmoidal foramina. Two lacrimal foramina can be found on or close to the rostral margin, and these open into the large open fossa sacci lacrimalis which is located in the medial orbital canthus on the orbital face of the lacrimal bone. The zygomatic bone continues caudally with the processus temporalis, which together with the processus zygomaticus of the temporal bone forms a thick, dorsally convex zygomatic arch (Figures 2 and 3). The zygomatic, lacrimal and frontal bones that form the aditus orbitae are all pneumatized bones. The lacrimal sinus (sinus lacrimalis) is an excavation into the lacrimal bone. It borders ventromedially on the lacrimal canal

and the maxillary sinus, medially and dorsally on the rostral sinuses, and caudally on the rostromedial wall of the orbit. The zygomatic bone is pneumatized by the maxillary sinus extending all the way to the processus temporalis ossis zygomatici. The sphenoid sinus (sinus sphenoidalis) is a paired sinus (right and left sides) divided by a septum (septum sinuum sphenoidalium). It excavates into the presphenoid, basis phenoid and temporal bones, creating a sinus in the medial wall of the orbit, in close proximity to the chiasma opticum. It extends laterally and dorsally, excavating into the squamous part of the temporal bones, and reaching into the zygomatic process (Figures 2 and 3).

MRI findings

Soft tissue structures such as the mucosal covering of the conchae and paranasal sinuses, the detailed structure of the ectoturbinalia and endoturbinalia of the labyrinthus ethmoidalis, and muscular tissue are all shown in clear detail in the MR images (Figures 4 and 5).

The globe and the other orbital tissue structures are surrounded by orbital fat. This orbital fat starts as a dense connective tissue at the aditus orbitae and extends dorsally towards the roof of the orbit and ventrally towards the pterygopalatine fossa as an intermuscular fat pad. The orbit is lined by a continuous fibrous membrane, the periorbita, which forms a dense condensation in close proximity to the orbital margin.

MRI clearly facilitates the differentiation of extraocular muscle groups. The dorsal and ventral oblique muscles of the eye bulb (m. obliquus dorsalis and ventralis oculi) are easily discernible from straight muscles of the bulbus (m. rectus bulbi dorsalis, ventralis, medialis and lateralis) which however cannot be distinguished from the retractor muscle of the bulbus (m. retractor bulbi) except at their origins on the basis of sphenoid and presphenoid bones. The temporal muscle (musculus temporalis) originates in the temporal fossa or planum parietale and inserts into the internal side of the coronoid process of the mandible (Figures 4 and 5). This insertion occupies the entire rostral region down to the level of the third molar tooth.

Surgical anatomy of the orbit

The pig orbit is a cavity delineated by four walls, all but one of which is formed by bones. The medial wall is almost rectangular. It comprises the lacrimal bone, the zygomatic bone rostrally and medially and maxilla ventromedially. The thick bone of the medial wall covers the underlying sphenoid paranasal sinus caudally and the frontomaxillary sinus rostrally. It also adjoins the optic canal and the supraorbital opening

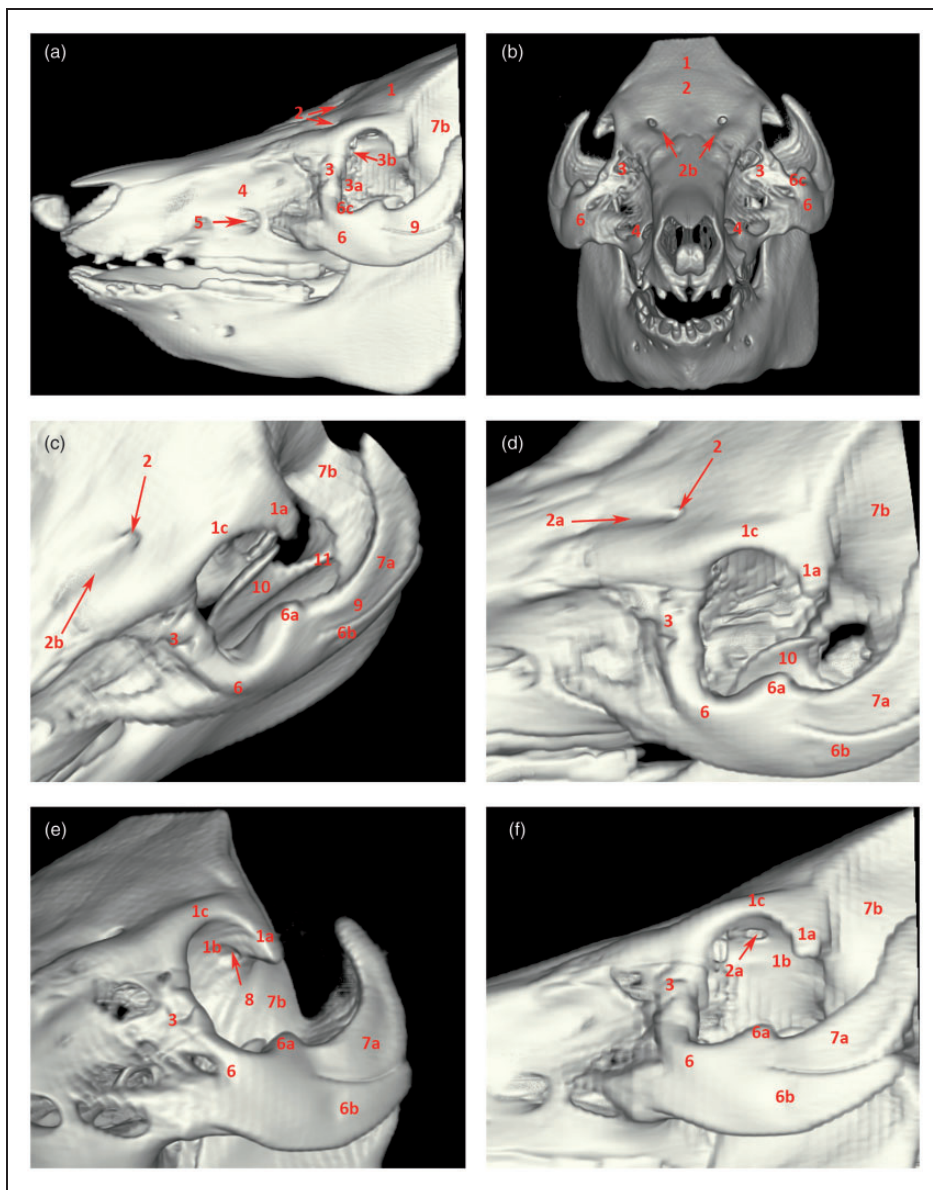


Figure 2. Computed tomography 3D reconstruction of the porcine orbit. (a) Overview of the skull: lateral aspect. (b) Overview of the skull: rostral aspect. (c) Orbit: dorsal view. (d) Orbit: dorsolateral view. (e) Orbit: ventrolateral view. (f) Orbit: lateral view. 1: os frontale; 1 a: processus zygomaticus ossis frontalis; 1 b: os frontale – facies orbitalis; 1 c: margo supraorbitalis; 2: foramen supraorbitale – frontal opening; 2 a: foramen supraorbitale – orbital opening; 2 b: sulcus supraorbitalis; 3: os lacrimale; 3 a: os lacrimale – orbital surface; 3 b: foramen lacrimale; 4: maxilla; 5: foramen infraorbitale; 6: os zygomaticum; 6 a: processus frontalis ossis zygomatici; 6 b: processus temporalis ossis zygomatici; 6 c: margo infraorbitalis; 7 a: processus zygomaticus ossis temporalis; 7 b: squama ossis temporalis; 8: foramen ethmoidale; 9: arcus zygomaticus; 10: processus coronoideus mandibulae; 11: incisura mandibulae.

for the same artery and nerve. The lacrimal bone carries two lacrimal foramina (Figure 2). Ventrally it continues as the lamina pterygopalatina bordering the ventrally located fossa pterygopalatina filled with pterygoid musculature.

The roof consists of the frontal bone and a wing of the sphenoid bone (Figures 2 and 3). It is composed of very thick bone pneumatized by the frontal lateral sinus

(Figure 4). The ventral aspect of the orbital roof lodges a large and shallow fossa for trochlear attachment of the dorsalis obliquus muscle. The lacrimal gland is housed in a shallow fossa in the rostrolateral aspect of the roof where the zygomatic process of the frontal bone connects with the ligamentum orbitale (Figure 6).

The floor of the orbit is very short, extending only one centimetre behind the infraorbital edge and

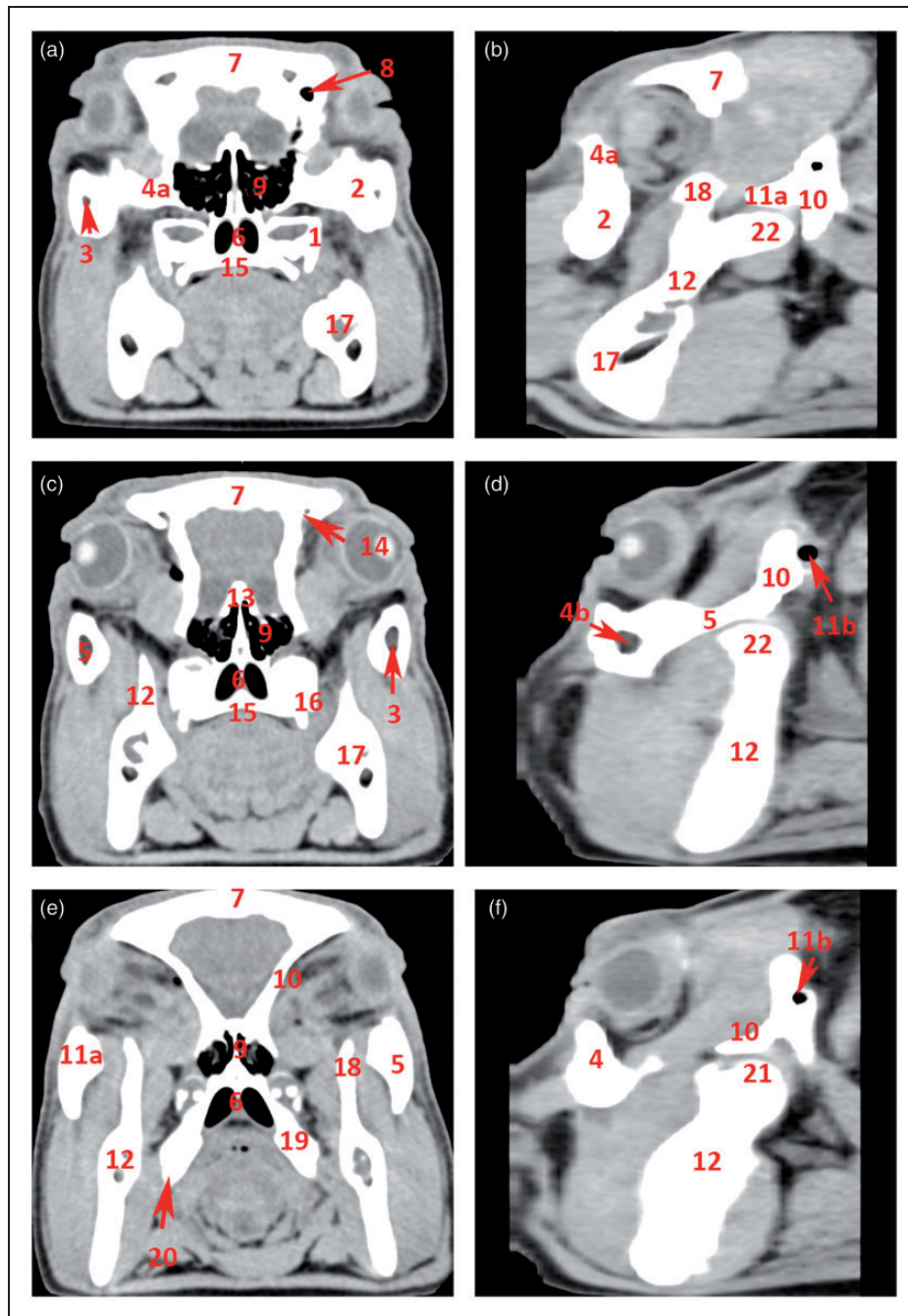


Figure 3. Computed tomography transverse sections through the orbit. (a) Transverse section through the cranial aspect of the orbit. (b) Sagittal section through the lateral aspect of the arcus zygomaticus. (c) Transverse section through the mid-part of the orbit. (d) Sagittal section through the middle of the arcus zygomaticus. (e) Transverse section through the caudal part of the orbit. (f) Sagittal section medially from the arcus zygomaticus. 1: maxilla; 2: os zygomaticum; 3: sinus maxillaris; 4: margo infraorbitalis; 4 a: os lacrimale; 4 b: sinus lacrimalis; 5: arcus zygomaticus; 6: choana; 7: os frontale; 8: sinus frontalis rostralis; 9: labyrinthus ethmoidalis; 10: os temporale – squama ossis temporalis; 11 a: os temporale – processus zygomaticus; 11 b: os temporale – meatus acusticus externus; 12: ramus mandibulae; 13: os ethmoidale; 14: foramen supraorbitale – orbital opening; 15: palatum durum; 16: processus pterygoideus ossis palatini; 17: corpus mandibulae; 18: processus coronoideus mandibulae; 19: os pterygoideum; 20: hamulus pterygoideus; 21: processus condylaris mandibulae.

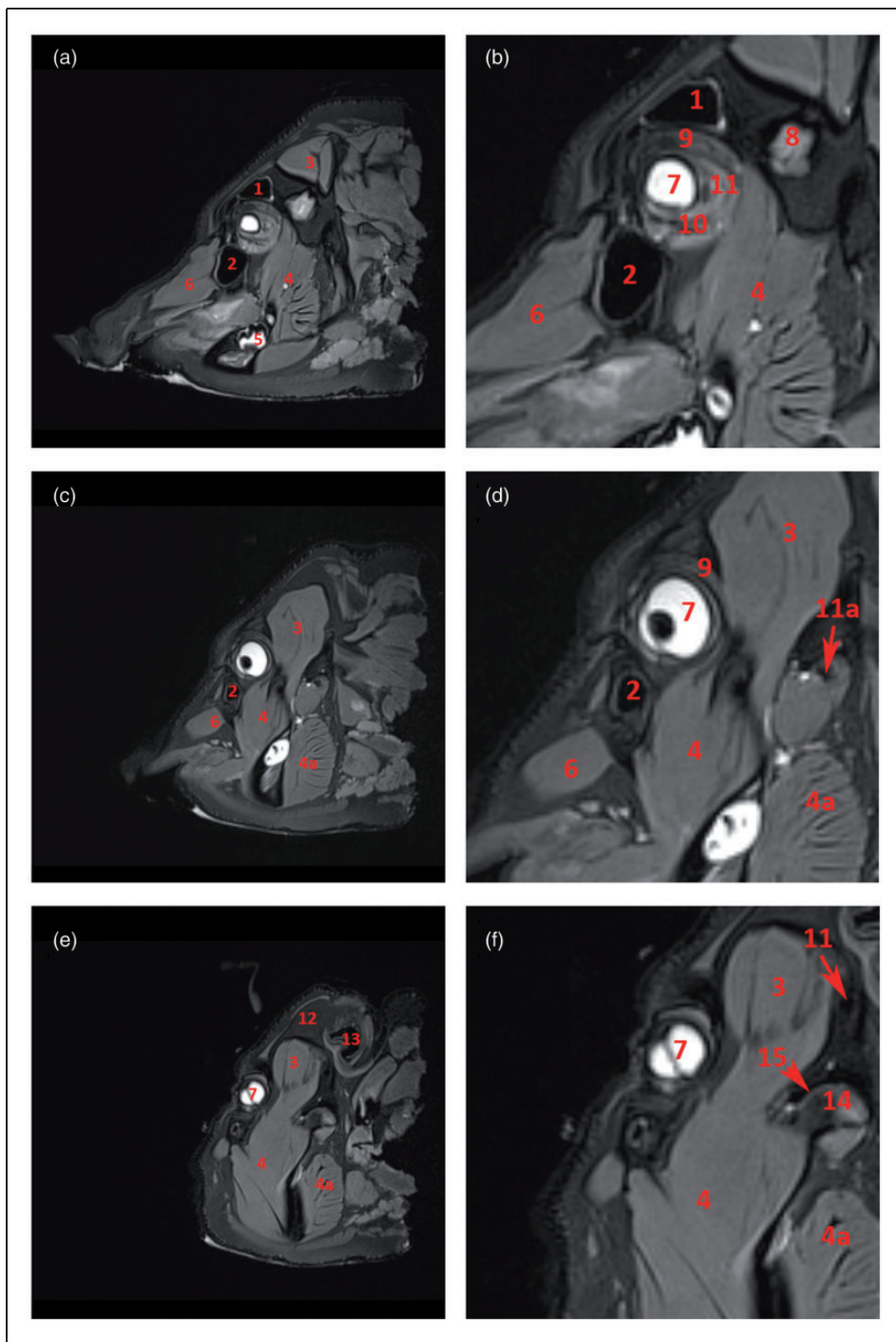


Figure 4. Magnetic resonance imaging: T1-weighted sagittal sections of the orbit. (a) Sagittal section of the porcine head at the level of the medial orbit. (b) Detail of the orbit. (c) Sagittal section of the porcine head through the centre of the orbit. (d) Detail of the orbit. (e) Sagittal section of the porcine head at the level of the lateral orbit. (f) Detail of the orbit. 1: sinus frontalis; 2: sinus lacrimalis; 3: musculus temporalis; 4: musculus pterygoideus lateralis; 5: fourth mandibular molar tooth; 6: musculus levator nasolabialis; 7: bulbus oculi; 8: squama ossis temporalis; 9: musculus rectus bulbi dorsalis; 10: musculus rectus bulbi ventralis; 11: musculus retractor bulbi; 11 a: meatus acusticus externus; 12: os frontale; 13: auris externa; 14: condylus mandibulae; 15: discus articularis.

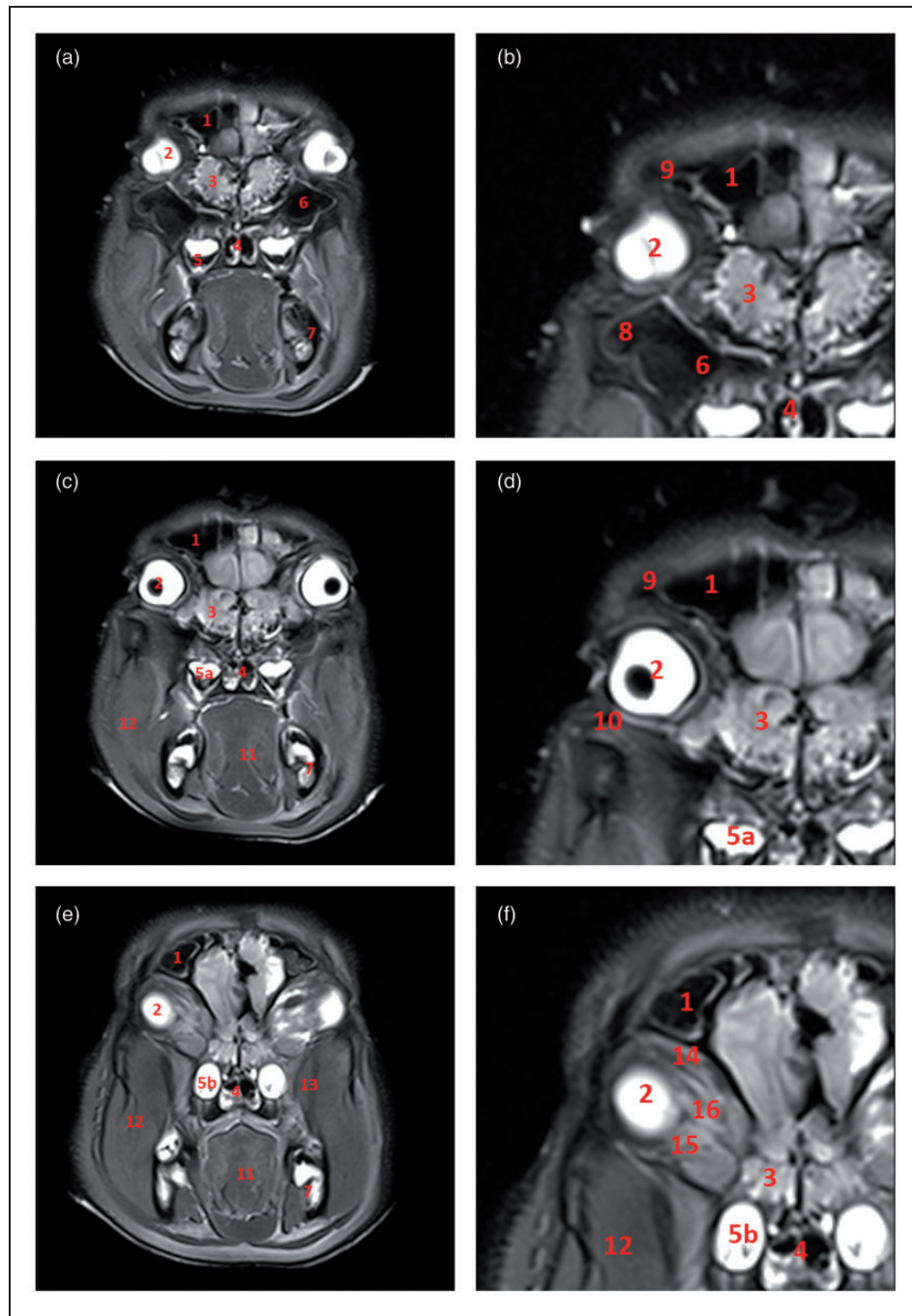


Figure 5. Magnetic resonance imaging: T1-weighted transverse sections of the orbit. (a) Transverse section of the porcine head at the level of the second maxillary molar tooth. (b) Detail of the orbit. (c) Transverse section of the porcine head at the level of the third maxillary molar tooth. (d) Detail of the orbit. (e) Transverse section of the porcine head at the level of the fourth maxillary molar tooth. (f) Detail of the orbit. 1: sinus frontalis; 2: bulbus oculi; 3: labyrinthus ethmoidalis; 4: choana; 5: second maxillary molar tooth; 5a: third maxillary molar tooth; 5b: fourth maxillary molar tooth; 6: sinus maxillaris; 7: corpus mandibulae; 8: sinus zygomaticus; 9: os frontale; 10: os zygomaticum; 11: lingua; 12: musculus masseter; 13: musculus pterygoideus lateralis; 14: musculus rectus bulbi dorsalis; 15: musculus rectus bulbi ventralis; 16: musculus retractor bulbi.

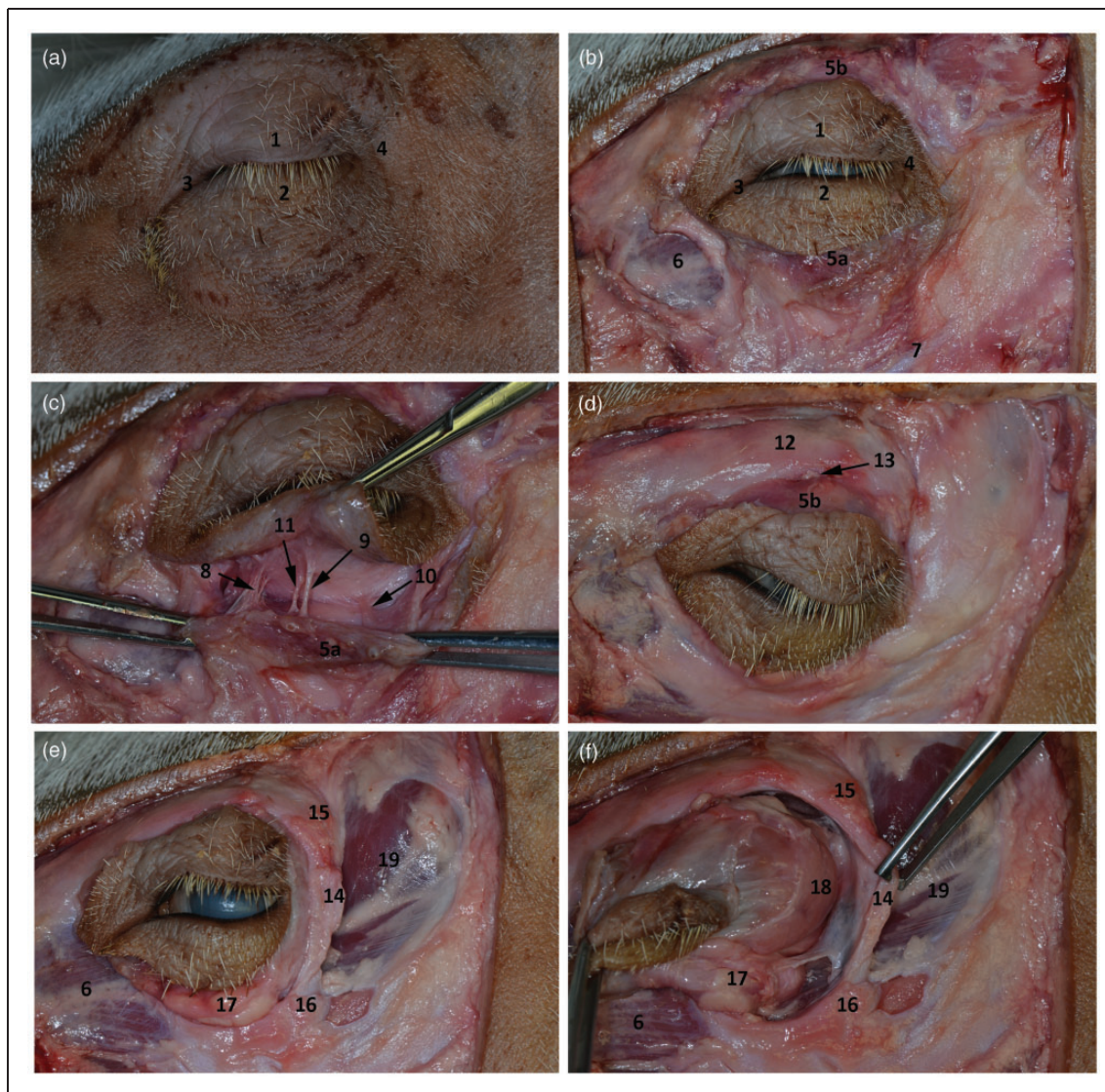


Figure 6. Surgical anatomy of the orbit. 1: palpebra superior; 2: palpebra inferior; 3: canthus medialis; 4: canthus lateralis; 5a: musculus orbicularis oculi pars inferior; 5b: musculus orbicularis oculi pars superior; 6: musculus malaris; 7: musculus zygomaticus – tendo originis; 8: nervus zygomatico facialis accessorius; 9: nervus zygomaticofacialis; 10: ramus communicans cum nervus buccalis; 11: arteria malaris; 12: margo supraorbitalis; 13: nervus trochlearis; 14: ligamentum orbitale; 15: processus zygomaticus ossis frontalis; 16: processus frontalis ossis zygomatici; 17: corpus adiposum periorbitae; 18: glandula lacrimalis; 19: musculus temporalis.

descending sharply into the fossa pterygopalatina (Figure 6). This is occupied mainly by an infraorbital fat pad (Figure 6) which continues ventrally into the fossa pterygopalatina between the lateral and medial pterygoid muscles, protecting the large neurovascular bundle comprising the maxillary artery, and its branches and branches of the trigeminal nerve.

The caudolateral wall is composed of soft tissues represented by a ligament (ligamentum orbitale) that extends between the zygomatic process of the frontal bone and the frontal process of the zygomatic bone

(Figures 2, 3 and 6). Caudally and ventrally it opens widely into the infratemporal fossa, which contains the terminal fibres of the temporalis muscle, the maxillary artery, and the maxillary vein.

The orbicularis muscle underlying the eyelids is composed of two layers of muscular tissue and is anchored with short ligaments to the medial and lateral aspects of the orbital opening. Its innervation arises from the trigeminal origin of the zygomatic nerve branches located on the ventral margin of the orbit and dorsally from the trochlear nerve. The blood supply of the ventral part of

the orbit is provided by the arteria malaris, and of the dorsal part by the arteria supraorbitalis (Figure 6).

Discussion

The porcine orbit is larger than its human counterpart. They however share the oval shape. Morphometric assessment of human orbits shown on the CT scans of Caucasian individuals have orbits with an average height of 32.0 mm and an average width of 36.9 mm, making them slightly horizontally oval shaped.¹⁹ Our study revealed that the porcine orbit is vertically oval shaped, with a significantly taller orbital opening than that of humans. The bone anatomy of the porcine orbit is similar to that of humans where seven bones in total contribute to its formation. As shown in our study, the same number of bones forms the orbit in pigs, with the maxilla contributing to the formation of the ventromedial part of the orbit. Furthermore, the infraorbital margin of the bony orbit is very narrow in pigs and the orbit is ventrally open to the pterygopalatine fossa. The human orbit has a ventral floor which is formed by the lacrimal and zygomatic bones.²⁰

As well as differing from the porcine orbit in size and shape, the human orbit is considered to be enclosed while the porcine orbit is open or incomplete.²¹ The enclosed orbit is formed by bones along its whole circumference, whereas the open orbit, such as in the pig, lacks bones at its caudolateral aspect. This gap is bridged by a strong band of collagen fibres, the orbital ligament, which completes the orbit. It is believed that the enclosed orbit is essential for protection and skull reinforcement during dominance rituals (such as the one in a large animal) and chewing; whereas the open orbit allows a better ability to open jaws widely, with reduced orbital closure.²¹

All the bones contributing to the formation of the orbit in pigs are pneumatized, forming paranasal sinuses. Some reports regarding the extent of the paranasal sinuses in pigs are contradictory.^{17,20} The extent of paranasal sinuses in our study was found to be the same in all the skulls investigated. The disagreements between different anatomical studies and textbooks could be explained by different breeds of pigs, with differences in development of the skulls varying from almost brachycephalic to dolichocephalic breeds. Paranasal sinuses in pigs seem to be more extensive than those of the human skull, which could be explained by the size of the skull. Pigs' skulls are larger and heavier, and the paranasal sinuses create empty cavities within the bone, adding to the bone mass while maintaining a low weight.¹⁷

Orbital fasciae in pigs are separated by the adipose tissue that fill the dead space in the orbit and between the extraocular muscles, which acts as a protective

cushion for the eye bulb and muscles and therefore makes the periorbital and orbital anatomy in this aspect identical to that of humans.¹⁸ Porcine eyelids are relatively thick and their movement is limited due to their considerably thicker dermis and also to the amount of fat under the skin and the conjunctiva. The upper eyelids contain heavy cilia but the lower eyelids lack them, unlike in humans. The porcine conjunctiva, unlike that of humans, has developed a third eyelid which is located in the medial canthus of the eye. It contains a cartilaginous plate which serves as an attachment of smooth muscle and third eyelid gland. It is believed to be involved in immunological defence of the conjunctiva, photoprotection and pheromone production.²²

Despite certain anatomical differences between human and porcine orbits, the pig is an important anatomical and surgical model as described in other studies²³⁻²⁵ and has to be considered in many areas of maxillofacial trauma and aesthetic surgery training. The porcine model can be very useful in simulating reconstruction of an injured eye bulbus, eye muscles, oculomotor or optic nerves of the lateral, upper and/or lower orbital wall, or reconstructions after oncological resections.^{1,18}

However some conditions and surgeries cannot be simulated in the pig model due to differences in the structure and thickness of the orbit-forming bones between pigs and humans. Most orbital injuries in humans occur due to impact forces acting on the very thin (sometimes described as 'paper-thin') bone forming the floor and the medial wall. Upon impact on the bulbus, hydrodynamic forces lead to breakage of these thin bones with subsequent prolapse of the orbital tissues and their incarceration into the fracture lines,²⁶ known as a 'trap door' fracture. This type of fracture however cannot be modelled in the porcine orbit due to the different anatomical arrangement of the bones, namely formation of the caudolateral wall of the orbit by fibrous tissue in the form of a ligament, and the significantly thicker orbital bones.

There are many other pathologies affecting the human orbit. In addition to orbital trauma, pathological processes such as damage to the brainstem or cortical centre scan can lead to individual orbital nerve defects.²⁶ Defects of mobility or binocular vision which are caused by mechanical disruption or by changes of orbital volume are also common in humans. The causes might be infraorbital and/or extraorbital and may be due to trauma, tumours or other orbit-located expansive processes (such as orbital thyreopathy).^{26,27} Other causes include pathologies leading to expansion of the paranasal cavity or myogenic pathologies caused by illness or by incarceration of eye muscles. The location and composition of the porcine orbit do not allow

modelling situations requiring coordination of both eyes.^{26,28} It is not possible to identify a disruption of binocular sight after carrying out the simulated surgical procedure. It is also impossible to simulate surgeries aimed at modifying optical properties of the eye.²⁹

Surgical approaches into the orbit

Surgical approaches to the orbit used in human medicine are well described, and require particular attention to ensure a good aesthetic result and to prevent damage to the optic nerve, oculomotor muscles and nerves, and damage to the eyelids (entropion and ectropion). These surgical approaches are based on detailed knowledge of human orbital anatomy. The surgeon must be aware of the limited volume of the orbit, which must not be altered during the surgical procedure. Any change in the volume or violation of the closed space can lead to a shift of the bulbus and thus to disruption of binocular vision.^{27,30–33} The surgical approaches involving the skin of the lower eyelid – subciliary, subtarsal, or transconjunctival – are employed for surgeries concerning the edge of the orbit or of the orbit itself. The decision about a particular incision the surgeon is going to perform is in large part dependent on the experience and surgical skills of the surgeon.^{34–36}

A supraorbital approach offers direct access to the upper lateral edge and fronto-zygomatic suture. Disadvantages include a skin scar and possible disruption of branches of the trigeminal and facial nerves or the lacrimal gland.^{26,27,37–39}

These routes of access can also be practised on the pig; it is however necessary to take into consideration the differences in the supraorbital nerve outlet and in the course of the facial nerve. In addition, the lacrimal gland is located dorsomedially from the orbital ligament.

The transconjunctival incision is another of the possible approaches into the lower part of the orbit. With this approach the skin remains intact, the scar is hidden in the conjunctiva (although this approach could be extended through the lateral cantus as a skin incision), and if the surgery is performed correctly there is a minimal risk of complications. The incision can be made in both the preseptal or retroseptal area, however this method requires a certain degree of surgical experience and practice.^{40–42}

Since the porcine orbit is a suitable model for this type of approach, appropriate experience can be gained using the pig.

A transantral endoscopy-assisted approach provides direct access to the bottom of the orbit through the maxillary sinus. Due to possible complications associated with incisions to the lower eyelids, this approach is currently used to reposition tissues of the orbit and to insert osteosynthesis mesh. Its advantage is the

avoidance of damage to soft tissues around the eye, resulting in no scarring and no risk of extropion. The disadvantages however lie in the long surgical time required in comparison with other surgical approaches, in the requirement for specific instrumentation, and the need for surgeons experienced in endoscopic surgery.^{43–45} The skin remains intact but this approach is technically difficult due to the limited space within the maxillary sinus.

The porcine model is however not suitable for practising this approach due to anatomical differences between pigs and humans, particularly in the layout of the orbit and the maxillary sinus.

The aim of surgeries of the orbit is to restore function and to reconstruct the orbit in order to achieve an outcome as close as possible to its normal anatomy. There is no ‘one size fits all’ surgical approach, and a wide range of techniques, materials and approaches are available for specific case scenarios. Therefore, careful pre-surgical planning is necessary and the porcine orbit can serve as a training model and can help to establish the advantages and disadvantages of each technique in different situations.

In conclusion, the porcine orbit is a suitable model for experimental medicine. However, if used in research, its anatomical differences and the breed of pigs must be taken into consideration. Consequently, the porcine orbit could serve as a suitable model for the training of surgeons, allowing them to gain necessary experience. All the most common surgical approaches used in human orbital surgery can be performed on a porcine head; therefore, the pig is a suitable model for practical training.

Declaration of conflicting interests

The authors declared no potential conflicts of interest with respect to the research, authorship, and/or publication of this article.

Funding

This work was supported by the Ministry of Health of the Czech Republic (project 3 RVO-FNOs/2014).

References

1. Štembírek J, Kyllar M, Putnová I, Stehlik L and Buchtová M. The pig as an experimental model for clinical craniofacial research. *Lab Anim* 2012; 46: 269–279.
2. Asai S, Shimizu Y and Ooya K. Maxillary sinus augmentation model in rabbits: effect of occluded nasal ostium on new bone formation. *Clin Oral Implants Res* 2002; 13: 405–409.
3. Haas R, Haidvogel D, Donath K and Watzek G. Freeze-dried homogeneous and heterogeneous bone for sinus augmentation in sheep. Part I: histological findings. *Clin Oral Implants Res* 2002; 13: 396–404.

4. Jakse N, Tangl S, Gill R, et al. Influence of PRP on autogenous sinus grafts: an experimental study on sheep. *Clin Oral Implants Res* 2003; 14: 578–583.
5. Roldan JC, Jepsen S, Schmidt C, et al. Sinus floor augmentation with simultaneous placement of dental implants in the presence of platelet-rich plasma or recombinant human bone morphogenetic protein-7. *Clin Oral Implants Res* 2004; 15: 716–723.
6. Lee SH, Choi BH, Li J, Jeong SM, Kim HS and Ko CY. Comparison of corticocancellous block and particulate bone grafts in maxillary sinus floor augmentation for bone healing around dental implants. *Oral Surg Oral Med Oral Pathol Oral Radiol Endod* 2007; 104: 324–328.
7. Estaca E, Cabezas J, Uson J, Sanchez-Margallo F, Morell E and Latorre R. Maxillary sinus-floor elevation: an animal model. *Clin Oral Implants Res* 2008; 19: 1044–1048.
8. vonWilmowsky C, Bauer S, Lutz R, et al. In vivo evaluation of anodic TiO₂ nanotubes: an experimental study in the pig. *J Biomed Mater Res Part B: Appl Biomater* 2009; 89: 165–171.
9. Pearce AI, Richards RG, Milz S, Schneider E and Pearce SG. Animal models for implant biomaterial research in bone: a review. *Cell Mater* 2007; 13: 1–10.
10. Beatty RG and Vertucci FJ. The porcine jaw: an aid for teaching endodontic surgery. *J Endodon* 1984; 10: 335–337.
11. Eufinger H, Konig S, Eufinger A and Machtens E. Significance of the height and width of the alveolar ridge in implantology in the edentulous maxilla. Analysis of 95 cadaver jaws and 24 consecutive patients. *Mund Kiefer Gesichtschirurgie* 1999; 3(Suppl. 1): 14–18.
12. Nieblerová J, Foltán R, Hanzelka T, et al. Stability of the miniplate osteosynthesis used for sagittal split osteotomy for closing an anterior open bite: an experimental study in mini-pigs. *Int J Oral Maxillofac Surg* 2012; 41: 482–488.
13. Folkestad L and Granstrom G. A prospective study of orbital fracture sequelae after change of surgical routines. *J Oral Maxillofac Surg* 2003; 61: 1038–1044.
14. Chacon-Moya E, Gallegos-Hernandez JF, Pina-Cabrales S, Cohn-Zurita F and Gone-Fernandez A. Cranial vault reconstruction using computer-designed polyetheretherketone (PEEK) implant: case report. *Cir Cir* 2009; 77: 437–440.
15. Botchwey EA, Pollack SR, El-Amin S, Levine EM, Tuan RS and Laurencin CT. Human osteoblast-like cells in three-dimensional culture with fluid flow. *Biorheology* 2003; 40: 299–306.
16. Stelzle F and Benner KU. Evaluation of different methods of indirect sinus floor elevation for elevation heights of 10mm: an experimental ex vivo study. *Clin Implant Dent Relat Res* 2009; 3: 167–177.
17. Getty R. *The anatomy of the domestic animals: porcine*, 5th ed. Philadelphia: WB Saunders, 1975, pp.1409–1416.
18. Kyllar M, Stembirek J, Putnova I, Stehlik L, Odehnalova S and Buchtova M. Radiography, computed tomography and magnetic resonance imaging of craniofacial structures in pig. *J Anat Histol Embryol* 2014; 43: 435–452.
19. Weaver AA, Loftis KL, Tan JC, Duma SM and Stitzel JD. CT based three-dimensional measurement of orbit and eye antropometry. *Invest Ophthalmol Vis Sci* 2010; 51: 4892–4897.
20. Koenig HE and Liebich HG. *Veterinary anatomy of domestic mammals*, 4th ed. Stuttgart: Schattauer, 2009, pp.568–575.
21. Prince JH. *Comparative anatomy of the eye*. Springfield, IL: Charles C.Thomas, 1956.
22. Payne AP. The harderian gland: a tercentennial review. *J Anat* 1994; 175: 1–49.
23. Uhlig CE and Gerding H. Illuminated artificial orbit for the training of vitreoretinal surgery in vitro. *Eye* 2004; 18: 183–187.
24. Kivell TL, Doyle SK, Madden RH, Mitchell TL and Sims EL. An interactive method for teaching anatomy of the human eye for medical students in ophthalmology clinical rotations. *Anat Sci Educ* 2009; 2: 173–178.
25. Suner S, Simmons W and Savitt DL. A porcine model for instruction of lateral canthotomy. *Acad Emerg Med* 2000; 7: 837–838.
26. Schendel SA. The orbit. *Oral Maxillofac Surg Clin North Am* 2012; 24: 525–720.
27. Ellis E and Zide MF. *Surgical approaches to the facial skeleton*, 2nd ed. Philadelphia: Lippincott Williams & Wilkins, 2006.
28. van der Meulen JC and Gruss JS. *Ocular plastic surgery*. London: Mosby-Wolfe, 1996.
29. Adams RD, Victor M and Ropper AH. *Adams and Victor's principles of neurology*, 7th ed. New York: McGraw-Hill, 2001.
30. Crumpton KL and Shockley LW. Ocular trauma: a quick, illustrated guide to treatment, triage, and medicolegal implications. *Emerg Med Rep* 1997; 18: 223–234.
31. Granström G. Invited review: craniofacial osseointegration. *Oral Dis* 2007; 13: 261–269.
32. Yanoff MY and Duer JS. *Ophthalmology*, 3rd ed. St Louis, MO: Mosby, 2008.
33. Scolozzi P. Reconstruction of severe medial orbital wall fractures using titanium mesh plates placed using transcaruncular–transconjunctival approach: a successful combination of 2 techniques. *J Oral Maxillofac Surg* 2011; 69: 1415–1420.
34. Rohrich RJ, Janis JE and Adams WP Jr. Subciliary versus subtarsal approaches to orbitozygomatic fractures. *Plast Reconstr Surg* 2003; 111: 1708–1714.
35. Kim YK and Kim JW. Evaluation of subciliary incision used in blowout fracture treatment: pretarsal flattening after lower eyelid surgery. *Plast Reconstr Surg* 2010; 125: 1479–1484.
36. Feldman EM, Brune TWR, Sharabi SE, Koshy JC and Hollier LH Jr. The subtarsal incision: where should it be placed? *J Oral Maxillofac Surg* 2011; 69: 2419–2423.
37. Neel HB 3rd, McDonald TJ and Facer GW. Modified Lynch procedure for chronic frontal sinus diseases: rationale, technique, and long-term results. *Laryngoscope* 1987; 97: 1274–1279.
38. Katowitz JA, Welsh MG and Bersani TA. Lid crease approach for medial wall fracture repair. *Ophthalmic Surg* 1987; 18: 288–290.

39. Wright JE, Stewart WB and Krohel GB. Clinical presentation and management of lacrimal gland tumours. *Br J Ophthalmol* 1979; 63: 600–606.
40. Baumann A and Ewers R. Use of the preseptal transconjunctival approach in orbit reconstruction surgery. *J Oral Maxillofac Surg* 2001; 59: 287–291.
41. Edgin WE, Morgan-Marshall A and Fitzsimmons TD. Transcaruncular approach to medial orbital wall fractures. *J Oral Maxillofac Surg* 2007; 65: 2345–2349.
42. Lee CS, Yoon JS and Lee SY. Combined transconjunctival and transcaruncular approach for repair of large medial orbital wall fractures. *Arch Ophthalmol* 2009; 127: 291–296.
43. Maturo SC, Wiseman J and Mair E. Transantral endoscopic repair of orbital floor fractures with the use of a flexible endoscope holder: a cadaver study. *Ear Nose Throat J* 2008; 87: 693–695.
44. Cheong EC, Chen CT and Chen YR. Endoscopic management of orbital floor fractures. *Facial Plast Surg* 2009; 25: 8–16.
45. Ducic Y and Verret DJ. Endoscopic transantral repair of orbital floor fractures. *Otolaryngol Head Neck Surg* 2009; 140: 849–854.

Komentář k přiložené publikaci č. 10

Juraj TIMKOVIC, Jiri STRANSKY, Katerina JANUROVA, Petr HANDLOS a Jan STEMBIREK ***(corresponding author)**. Role of orthoptics and scoring system for orbital floor blowout fracture: surgical or conservative treatment. *International Journal of Ophthalmology* [online]. 2021, **14**(12), 1928–1934. ISSN 2222-3959. Dostupné z: doi:[10.18240/ijo.2021.12.18](https://doi.org/10.18240/ijo.2021.12.18)

IF = 1,645; kvartil OPHTHALMOLOGY Q4

V této práci jsme se zabývali úspěšností léčby pacientů s retromaginální zlomeninou očnice ve Fakultní nemocnici Ostrava, analyzovali jsme vztahy mezi výsledky CT a ortoptických vyšetření na jedné straně a úspěšností výběru konzervativní či chirurgické léčby na straně druhé. U konzervativní léčby jsme u 35 pacientů dosáhli **97 %** úspěšnosti terapie. Při závěrečném ortoptickém vyšetření byla diplopie zjištěna pouze u jednoho pacienta (3%) léčeného konzervativně, v daném případě však byla způsobena obrnou trochleárního nervu a chirurgická léčba by v takovém případě pravděpodobně rovněž neměla žádný efekt. Z tohoto pohledu můžeme považovat úspěšnost indikace pacientů ke konzervativní terapii prakticky za 100% (přesněji řečeno, nikdo z pacientů, kteří byli indikováni ke konzervativní léčbě, by neprofitoval z chirurgické léčby).

Chirurgická léčba byla zvolena u 34 pacientů, z čehož jsme absolutní nebo částečnou úspěšnost zaznamenali u **80 %** pacientů. Terapie byla bez efektu u 15 % (5 pacientů), u kterých přetrvávaly minoritní okohybné poruchy v podobě nepřímé diplopie, tj. pouze v jednom z dalších osmi směrů pohledu. U dvou chirurgicky léčených pacientů (6 %) byla terapie neúspěšná (porucha oční motility a binokulární diplopie přetrvávala i v přímé poloze). U obou těchto pacientů byla binokulární diplopie, která byla pacientem špatně tolerovaná, úspěšně eliminována předepsáním prizmatické korekce v brýlích; v jednom případě byl proveden další chirurgický zákrok řešící strabismus. Nicméně pacienti, u kterých chirurgická terapie nebyla úspěšná, přicházeli s relativně závažnými poraněními očnice a nedá se očekávat, že by u nich konzervativní terapie přinesla lepší výsledky. Z tohoto důvodu můžeme považovat rozpoznání pacientů indikovaných k chirurgické léčbě rovněž za úspěšné. Naše výsledky ukazují, že pro správné rozhodnutí o indikaci ke konzervativní nebo chirurgické terapii je zásadní provedení

komplexního ortoptického vyšetření a zhodnocení poruchy oční motility. Ortoptické vyšetření je pak důležitým pomocníkem i v průběhu rehabilitační fáze.

Rozhodnutí ohledně konzervativní nebo chirurgické terapie v současné době zůstává na zkušenosti lékařů, kteří se problematikou zabývají. Proto jsme na základě našich výsledků vyvinuli skórovací systém, který si klade za cíl poskytnout při tomto rozhodování pomoci (viz Tabulka č. 1). V naší studii se ukázalo, že 80% pacientů s hodnotou <22 bodů ve skórovacím systému bylo léčeno konzervativně (s excelentními výsledky, viz výše), zatímco 80 % pacientů s hodnotou >35 bylo indikováno k chirurgické léčbě. Výsledek skórovacího systému tak nedefinuje jednoznačně indikaci ke konzervativní nebo chirurgické terapii a není absolutní, cílem je, aby skórovací systém mohl fungovat jako pomocný nástroj při tomto rozhodování. Je třeba rovněž upozornit, že tento skórovací systém neslouží k predikci výsledků léčby. Vždy je nutno mít při rozhodování mezi chirurgickou a konzervativní terapií individuální přístup a zohlednit další faktory, jako jsou věk pacienta, celkový zdravotní stav nebo přesné místo defektu, a dle toho se rozhodnout. To platí zejména tam, kde pacienti spadají mezi výsledné hodnoty 23 - 34 bodů. V tomto rozmezí strmě rostla indikace k chirurgické léčbě, ale nebyla vždy jednoznačná (např. skóre 29 bodů bylo spojeno s 50 % pravděpodobností operace). Zajímavostí je, že silnými faktory ve skórovacím systému byly zejména elevace očního bulbu na Lancasterově plátně a poměrná velikost defektu ku velikosti spodiny, a to více jak 25%.

Tabulka č. 1: Skórovací systém indikace operace fraktury spodiny očnice, kde nejsilnějšími faktory jsou elevace očního bulbu na Lancasterově plátně a více jak 25% relativní velikost defektu spodiny očnice.

PROPOSED THRESHOLD VALUES:	
- CONSERVATIVE SOLUTION	<22
- SURGICAL SOLUTION	>35
- 50% PROBABILITY OF SURGERY	29
AWARDED POINTS:	
LANCASTER – ELEVATION	19
* RFA > 25 % – 2D	19
VERTICAL DEVIATION – PRISM COVER TEST	7
LANCASTER – DEPRESSION	5
DIPLOPIA	4
LANCASTER – VERTICAL DEVIATION (PRIMARY POSITION)	2

Jednoznačným omezením studie je, že si nemůžeme být zcela jisti, že u některých pacientů, kteří byli indikováni k chirurgické léčbě, by nedostačovala konzervativní terapie, zvláště u pacientů s výsledným skóre 24-34 bodů. Ke zvážení je proto možné ověření námi vyvinutého skórovacího systému na větším souboru pacientů v podobě multicentrické studie, popř. jeho nahrazení algoritmickým schématem a postupné zavedení do klinické praxe.

Role of orthoptics and scoring system for orbital floor blowout fracture: surgical or conservative treatment

Juraj Timkovic^{1,2}, Jiri Stransky³, Katerina Janurova⁴, Petr Handlos⁵, Jan Stembirek^{3,6}

¹Clinic of Ophthalmology, University Hospital Ostrava, 17. Listopadu 1790/5, Ostrava 708 52, Czech Republic

²Department of Craniofacial Surgery, Faculty of Medicine, Ostrava University, Syllabova 19, Ostrava 703 00, Czech Republic

³Clinic of Oral and Maxillofacial Surgery, University Hospital Ostrava, 17. Listopadu 1790/5, Ostrava 708 52, Czech Republic

⁴IT4Innovations, VSB-Technical University of Ostrava, Studentská 6231, Ostrava 708 33, Czech Republic

⁵Department of Forensic Medicine, University Hospital Ostrava, 17. Listopadu 1790/5, Ostrava 708 52, Czech Republic

⁶Laboratory of Molecular Morphogenesis, Institute of Animal Physiology and Genetics CAS, Veveří 97, Brno 602 00, Czech Republic

Correspondence to: Jan Stembirek. Clinic of Oral and Maxillofacial Surgery, University Hospital Ostrava, 17. Listopadu 1790/5, Ostrava, 708 52, Czech Republic. stembirek@iach.cz

Received: 2020-11-27 Accepted: 2021-04-22

Abstract

• **AIM:** To assess the role of orthoptics in referring patients with orbital floor blowout fracture (OFBF) for conservative or surgical treatment and based on the results, to propose a scoring system for such decision making.

• **METHODS:** A retrospective analysis of 69 patients with OFBF was performed (35 treated conservatively, 34 surgically). The role of orthoptics in referring to surgery or conservative treatment was retrospectively evaluated, the factors with the highest significance for decision making were identified, and a scoring system proposed using Logistic regression.

• **RESULTS:** According to defined criteria, the treatment was unsuccessful in 2 (6%) surgically treated and only in one (3%) conservatively treated patient. The proposed scoring system includes the defect size and several values resulting from the orthoptic examination, the elevation of the eyeball measured on Lancaster screen being the most significant.

• **CONCLUSION:** The study demonstrates the benefits of orthoptic examination when making decisions on conservative or surgical treatment and for diagnosing ocular motility disorder (with or without binocular diplopia) in OFBF patients. The proposed scoring system could, following verification in a prospective study, become a valuable adjunctive tool.

• **KEYWORDS:** orbital floor blowout fracture; scoring system; orthoptics; ocular motility; diplopia; conservative treatment; surgical treatment

DOI:10.18240/ijo.2021.12.18

Citation: Timkovic J, Stransky J, Janurova K, Handlos P, Stembirek J. Role of orthoptics and scoring system for orbital floor blowout fracture: surgical or conservative treatment. *Int J Ophthalmol* 2021;14(12):1928-1934

INTRODUCTION

In patients with orbital floor blowout fractures (OFBF), two principal treatment options are available: conservative and surgical treatment. At present, no guidelines facilitating the decision making which of those treatment options to choose and the decisions depend to a great degree on the general experience and habitual practices of the individual departments^[1]. The most common criteria include the size of the defect exceeding one-third of the orbital floor or binocular diplopia resulting from the disruption of ocular motility due to the herniation of soft tissues into the defect^[2]. Here, it is, however, necessary to mention that binocular diplopia may not be obvious and in some cases, it can be altogether missing despite the presence of a clear ocular motility disorder (*e.g.* patients with preexisting concomitant strabismus with an alternating suppression)^[3-5]. The diagnosis and treatment of ocular motility disorders are a complex process^[6]. As orthoptic examination is the best-suited method for diagnosing ocular motility disorders, the fact that its use in the decision making related to OFBF treatment is largely neglected is actually quite surprising^[7-8].

The aims of the presented study were to retrospectively evaluate the results of the conservative and surgical treatment

of isolated blowout fractures at our department based on given criteria of therapy success. Providing that the success rate was good, additional aims were to identify possible factors, the presence of which can be associated with the chosen treatment path and based on a detailed analysis of those factors, to propose an easy-to-use pilot scoring system for individualized referring to surgical or conservative treatment.

SUBJECTS AND METHODS

Ethical Approval This study was performed in accordance with the Declaration of Helsinki and approved by the Ethics Committee of the University Hospital Ostrava, Approval No.397/2017.

Patients A retrospective analysis of the documentation of all patients who were treated for isolated blowout orbital fracture and followed up between September 2013 and October 2016 was performed. All patients meeting the following inclusion criteria were included in the study: age at the time of injury 15-80y, isolated one-sided orbital floor fracture confirmed by CT scan, a full orthoptic examination performed per our standard procedure, normal retinal correspondence, normal direct and indirect pupillary light reflex, and known long-term results of the therapy (at least 6-months follow up). Preexisting concomitant strabismus with an alternating suppression was an exclusion criterion.

Treatment Procedures at Our Hospital In each patient, a CT scan with slices below 1 mm was performed, meeting the guidelines and criteria set by the American College of Radiology^[9]. The size of the orbital floor defect was measured using defect-delineating and orbital floor delineating tangents in the xVisionViewer software (Vidis, s.r.o, Prague, Czech Republic) and evaluated both in the mediolateral and anteroposterior axes on frontal and sagittal slices of the orbit. The convex shape of the orbital floor was not considered due to the software capabilities. The acquired data were subsequently used for calculating a percentage of the defect in the direction of each axis and of the orbital floor area.

All patients were examined by a maxillofacial surgeon and by an ophthalmologist. The complex examination by an ophthalmologist took place several days after the injury, which allowed time for the initial swelling to partially subside and, therefore, to help us distinguish between ocular motility disorders caused by intraorbital swelling/bleeding from true ocular motility disorders. The examination included the evaluation of refraction, near and far vision, intraocular pressure, biomicroscopic examination of the anterior and posterior segments of both eyes, examination of motility, fixation, accommodation and convergence, of binocular spatial functions using colour filters, Worth four lights and Bagolini striated glasses tests, the degree of strabismus in prism cover test and by synoptophore. The eye position

in the anterior-posterior orbital axis was assessed using Hertel exophthalmometer. The ocular motility disorders were objectively assessed and documented by the Lancaster screen test. Based on all those findings, a team consisting of a maxillofacial surgeon and ophthalmologist decided about the treatment methods (conservative/surgical revision with orbital floor reconstruction). The decision whether or not to operate was made strictly individually in each patient, considering multiple factors, among others the defect size and position, enophthalmos on the affected side >2 mm, or ocular motility disorder (with or without binocular diplopia). All the above examinations were repeated during follow-ups.

Where the decision to perform surgery was made, the intervention was performed once the swelling had subsided. We operate through a combination of subciliary and subtarsal approaches in the region of the lower eyelid, accessing the periorbita through the orbitalis oculi muscle. Cutting through the periorbita and exposing the orbital floor defect, herniated tissues are released. The defect is subsequently reconstructed using a resorbable RapidSorb Orbfloor PI plate (DePuy Synthes, Massachusetts, USA), which is during the surgery shaped to fit the orbital floor and fixed to the edge of the defect with two resorbable stitches. Finally, the plate position and ocular motility are evaluated using the forced duction test and close the wound.

The rehabilitation of ocular motility and, if need be, prismatic correction were managed by an ophthalmologist. The recorded parameters included the need for revision of the original surgery of the orbital floor fracture, the need for surgical correction of an ocular motility disorder and eventual prism correction using glasses.

For evaluating the long-term results of the treatments, the criteria of success/failure of the treatment were set as detailed in Table 1.

Methods of descriptive statistics were used for the initial evaluation of data; namely, the sample mean, sample standard deviation, sample median, minimum and maximum values and the number of patients were used for the continuous variables [relative fracture area (RFA) and lengths in individual axes, age of patients, follow-up period] and sample relative and absolute frequency for categorical variables (all remaining variables used only a binary differentiation between normal/abnormal finding was used for orthoptic variables). Subsequently, the statistical significance of individual factors for their referring to conservative or surgical treatment was assessed using Mann-Whitney test for continuous data and contingency tables with χ^2 -test for categorical data at the level of $P < 0.05$. The null hypothesis was H_0 : the variables in the contingency table are independent. "To achieve a better approximation, Yates correction was used for selected contingency table analyses.

Table 1 Criteria of the success/failure of the treatment

Result of treatment	Conservative treatment	Surgical treatment
Successful	<p>The patient had neither ocular motility disorder nor binocular diplopia during the initial examination and none of these problems developed by the end of the follow-up period</p> <p>The patient had either ocular motility disorder or binocular diplopia (regardless of whether in primary or non-primary position) during the initial examination and these regressed spontaneously without surgical intervention</p>	<p>The patient had neither ocular motility disorder nor binocular diplopia during the initial examination and none of these problems developed by the end of the follow-up period</p> <p>The patient had either ocular motility disorder or any form of binocular diplopia (or both) during the initial examination and these disappeared after surgical intervention</p>
Partially successful	-	The patient had either ocular motility disorder or binocular diplopia (or both) in the primary position during the initial examination but after surgery, it only persisted in the secondary position.
No effect	-	The patient had either ocular motility disorder or binocular diplopia (or both) in a non-primary position during the initial examination and these persisted even after surgical intervention (the patient's condition remained unchanged)
Unsuccessful	<p>The patient had neither ocular motility disorder nor binocular diplopia during the initial examination but any of these developed by the end of the follow-up period</p> <p>The patient had an ocular motility disorder with binocular diplopia in the primary and/or non-primary position during the initial examination and these persisted for longer than 6mo or surgical revision was subsequently needed</p>	<p>The patient had neither ocular motility disorder nor (any) binocular diplopia during the initial examination but these developed after surgery</p> <p>The patient had an ocular motility disorder or binocular diplopia in primary position (or both) during the initial examination and these persisted in the primary position after the surgery</p> <p>The patient had an ocular motility disorder or binocular diplopia (or both) outside the primary position during the initial examination and after the surgery, these were present in the primary position</p>

Individual variables were subsequently sorted according to the relative risk of being referred to the surgical treatment and strong and weak factors were determined. Correlations between individual variables were determined and uncorrelated variables were subsequently used for creating a pilot scoring system by Logistic regression. Statistical evaluation was performed in the R (R Core Team, 2018) and Microsoft Excel 2010 (Microsoft Corporation, Redmond, Washington, USA).

RESULTS

From September 2013 till October 2016, 69 patients were treated for isolated one-sided orbital floor fracture, 47 of which were male and 22 female. The mean age was 43y (SD=19, median age 42y, min-max 15-80y). Mann-Whitney test revealed no statistically significant difference between the age of patients who were and were not referred to surgery (P=0.94). The median time from the injury to the orthoptic examination was 7d (mean 9d, min-max 1-19d). The median time from the injury to surgery (if performed) was 10d (mean 16d, min-max 5-21d).

Surgical treatment was performed and the orbital floor reconstructed (always after a thorough evaluation of the patient by both the maxillofacial surgeon and the ophthalmologist) in

34 patients (49%) while the remaining 35 patients (51%) were treated conservatively. The mean follow-up period was 26mo in patients after surgical intervention (median 24mo, min-max 12-50mo), and 24mo in patients treated conservatively (median 21mo, min-max 12-51mo). No statistically significant difference in the length of the follow-up period was found between patients treated conservatively and those who underwent surgical treatment (Mann-Whitney test, P=0.453).

The mean orbital floor defect size was 279 mm² in patients who underwent surgical intervention (SD=124, median 276 mm², min-max 77-498 mm²) while in conservatively treated patients, the mean was 177 mm² (SD=98, median 178 mm², min-max 40-481 mm²). The difference in defect size between both groups was statistically significant (Mann-Whitney, P=0.003). The comparison of the results of the orthoptic examination between the groups can be found in Table 2.

By the end of the follow-up period, we recorded success in 97% of patients who were conservatively treated. Only in one (3%) patient treated conservatively, the final orthoptic examination revealed an ocular motility defect with binocular diplopia; this defect was, however, caused by a partial paralysis of the trochlear nerve, hence the surgical treatment would

Table 2 Results of orthoptic examination, comparison of the presence of individual disorders between the conservatively treated and surgically treated patient groups

Result of orthoptic examination	Conservative		Surgical		P
	n	%	n	%	
Any form of binocular diplopia	12	29	29	71	<0.001
Binocular diplopia in primary position	1	9	10	91	<0.001
Binocular diplopia in a non-primary position only	12	29	29	71	<0.001
Anterior/posterior shift (Hertel)	12	32	25	68	<0.001
Enophthalmos (Hertel)	8	42	11	58	<0.002
Vertical deviation (Prism cover test)	2	12	14	88	<0.009
Vertical deviation (Lancaster)	7	25	21	75	<0.001
Horizontal motility disorder (Lancaster)	6	23	20	77	<0.001
Vertical motility disorder (Lancaster)	9	24	29	76	<0.001
Combined motility disorder (Lancaster)	4	23	13	77	<0.008
Patients total	35	51	34	49	

All parameters derived from Lancaster test describe the injured side only.

in all likelihood not have any effect anyway. Where surgical treatment is concerned, we recorded absolute or partial success in 80% of patients. The therapy was without effect in 15% (5 patients) in whom minor ocular motility disorders persisted, namely binocular diplopia in non-primary position, *i.e.*, only in one of the other eight cardinal directions of gaze. In two surgically treated patients (6%), the therapy was unsuccessful (the ocular motility disorder and binocular diplopia persisted even in the primary position). In both these patients, the binocular diplopia that was poorly tolerated by the patient was successfully eliminated by prescription of prism correction in eyeglasses; in one case, an additional surgical procedure addressing strabismus was performed.

Results of the subsequent calculation of relative risks and odds ratios of individual parameters for their referring to the surgical treatment is shown in Table 3. Subsequently, Logistic regression was used to propose a pilot scoring system (Table 4). Models using multiple values of the RFA derived from the CT scans were tested; of those, 25% RFA yielded the best results and hence, this value was used in the developed scoring system. The RFA and limitation of the eyeball elevation detected by the Lancaster screen test were the strongest predictors and assigned the highest values in the scoring system. Additional factors included changes in the ocular motility and position assessed on the Lancaster screen test, presence of any form of binocular diplopia and evaluation of the ocular motility disorder in the vertical direction using the prism cover test.

The threshold values for the scoring system were determined as values associated with an 80% probability of being referred to surgery or conservative treatment in our retrospective study. The use of the scoring system is simple-all factors with assigned values that are present in the patient are to be summed

Table 3 Relative risk of referring patients with named factors for surgical treatment

Disorder (presence of):	Relative risk (confidence interval)
Vertical deviation (Prism cover test)	6.72 (1.63; 27.76)
Vertical motility disorder-depression (Lancaster)	6.42 (2.51; 16.44)
Horizontal motility disorder-adduction (Lancaster)	5.30 (1.68; 16.69)
Vertical motility disorder-elevation (Lancaster)	4.37 (2.24; 8.50)
Horizontal motility disorder-abduction (Lancaster)	3.67 (1.33; 10.08)
Vertical deviation (Synoptophore)	3.67 (1.10; 12.22)
Vertical deviation (Lancaster)	3.14 (1.55; 6.39)
Any form of binocular diplopia	2.78 (1.69; 4.55)
Relative fracture area >25%	2.55 (1.47; 4.43)
Anterior/posterior shift (Hertel)	2.00 (1.15; 3.47)
Horizontal deviation (Lancaster)	1.83 (0.88; 3.83)
Horizontal deviation (Prism cover test)	1.57 (0.67; 3.66)
Horizontal deviation (Synoptophore)	1.17 (0.46; 2.95)

Factors were distinguished in a binary way only (normal/abnormal finding). Where the confidence interval included the value of 1.00, the relationship was considered weak and not taken into account for subsequent modeling.

up; if the total is 22 or less, the patient should be treated conservatively while where it exceeds the threshold value of 35 points, the patient is referred for surgical treatment. This is, of course, valid unless a clear contraindication for either decision is present (*e.g.*, when the patient's condition prevents surgery). Between those two values, the dependency is almost linear, with a score of 29 denoting a 50% likelihood for being referred for either treatment.

DISCUSSION

Results of Treatment In our patient group, success was recorded in 97% of conservatively treated and 80% of surgically treated patients. All patients with conservative treatment healed well; in the only patient with persisting

Table 4 A pilot scoring system for decision for surgical or conservative treatment of orbital floor blowout fracture

Proposed threshold values	Score/awarded points
Conservative solution	≤22
Surgical solution	>35
50% probability of surgery	=29
Awarded points (if disorder present):	
Vertical motility disorder-elevation (Lancaster)	19
RFA>25%	19
Vertical deviation (prism cover test)	7
Vertical motility disorder-depression (Lancaster)	5
Any form of binocular diplopia	4
Vertical deviation (Lancaster)	2

The threshold values were set as values where more than 80% of patients reaching that score (23 and less for conservative or 36 and more for surgical) were indicated for the respective therapy; with a score of 29, the probability of either therapy was equal. RFA: Relative fracture area.

problems, those were caused by a reason outside the orbit, namely paralysis of the trochlear nerve. Of seven surgically treated patients in whom the surgical treatment was regarded as ineffective or unsuccessful according to the set criteria, the condition after surgery was better than before it in 4 patients out of 7.

Our results indicate that none of the patients who were referred for conservative treatment would benefit from surgical treatment and we can thus state that the decision not to operate was correct in all of them. In surgically treated patients, the condition worsened in one patient and failed to improve in two patients. Although the surgical therapy was unsuccessful in these patients, we still believe that the decision to operate was correct as the character of the injuries was so serious (RFA over 30 % of the orbital floor and objectively detected ocular motility disorder) that conservative therapy could in no way yield a better result.

In patients with surgical therapy, the defect size was typically larger than in patients with conservative therapy, which was also associated with a higher risk of complications and represented another reason for a seemingly lower success rate in these patients. Even relatively small defects may in some cases require surgical intervention. As an example, we can mention a patient with the RFA of only 20% of the orbital floor in whom however a decision to operate was made. The main reason for such decision was the localization of the defect in the medial axis of the orbital floor and the consequent definite restriction of movement of the inferior rectus muscle with binocular diplopia. It is, therefore, necessary to emphasize that especially where the decision whether to operate or

not is close, it is also necessary to take the site of the defect into account as centrally located defects are associated with herniation of oculomotor muscles much more often than even larger defects localized outside the axial position.

Risk Factors and Scoring System The decision whether or not to operate a patient with an orbital blowout fracture can be a complicated one, especially since subjective complaints of the patient may be changing over time-both in the sense of spontaneous regression of the ocular motility disorder (potentially including binocular diplopia) and recovery of the facial sensitivity and, conversely, in the sense of developing late complications such as ocular motility disorders due to the late change in the volume of orbital soft tissues that can be caused by fading of the swelling or by atrophy of (usually adipose) tissue occurring over a longer period after the injury. It is therefore necessary to evaluate each patient individually and to consider the possible benefits even in patients who show no subjective complaints in the early post-injury period. At present, there is no scoring system that could help clinicians in decision making. According to existing papers, the most common indication criteria for surgical solution are enophthalmos over 2 mm and RFA over 50% of the orbital floor with persisting herniation of soft tissues of the periorbit, binocular diplopia and affected ocular motility resulting from herniation of oculomotor muscles^[3,10-16].

Our results confirm that the defect size determined by CT and its accurate measurement is indeed one of the most important criteria in decision making. A detailed analysis of CT scans in both sagittal and frontal slices can provide information both on the size and localization of the defect. Kovář *et al*^[17] performed a retrospective study on 80 patients where they attempted to determine indication criteria for surgical intervention based on the volume of the prolapsed tissue. According to their findings, the threshold for surgical intervention was 500 mm³ in anterior and posterior fractures and 1400 mm³ in anterior-posterior fractures. Chiason and Matic^[18] used the CT-derived ratio of width and length of inferior and medial rectus muscles in their study on 18 patients. In their study, the indication criterion was the length/width ratio of 1.0 for the inferior rectus muscle and 0.7 for the medial rectus muscle.

The change of the eyeball position in the anterior-posterior direction in the sense of enophthalmos, if present, is generally considered to be an indication for surgery^[3,11-14,16]. While we observed a statistically significant difference between the presence of a defect in the anterior/posterior shift of the eye by Hertel test, the effect was relatively weak when compared to most of the others and its addition into the scoring system was not shown to have a notable effect on the accuracy. We can also find support for this finding in the literature. For example, Alinasab *et al*^[19] who studied the relationship

between herniation of soft tissues and enophthalmos disproved the opinion that herniation of 1 mL of orbital soft tissues into maxillary sinus leads to 1 mm eyeball shift in the anterior-posterior axis. Another study described a conservative treatment in patients with blowout fractures, 22% of whom presented with enophthalmos with more than 2 mm and despite that, all of them resolved without surgical treatment over time^[20]. We believe that the main reason is the fact that in the early post-injury period, the presence of enophthalmos is often confounded by changes in the orbital tissues (swelling of orbital soft tissues, bleeding or the presence of pneumo-orbit caused by penetration of the air from paranasal sinuses)^[19]. Besides, enophthalmos is largely a cosmetic problem and as such, it can be resolved through surgery at a later time if the patient is treated conservatively and enophthalmos persists. Therefore, disregarding enophthalmos as an indication criterion in the initial decision making does not pose a significant risk (if any) to the patient^[21].

Our experience shows that performing a full orthoptic examination and evaluation of the ocular motility disorder before indicating the patient for conservative or surgical treatment as well as during the rehabilitation is crucial. In the early post-injury period, orthoptic examination allows a more accurate evaluation of motility and position of the eye in the orbit and differentiation between dynamic and restrictive strabismus. From this perspective, the Lancaster screen test is of utmost importance, providing among other data also information about the extent of incomitant, usually restrictive, strabismus. The possibility to evaluate the development of individual parameters over time further underlines the importance of complex orthoptic examination.

The ocular motility disorders represent a frequent, diagnostically very important, symptom of orbital fractures as well as one of their most serious complications. Vertical ocular motility disorders are more common than horizontal in orbital fractures^[2]. In our study, the limitations to the vertical ocular motility documented on the Lancaster screen, together with the vertical strabismus deviation detected by cover prism test, represent crucial factors affecting to a great degree the decision whether or not to indicate surgical intervention.

The most typical subjective presentation of ocular motility disorders is binocular diplopia. From this point of view, the relatively low importance of binocular diplopia for the indication for surgery revealed by Logistic regression in our model is surprising. Although the presence of binocular diplopia was an important and statistically significant factor in our study, it was awarded only 4 points in the scoring system, which makes it a parameter of substantially lower importance than the RFA or elevation abnormalities detected on Lancaster screen. The likely reason is that in the early post-injury period,

binocular diplopia can be to a major degree masked by the swelling of orbital soft tissues with a drooping upper eyelid. Besides, in the long term, binocular diplopia can be obscured by neuroadaptation and suppression that is highly individual.

The presented scoring system aims to provide help in deciding whether or not to operate in patients with orbital blowout fracture. In our experience, the results of orthoptic examinations are more important than the RFA on itself and/or a focus on the presence of binocular diplopia. It is of course necessary to further improve the accuracy and verification of the system and we need to emphasize that we present this system as an adjunctive tool, especially at this stage. The proposed thresholds of ≤ 22 points for conservative treatment and >35 for surgical treatment correspond to 80% probability to be referred for either treatment in our retrospective study. Our recommendation to refer patients with scores ≤ 22 points for conservative treatment and those with scores >35 for surgery is, however, obviously not absolute-the scoring system aims to provide guidance but in every single case, an individual approach taking additional factors into account, such as the patient's age, overall health condition or exact site of the defect, is necessary. This is especially true where patients with a score falling between the proposed threshold values are concerned (*i.e.*, in the range where the relative frequency of the indication to surgery steeply and almost linearly increases). The total score of 29 points was associated with a 50% probability of surgery.

Study Limitations It must be of course emphasised that as this is a retrospective study, it is burdened with autocorrelation. Hence, we present it rather as a basis for further prospective studies and, at this moment, an adjunctive tool; in other words, the proposed scoring system should not be interpreted as the only correct decision-making procedure but rather as a procedure that would lead to results identical to ours (which are, however, very good).

Speaking of results of our treatment, an objection can be made that all patients including those whose therapy was not fully successful were included in modelling. Here, we would like to point out that this scoring system is not used for predicting results of the treatment but only for selecting the treatment method. Not even the best therapy can resolve all defects without any consequences and the injuries of patients in whom we did not record full success were very serious (scores 37 to 56); hence, we believe that their referring to surgery was correct and that their inclusion into the model was, therefore, justified.

An obvious limitation of the study is that although we can be quite sure that none of the patients who were referred for conservative treatment would have benefited from surgery, we cannot be certain that conservative treatment would not

be sufficient in some patients who were referred to surgery. In the retrospective view and knowing the results of our scoring system, there were patients with low scores who were referred to surgery. This, however, only underlines the potential value of the presented scoring system in preventing surgery in such patients, *i.e.*, patients who would in all likelihood not benefit from it.

In conclusion, referring patients with orbital blow-out fracture to surgical or conservative treatment is a complex and complicated problem. The decision must be therefore made individually for each patient and consider surgical revision even in patients without subjective complaints in the early post-injury period with relatively smaller orbital floor defects. In our experience, a full orthoptic examination by an experienced ophthalmologist should form an indispensable part of the examination of each patient with orbital blowout fracture, both to provide data necessary for treatment decision, for the rehabilitation of ocular motility disorders and for evaluation of the therapeutic success. The proposed scoring system could become a valuable adjunctive tool for deciding which path to take in the treatment of isolated orbital blowout fractures in everyday practice.

ACKNOWLEDGEMENTS

Foundation: Supported by the Ministry of Health, Czech Republic Conceptual Development of Research Organization (FNOs/2017).

Conflicts of Interest: Timkovic J, None; Stransky J, None; Janurova K, None; Handlos P, None; Stembirek J, None.

REFERENCES

- Felding UNA. Blowout fractures-clinic, imaging and applied anatomy of the orbit. *Dan Med J* 2018;65(3):B5459.
- Marano R, Lino PRS, Zanetti F, Tincani AJ, Oliveira L. Is specialized ophthalmologic evaluation necessary after orbital fractures? A prospective 64-case study. *Oral Maxillofac Surg* 2019;23(3):325-329.
- Gosse EM, Ferguson AW, Lymburn EG, Gilmour C, MacEwen CJ. Blow-out fractures: patterns of ocular motility and effect of surgical repair. *Br J Oral Maxillofac Surg* 2010;48(1):40-43.
- Loba P, Kozakiewicz M, Nowakowska O, Omulecki W, Broniarczyk-Loba A. Management of persistent diplopia after surgical repair of orbital fractures. *J AAPOS* 2012;16(6):548-553.
- Steinegger K, De Haller R, Courvoisier D, Scolozzi P. Orthoptic sequelae following conservative management of pure blowout orbital fractures: anecdotal or clinically relevant? *J Craniofac Surg* 2015;26(5):e433-e437.
- Zeng CJ, Fan CJ, Liu JL, Xiao Q, Zhu YW, Song XF, Chen HF. Gradual oculomotor training in blow-out orbital fracture reconstruction recovery. *J Int Med Res* 2020;48(4):300060519893846.
- Laurentjoye M, Bondaz M, Majoufre-Lefebvre C, Huslin V, Caix P, Ricard AS. When should an orthoptic evaluation be prescribed in the management of orbital floor fracture? A prospective study of 47 fractures. *Rev Stomatol Chir Maxillofac Chir Orale* 2014;115(5):274-278.
- Arrico L, Migliorini R, Bianchini D, Salducci M, Collini S, Malagola R. Ocular motility alterations in orbital fractures: pre-post evaluation in maxillofacial surgical treatment. *G Chir* 2018;39(6):363-367.
- AASC, *ACR-ASNR-SPR practice parameter for the performance of computed tomography (CT) of the extracranial head and neck*. <https://www.asnr.org/guidelines-standards/acr-asnr-spr-practice-parameter-for-the-performance-of-computed-tomography-ct-of-the-extracranial-head-and-neck-res-14-2016/>.
- Dunphy L. Maxillofacial trauma and esthetic facial reconstruction, 2nd edition. *Br Dent J* 2012;212(11):568.
- Boyette JR, Pemberton JD, Bonilla-Velez J. Management of orbital fractures: challenges and solutions. *Clin Ophthalmol* 2015;9:2127-2137.
- Harris GJ, Garcia GH, Logani SC, Murphy ML, Sheth BP, Seth AK. Orbital blow-out fractures: correlation of preoperative computed tomography and postoperative ocular motility. *Trans Am Ophthalmol Soc* 1998;96:329-347; discussion 347-353.
- Harris GJ. Orbital blow-out fractures: surgical timing and technique. *Eye (Lond)* 2006;20(10):1207-1212.
- Gosau M, Schöneich M, Draenert FG, Ettl T, Driemel O, Reichert TE. Retrospective analysis of orbital floor fractures—complications, outcome, and review of literature. *Clin Oral Invest* 2011;15(3):305-313.
- Koenen L and Waseem M, *Orbital Floor (Blowout) Fracture*, in *StatPearls*. 2020, StatPearls Publishing: Treasure Island (FL).
- Homer N, Huggins A, Durairaj VD. Contemporary management of orbital blowout fractures. *Curr Opin Otolaryngol Head Neck Surg* 2019;27(4):310-316.
- Kovar D, Voldrich Z, Voska P, Lestak J, Astl J. Indications for repositioning of blow-out fractures of the orbital floor based on new objective criteria-tissue protrusion volumetry. *Biomed Pap Med Fac Univ Palacky Olomouc Czech Repub* 2017;161(4):403-406.
- Chiasson G, Matic DB. Muscle shape as a predictor of traumatic enophthalmos. *Craniofac Trauma Reconstr* 2010;3(3):125-130.
- Alinasab B, Beckman MO, Pansell T, Abdi S, Westermark AH, Stjärne P. Relative difference in orbital volume as an indication for surgical reconstruction in isolated orbital floor fractures. *Craniofac Trauma Reconstr* 2011;4(4):203-212.
- Pansell T, Alinasab B, Westermark A, Beckman M, Abdi S. Ophthalmologic findings in patients with non-surgically treated blowout fractures. *Craniofac Trauma Reconstr* 2012;5(1):1-6.
- Nkenke E, Vairaktaris E, Spitzer M, Kramer M, Stamminger M, Holbach L, Knipfer C, Stelzle F. Secondary reconstruction of posttraumatic enophthalmos: prefabricated implants vs titanium mesh. *Arch Facial Plast Surg* 2011;13(4):271-277.

Komentář k přiložené publikaci č. 11

Juraj TIMKOVIC, Jiri STRANSKY, Petr HANDLOS, Jaroslav JANOSEK, Hana TOMASKOVA a **Jan STEMBIREK **(corresponding author)****. Detecting Binocular Diplopia in Orbital Floor Blowout Fractures: Superiority of the Orthoptic Approach. *Medicina-Lithuania* [online]. 2021, **57**(9), 989. ISSN 1010-660X. Dostupné z: doi:[10.3390/medicina57090989](https://doi.org/10.3390/medicina57090989)

IF = 2,948; Kvartil: MEDICINE, GENERAL & INTERNAL Q3

Za základní klinickou vyšetřovací metodu pro detekci okohybné poruchy u pacientů s retromarginální zlomeninou očnice je obecně považována metoda využívající pohybu prstu před obličejem v osmi směrech. V této studii jsme se zabývali otázkou, zda je toto vyšetření pro detekci okohybné poruchy dostatečné. Proto jsme v rámci této naší práce srovnali úspěšnost klinického vyšetření pomocí pohybu prstu s výsledky komplexního ortoptického vyšetření u pacientů s retromarginální zlomeninou očnice.

V souboru bylo zahrnuto 66 pacientů s izolovanou frakturou spodiny očnice (31 operovaných, 35 neoperovaných), u kterých bylo provedeno klinické vyšetření maxilofaciálním chirurgem pomocí pohybu prstu i kompletní ortoptické vyšetření.

Zajímavostí naší studie bylo, že mezi konzervativně léčenými pacienty ze studijního souboru bylo dvanáct konzervativně léčených pacientů, kterým byla při vyšetření prokázána porucha oční motility a měli také diplopii, která může být obecně považována za indikaci k chirurgické léčbě. Na základě komplexního ortoptického vyšetření a výsledků CT vyšetření jsme nicméně u těchto pacientů diplopii považovali pouze za následek otoku měkkých tkání, což se ukázalo jako správná diagnóza a všichni tito pacienti se při konzervativní terapii plně zhojili.

Nejdůležitějším výsledkem této studie bylo, že vyšetření pomocí pohybu prstu prokázalo diplopii pouze u **23 %** pacientů, zatímco plné ortoptické vyšetření se ukázalo mnohem efektivnější a odhalilo poruchu oční motility u **65 %** pacientů. Jako nejúčinnější test se ukázalo vyšetření na Lancasterově plátně, které odhalilo 97,7 % okohybných poruch. Dle ortoptického vyšetření u 4 konzervativně řešených pacientů přetrvávala ortopticky detekovaná porucha oční motility až do konce doby sledování; pouze u jednoho pacienta se

však projevila ve formě diplopie a žádný z těchto pacientů si nestěžoval na problémy v každodenním životě. Kromě toho se u žádného z pacientů indikovaných ke konzervativní terapii nerozvinula okohybná porucha, kterou by prvotní ortoptické vyšetření neodhalilo.




U 30 chirurgicky léčených pacientů z 31 jsme pomocí ortoptiky odhalili okohybnou poruchu. Jediný pacient, který podstoupil chirurgický výkon a neměl známky okohybné poruchy dle ortoptiky, byl operován pro velký rozsah defektu dna očnice (více než polovina plochy dna očnice). U 19 z 31 chirurgicky léčených pacientů klinické vyšetření neodhalilo žádnou diplopii.

Úspěch (absolutní nebo částečný) jsme zaznamenali u 77 % chirurgicky léčených pacientů. Operace neměla žádný efekt u 16 % (5 pacientů), u kterých po operaci přetrvávaly drobné poruchy (binokulární diplopie v jednom z osmi neprimárních směrů pohledu). U dalších dvou pacientů, kteří podstoupili operaci (6 %), přetrvávala binokulární diplopie v primární poloze. Jeden z těchto dvou pacientů podstoupil operaci k řešení strabismu, u obou pak byla nutná další prizmatická brýlová korekce, která přinesla uspokojivé výsledky.

Z našich závěrů vyplývá, že vzhledem k tomu, že přítomnost okohybné poruchy je důležitým indikačním kritériem pro operační řešení retromarginální zlomeniny očnice, mělo by vždy kromě klasického klinického a CT vyšetření provedeno kompletní ortoptické vyšetření s následnou dispenzarizací pro riziko rozvoje možné okohybné poruchy.

Article

Detecting Binocular Diplopia in Orbital Floor Blowout Fractures: Superiority of the Orthoptic Approach

Juraj Timkovic^{1,2} , Jiri Stransky^{2,3}, Petr Handlos⁴, Jaroslav Janosek⁵ , Hana Tomaskova⁶ 
and Jan Stembirek^{2,3,7,*}

- ¹ Clinic of Ophthalmology, University Hospital Ostrava, 17. Listopadu 1790/5, 708 52 Ostrava, Czech Republic; timkovic.j@bluepoint.sk
 - ² Department of Craniofacial Surgery, Faculty of Medicine, University of Ostrava, 703 00 Ostrava, Czech Republic; jiri.stransky@fno.cz
 - ³ Clinic of Oral and Maxillofacial Surgery, University Hospital Ostrava, 708 52 Ostrava, Czech Republic
 - ⁴ Department of Forensic Medicine, University Hospital Ostrava, 708 52 Ostrava, Czech Republic; petr.handlos@fno.cz
 - ⁵ Center for Health Research, Faculty of Medicine, University of Ostrava, 703 00 Ostrava, Czech Republic; janosek@correcta.cz
 - ⁶ Department of Epidemiology and Public Health, Faculty of Medicine, University of Ostrava, 703 00 Ostrava, Czech Republic; hana.tomaskova@osu.cz
 - ⁷ Laboratory of Molecular Morphogenesis, Institute of Animal Physiology and Genetics CAS, 602 00 Brno, Czech Republic
- * Correspondence: jan.stembirek@fno.cz; Tel.: +420-777-136-039



Citation: Timkovic, J.; Stransky, J.; Handlos, P.; Janosek, J.; Tomaskova, H.; Stembirek, J. Detecting Binocular Diplopia in Orbital Floor Blowout Fractures: Superiority of the Orthoptic Approach. *Medicina* **2021**, *57*, 989. <https://doi.org/10.3390/medicina57090989>

Academic Editor: David Madrid-Costa

Received: 11 August 2021

Accepted: 18 September 2021

Published: 19 September 2021

Publisher's Note: MDPI stays neutral with regard to jurisdictional claims in published maps and institutional affiliations.



Copyright: © 2021 by the authors. Licensee MDPI, Basel, Switzerland. This article is an open access article distributed under the terms and conditions of the Creative Commons Attribution (CC BY) license (<https://creativecommons.org/licenses/by/4.0/>).

Abstract: *Background and Objectives:* In patients with orbital floor blowout fracture (OFBF), accurate diagnosis of ocular motility disorder is important for decisions about conservative or surgical therapy. However, the accuracy of the traditional test for detecting binocular diplopia/ocular motility disorder using a moving pencil or finger (hereinafter, “finger test”) has been generally accepted as correct and has not been subject to scrutiny so far. Hence, its accuracy relative to full orthoptic examination is unknown. *Materials and Methods:* In this paper, the results of the “finger test” were compared with those derived from a complex examination by orthoptic tests (considered “true” value in patients with OFBF). *Results:* “Finger test” detected ocular motility disorder in 23% of patients while the full orthoptic examination proved much more efficient, detecting ocular motility disorder in 65% of patients. Lancaster screen test and test with color filters were the most important tests in the battery of the orthoptic tests, capable of identifying 97.7% and 95.3% of patients with ocular motility disorder, respectively. Still, none of the tests were able to correctly detect all patients with ocular motility disorder in itself. *Conclusions:* As the presence of ocular motility disorder/binocular diplopia is an important indication criterion for the surgical solution of the orbital floor blowout fracture, we conclude that a complex orthoptic evaluation should be always performed in these patients.

Keywords: diplopia; orthoptic examination; orbital blowout fractures; orbit; maxillofacial surgery; ocular motility disorder

1. Introduction

Binocular diplopia is one of the most common problems arising as a result of orbital floor blowout fractures (OFBF) and, at the same time, an important criterion in deciding whether to treat the patient conservatively or surgically [1,2]. It is, however, necessary to note that binocular diplopia is just one manifestation of the ocular motility disorder (OMD) that can arise as a result of herniation of soft orbital tissues in the defect and that such herniation is, in principle, the cause for referring patients for surgical solution [3–5].

Still, in clinical practice, binocular diplopia (not OMD in itself) is considered an important indication criterion for the surgical solution [4]. The most widely used method of diagnosing binocular diplopia is a simple test where the surgeon moves an object (often

a pencil or a finger; hence, hereinafter, we will call this method a “finger test”) in front of the patient’s eyes. A full orthoptic examination represents an alternative to this method that is capable, thanks to its complexity, of detecting a wider range of OMDs and of its objective quantification [2,3,6–8]; it is, however, not widely used [4]. Surprisingly, even after an extensive search, we have found no valid head-to-head evaluation of these two methods in the literature and for this reason, we have decided to perform this study on the differences in the performance of these two methods in diagnosing binocular diplopia resulting from OFBF.

2. Materials and Methods

The study was performed in accordance with the Declaration of Helsinki and approved by the local Ethics Committee. All patients signed informed consent to participate in the study.

Sixty-six patients with orbital floor blowout fracture aged 15–80 with a computed tomography- (CT-) proven OFBF were included in the study. Exclusion criteria were: known pre-existing ocular motility disorder, diplopia, or spatial vision disorder. The binocular diplopia was determined in these patients after a complex clinical examination and exclusion of other trauma to the facial skeleton using two methods: (i) the most widely used examination of ocular motility, i.e., a simple clinical test when the patient followed the surgeon’s finger moving in eight gaze directions (up, down, left, right, and four diagonal directions) and convergence. Hereinafter, we will refer to this examination as a “finger test”, which is typically performed by a maxillofacial surgeon and diplopia is reported by the patient; and (ii) by a complex ophthalmological (evaluation of refraction, near and far vision, intraocular pressure, biomicroscopic examination of the anterior and posterior segments of both eyes) and orthoptic examination (consisting of the “finger test” itself combined with examination of fixation, accommodation and convergence, of binocular spatial functions using color filters, Worth four lights and Bagolini striated glasses tests, the degree of strabismus in prism cover test and by synoptophore, and Lancaster screen test) performed by an ophthalmologist. Both examinations were performed on the same day and never later than two weeks after the injury (sooner if the swelling of soft tissues subsided before that). The combined result of the complex evaluation was used as a reference value (i.e., our “gold standard” for diplopia) for subsequent test performance evaluations.

The difference between the results of both tests was evaluated using the chi-square test in the contingency table. Performances of the individual tests relative to the “true” value (i.e., presence of the ocular motility disorder measured as a complex combination of all orthoptic examinations based on the standard methodology of orthoptics) were calculated in Stata v.14 (StataCorp LLC, College Station, TX, USA). The raw data is available from <https://doi.org/10.6084/m9.figshare.14538111.v1> (accessed on 10 September 2021).

3. Results

The mean age in our patient group was 43 years (SD = 19; median age 42 years, min-max 15–81 years). Out of the 66 patients participating in our study, 45 were male and 21 were female. 31 patients were treated surgically, 35 conservatively. 43 patients (65.2%) with isolated orbital floor blowout fracture had an ocular motility disorder and out of these, 41 suffered from binocular diplopia detected by a complex orthoptic examination.

Thirteen patients in our group were treated conservatively despite having ocular motility disorder. Out of these, 6 (46.1%) had detectable strabismus that were neither on synoptophore nor on the cover test. In 10 of these patients (76.9%), Lancaster screen proved the limitation of ocular motility on the affected side, which was most likely caused by a swelling of the orbital soft tissues that regressed spontaneously over time. Twelve conservatively treated patients with ocular motility disorder had also diplopia but were not surgically treated because, based on the complex orthoptic examination and CT results, the diplopia was, at the time, judged to be a result of soft tissue swelling. In 4 such patients (30.8%), ocular motility disorder detected by orthoptics persisted until the end of the

follow-up period; only one patient, however, suffered from diplopia as well and none of these patients complained of problems in everyday life. The one patient with persisting diplopia had binocular diplopia and ocular motility disorder already during the original examination and, due to a suspected herniation of the inferior rectus muscle, was originally referred for surgery. However, as he suffered from severe renal insufficiency, the surgery in general anaesthesia was abandoned. After a partial recovery of the renal functions (2 months later), he was no longer eligible for surgery due to the long period from the injury and a fully developed orbital scarring. The last conservatively treated patient who had an ocular motility disorder but no binocular diplopia did not develop diplopia by the end of the follow-up period. None of the patients in whom orthoptic examination revealed no ocular motility disorder and who were treated conservatively (22 patients) developed any ocular motility disorder by the end of the follow-up period.

All but one of the 31 patients who underwent surgery had an ocular motility disorder diagnosed by the complex orthoptic examination. The single patient who underwent reconstruction of the orbital floor, despite having no signs of an ocular motility disorder, was operated due to the large size of the orbital floor defect (more than half of the orbital floor area). In 19 of the surgically treated patients, the “finger test” revealed no diplopia.

We recorded success (absolute or partial) in 77% of surgically treated patients. Surgery had no effect in 16% (5 patients) in whom minor disorders persisted after surgery (binocular diplopia in one of the eight non-primary gaze directions). In two more patients who underwent surgery (6%), binocular diplopia persisted in the primary position. One of these two patients underwent surgery to address strabism. Nevertheless, additional prism correction in eyeglasses was necessary in both these patients and yielded satisfactory results.

In all, the standard “finger test” revealed only 15 out of 41 patients with binocular diplopia and 15 out of 43 patients with ocular motility disorder. Therefore, while the “finger test” revealed binocular diplopia only in 23% out of 66 patients with OFBF, the complex orthoptic examination detected ocular motility disorder in 65% of such patients ($p < 0.01$). If considering the full orthoptic examination as a reference method, we detected 15 true positives, 2 false positives, 21 true negatives, and 28 false negatives. In other words, the sensitivity of the “finger test” was 34.8% (95% confidence interval 21.5–51.0%), specificity was 91.3% (70.5–98.5%), negative predictive value was only 42.9% (29.1–57.7%), and positive predictive value was 88.2% (62.3–97.9%).

The performance of selected individual tests from the battery of orthoptic tests, i.e., their capability to detect the binocular diplopia revealed by the entire battery, is detailed in Table 1.

Table 1. The performance of individual tests from the battery of orthoptic examinations in detecting ocular motility disorders resulting from OFBF (complex combined evaluation used as a reference value, results are presented as estimates with 95% confidence intervals in brackets).

Disorder—Method of Measurement	Sensitivity	Specificity	PPV	NPV
Binocular disparity—color filter test	95.3 (84.2–99.4)	100 (85.2–100)	100 (91.4–100)	92.0 (74.0–99.0)
Strabismus—synoptophore	39.5 (25.0–55.6)	87.0 (66.4–97.2)	85.0 (62.1–96.8)	43.5 (28.9–58.9)
Strabismus—prism cover test	46.5 (31.2–62.3)	91.3 (72.0–98.9)	90.9 (70.8–98.9)	47.7 (32.5–63.3)
Bulbus deviation—Lancaster screen	76.7 (61.4–88.2)	91.3 (72.0–98.9)	94.3 (80.8–99.3)	67.7 (48.6–83.3)
Motility insufficiency—Lancaster screen	93.0 (80.9–98.5)	91.3 (72–98.9)	95.2 (83.8–99.4)	87.5 (67.6–97.3)
Lancaster screen combined	97.7 (87.7–99.9)	91.3 (72.0–98.9)	95.5 (84.5–99.4)	95.5 (77.2–99.9)

PPV—positive predictive value; NPV—negative predictive value; Lancaster screen combined—if any abnormality was detected in any of Lancaster parameters, this parameter was considered abnormal.

4. Discussion

Ocular motility disorders resulting from orbital floor blowout fracture are well manageable if a complex diagnostic approach is used. The overall treatment success in our group was high. Out of 34 patients originally referred for conservative treatment, only a minor ocular motility disorder unaffacting the patients in their normal life persisted in 3 patients at the end of the follow-up period. One patient treated conservatively was origi-

nally referred for surgery, which could not be performed due to his overall condition; in his case, binocular diplopia persisted. 77% of surgically treated patients healed completely and the remaining patients in whom some problems persisted suffered from injuries so serious that it is highly unlikely that conservative treatment would yield better results than the surgical approach.

The difference between the detection success of the most commonly used method, the “finger test” and full orthoptic examination, is astounding. The “finger test” actually failed to capture 65.1% of patients suffering from ocular motility disorder as a result of the OFBF. Surprisingly, this crucial information has been completely missing in the literature so far.

Of course, one can object that we could not have even expected the good fit of these as binocular diplopia is just a subgroup of ocular motility disorders; however, we must still bear in mind that in this paper, we discuss patients with OFBF in whom ocular motility disorder is likely caused by herniation. Besides, comparing the results of the “finger test” with those of the color filters test (targeting binocular disparity, i.e., the closest test to detecting solely binocular diplopia of the entire orthoptic battery), the difference is still big. The likely reason is that in the early post-injury period, binocular diplopia can be, in the case of the “finger test”, to a major degree masked by the swelling of orbital soft tissues with drooping upper eyelid, which eliminates the picture projected by the respective injured (squinting) eye, and the patient may not realize the binocular diplopia at all in such conditions. The same applies even when performing a full orthoptic examination, especially when binocular diplopia with vertical disparity in the extreme eye positions is concerned (in particular when looking upwards). However, the full orthoptic examination, unlike the “finger test”, facilitates the exact quantification of the ocular motility disorder and of its dynamics over time. Besides, it also allows detection of a pre-existing ocular motility disorder in patients with strabismus and can distinguish between incomitant and concomitant ocular motility disorder.

Lancaster red–green test appears to be the single most important test of the battery of orthoptic tests, as the combined result of both provided outcomes objectively detected diplopia in 97.7% of cases. The only patient in whom this test failed to detect the ocular motility disorder was a patient with the disorder only apparent in the extreme position (i.e., outside the size of the Lancaster screen). Theoretically, a patient’s non-compliance (shift in the head position) can also confound the result. Patients with “false positive” results in the Lancaster screen test suffered from pre-existing strabismus. The second most important test was the test with color filters for binocular diplopia detection, which missed only two patients with ocular motility disorder and yielded no false positives. Still, none of the individual tests were able to accurately detect all patients with an ocular motility disorder resulting from OFBF, which emphasizes the need for performing the full orthoptic examination. Moreover, it is necessary to note that, for example, performing only Lancaster screen and color filters tests could (i) miss the same patients and (ii) provide false positive results (i.e., had we considered Lancaster screen as a proof of herniation and ocular motility disorder associated with orbital floor blowout fracture, we would come to false conclusions).

The revelation that the “finger test” performs so poorly in comparison to orthoptics has great potential implications for practice. As the presence of binocular diplopia indicates that some parts of the ocular motility apparatus are trapped in the fracture and need to be released, binocular diplopia remains one of the widely recognized indication criteria for surgical resolution of OFBF. Our results suggest that more than half of the patients with binocular diplopia after this injury fail to be detected during a conventional examination. Although binocular diplopia (representing an ocular motility disorder) is not the only indication for surgical therapy, failure to detect it because of using an unsuitable method of examination can lead to erroneous decision to treat the patient conservatively. For this reason, we believe that, where available, a full orthoptic examination should always be performed in patients with OFBF, rather than a simple finger test. The primary aim of treatment is to prevent or eliminate the binocular diplopia limiting the patient’s life and

orthoptics facilitates the evaluation of the dynamics, as well as of the rehabilitation success of the ocular motility disorder in both conservative (spatial vision exercises, compensation of strabismus using prismatic glasses) and surgical solutions. This recommendation of the use of orthoptics in patients with OFBF is also in accordance with the proposal by Laurentjoye et al. [5].

The limitation of our study is that it is a single center study. Additionally, we should consider that its results are valid only in the indication of orbital floor blowout fracture and cannot be generalized to any possible ocular motility disorder (although it is likely that similar results would be found there as well). Our results, therefore, need to be confirmed by larger, prospective, multicenter studies; nevertheless, the success rate of our treatment indicates that our method of referring the patients to surgical or conservative treatment based on orthoptics is correct and, therefore, supports the notion that orthoptics is superior to the standard “finger test” in determining ocular motility disorder in patients with OFBF.

5. Conclusions

We consider the fact that compared to the full orthoptic examination, the “finger test” usually performed for diagnosing ocular motility disorders failed to reveal 65% of cases, to be of the utmost importance and to be a strong reason for advocating full orthoptic examination in these patients.

Author Contributions: J.T., J.S. (Jan Stembirek)—study conception, data acquisition, data interpretation, critical review of the manuscript, final approval of the manuscript, J.S. (Jiri Stransky)—study management, funding acquisition, critical review of the manuscript, final approval of the manuscript; P.H.—methodology, data acquisition, critical review of the manuscript, final approval of the manuscript; J.J.—data analysis and interpretation, initial draft of the manuscript, final approval of the manuscript; H.T.—data analysis, critical review of the manuscript, final approval of the manuscript. All authors have read and agreed to the published version of the manuscript.

Funding: This work was supported by the internal Grant by the University Hospital Ostrava “Diagnosis, treatment and subsequent care for patients with the orbital floor blowout fracture”, Grant No.-MZCR-RVO-FNOs/2017.

Institutional Review Board Statement: The study was conducted according to the guidelines of the Declaration of Helsinki, and approved by the Ethics Committee of the University Hospital Ostrava (Approval No 397/2017 from 27 April 2017).

Informed Consent Statement: Written informed consent has been obtained from the patient(s) to publish this paper (all patients in our hospital whose data are available for retrospective analysis have signed a consent with anonymous data use for retrospective studies).

Data Availability Statement: The raw data is available from <https://doi.org/10.6084/m9.figshare.14538111.v1> (accessed on 10 September 2021).

Conflicts of Interest: All Authors declare that they have no conflict of interest.

References

1. Gosse, E.M.; Ferguson, A.W.; Lymburn, E.G.; Gilmour, C.; MacEwen, C.J. Blow-out Fractures: Patterns of Ocular Motility and Effect of Surgical Repair. *Br. J. Oral Maxillofac. Surg.* **2010**, *48*, 40–43. [[CrossRef](#)] [[PubMed](#)]
2. Marano, R.; Lino, P.R.S.; Zanetti, F.; Tincani, A.J.; Oliveira, L. Is Specialized Ophthalmologic Evaluation Necessary after Orbital Fractures? A Prospective 64-Case Study. *Oral Maxillofac. Surg.* **2019**, *23*, 325–329. [[CrossRef](#)] [[PubMed](#)]
3. Boyette, J.R.; Pemberton, J.D.; Bonilla-Velez, J. Management of Orbital Fractures: Challenges and Solutions. *Clin. Ophthalmol.* **2015**, *9*, 2127–2137. [[CrossRef](#)] [[PubMed](#)]
4. Shin, J.W.; Lim, J.S.; Yoo, G.; Byeon, J.H. An analysis of pure blowout fractures and associated ocular symptoms. *J. Craniofac. Surg.* **2013**, *24*, 703–707. [[CrossRef](#)] [[PubMed](#)]
5. Laurentjoye, M.; Bondaz, M.; Majoufre-Lefebvre, C.; Huslin, V.; Caix, P.; Ricard, A.S. When Should an Orthoptic Evaluation Be Prescribed in the Management of Orbital Floor Fracture? A Prospective Study of 47 Fractures. *Rev. Stomatol. Chir. Maxillofac. Chir. Orale* **2014**, *115*, 274–278. [[PubMed](#)]
6. Liu, S.R.; Song, X.F.; Li, Z.K.; Shen, Q.; Fan, X.Q. Postoperative Improvement of Diplopia and Extraocular Muscle Movement in Patients With Reconstructive Surgeries for Orbital Floor Fractures. *J. Craniofac. Surg.* **2016**, *27*, 2043–2049. [[CrossRef](#)] [[PubMed](#)]

7. O'Connell, J.E.; Hartnett, C.; Hickey-Dwyer, M.; Kearns, G.J. Reconstruction of orbital floor blow-out fractures with autogenous iliac crest bone: A retrospective study including maxillofacial and ophthalmology perspectives. *J. Craniomaxillofac. Surg.* **2015**, *43*, 192–198. [[CrossRef](#)] [[PubMed](#)]
8. Kozakiewicz, M.; Elgalal, M.; Piotr, L.; Broniarczyk-Loba, A.; Stefanczyk, L. Treatment with individual orbital wall implants in humans—1-Year ophthalmologic evaluation. *J. Craniomaxillofac. Surg.* **2011**, *39*, 30–36. [[CrossRef](#)] [[PubMed](#)]

Komentář k přiložené publikaci č. 12

Jiří STRÁNSKÝ, Jan ŠTEMBÍREK a Juraj TIMKOVIČ. Fraktury orbity. In: *Dětská oftalmologie: klinické a mezioborové souvislosti*. Praha: Grada, 2022, s. 425-428. ISBN 978-80-271-3052-8.

Kapitola v knize, která shrnuje naše klinické zkušenosti a ukazuje multioborový pohled na zlomeniny očnice v dětském věku, které mohou být rozdílné oproti dospělým. Jednou z odlišností je i tvar zlomeniny. U dětí převládá výskyt „blow-out“ zlomenin očnice, ale relativně často, že může objevovat i zlomenina typu „padacích dvířek“ (*trapdoor fracture*), kdy dislokovaný fragment kosti se vlastní elasticitou vrací do původní polohy a přitom dochází k uskřínutí měkkých tkání. Tento mechanismus poté vede k poruše oční motility a možné diplopii. Mezi poslední typ, který u dětí nalézáme jsou pak zlomeniny „blow-in“, u kterých dochází k dislokaci fragmentu kosti dovnitř očnice a tím redukuje její obsah, což se klinicky může projevit okohybnou poruchou.

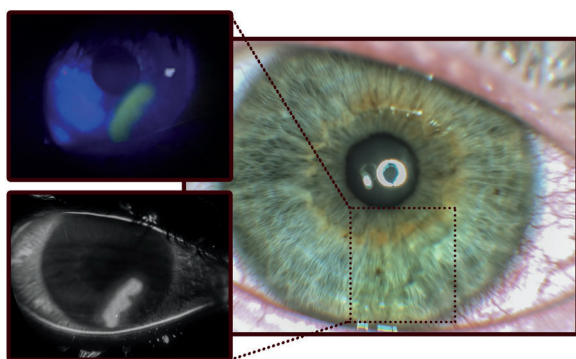
V klinickém obrazu nemusí být nutně u dětí přítomen žádný z typických lokálních příznaků (sufúze spojivky, hematom, porucha motility bulbu), ale jen nauzea, zvracení, někdy i bradykardie v důsledku okulokardiálního reflexu. Někdy dokonce dětské pacienti nepocítují žádné subjektivní ani objektivní potíže. I tak je s výhodou při podezření na úraz očnice vhodné doplnit CT vyšetření.

Před vlastní terapií vždy doplňujeme ortoptické vyšetření, které nám pomáhá přesně určit možnou okohybnou poruchu a rozhodnout se k případné chirurgické terapii, která u dětských pacientů je většinou na druhém místě.

sobením přímé síly na povrch oka. Nejčastěji se jedná o zasažení drobnými stolními předměty, hračkou, prstem, rostlinou, sportovním náčiním a dalšími.

Klinický obraz: Může být v závislosti na lokalizaci léze, její velikosti a prahu bolesti postiženého dítěte značně variabilní a rozmanitý. Nejčastěji se setkáváme s pocitem cizího tělesa v oku nebo bolesti postiženého oka, která bývá většinou mírného charakteru. Nežádka, zejména u menších dětí, může být přítomná světloplachost (fotofobie) až křečovitě sevření víček (blefarospasmus). Spojivka na postiženém oku bývá prokrvená a lehce oteklá. Zraková ostrost bývá normální nebo lehce snížená.

Diagnóza: Opírá se o výše zmíněné příznaky postižení, a zejména u dětí v preverbálním věku o pečlivě odebranou anamnézu úrazového děje od doprovodu dítěte. Základem pro stanovení správné diagnózy je biomikroskopické vyšetření předního segmentu oka ruční či stolní štěrbinovou lampou, které obvykle prokáže přítomnost různé velikého povrchového defektu epitelu rohovky či hlubšího lamelárního defektu (obr. 20.5). Velmi nápomocné, zejména u dětí méně spolupracujících, je vkápnutí fluoresceinu do spojivkového vaku, kdy v typickém případě dochází k obarvení defektu, které je dobře patrné při použití modrého kobaltového světla štěrbinové lampy či přímého oftalmoskopu. Neměli bychom opomíjet rovněž kontrolu obou fornixů (včetně everze horního víčka), kdy pátráme po přítomnosti cizího tělíska na tarzální spojivce, které bývá často zdrojem zmíněných potíží.



Obr. 20.5 Eroze rohovky

Léčba:

- Lokální aplikace antibiotické masti a mydriatik s cílem zabránění vývoje sekundární infekce.
- K zmírnění bolestivých projevů mohou přispět topicky aplikovaná nesteroidní antiflogistika a oční lubrikancia ve formě gelu či masti.

- U těžších případů může pomoci ke zmírnění bolestivých projevů rovněž aplikace terapeutické kontaktní čočky, která je však spojena s prodloužením doby hojení a rizikem možného vývoje syndromu recidivující eroze.

Prognóza: U povrchových defektů epitelu rohovky je prognóza zpravidla dobrá, plné zhojení lze v závislosti na velikosti léze očekávat do několika dnů od zahájení léčby. Hlubší, lamelární defekty se obvykle hojí rohovkovou jizvou, která může být podle lokalizace léze zcela asymptomatická, ale v případě centrální lokalizace může vést k poklesu zrakové ostrosti různého stupně. **U malých dětí může být i jemná jizva v této lokalizaci spouštěcím mechanismem tupozrakosti!**

U zhruba 7–8 % pacientů s traumatickou erozí může dojít k zhojení defektu méněcenným epitelem, který je pak zdrojem protrahovaných potíží ve smyslu **vývoje syndromu recidivující eroze**. Příčinou tohoto stavu je neobvykle slabá vazba mezi bazálními buňkami epitelu rohovky a jejich bazální membránou. Léčba těchto stavů je svízelná. Jednak může zahrnovat dlouhodobou aplikaci očních lubrikantů ve formě gelů nebo mastí, u části pacientů pak aplikaci hyperosmotických látek (5% chlorid sodný ve formě kapek nebo masti) po dobu několika týdnů. Další možností je dlouhodobé nošení terapeutické kontaktní čočky. V poslední řadě pak může dojít k léčbě chirurgické, zahrnující fototerapeutickou keratektomií excimerovým laserem.

20.3 Orbitální traumata

20.3.1 Fraktury orbity

Jiří Stránský, Jan Štembírek, Juraj Timkovič

Zlomeniny očnice patří mezi běžná obličejová poranění. V zásadě je lze rozdělit do dvou typů: **zlomeniny s porušením okraje orbity, resp. orbitálního vchodu**, které bývají součástí kombinovaných obličejových fraktur (zlomeniny typu Le Fort II a III, zlomeniny zygomaticomaxilárního či nazomaxilárního komplexu, frontobazální zlomeniny) a **zlomeniny retromarginální, tedy izolované zlomeniny očnice**.

Úrazy prvního typu se dostatečně zabývá literatura maxilofaciální chirurgie, otorinolaryngologie a neurochirurgie, v tomto textu se budeme věnovat pouze skupině druhé čili izolovaným retromarginálním zlomeninám očnice.

Dětský věk z pohledu maxilofaciální traumatologie

Maxilofaciální poranění jsou u dětí daleko méně častá než u adolescentů a dospělých, ale i u dětských pacientů převažují chlapci nad dívkami. Přibližně do věku 5 let žije většina dětí v prostředí, které je relativně chrání proti vážným úrazům, bývají víceméně pod stálým dozorem dospělých. V tomto věku jsou časté pády z malé výše, s nízkou traumatizující silou, která je obvykle absorbována elastickým skeletem. Věk 5–7 let je charakterizován rychlou progresí neuromotorického vývoje, jsou častější interakce s jinými dětmi, objevuje se široká škála aktivit mimo domov, postupně jsou omezeny možnosti neustálého dohledu. Dítě se stále více pohybuje ve venkovním prostředí, dostává se do kontaktu s dopravním provozem. Tyto faktory vedou ke zvýšenému riziku obličejového poranění.

V maxilofaciální traumatologii dětského věku hraje zásadní roli vývoj lebečního skeletu. Počáteční roky života jsou charakterizovány nedostatečným vývojem paranazálních dutin, obličejová část je relativně nízká a široká s prominencí čela, traumatologicky exponována je zejména frontální a horní orbitální oblast. Kolem 4. roku života začíná rozvoj sinů a pokračuje až do adolescence. Pneumatizované paranazální dutiny působí jako oslabená místa mezi pilíři obličejového skeletu, což umožňuje vznik zlomenin. Na druhou stranu vysoce osteogenní dětský periost vede k rychlému hojení fraktury se značnou schopností remodelace.

Děti obecně mají pružnější kosti a flexibilní linie švů. Z těchto důvodů jsou pediatrické zlomeniny mnohem častěji nekompletní, s minimální dislokací, a proto také daleko méně často vyžadují chirurgickou intervenci.

Nejčastější příčinou dětských obličejových fraktur jsou dopravní nehody, jejich incidence stoupá s věkem stejně jako počet úrazů vyžadujících chirurgické ošetření.

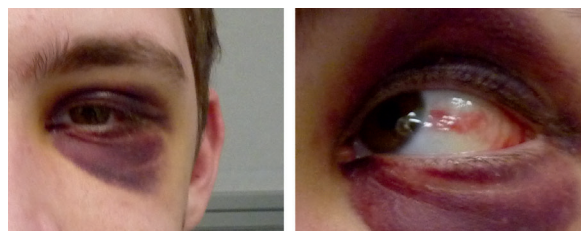
Izolovaná zlomenina očnice u dětí

U izolované retromarginální zlomeniny očnice je nutná přítomnost pneumatizovaného sinu, což bývá okolo 7. roku života, u mladších jsou tyto zlomeniny vzácné a spíše se setkáváme s postižením stropu očnice. Tato fraktura vzniká na principu přenosu tlaku mezi měkkými tkáněmi a kostěnou schránkou. Protože měkké tkáně vykazují větší pružnost než kostěné struktury, dochází k přenosu síly, sumaci a prolomení stěny očnice. Po vyrovnání tlaku v orbitě se měkké tkáně vrací na základě elasticity do původní polohy. Mohou však zůstat herniovány do kostního defektu. Takovouto zlomeninu označujeme jako **hydraulickou nebo „blow-out“**, obvykle postihuje spodinu, ale poranění mohou

být i ostatní části očnice. Pro dětský věk je příznačná zlomenina **typu padacích dvířek (trapdoor fracture)**, kdy fragment kosti, dislokovaný do sinu (nejčastěji maxilárního), se vlastní elasticitou vrací do původní polohy a přitom dochází k uskrínutí měkkých tkání, což vede k poruše motility bulbu a diplopii. Podle některých zdrojů téměř polovina dětských orbitálních zlomenin vykazuje tento mechanismus.

Jiným typem poranění kostěné očnice jsou pak zlomeniny **„blow-in“**, rovněž častější u dětí. Podstatou je fragment kosti dislokovaný dovnitř očnice, a redukuje tak její obsah. Může také dojít k poranění okohybných svalů, očního bulbu či optického nervu. Izolovaná „blow-in“ zlomenina očnice je poměrně vzácná.

Klinický obraz: U izolovaných pediatrických zlomenin očnice bývá chudý. Bolestivost nemusí být výrazná, můžeme vidět různě veliký hematom v okolí očnice a sufuzi spojivky (obr. 20.6). U fraktur spodiny očnice se setkáváme s poruchou senzitivity v inervační oblasti druhé větve trojklaného nervu (důvodem je jeho anatomický průběh infraorbitálním kanálem). Při retromarginální zlomenině očnice často dochází k provalení měkkých tkání orbity do defektu a jejich herniaci, případně až inkarceraci do sinu, nejčastěji maxilárního, což může mít za následek poruchu postavení a motility bulbu, enoftalmus (z důvodu prolapsu tukové tkáně na spodině), nebo i exoftalmus (pro výrazný otok uvnitř orbity, který bulbus tlačí ven z očnice) a/nebo diplopii. Tyto příznaky mohou být přítomny i bez uskrínutí měkkých tkání.



Obr. 20.6 Klinický obraz zlomeniny očnice

U dětí nemusí být přítomen žádný ze zmíněných příznaků, ale jen nauzea, zvracení, někdy i bradykardie v důsledku okulokardiálního reflexu. Dětské zlomeniny typu padacích dvířek mohou být velmi malého rozsahu, s minimální inkarcerací měkkých tkání, mnohdy sotva patrné na CT. Zjištění poruchy oční motility a nevolnost/zvracení by měly upozornit na možnost takového úrazu a potřebu včasné chirurgické intervence.

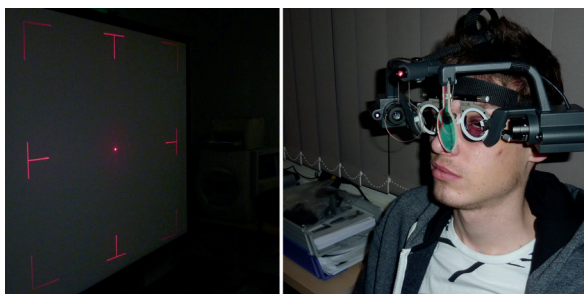
Výjimkou ovšem nejsou ani případy, kdy pacient nepocituje žádné obtíže a ani objektivní klinické zhodnocení stavu nenaznačuje poruchu. Pokud ne-

jsou tyto případy diagnostikovány pomocí zobrazovacích metod, mohou se komplikace projevit až několik měsíců po traumatu, kdy jsou hůře řešitelné. Proto **při podezření na trauma očnice je vhodné vždy provést CT vyšetření.**

Diagnóza: Vyšetřovací postup je stejný jako u všech pacientů s úrazem v obličeji, pouze u nezletilých je nutná přítomnost zákonného zástupce během vyšetření. Po pečlivě odebrané anamnéze stran úrazu a celkového stavu pacienta je nutno vyloučit mozkové poranění. Po celkovém klinickém vyšetření a vyloučení ostatních možných traumat se zaměřujeme na vyšetření očí a očnice. Postupně kontrolujeme stav zrakových funkcí, rozsah poranění oka a periokulární krajiny. Palpací vyšetřujeme okraje očnice a citlivost v obličeji (pro vyloučení zranění nervus infraorbitalis).

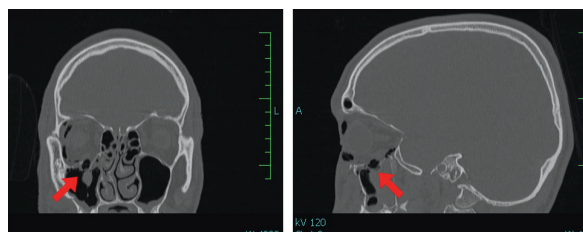
Zlatý standard v hodnocení těchto stavů představuje i nadále **ortoptické vyšetření**, které dokáže spolehlivě, a zejména objektivně zhodnotit charakter a rozsah případné okoohybné poruchy. Navíc umožňuje jednotlivé parametry, a tím i dynamiku celého procesu hojení sledovat v čase. Kromě základního oftalmologického vyšetření by měla tedy diagnostika zahrnovat rovněž zhodnocení postavení očí, motility v osmi pohledových směrech, fixace, akomodace a konvergence, vyšetření binokulárních funkcí v prostoru pomocí různých testů (barevné filtry, Worthova světla, Bagoliniho skla), velikosti úchylky šilhání v prizmatických dioptriích a na troposkopu. Polohu očí v předozadní ose očnice hodnotíme pomocí Hertelova exoftalmometru. Objektivizaci okoohybné poruchy tradičně provádíme na Lancasterově či Hessově plátně (viz kap. 6), event. využitím některého z nových moderních sofistikovaných systémů pracujících na podobném principu disociace obrazů obou očí (GazeLab apod.) (obr. 20.7). Výsledky ortoptického vyšetření nám významnou měrou napomáhají v procesu rozhodování, zda pacient bude léčen konzervativně, nebo chirurgicky.

Pro diagnostiku orbitálních fraktur jsou naprosto nezbytné zobrazovací metody, jelikož klinické vyšet-



Obr. 20.7 Vyšetření postavení a hybnosti očí při fraktuře očnice

ření nedokáže do detailu zhodnotit jejich přítomnost a závažnost. K ozřejmění a potvrzení diagnózy je obvykle zapotřebí **CT vyšetření hlavy v koronárním a sagitálním řezu**, jež hodnotícímu lékaři umožní posoudit rozsah kostěného defektu ve spodině očnice (obr. 20.8). Typickým nálezem u retromarginálních fraktur je různě velký kostěný fragment prolomený do maxilárního sinu, často doprovázený výše zmíněnou herniací měkkých tkání do defektu orbity. Geometricky defekt většinou připomíná nepravidelnou elipsu s různými velikostmi průměrů a různou velikostí herniace měkkých tkání orbity, zasazenou do trojúhelníkovitě tvarované spodiny očnice.



Obr. 20.8 CT vyšetření zlomené očnice

Léčba: Terapie zlomenin očnice v zásadě zahrnuje **konzervativní a chirurgické postupy**. Při rozhodování o způsobu léčby těchto úrazů u dětských pacientů je nutno vzít v potaz jak **riziko poruchy růstu**, způsobené chirurgickým výkonem, tak hledisko prevence **malpozice očního bulbu a problémů s jeho motilitou**. Přístup k ošetření pediatrických orbitálních fraktur je odlišný od pacientů dospělých; není-li přítomna inkarcerace, akutní enoftalmus či pokles bulbu, volíme konzervativnější postup.

Konzervativní léčba

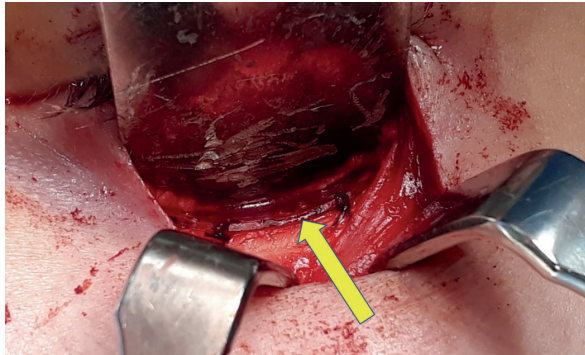
Dětské fraktury orbitálních stěn s propagací fragmentu do okolních sinů bývají povahy vrbového proutku. Většinou dojde v průběhu několika dnů observace ke spontánní úpravě a návratu úlomku do původní polohy; vhodná je aplikace antiedematózní léčby, celková antibiotická terapie v rámci prevence sekundární infekce a režimová opatření (nesmrkat) zabraňující průniku vzduchu a infekce z paranazálních dutin do měkkých tkání očnice. Nutná je ovšem pečlivá observace, nejlépe v rámci mezioborové spolupráce maxilofaciálního chirurga, ORL lékaře a oftalmologa se zkušenostmi s diagnostikou a léčbou okoohybných poruch.

Chirurgická léčba

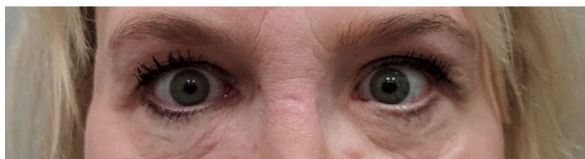
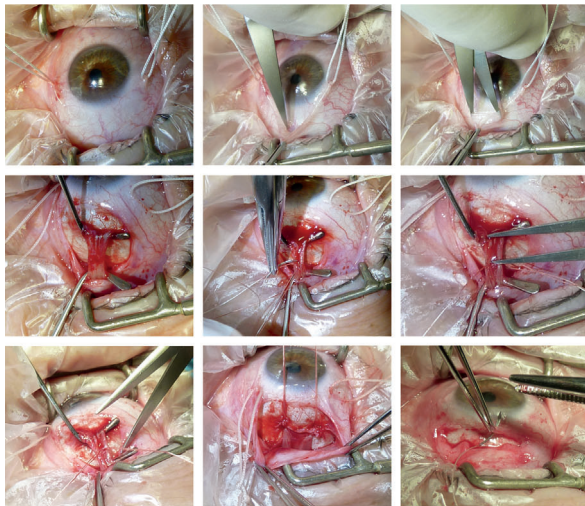
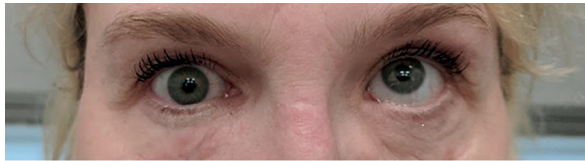
Výhodou chirurgické terapie je prevence vzniku okoohybné poruchy (není-li již přítomná) s diplopií, nevý-

hodou pak samotný chirurgický výkon se všemi potenciálními konsekvencemi včetně rizika traumatizace infraorbitálního nervu.

Indikační kritéria chirurgické intervence nejsou jednoznačně dána a obvykle se odvíjejí od zkušenosti zúčastněných specialistů. Uvádí se diplopie v důsledku uskřínutí okoohybného svalu, enoftalmus větší než 2 mm po vymizení otoku měkkých tkání a defekt spodiny očníce větší než 1 cm².



Obr. 20.9 Chirurgická léčba fraktury spodiny očníce



Obr. 20.10 Okoohybná porucha po obličejovém poranění s frakturou spodiny očníce

Hlavním indikačním kritériem pro chirurgickou intervenci by však měla být **okoohybná porucha restriktivního charakteru**, kterou je nutno odlišit od omezení motility bulbu způsobené otokem měkkých tkání očníce. Indikace k chirurgické intervenci by měla být navíc přísně individuální, zohledňující lokalizaci a velikost defektu. I malé defekty lokalizované axiálně mohou snadněji vést k restrikci okoohybného svalu než častokrát i větší léze lokalizované excentricky na okrajích spodiny očníce.

Podstatou ošetření je revize zlomeniny, uvolnění inkarcerovaných tkání a případně rekonstrukce kostního defektu. Chirurgickou intervenci provádíme u pediatrického pacienta obvykle v průběhu 7–10 dnů, k rekonstrukci u dětí používáme resorbovatelný materiál nebo autologní štěp (obr. 20.9).

Není-li indikace k chirurgickému ošetření jednoznačná, je nutné pečlivě sledování, protože hojení dětského pacienta je velmi rychlé a hrozí trvalá cikatrizace.

Prognóza: U retromarginálních zlomenin očníce u dětí je variabilní v závislosti na rozsahu přidruženého obličejového či multiorgánového postižení. Plné zhojení u chirurgicky řešených nekomplikovaných izolovaných jednostranných retromarginálních zlomenin očníce lze očekávat v horizontu osmi až dvanácti týdnů od provedené intervence.

Rehabilitace hybnosti očního bulbu či případná korekce okoohybné poruchy jsou prováděny pod vedením očního lékaře se zkušenostmi v oblasti diagnostiky a léčby okoohybných poruch. Zahrnují jak postupy konzervativní (předpis optimální prismatické korekce), tak i postupy chirurgické (operace restriktivního šilhání) (obr. 20.10).

U dětských pacientů je potřebná pravidelná dispenzarizace do dokončení růstu pro riziko vývoje pozdních komplikací (např. okoohybná porucha s diplopií na podkladě jizevnatých změn v očníce) a dále jsou vhodné kontroly senzitivity v oblasti výstupu druhé větve trojklaného nervu při jeho traumatizaci.

20.3.2 Uzavřená a otevřená poranění víček

Adam Kopecký, Juraj Timkovič, Lukáš Kolarčík

Víčka představují přirozenou a důležitou ochranu očního bulbu před následky poranění různé etiologie. Statisticky je prokázáno, že poranění víček spojená s otevřeným poraněním očního bulbu jsou častější v populaci dětí do 10 let než v populaci dospělých.

Každé dítě s poraněním víček, zvláště otevřeným, musíme důsledně vyšetřit a jednoznačně u něj vyloučit poranění očního bulbu!

Závěr

Předkládaná práce sumarizuje výsledky, které byly získány jak z bazálního výzkumu, tak z klinické praxe. Vzhledem ke stále se zdokonalujícím laboratorním metodám dokážeme v posledních desetiletích mnohem lépe pronikat do problematiky fungování buněk, regulačních systémů či celých organismů. Ruku v ruce s tím se rozšiřují i možnosti detailnějších diagnostických metod, které již nezahrnují pouze zobrazovací nebo histologické metody, ale do rutinní klinické praxe čím dál více pronikají i metody na molekulární úrovni, jako je sekvenace genů, single-cell RNA sequencing (scRNA-seq) nebo microarray. V rámci mojí specializace tento trend pozoruji zejména v oblasti orofaciální onkologie, kde je současný progres nejpatrnější a i naše pracoviště má v týmu molekulární biologie.

Doufám, že výsledky naší práce poskytnou důležité informace dalším vědeckým skupinám, které danou problematiku posunou opět dále, a právě takovými drobnými krůčky a multioborovou spoluprací dokážeme tyto znalosti převést do klinické praxe a ke konkrétním pacientům.

Z mého pohledu v dnešní době nelze pouze shrnovat klinická data o pacientech, ale je nutné klinický tým rozšířit o výzkumníky z oblasti molekulární genetiky nebo buněčné biologie, kteří dokáží na daný problém nahlédnout jinou optikou a prozkoumat jej až na molekulární úrovni.

Nutná je ovšem i opačná cesta, tzn. interpretace obrovského množství zjištěných dat vědeckými pracovníky a postupné převedení těchto poznatků do klinické praxe. To vyžaduje enormní komplexitu, mezioborovou spolupráci, znalosti a praktické poznatky nejen z klinické medicíny, ale právě i ze spolupracujících vědních oborů. Jedinec může jen těžko obsáhnout celou komplexitu takovéto problematiky, proto pro zodpovězení otázek, které se neustále objevují, je nutný multioborový přístup, který kombinuje bazální výzkum s klinickou praxí. Tohoto přístupu je možné dosáhnout pouze pomocí tvorby úzce spolupracujících týmů sdružujících vědce různých oborů.

Literatura

Abrahamsson H, Eriksson L, Abrahamsson P, Häggman-Henrikson B. Treatment of temporomandibular joint luxation: a systematic literature review. *Clin Oral Investig*. 2020 Jan;24(1):61-70. doi: 10.1007/s00784-019-03126-1. Epub 2019 Nov 15. PMID: 31729577.

AlSubaie MF, Al-Sharydah AM, Nassim HM, Alhawsawi A. Orbital Floor Blowout Fracture Reconstruction Using Moldable Polymethyl Methacrylate: A Report of Two Cases and Their Imaging Findings. *Open Access Emerg Med*. 2022 May 25;14:223-232. doi: 10.2147/OAEM.S359173. PMID: 35656329; PMCID: PMC9153998.

Bazina F, Brouxhon SM, Kyrkanides S. Partial epithelial-mesenchymal transition during enamel development. *Clin Exp Dent Res*. 2022 Apr;8(2):513-518. doi: 10.1002/cre2.543. Epub 2022 Feb 19. PMID: 35182458; PMCID: PMC9033535.

Beger HG, Schwarz A. Clinical research in surgery: questions but few answers. *Langenbecks Arch Surg*. 1998 Oct;383(5):300-5. doi: 10.1007/s004230050137. PMID: 9860220.

Borello,U.,Buffa,V.,Sonnino,C.,Melchionna,R.,Vivarelli,E.,and Cossu,G.(1999).Differential expression of the Wnt putative receptors Frizzled during mouse somitogenesis. *Mech.Dev*. 89,173–177. doi:10.1016/S0925-4773(99)00205-1

Boyette JR, Pemberton JD, Bonilla-Velez J: Management of orbital fractures: challenges and solutions. *ClinOphthalmol*. 2015 Nov 17;9:2127-37.

Campanelli G. Basic research, experimental surgery and clinical research: where there is science, there is better treatment. *Hernia*. 2020 Aug;24(4):681-682. doi: 10.1007/s10029-020-02261-z. PMID: 32681378.

Ferri J, Potier J, Maes JM, Rakotomalala H, Lauwers L, Cotellet M, Nicot R. Temporomandibular joint arthritis: Clinical, orthodontic, orthopaedic and surgical approaches. *Int Orthod*. 2018 Sep;16(3):545-561. doi: 10.1016/j.ortho.2018.06.019. Epub 2018 Jul 13. PMID: 30017770.

Gong S, Emperumal CP, Al-Eryani K, Enciso R. Regeneration of temporomandibular joint using in vitro human stem cells: A review. *J Tissue Eng Regen Med*. 2022 Jul;16(7):591-604. doi: 10.1002/term.3302. Epub 2022 Mar 31. PMID: 35357772; PMCID: PMC9310826.

Gosau M, Schöneich M, Draenert FG, Ettl T, Driemel O, Reichert TE. Retrospective analysis of orbital floor fractures--complications, outcome, and review of literature. *Clin Oral Investig*. 2011 Jun;15(3):305-13

Gosse EM, Ferguson AW, Lymburn EG, Gilmour C, MacEwen CJ. Blow-out fractures: patterns of ocular motility and effect of surgical repair. *Br J Oral Maxillofac Surg*. 2010 Jan;48(1):40-3.

Gulses A, Bayar GR, Aydintug YS, Sencimen M, Erdogan E, Agaoglu R. Histological evaluation of the changes in temporomandibular joint capsule and retrodiscal ligaments following autologous blood injection. *J Craniomaxillofac Surg*. 2013 Jun;41(4):316-20. doi: 10.1016/j.jcms.2012.10.010. Epub 2012 Dec 1. PMID: 23207064.

HAMPL M, CELA P, SZABO-ROGERS HL, KUNOVA BOSAKOVA M, DOSEDELOVA H, KREJCI P, BUCHTOVA M. Role of Primary Cilia in Odontogenesis. *J Dent Res*. 2017 Aug;96(9):965-974. doi: 10.1177/0022034517713688. Epub 2017 Jun 12. PMID: 28605602; PMCID: PMC5524235.

Harris G. Orbital blow-out fractures: surgical timing and technique. *Eye (Lond)*. 2006 Oct;20(10):1207-12.

Harris GJ., Garcia GH., Logani SC., Murphy ML., Sheth BP., Seth AK.: Orbital blow-out fractures: correlation of preoperative computed tomography and postoperative ocular motility. *Trans Am Ophthalmol Soc*. 1998;96:329-47; 347-53.

Higgins M, Obaidi I, McMorrow T. Primary cilia and their role in cancer. *Oncol Lett*. 2019 Mar;17(3):3041-3047. doi: 10.3892/ol.2019.9942. Epub 2019 Jan 17. PMID: 30867732; PMCID: PMC6396132.

Hirjak D, Machoň V. Traumatologie skeletu tváře, WestMedical, 2013 str. 99-100

Chang,H.,Smallwood,P.M.,Williams,J.,and Nathans,J.(2016).The spatio-temporal domains of Frizzled6 action in planar polarity control of hair follicle orientation. *Dev.Biol*. 409,181–193.doi:10.1016/j.ydbio.2015.10.027

Chattopadhyay C, Dev V, Pilia D, Harsh A. Reconstruction of Orbital Floor Fractures with Titanium Micromesh: Our Experience. *J Maxillofac Oral Surg*. 2022 Jun;21(2):369-378. doi: 10.1007/s12663-020-01407-x. Epub 2020 Jul 9. PMID: 35712422; PMCID: PMC9192857.

Kaneko H, Hashimoto S, Enokiya Y, Ogiuchi, Shimono M. Cell proliferation and death of Hertwig's epithelial root sheath in the rat. *Cell Tissue Res* 1999; 298:95–103.

Kang P, Svoboda KK. Epithelial-mesenchymal transformation during craniofacial development. *J Dent Res* 2005; 84(8):678-90.

Kim HY, Li S, Lee DJ, Park JH, Muramatsu T, Harada H, Jung YS, Jung HS. Activation of Wnt signalling reduces the population of cancer stem cells in ameloblastoma. *Cell Prolif*. 2021 Jul;54(7):e13073. doi: 10.1111/cpr.13073. Epub 2021 Jun 6. PMID: 34096124; PMCID: PMC8249789.

Kitisubkanchana J, Reduwan NH, Poomsawat S, Pornprasertsuk-Damrongsri S, Wongchuensoontorn C. Odontogenic keratocyst and ameloblastoma: radiographic

evaluation. *Oral Radiol.* 2021 Jan;37(1):55-65. doi: 10.1007/s11282-020-00425-2. Epub 2020 Feb 6. Erratum in: *Oral Radiol.* 2021 Oct;37(4):715-717. PMID: 32030659.

Kovar D, Voldrich Z, Voska P, Lestak J, Astl J. Indications for repositioning of blow-out fractures of the orbital floor based on new objective criteria - tissue protrusion volumometry. *Biomed Pap Med Fac Univ Palacky Olomouc Czech Repub.* 2017 Dec;161(4):403-406. doi: 10.5507/bp.2017.036. Epub 2017 Aug 31. PMID: 28983121.

Kreppel M, Zöller J. Ameloblastoma-Clinical, radiological, and therapeutic findings. *Oral Dis.* 2018 Mar;24(1-2):63-66. doi: 10.1111/odi.12702. PMID: 29480593.

Krivanek, J., Adameyko, I., Fried, K., 2017. Heterogeneity and Developmental Connections between Cell Types Inhabiting Teeth. *Front. Physiol.* 8. <https://doi.org/10.3389/fphys.2017.00376>

Krivanek, J., Soldatov, R.A., Kastriti, M.E., Chontorotzea, T., Herdina, A.N., Petersen, J., Szarowska, B., Landova, M., Matejova, V.K., Holla, L.I., Kuchler, U., Zdrilic, I.V., Vijaykumar, A., Balic, A., Marangoni, P., Klein, O.D., Neves, V.C.M., Yianni, V., Sharpe, P.T., Harkany, T., Metscher, B.D., Bajénoff, M., Mina, M., Fried, K., Kharchenko, P.V., Adameyko, I., 2020. Dental cell type atlas reveals stem and differentiated cell types in mouse and human teeth. *Nat. Commun.* 11, 4816. <https://doi.org/10.1038/s41467-020-18512-7>

Lee SH, Bédard O, Buchtová M, Fu K, Richman JM. A new origin for the maxillary jaw. *Dev Biol.* 2004; 276(1):207-24.

Li S, Zhang H, Sun Y. Primary cilia in hard tissue development and diseases. *Front Med.* 2021 Oct;15(5):657-678. doi: 10.1007/s11684-021-0829-6. Epub 2021 Sep 13. PMID: 34515939.

Lin CH, Lee SS, Wen Lin I, Su WJ. Is Surgery Needed for Diplopia after Blowout Fractures? A Clarified Algorithm to Assist Decision-making. *Plast Reconstr Surg Glob Open.* 2022 May 9;10(5):e4308. doi: 10.1097/GOX.0000000000004308. PMID: 35558136; PMCID: PMC9084434.

Liu SS, Xu LL, Fan S, Lu SJ, Jin L, Liu LK, Yao Y, Cai B. Effect of platelet-rich plasma injection combined with individualised comprehensive physical therapy on temporomandibular joint osteoarthritis: A prospective cohort study. *J Oral Rehabil.* 2022 Feb;49(2):150-159. doi: 10.1111/joor.13261. Epub 2021 Oct 4. PMID: 34562321.

Liu XY, Zhang LT, Han D. [Research progress in studies on tooth development based on diphyodont mammals]. *Zhonghua Kou Qiang Yi Xue Za Zhi.* 2021 May 9;56(5):497-501. Chinese. doi: 10.3760/cma.j.cn112144-20200604-00314. PMID: 33904287.

Logan,C.Y.,and Nusse,R.(2004).The Wnt signaling pathway in development and disease. *Annu.Rev.CellDev.Biol.* 20,781–810. doi:10.1146/annurev.cellbio.20.010403.113126

Machon V, Levorova J, Hirjak D, Wisniewski M, Drahos M, Sidebottom A, Foltan R. A prospective assessment of outcomes following the use of autologous blood for the management of recurrent temporomandibular joint dislocation. *Oral Maxillofac Surg.* 2018 Mar;22(1):53-57. doi: 10.1007/s10006-017-0666-6. Epub 2017 Nov 30. PMID: 29189955.

Machoň V.: Užití autologní krve při léčbě chronické hypermobility čelistního kloubu, LKS č.1, leden 2006, ročník 16.

Matalova E, Tucker AS, Sharpe PT. Death in the life of a tooth. *J Dent Res* 2004; 83(1):11-6.

Mendenhall WM, Werning JW, Fernandes R, Malyapa RS, Mendenhall NP. Ameloblastoma. *Am J Clin Oncol*. 2007 Dec;30(6):645-8. doi: 10.1097/COC.0b013e3181573e59. PMID: 18091060.

Morikawa S, Ouchi T, Shibata S, Fujimura T, Kawana H, Okano H, Nakagawa T. Applications of Mesenchymal Stem Cells and Neural Crest Cells in Craniofacial Skeletal Research. *Stem Cells Int*. 2016;2016:2849879. doi: 10.1155/2016/2849879. Epub 2016 Feb 24. PMID: 27006661; PMCID: PMC4783549.

Murray-Douglass A, Snoswell C, Winter C, Harris R. Three-dimensional (3D) printing for post-traumatic orbital reconstruction, a systematic review and meta-analysis. *Br J Oral Maxillofac Surg*. 2022 Nov;60(9):1176-1183. doi: 10.1016/j.bjoms.2022.07.001. Epub 2022 Jul 16. PMID: 35931592.

Ottria L, Candotto V, Guzzo F, Gargari M, Barlattani A. Temporomandibular joint and related structures: anatomical and Histological aspects. *J Biol Regul Homeost Agents*. 2018 Jan-Feb;32(2 Suppl. 1):203-207. PMID: 29460542.

Ozturker C, Sari Y, Ozbilen KT, Ceylan NA, Tuncer S. Surgical Repair of Orbital Blow-Out Fractures: Outcomes and Complications. *Beyoglu Eye J*. 2022 Aug 5;7(3):199-206. doi: 10.14744/bej.2022.88156. PMID: 36185982; PMCID: PMC9522991.

Pagotto LEC, de Santana Santos T, Pastore GP. The efficacy of mesenchymal stem cells in regenerating structures associated with the temporomandibular joint: A systematic review. *Arch Oral Biol*. 2021 May;125:105104. doi: 10.1016/j.archoralbio.2021.105104. Epub 2021 Mar 6. PMID: 33706151.

Palanisamy JC, Jenzer AC. Ameloblastoma. 2022 Jul 4. In: StatPearls [Internet]. Treasure Island (FL): StatPearls Publishing; 2022 Jan-. PMID: 31424749.

Shi HA, Ng CWB, Kwa CT, Sim QXC. Ameloblastoma: A succinct review of the classification, genetic understanding and novel molecular targeted therapies. *Surgeon*. 2021 Aug;19(4):238-243. doi: 10.1016/j.surge.2020.06.009. Epub 2020 Jul 22. PMID: 32712102.

Shu J, Li A, Shao B, Chong Dyr, Yao J, Liu Z. Descriptions of the dynamic joint space of the temporomandibular joint. *Comput Methods Programs Biomed*. 2022 Nov;226:107149. doi: 10.1016/j.cmpb.2022.107149. Epub 2022 Sep 20. PMID: 36179656.

Siar CH, Nagatsuka H, Han PP, Buery RR, Tsujigiwa H, Nakano K, Ng KH, Kawakami T. Differential expression of canonical and non-canonical Wnt ligands in ameloblastoma. *J Oral Pathol Med*. 2012 Apr;41(4):332-9. doi: 10.1111/j.1600-0714.2011.01104.x. Epub 2011 Nov 14. PMID: 22077561.

Singh HP, S H T, Gandhi P, Salgotra V, Choudhary S, Agarwal R. A Retrospective Study to Evaluate Biopsies of Oral and Maxillofacial Lesions. *J Pharm Bioallied Sci.* 2021 Jun;13(Suppl 1):S116-S119. doi: 10.4103/jpbs.JPBS_597_20. Epub 2021 Jun 5. PMID: 34447057; PMCID: PMC8375871.

Stembirek J., Matalova E., Buchtova M., Machon V., Misek M. Investigation of an autologous blood treatment strategy for temporomandibular joint hypermobility in a pig model, *Int J Oral Maxillofac Surg* 2013; 42:369–375.

ŠTEMBÍREK, Jan, Anna ŠČERBOVÁ, Martina LITSCHMANNOVÁ, Oldřich RES a Jiří STRÁNSKÝ. Konzervativní a chirurgická terapie zlomenin kloubního výběžku mandibuly u dospělých. *Úrazová chirurgie: časopis České společnosti pro úrazovou chirurgii.* 2018, 26(4), 154–157. ISSN 1211-7080.

Taşkesen F, Cezairli B. Efficacy of prolotherapy and arthrocentesis in management of temporomandibular joint hypermobility. *Cranio.* 2020 Dec 16:1-9. doi: 10.1080/08869634.2020.1861887. Epub ahead of print. PMID: 33326351.

Ten Cate AR. The role of epithelium in the development, structure and function of the tissues of tooth support. *Oral Dis* 1996; 2:55–62.

Thesslef I, Vaahtokari A, Partanen AM. Regulation of organogenesis. Common molecular mechanism regulating the development of teeth and other organs. *Int. J. Dev. Biol* 1995; 39:35-50.

TIMKOVIC, Juraj, Jiri STRANSKY, Petr HANDLOS, Jaroslav JANOSEK, Hana TOMASKOVA a Jan STEMBIREK. Detecting Binocular Diplopia in Orbital Floor Blowout Fractures: Superiority of the Orthoptic Approach. *Medicina-Lithuania* [online]. 2021, 57(9), 989. ISSN 1010-660X. Dostupné z: doi:10.3390/medicina57090989

Warwar RE., Bullock JD., Ballal RD.: Mechanism of orbital floorfractures: a clinical, experimental, and theoretical study. *Ophthal Plast ReconstrSurg* 16:188 – 200, 2000

Xiong, J., Gronthos, S., Bartold, P.M., 2013. Role of the epithelial cell rests of Malassez in the development, maintenance and regeneration of periodontal ligament tissues. *Periodontol.* 2000 63, 217–233. <https://doi.org/10.1111/prd.12023>

Zeichner-David M, Oishi K, Su Z, Zakartchenko V, Chen LS, Arzate H. Role of Hertwig's epithelial root sheath cells in tooth root development. *Dev Dyn* 2003; 228:651-663.

Zemen J.: konzervativní léčba temporomandibulárních poruch, Galén, Praha, 199, str.: 14-36, 162-166.